University of Nottingham
UK | CHINA | MALAYSIA

Faculty of Engineering
Department of Architecture and Built Environment

INVESTIGATION OF THE VENTILATION AND THERMAL PERFORMANCE OF MASHRABIYA FOR RESIDENTIAL BUILDINGS IN THE HOT-HUMID CLIMATE OF SAUDI ARABIA

By

Abdullah Abdulhameed Bagasi

B. Arch, MSc

Thesis submitted to the University of Nottingham
for the degree of Doctor of Philosophy
June 2022

In the Name of Allah, the Most Beneficent, the Most Merciful.

ABSTRACT

The residential sector in Saudi Arabia is the most energy-consuming building sector, accounting for about 50% of the total energy generated. A large proportion of this energy is used to maintain the indoor air temperature at the required comfort level. While the lack of optimal use of natural resources in buildings, such as natural ventilation also contributes to the rising consumption. Traditionally, the Saudi buildings were characterised by different architectural solutions and elements such as the mashrabiya, which was closely related to the local environment and responded to many factors, such as climatic conditions and occupants needs. Mashrabiya is an opening covered with a wooden lattice for ventilation, daylight, privacy, and an aesthetic appeal for houses. Although there are many studies and research on the mashrabiya, most studies addressed either the ventilation or daylight aspect and few included evaporative cooling without conducting field tests or validated modelling to investigate its actual performance and the extent of its impact on the internal thermal environment.

Therefore, this research aims to investigate the effect of the mashrabiya on the indoor thermal environment and develop a mashrabiya design to enhance indoor thermal comfort in the residential buildings in hot climates with reference to Jeddah, Saudi Arabiya. The research, besides the literature review, includes field experiments and simulation works.

The field experiment results indicated that opening the mashrabiya allowed more airflow into the room and reduced the indoor temperature by up to 2.4 °C compared to the closed mashrabiya. Furthermore, by integrating evaporative cooling strategies (pots, water sprays, and wet cloth) with the open mashrabiya, it was found that the most effective approach to improving the room air temperature was hanging a wet cloth and the average room temperature reduced by up to 6.8°C. Along with that, the thermal mass played a significant role in reducing indoor air temperatures' thermal swings. In order to expand its scope in the study and examination of the mashrabiya, a computational fluid dynamic simulation tool was used. The results of the base case of the mashrabiya in the simulation generally indicated that the slats' inclination plays a vital role in the direction of the airflow into the room, and this is evident with tilting the slats angle to +30 or -30, as the airflow becomes more directed and sharper to the ceiling or the floor. Also, compared to the benchmark case, the mashrabiya contributed to

increasing the proportion of airflow into the room. This study also introduced the concept of integrating heat transfer devices into the mashrabiya to reduce the indoor temperature further. Overall, while the outdoor temperature was set at 40 C°, based on the average outdoor temperatures monitored from field experiment measurements during the summer season, the technique has been able to decrease the indoor air temperature by up to 7.5°C (18.8%).

This research presents comprehensive theoretical, experimental and computational methods of the evaluation of the performance of the mashrabiya and some strategies used to enhance thermal comfort. It can be summarized from the field studies that integrating evaporative cooling strategies, particularly the cloth strategy with mashrabiya in addition to the thermal mass, contributed to enhancing comfort. It can be concluded from the simulation work that the Ansys Fluent as a CFD tool gave flexibility in allowing testing and analysis of different designs and models, which contributed to a more accurate and better understanding than the fieldwork of the performance and effect of mashrabiya on ventilation, temperature and thermal comfort. In addition, the incorporation of heat transfer devices contributed to enhancing thermal performance and thus the achievement of simulation aim and objectives.

DEDICATION

I dedicate this thesis to my family, especially:

To **my great father "Abdulhameed" & mother "Abeer"**, who raised me and did everything they could for me, they have the credit after Allah for what I achieved from successes until this stage.

To **my beloved wife** "Alaa", the mother of my children, who always stands beside me, supports me and believes in my abilities.

To **my children (Hala, Abdulhameed, Taliah)** to encourage them to persevere, be patient and hope to achieve their goals

To **my brothers (Ahmed, Abdulrahman, Hashim) & my sisters (Laila, Asmaa, Rahmah)** & all my siblings who are an integral part and who support me and wish the best for me

ACKNOWLEDGMENTS

PUBLICATIONS

Journal Papers

BAGASI, A. A., CALAUTIT, J. K. & KARBAN, A. S. 2021. Evaluation of the Integration of the Traditional Architectural Element Mashrabiya into the Ventilation Strategy for Buildings in Hot Climates. *Energies*, 14, 530. doi:https://doi.org/10.3390/en14030530

BAGASI, A. A. & CALAUTIT, J. K. 2020. Experimental field study of the integration of passive and evaporative cooling techniques with Mashrabiya in hot climates. *Energy and Buildings*, 225, 110325. doi:https://doi.org/10.1016/j.enbuild.2020.110325

Conference papers:

BAGASI, A. A. & CALAUTIT, J. K. (2021). 'Investigation of the novel integration of mashrabiya and heat transfer devices for buildings in hot climates', *Applied Energy Symposium 2021: Low carbon cities and urban energy systems*, September 4-8, 2021, Matsue, Japan, 47.

BAGASI, A. A. & CALAUTIT, J. K. (2020). 'Experimental Field Study of the Integration of Passive and Evaporative Cooling Techniques with Mashrabiya in Hot Climates', *4th South East European Conference on Sustainable Development of Energy, Water, And Environment Systems.* Sarajevo, 28 June- 2 July. Bosnia and Herzegovina, 207.

BAGASI, A. A. & CALAUTIT, J. K. (2020). 'Evaluation of the Integration of Mashrabiya into the Ventilation Strategy for Buildings in Hot Climates', *4th South East European Conference on Sustainable Development of Energy, Water, And Environment Systems.* Sarajevo, 28 June- 2 July. Bosnia and Herzegovina, 212.

TABLE OF CONTENTS

LIST OF FIGURES

LIST OF TABLES

LIST OF ACRONYMS

AIAA	American Institute of Aeronautics and Astronautics
ASHRAE	American Society of Heating, Refrigerating, and Air conditioning Engineers
AC	Air Conditioning
Avg	Average
CAD	Computer-aided Design
CIBSE	Chartered Institution of Building Services Engineers
CFD	Computational Fluid Dynamics
clo	clothing insulation (clo)
D	Depth
DBT	Dry Bulb Temperature
DEC	Direct Evaporative Cooling
DF	Daylight Factor
FDM	Finite Difference Method
FEM	Finite Element Method
FVM	Finite Volume Method
GRC	Glass Reinforced Concrete
H	Height
HVAC	Heating, Ventilation, and Air Conditioning
IAQ	Indoor Air Quality
IDEC	Indirect Evaporative Cooling
L	Length
Max	Maximum
Min	Minimum
MRT	Mean radiant temperature
OPEC	Organization of the Petroleum Exporting Countries
PIV	Particle Image Velocimetry
PMF	Predicted Mean Vote
PPD	Predicted Percentage of Dissatisfied
RH	Relative Humidity
S.D.	Standard Deviation
SC	Shading Coefficient
SD	Secure Digital
SHGC	Solar Heat Gain Coefficient
SHGF	Solar Heat Gain Factor
SEC	Saudi Electricity Company
SEEC	Saudi Energy Efficiency Center
SST	Shear-Stress Transport
TA	Air Temperature
Tc	Comfort Temperature
T_o	Outdoot Temperature
UK	United Kingdom
UAE	United Arab Emirates
UoN	University of Nottingham
UNESCO	United Nations Educational, Scientific and Cultural Organization
USA	United States of America
W	Width

NOMENCLATURE

$\vec{a}$	Acceleration (m/s2)
$\vec{j}_j$	Diffusion flux of species j (mol/m^{2}s)
Γ_e	Diffusion coefficient (m^2/s)
K_{eff}	Effective conductivity, (W/m.K)
H	Enthalpy
ρ	Fluid density (kg/m^3)
$\vec{F}$	Force vector (Newtons)
$\vec{g}$	Gravitational acceleration (m/s^2)
c_p	Heat capacity (J/kg.K)
m	Mass (g, kg)
S_m	Mass added to the continuous phase from the dispersed second phase (kg)
$\boldsymbol{\mu}$	Molecular viscosity (Pa s)
∂	Partial derivative
$\boldsymbol{p}$	Pressure (Pa)
T_{ref}	Reference temperature (K)
$\bar{\bar{\boldsymbol{\tau}}}$	Stress tensor (Pa)
k	Thermal conductivity (W/m.K)
t	Time (s)
∇	The partial derivative of a quantity with respect to directions in the Cartesian coordinate system.
ε	Turbulence dissipation rate (m^2/s^3)
$S\varepsilon$	User defined source term for energy dissipation rate (m^2/s^3)
$\bar{\phi}$	Variable (changing property)
$\vec{u}$	Velocity vector (m/s)
S_h	Volumetric heat sources (W)
U	Wind velocity/Velocity magnitude (m/s)

CHAPTER 1

INTRODUCTION

Background
Problem Statement
Research Aim and Objectives
Research Questions
Scope and Limitations
Research Methodology
Thesis Structure

1. INTRODUCTION

1.1 Background

The rapid development witnessed by the Kingdom of Saudi Arabia during the past decades
has led to significant changes in the economic and social fields and buildings, accompanied
by a significant increase in energy demand. Saudi Arabia's climate is classified among the hot
climates, as it witnesses a rise in high temperatures most of the year. Mechanical cooling
systems consume a large proportion of energy to provide comfort to occupants of residential
buildings in the Kingdom of Saudi Arabia and maintain the indoor air temperature in buildings
at the required comfort temperature. While the lack of optimal use of natural resources in
buildings, such as daylight and ventilation also contribute to raising this consumption. As a
result, the residential sector in Saudi Arabia is the most energy-consuming building sector,
accounting for about 50% of the total energy generated (SEEC, 2019).

Referring to the past, vernacular buildings in Saudi Arabia have been closely related to the
local environment and responded to many factors, such as climatic conditions, comfort and
occupants' needs. Traditionally, Saudi buildings have used different passive cooling
techniques such as high thermal mass, shading devices, and evaporative cooling to reduce
the heat gains in the buildings. Consequently, several architectural elements were adapted
and employed effectively and on a large scale in traditional housing in Saudi Arabia, such as
the mashrabiya, courtyards, and wind towers that have been proven to meet the occupants'
needs and have strong compatibility with the local climate. Mashrabiya is one of the most
prominent traditional architectural elements in the Middle East, such as Jeddah, Makkah,
Yanbu, Baghdad, Cairo, Damascus, and Tunis. Moreover, mashrabiya has spread and been
adopted in different regions worldwide, from the Far East to South America, such as India,
Japan, China, Portugal, and Spain. Mashrabiya can be described as a wooden frame
covering a window opening and decorating the building facade.

Although there are many studies and research on the traditional mashrabiya, most studies
handled introducing and emphasising the importance of the mashrabiya and its functional

purposes or developing mashrabiya without field testing and looking at it its actual

performance and the extent of its impact on the internal thermal environment.

Therefore, this study aims to broaden our knowledge about mashrabiya and investigate its

impact on the internal thermal environment and develop it through implementing a number of

procedures, starting with a comprehensive literature review, then field experiments, and

ending with simulation work.

1.2 Problem Statement

From oil exploration in Saudi Arabia until the present, many changes and developments have

taken place in different sectors due to the economic boom, and Saudi Arabia has made great

strides towards urban development and construction in many fields. During this process of

modernisation, the buildings became one of the most important sectors that developed

significantly but regrettably contributed to some issues. Modern buildings relied on active

systems, especially ventilation, instead of optimising natural resources, which led to increased

energy consumption. Besides that, most modern buildings have lost the local and original

architectural style and identity. Along with Saudi Arabia's hot climate, these factors have

contributed to increased energy use in modern residential buildings, consuming about 50% of

the generated energy. Saudi Energy Efficiency Center (2017) reported that air conditioning,

lighting, equipment, and other devices, in buildings consume about 80% of the electricity

produced in Saudi Arabia and about half this ratio is consumed in air conditioning use.

Therefore, providing indoor thermal comfort to occupants of residential buildings is one of the

essential needs and requirements in the past and present. Referring to the past, the vernacular

residential buildings of Saudi Arabia featured different traditional architectural elements with

convenient solutions for the local environment. Mashrabiya, which has been used since the last

century, considers one of the elements characterised by its functions and features. Nowadays,

mashrabiya is no longer used widely and functionally as used in the past due to not being

compatible with the current era with building requirements and occupant needs. With the rapid

development and availability of mechanical systems that meet thermal comfort's human needs,

reliance on these uses has contributed to the increased consumption of energy resources. In

recent years, many research, experiments, and studies have been carried out to revive

mashrabiya with several solutions and methods. However, mashrabiya still needs more studies regarding its actual impact, especially concerning achieving thermal comfort and thus reintegrating it into modern buildings in line with the needs of the inhabitants and the requirements of modern buildings and the environment in a way that improves the energy efficiency of buildings.

1.3 Research Aim and Objectives

This research aims to investigate the effect of mashrabiya on the indoor thermal environment and develop mashrabiya design to enhance indoor ventilation and thermal comfort in residential buildings in hot climates with reference to Jeddah, Saudi Arabiya.

The main objectives of this research to achieve this aim are the following:

- Review studies on mashrabiya as a shading device and its integration with residential buildings in different regions.
- Review the literature on the developments on mashrabiya regarding its daylight, ventilation and thermal performance and the techniques or strategies integrated with it.
- Investigate and evaluate the performance of a traditional mashrabiya related to the indoor environment and thermal comfort using field experiments.
- Investigate and evaluate the effect of integrating passive cooling strategies (water spray, wet cloth, and water pots) with the mashrabiya, including thermal mass.
- Create a valid numerical model to evaluate the ventilation and thermal performance of mashrabiya through a computational fluid dynamics CFD tool in addition to obtaining a valid model prepared for development.
- Develop the mashrabiya design by integrating cooling techniques " heat transfer devices" and determine its impact on indoor ventilation, air temperature, and thermal comfort.

1.4 Research Questions

- What is the actual role and impact of a traditional mashrabiya on the environmental factors of thermal comfort in a residential building in Jeddah?
- What is the impact on the ventilation and thermal performance of a mashrabiya integrated to a residential building in hot climates?

- Does adding evaporative cooling strategies affect the performance and effectiveness of the traditional mashrabiya in a hot-humid climate of Saudi Arabia?

- Does the strategy of heat transfer devices increase the mashrabiya performance's effectiveness and achieve the comfort level in hot climates?

1.5 Scope and Limitations

This study focused on investigating the performance of the mashrabiya in the hot and humid climate in Saudi Arabia in terms of indoor thermal comfort. The field experiments were conducted in a historical building in Jeddah during two summers, 2018 and 2019. The first evaluated the traditional mashrabiya's performance comparing different opening configurations. The second assessed the effect of combining passive evaporative cooling strategies with mashrabiya on the internal environmental and thermal comfort, and the role of thermal mass was evaluated.

After that, a base case was modelled using a CFD tool to extend our understanding of the performance of mashrabiya and develop the design through combined heat transfer devices to enhance thermal performance.

In this research, the assessment of thermal comfort was based only on environmental factors. Due to time constraints and the high cost of getting more equipment, the fieldwork investigated one type of mashrabiya in a single building at limited points. Moreover, during summer, field measurements were conducted while the other seasons were not covered due to limited time. The investigation of the simulation work was limited to studying one type and design of the standard mashrabiya. In addition, the computational modelling room was not studied as part of a building but was studied as isolated, and no obstructions such as furniture inside the room or glass pane in front of the mashrabiyas were considered. The tetrahedral type mesh was used for the base case and development phase instead of the hexahedral mesh with more correlation in the Particle Image Velocimetry "PIV" data to save time and compare to complex steps to prepare the solution of the hexahedral models.

1.6 Research Methodology

In an attempt to study and examine the performance of the mashrabiya in an organised and systematic way, this research is composed of two approaches: a theoretical and practical approach (Figure 1-1). Under these approaches, there are several procedures to achieve the research objectives, as shown in the following:

Theoretical approach

- Conduct a literature review on Saudi residential buildings and review the most important influences, climate treatments and influencing factors on energy efficiency.
- Conduct a literature review on mashrabiya: history, concept and structure, functions, advantages and disadvantages, previous studies and applications.
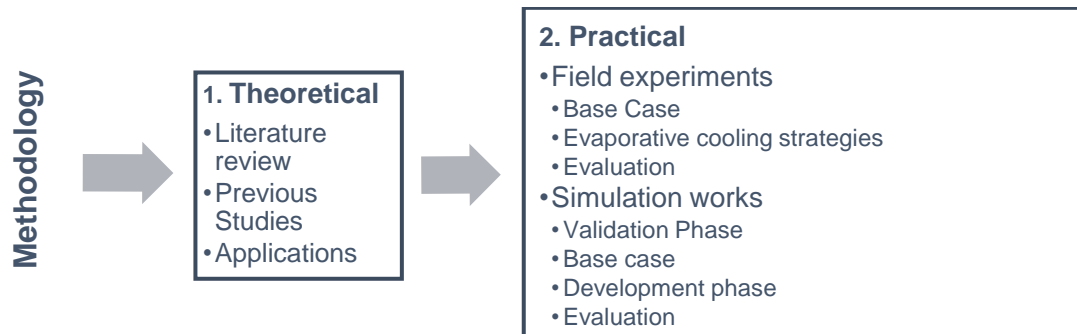
Figure 1-1 Thesis research methodology

Practical approach:

1. Select a case study among the historical buildings of Jeddah based on several criteria such as the mashrabiya's shape, function, and the building age, availability of drawings, the possibility of experiments, and access.

2. Specify the appropriate devices (data loggers) for measuring and monitoring outdoor and indoor thermal environments, based on several criteria; measurements range, accuracy, data display, recording, cost, and power requirements.

3. Carry out field measurements in a building with traditional mashrabiyas with various opening configurations.

4. Investigate and evaluate the integration of passive cooling evaporative strategies with mashrabiya.

5. Create a benchmark case numerical model of a crossflow ventilated building validated model with experimental data.

6. Generate a base case of the mashrabiya based on the benchmark model. Then, evaluate and determine the most effective inclination angle of the mashrabiya in terms of the airflow into the room

7. Optimize the mashrabiya ventilation and thermal performance by integrating cooling techniques such as heat transfer devices.

8. Evaluate and compare the base case with the benchmark model in terms of ventilation, temperature, and indoor thermal comfort.

9. Complete the investigations, analysing the results and providing conclusions and recommendations.

Overall, the thesis's overall scope and main procedures can be summarized in Figure 1-2.
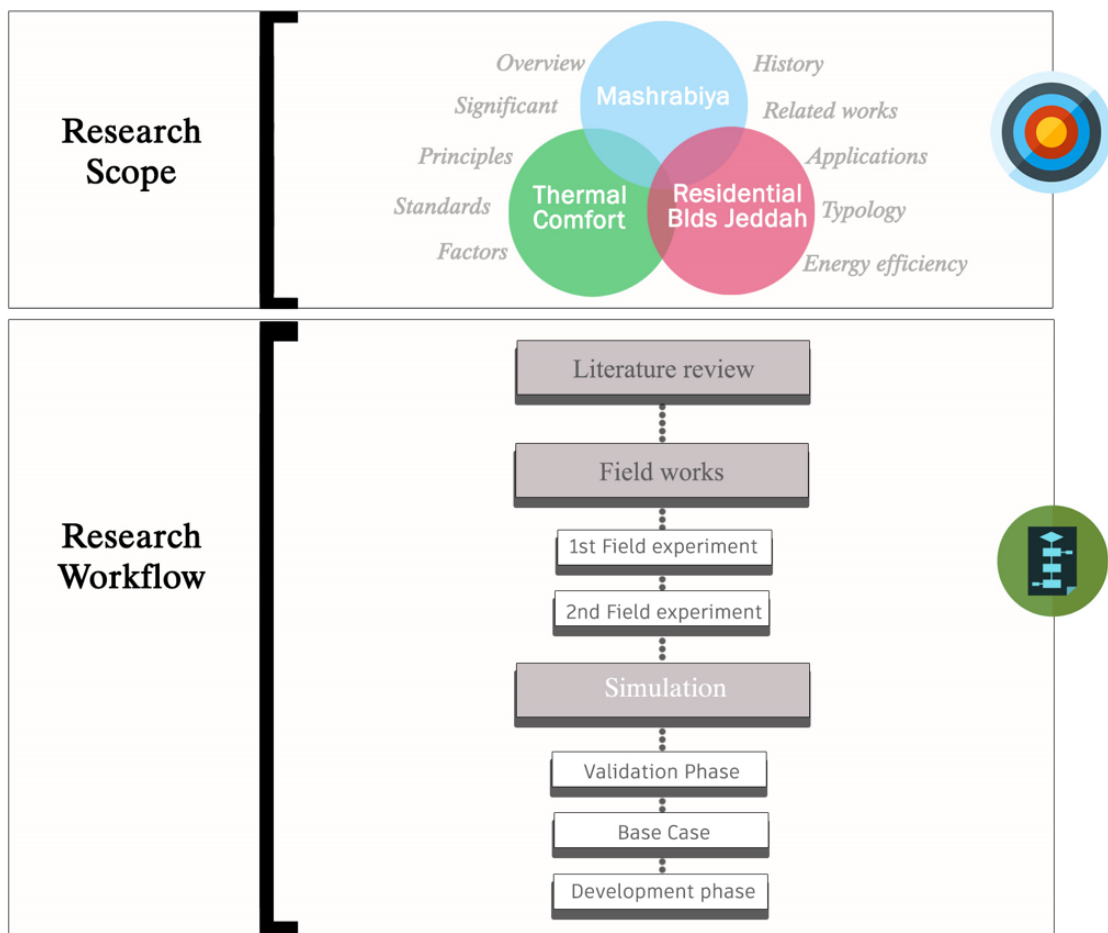
Figure 1-2 Diagram of thesis procedures

1.7 Novelty of the Research

Besides the privacy and beauty that the mashrabiya provided for traditional buildings, mashrabiya provided two main solutions that allowed occupants to benefit effectively from natural lighting and ventilation. Despite what was mentioned in several studies of the necessity of reviving and benefiting from local architectural elements such as the mashrabiya, there is a lack of studies on the mashrabiya from an environmental perspective where to the best of our knowledge the effect of mashrabiya on thermal condition practically in the field hasn't been investigated. Furthermore, most studies tend to focus on the history or development of the mashrabiya without testing or considering its actual performance and impact on the internal thermal environment. Therefore, the novelty of this study lies in the investigation and evaluation of the effect of a traditional mashrabiya on the indoor thermal environment through field experiments and resulting in a comprehensive assessment for understanding the mashrabiya performance on the indoor thermal condition. It is important to emphasize that passive evaporative cooling strategies have been integrated with mashrabiya to improve the thermal condition, while it should be noted that none of these strategies has been conducted previously on mashrabiya in the hot humid climate of Saudi Arabia.

Also, by using a CFD tool, testing, and analysis of different models, this research contributed to a more accurate and better understanding of the performance and effect of mashrabiya on airflow, and air temperature in detail. Furthermore, this research benefited from the use and application of integrated heat pipe heat transfer devices and thus was able to expand the efficiency of mashrabiya on the indoor thermal conditions and resulting in achieving thermal comfort.

1.8 Thesis Layout

As shown in Table 1-1, besides the introduction and conclusions chapters, the thesis consists of three main sections, which briefly can be described as 1) it covers chapters two to four that contain the research background and theoretical framework, 2) it includes chapter five which represents the case study and field experiments, and 3) it covers chapter six and seven that includes the validation modelling, the base case, and development phase.

The following is a brief overview of each chapter of this thesis:

Chapter 1 introduces an overview background of the study. Also, the chapter explained the research problem, the aim and objectives, research questions, scope and limitations, and methodology to achieve the aim and objectives of this study. Finally, the description for each chapter has been presented here, in addition to a table of thesis structure.

Chapter 2 contains a literature review of the energy efficiency of residential buildings in Saudi Arabia. Besides, an overview of traditional residential buildings and modem residential buildings in Saudi Arabia with a focus on the architecture of the study area is known as the Hijaz architecture.

Chapter 3 contains a literature review of the impact of building fabric on the thermal environment. The chapter discusses several parameters; facades and windows, daylighting, heat loss, heat gain, and ventilation. It also presents the significance of thermal comfort , including the factors and models, adaptive passive strategies in hot climates, and the comfort and residential buildings in Jeddah.

Chapter 4 covers mashrabiya from several aspects. First, it presents the definition of mashrabiya, the origin and meaning of the word, and its spread worldwide in different shapes and designs. It also reviews the history of mashrabiya, its designs and types, as well as its functions. Moreover, previous studies and applications have been reviewed with conclusions.

Chapter 5 represents the case study "Baeshen House" of the fieldwork. It presents an overview of the area of the case study and the local climate. Also, it presents information about the case study and the selection criteria. The chapter introduces the aim and objectives of the field experiments and the method, results and discussions, limitations, and the evaluation of thermal comfort for each field experiment.

Chapter 6 represents the basics of simulations related to CFD computational fluid dynamics. It also displays the objectives, plan, phases of the simulation, and model setup (geometry, meshing, boundary conditions, solver settings). Finally, it presents the cases and defines the benchmark case as a reference case for the subsequent phases.

Chapter 7 presents modelling the base case of the mashrabiya. Moreover, it includes the development phase represented in "heat pipes" while the model setup is covered for each phase. Finally, it concludes with comprehensive comparisons between the phases, defining the best case in terms of thermal comfort.

Chapter 8 summarises the main findings and the conclusion of the thesis on the importance of mashrabiya on thermal comfort in residential buildings in hot climates and the effect of incorporating passive evaporative cooling strategies. Summarises the processes followed during the study and the methods used to fill the gap in utilising mashrabiyas on comfort. Finally, it provides some recommendations for future research.

Table 1-1 The structural outline for the thesis chapters

Methodology	Proposed Chapter	Proposed Sub-Chapter
Investigation of the ventilation and thermal performance of mashrabiya for residential buildings in the hot-humid climate of Saudi Arabia		
Introduction	1. Background, Aim and Objectives, Methodology, Scope and limitations, Thesis Layout	
Background + Literature Review (Lead-in)	2. Energy Efficiency in Residential Buildings in Saudi Arabia	The context in Saudi: Geographical location, Climate, and regions
		Energy Consumption and Efficiency
		Housing Typology: types, characteristics, regulations
	3. Impact of Building Fabric on the Thermal Environment	Facades and Windows
		Daylight, Heat Loss, Heat Gain, Ventilation
		Thermal Comfort: Factors, models
		Adaptive Comfort Strategies Used in Hot Climates: Thermal mass, Ventilation, Evaporative Cooling
	4. Mashrabiya	History of Mashrabiya
		Design and Structure Details
		Functions & Characteristics
		Previous Studies and Applications
Field Experiments (Core)	5. Case Study	Baeshen House Description: Location, Climate, history, design
		Scope and Methods
		Field study 1: Results, Discussion, Limitations
		Field study 2: Results, Discussion, Limitations
Simulation and validation (Core)	6. Simulation and the Benchmark Model	Simulation Basis
		Simulation Plan
		Validation Model
		Results
Parametric Study (Core)	7. Design and Integration of Heat Transfer Devices with Mashrabiya	Models Setup
		The Base Case
		Single Row of Pipes Integrated with Mashrabiya
		Double Rows of Pipes Integrated with Mashrabiya
		Results and Discussion
Conclusions (Lead out)	8. Conclusions and further work	Conclusions
		Limitations
		Recommendation for Future Work

CHAPTER 2

Energy Efficiency and Residential Buildings in Saudi Arabia

Introduction
The context in Saudi Geographical location, Climate and Regions
Housing Typology (types, characteristics, regulations)
Energy performance and consumption

2. ENERGY EFFICIENCY IN RESIDENTIAL BUILDINGS IN SAUDI ARABIA

2.1 Introduction

Climate is one of the most critical factors affecting designs and construction materials used in buildings, and this is evident in traditional architecture, which showed more response to the climate than contemporary buildings. Baik and Boehm (2017) stated, "Regarding the climatic considerations, historical Jeddah houses are very effective, which was critical in shaping the morphology and the urban fabric of the historic city."

During the last decades, the accelerated development of Saudi Arabia led to major changes in the economic, social, and building fields and experienced a high increase in energy demand where the electricity demand has increased at an average annual rate of approximately 7% (Dehwah et al., 2018). The high temperatures throughout the year in Saudi Arabia make cooling systems necessary to achieve human comfort (Rafique et al., 2016). In general, a large portion of energy use is consumed globally to keep the indoor air temperature of buildings within the required comfort temperature (Shahzad et al., 2020). In Saudi Arabia, the residential building sector consumes about 50% of the total generated energy, mainly due to high outdoor temperatures, especially in the summer, leading to increased air conditioner use (Alaidroos and Krarti, 2015) (Felimban et al., 2019). Also, the lack of optimal utilisation of natural resources such as daylight and ventilation contributes to high energy consumption.

2.2 The context in Saudi

Saudi Arabia is dominated by desert and sub-Saharan climate where high temperature is dominant in most months of the year. The Kingdom of Saudi Arabia is located in the southwest of Asia between 16 and 32° latitude north, lying down in the middle of the Tropic of Cancer. Due to the difference in Saudi Arabia's topography (elevation from the earth's surface), besides the vast area, temperature, humidity, wind direction, and rain rates vary from one region to another. Besides, the climate of Saudi Arabia is affected by the surrounding water surfaces. Saudi is surrounded by two important water seas: the Arabian

Gulf from the east and the Red Sea from the west. It is also located near other large water

bodies, the Indian Ocean in the south of the Arabian Peninsula and the Mediterranean in the

northwest of the Arabian Peninsula. The temperature difference between water bodies and

the Earth and their natural properties, including the gain and loss of heat, results in different

regional pressure centres during the year and the air transmission affecting Saudi's climate

from different directions (Al-Shareef, 1996). According to the Köppen-Geiger climate

classification, Saudi Arabia can be categorised as a hot arid desert climate (BWh), as shown

in Figure 2-1. This system was deemed acceptable to describe a more general world climate

model since it is based on annual and monthly temperature and precipitation averages

(Kiamba, 2016). It should be noted that the western regions adjoining on the coast of the Red

Sea are classified as hot and humid climate (Alwetaishi, 2019).
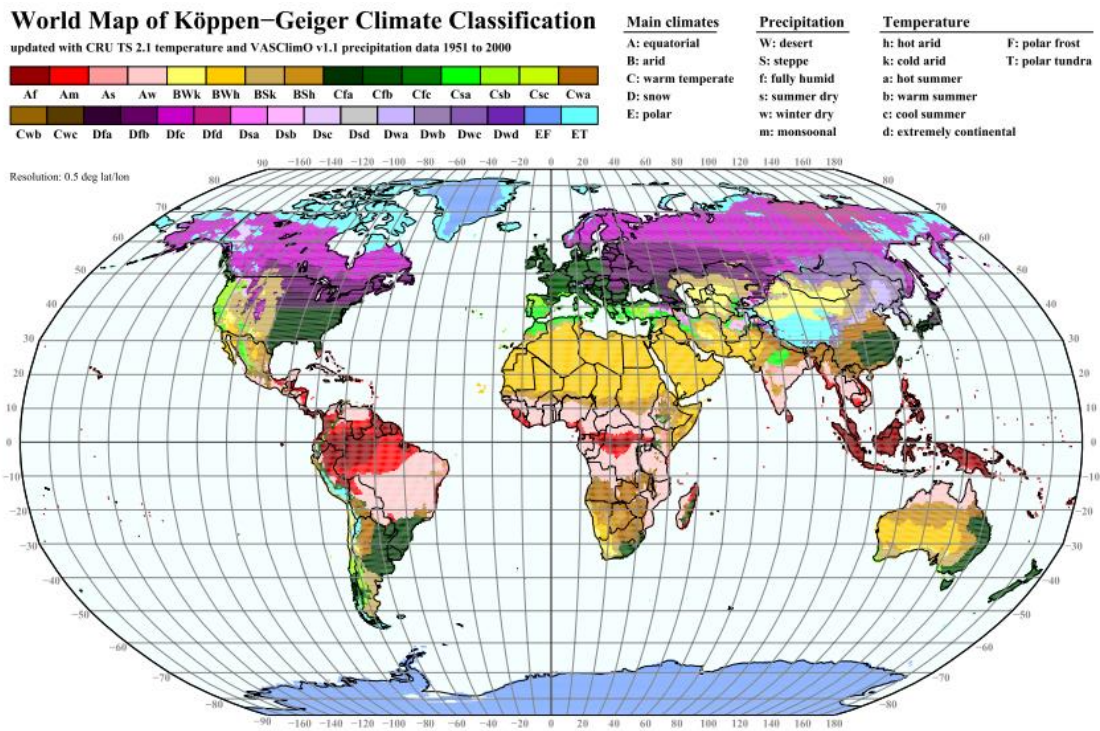
Figure 2-1 World Map of Koppen-Geiger Climate Classification. Reproduced from (Kottek et al., 2006)

Topography also plays an essential role in the region's climate variations due to the difference

in elevation and direction and surface crust composition. The natural shape of Saudi allows

air masses and winds coming from the open sides of the north, east and south to deepen in

its territory, while the western highlands limit the masses and wind that coming from the west

and south-west to deepen into the rest of Saudi Arabia's regions.

According to (Said et al., 2003), climate zones in Saudi Arabia can be classified into five climatic zones: Dhahran, Guriat, Riyadh, Jeddah, and Khamis Mushait, as seen in Figure 2-2.
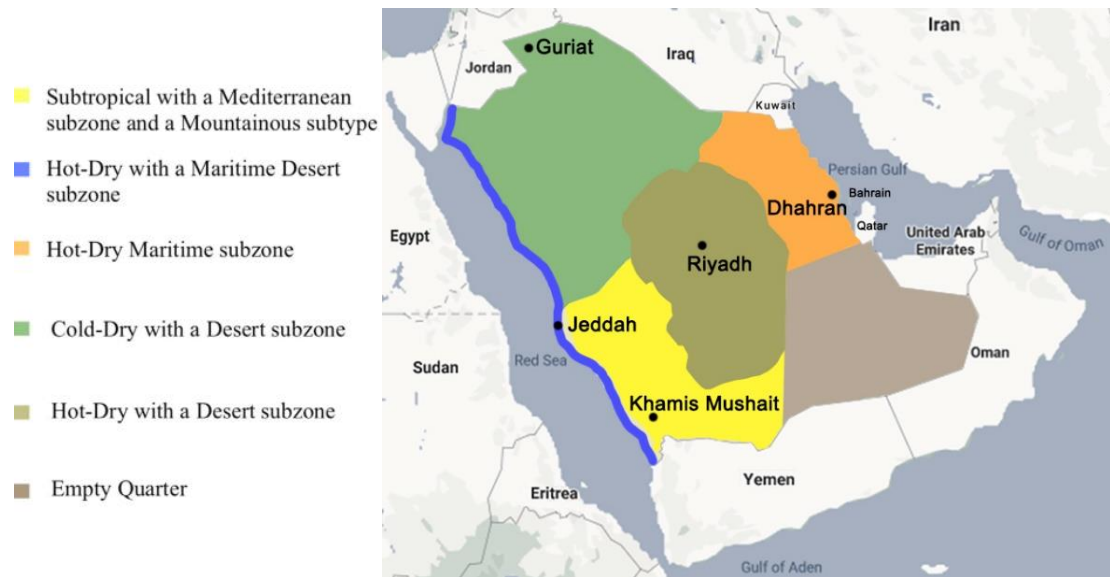
Figure 2-2 The climatic zones in Saudi Arabia. Amended from (Said et al., 2003)

The summer temperature is characterised by a rise in most Saudi Arabia areas except for the mountainous regions (Western and South-west highlands) and moderation in winter. Temperatures can reach over 45°C in the hot, dry zones in summer, while in the spring and autumn, temperatures average 29° C (Maghrabi, 2000). In the country's northern regions, the winter temperatures can drop below freezing point with a chance of some snow. The summer season in Saudi begin in March, and winter begins in October and November (Al-Ansari et al., 1986). Figure 2-3 shows the maximum and minimum historical monthly temperatures for Saudi Arabia from 1999 to 2019 for 20 years. All climatic data were taken from the collected data of 32 measuring stations in Saudi Arabia, without including weather stations at an altitude above 2090m (WorldData.info, 2020). The green zone in the graph represents the months' minimum averages, whereas the red zone demonstrates the maximum averages. Saudi Arabia is one of the most exposed countries to solar radiation during the year. The total solar radiation incident on a horizontal surface is called solar radiation, known as global horizontal radiation (GHI). Direct normal radiation (DNI), diffuse horizontal radiation (DHI), and radiation reflected from the earth are all included under solar radiation.
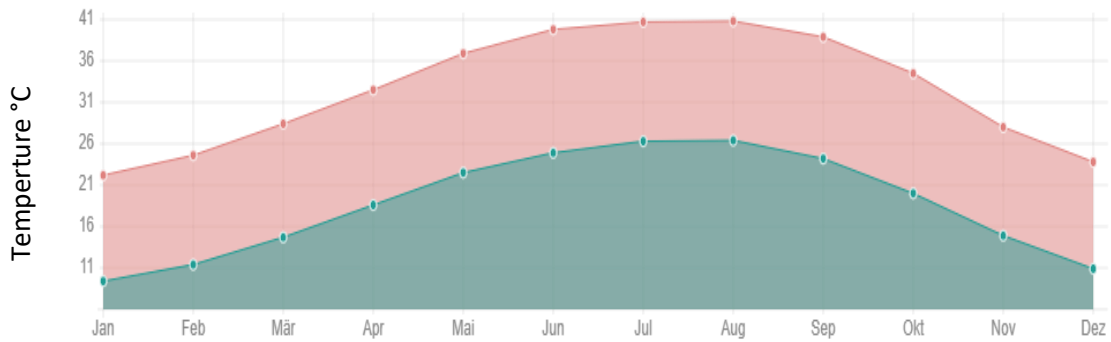
Figure 2-3 Average Monthly Air Temperature for Saudi Arabia from 1999 to 2019. Reproduced from (WorldData.info, 2020)

The annual average daily Global Horizontal Irradiance (GHI) ranges from around 5700 Watt-hour per square metre (Wh/m²) to 6700 Wh/m², with lower values along the shores and higher values inward (Maxwell et al., 1996). Figure 2-4 presents the average amount of GHI and DNI for all Saudi areas, where it shows that the southern part is the most exposed to the sun, with an average annual sum of GHI of more than 2400 kiloWatt-hour per square metre (Maxwell et al., 1996). In contrast, the north-eastern part is the least exposed to solar irradiance, with an average annual sum of GHI less than 2100 kWh/m2 (Maxwell et al., 1996).
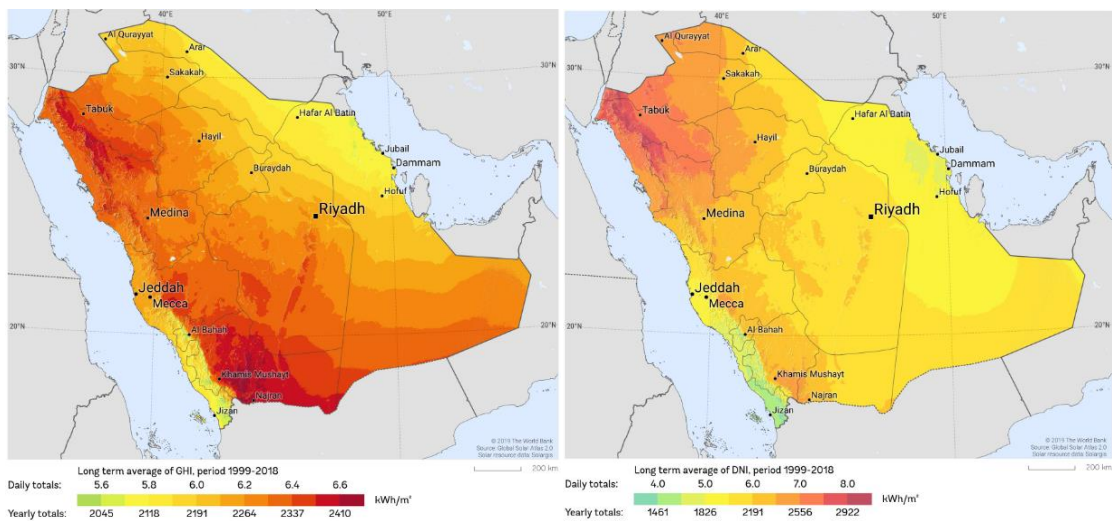
Figure 2-4 Average annual GHI (left) & DNI (right) for Saudi Arabia (SOLARGIS, 2018)

The rainfall over Saudi Arabia is generally very scanty only about a few inches a year on average except in the southwest. Rain in most Saudi parts except in the southwest is characterised by seasonality and difference in time, place, and quantity.

The amount of water vapour "Relative Humidity" varies in the atmosphere of Saudi from one area to another because of the difference in location of water bodies such as the sea and

other sources of humidity such as agricultural areas, in addition to the humid wind's path that blows over the country. However, the average monthly relative humidity ranges between 30 and 58%, Figure 2-5.
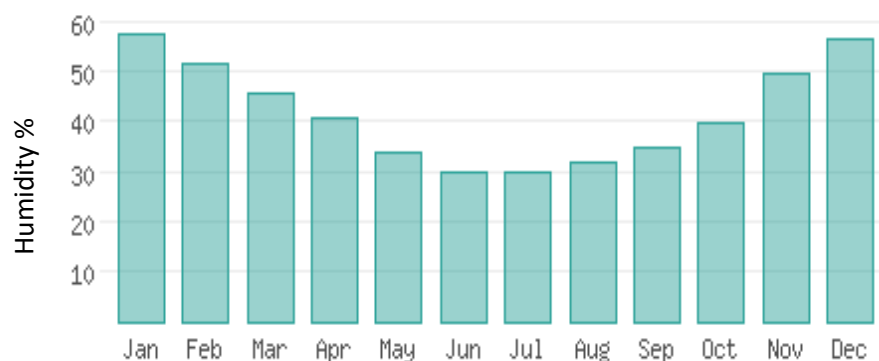
Figure 2-5 Average monthly relative humidity for Saudi Arabia from 1999 to 2019. Reproduced from (WorldData.info, 2020)

Wind speeds and directions are affected by several factors, such as the difference in heights of regions, the formation of the surface crust, water bodies and open areas. Generally, the natural shape of Saudi Arabia allows the air masses and winds coming from the open sides of the north, east and south to deepen in its lands, while the western highlands limit the masses and winds coming from the west and southwest to deepen the rest of Saudi Arabia. Although atmospheric pressure is commonly high and seasonal pressure differences are relatively small in most areas but causing non-gale winds. For instance, the most frequent winds from the Southwest blow through May to September and carry dust into Jeddah and thunderstorms in the South. The winds are strong, hot, and droughty during this period (Vincent, 2008).

To summarize, the climate of Saudi Arabia is generally classified as hot and dry, with high temperatures prevailing in most months of the year. So, Saudi Arabia is one of the most exposed countries to solar radiation during the year. Temperatures can reach over 45°C in the hot, dry zones in summer, while in the spring and autumn, temperatures average 29° C where the average monthly relative humidity range between 30 and 58%. Whereas the rainfall is generally very scanty, only about a few inches a year on average except in the south-west. Generally, the temperature, humidity, wind direction, and precipitation rates differ from one region to another due to the surrounding water surfaces and the difference in the topography and the vast area.

2.3 Housing Typology (types, characteristics and regulations)

Since Saudi Arabia's founding and then the discovery of oil, developments, and economic growth in Saudi Arabia until now, Saudi architecture can be divided into two classifications: traditional residential architecture and contemporary residential architecture. In traditional architecture built before oil discovery, architects and designers were fully aware of the importance of environmental and climatic factors and how to benefit from them and reflected clearly on those buildings. On the other hand, during economic development and modernity, the construction sector became one of the most important sectors that developed significantly but unfortunately contributed to some issues. The buildings became more dependent on energy systems with a weak dependence on environmental conditions and local climate, and the loss of original architectural buildings and cultural identity became evident. These factors influenced the urban movement, formed a clear gap between traditional and modern architecture, and increased energy consumption.

2.3.1 Traditional Residential Architecture

Talib (1984) said, "the design concepts, forms, and details of traditional architecture show an impressive climatic response to the vast desert environment of Saudi Arabia". Meeting the needs of human beings in the design of buildings and considering the climatic factors, including the diversity of cultures, are some of the main reasons that contributed significantly to the formation of a distinctive traditional architecture for each region in Saudi Arabia. Traditional residential buildings in Saudi Arabia are characterised by several architectural elements such as; mashrabiya, courtyard and windcatcher, which have achieved sustainability principles in different proportions (Figure 2-6).
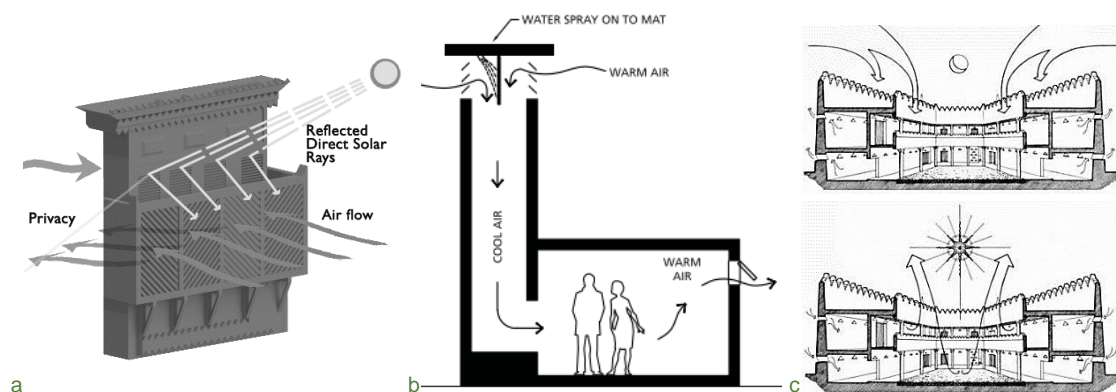
Figure 2-6 A typical design of a) Mashrabiya, b)Wind tower, c) Courtyard

In Saudi Arabia, there are generally four different types of traditional housing architecture: Hijaz architecture, Upland architecture, Najd architecture, and Eastern Province architecture (Ibrahim, 1995). These types emerged mainly due to differences in local environments, including local climate and topography, and different factors that affect these patterns, whether social or cultural. Despite the differences between these types, they all combine in the constants associated with Islamic values and local heritage (Figure 2-7). Each type of this architecture will be briefly addressed in the following, and since the study is based on Jeddah as a reference for the study, the Hijaz architecture that includes Jeddah will be explored and reviewed in more detail.
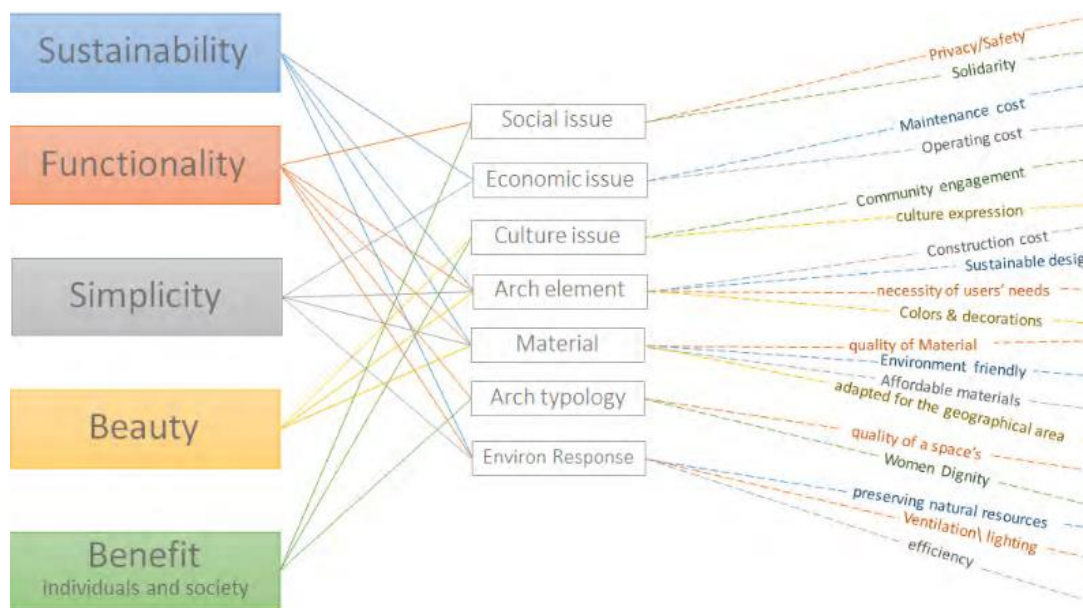
Figure 2-7 Principles and Design Strategy. Reproduced from (Alsharif, 2016)

Najd architecture

Najd architecture was a traditional type known in central Saudi Arabia for the hot and dry climate. In response to the region's harsh, hot and dry climate, buildings were built adjacently, to shade each other. The buildings depended on courtyards as a climatic solution to the harsh conditions. As shown in Figure 2-8, with the small and narrow external openings, all rooms are oriented to the house's inner courtyard, and a covered corridor around the courtyard protects the doors and windows of the rooms. The courtyard played an essential role in filtering dust, allowing more natural lighting and ventilation, and providing the highest level of privacy for the family inside the house. The buildings are generally made of clay with a wall

thickness of 45 to 75 cm. To provide a high degree of thermal stability inside the building, thick walls were built using stones with mud and sometimes with gypsum, while wood or palm trunks and branches were used to construct the roofs. The buildings are characterised by breadth and regular lines, with simple lines and a few external decorations, but they are rich in interior decoration and inscriptions (Ibrahim, 1995).

Figure 2-8 Typical Najdi internal courtyard. Reproduced from (Facey, 2015)

Upland Architecture

It is a distinctive traditional style of the southwestern region in Saudi Arabia, as Asir, Taif, and Abha. The nature of the high mountainous area and its cold climate influenced architectural characteristics in the region. The houses were built above the mountains while mountain slopes are exploited in agriculture. Due to the rough terrain in the region, the horizontal area of a building is relatively small; then it enlarges vertically to accommodate all of its basic needs. The buildings were built of clay and stone and characterised by stone rows of multiple and prominent "Madamek" at regular intervals in the form of full belts that extend around a building and protect it from weather fluctuations, especially from heavy rain. The buildings rise to four and five floors (Figure 2-9), in which the higher floors were assigned to women and family rooms.

Some buildings are rich in colourful geometric designs with vibrant colours such as red, green, yellow, and blue. These decorations appear in doors, windows, ceilings, openings, and external walls and these colourful decorations are considered common features in the region (Ibrahim, 1995).

Figure 2-9 Historical buildings in Asir. Reproduced from (Saudi, 2020)

Eastern Province architecture

It was a traditional pattern known near the Arabic Gulf. It includes Dhahran, Al-Khobar, and Dammam, which has a composite climate that fluctuates between hot-dry and hot-humid climates (Ibrahim, 1995). Some of the architectural areas were distinguished by wind catchers or badgirs, which were used to allow and control the incoming air and reduce the entry of dust (Figure 2-10).
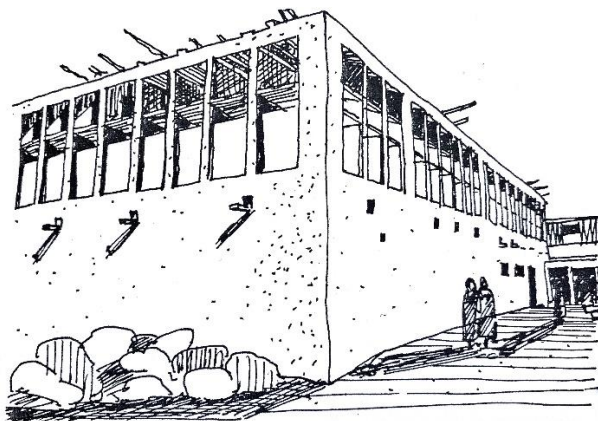
Figure 2-10 Wind towers in eastern province oasis. Reproduced from (Talib, 1984)

Also, the dwellings were characterised by the inner courtyard as a central element designed from more regular shapes than the courtyards in the Najd region. Usually, the buildings were built in monolithic rows, so that clusters of buildings shade each other. The buildings were placed in rows extending eastward - westward so that the house's interior living spaces are oriented north and south. The openings of doors and windows are on covered corridors around a courtyard, while the external openings are few, narrow, and provided by a wooden screen to protect the inner space from the glare of the sun and dust winds (Figure 2-11). The walls were constructed of stone 45 to 75 cm thick with clay and gypsum used as bonding to ensure thermal stability inside dwellings. The finishing materials were smooth with light colours and used to achieve direct sunlight reflection and resist humidity and rain.
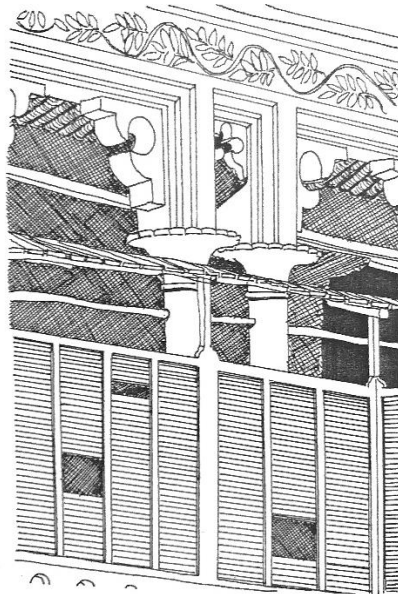
Figure 2-11 A wooden screen around a courtyard. Reproduced from (Talib, 1984)

2.3.1.1 Hijaz architecture

It is spread in the western region of Saudi Arabia where the hot, humid climate on the west coast and turns into hot and dry as we head east inland. Hijaz means the barrier that split the Middle (Najd) region of the Arabian Peninsula from the Western (Hijaz) by the Jabal Al-Sarawat mountain range, from the north part of Saudi Arabia near the Jordanian border to the south in Yemen (Kamal, 2014). This region includes many cities as Jeddah, Makkah, Medina, Taif, and Yanbu. Jeddah is the largest city in this region which was and still is a centre of cultural and commercial exchange between the region and countries of the Middle East, Asia,

and Europe. This exchange affected building technology in the Hejaz since the Ottoman era, as non-local building materials appeared and more developed and advanced construction methods were introduced. (Taleb, 2012) stated, "The traditional architecture of Hijaz reflects the influence of the Ottoman Empire, which controlled this region through much of its history". The movement of pilgrims entering the region through Jeddah from around the world cannot be overlooked. Therefore, this region's architecture is considered a natural continuation of the Islamic architecture in Egypt and the Levant (Sham), and this is evident in the beautiful mashrabiyas built on the openings and windows taken from Egyptian architecture. These mashrabiyas were developed to become rich in wood ornaments, and this widespread pattern in Jeddah has influenced the character of architecture in the dry and arid region of Makkah and Medina (Ibrahim, 1995).

Buildings in Hijaz rise up to four and five floors and sometimes to seven floors in response to the hot, humid climate so that the height allows the movement of air through a building. Talib (1984) said, "In hot-humid Jeddah the houses sometimes as high as six storeys, do not have courtyards, and feature mashrabiyas (projected decorative bay windows) for maximum ventilation and to provide cooling", see (Figure 2-12Figure 2-11).

Figure 2-12 A type of mashrabiyas in a historical building in Jeddah "Noorwali House"

Saudi Commission for Tourism and National Heritage (2016) stated: "The dwellings were characterised use wood ornate boxes called 'Roshans' covering the wall openings which controlled the airflow to spread it all around the house and also throw their shadows on the adjacent walls of the house to mitigate the effect of heat in summer". The buildings were built from brick and stone, whereas gypsum was used with stone as a bond material to ensure insulation, while floors and ceilings were made from wood. The exterior and interior design allow air to flow through the spaces and from lower to upper floors. Overall, the buildings are rich in wood ornaments or carved stucco in geometric or floral exquisite patterns, all of that provide large surfaces of shadows on the facades of buildings, thus strengthening the heat resistance property of the building. The buildings were built apart to allow for the airflow around them and give the largest possible surface for setting mashrabiyas, allowing air to pass inside the building (Ibrahim, 1995).

To conclude, the formation of traditional architecture for each region in Saudi Arabia was designed and built based on climatic factors, including meeting the needs of its inhabitants and the diversity of cultures from one region to another. In general, several architectural elements were common to each region that acted as effective climate solutions and achieved the principles of sustainability in different proportions, such as mashrabiyas, courtyards, wind catchers, and local materials stones.

2.3.2 Contemporary Residential Architecture

From exploring Oil 1930s in Saudi Arabia until today, many changes and developments occurred in different sectors due to the economic boom. Saudi Arabia has moved into great strides toward urban development and construction in various fields. Moreover, a significant increase in the number of domestic and immigrant workers, especially in the urban regions, has caused a crisis in providing suitable housing for individuals or families' needs. In 1970, many foreign architects, engineers, and construction experts were invited to Saudi Arabia to create a modern built environment (Taleb, 2012). In most cases, this involved importing modern designs, construction techniques, and construction materials developed and manufactured outside of the country (Taleb, 2012).

During this modernity process, the building sector became one of the most important sectors that have evolved significantly but unfortunately contributed to some issues. However, the

lack of buildings' dependence on environmental conditions and the local climate and the loss of buildings' original architectural, and cultural identity became evident. These factors influenced the urban movement and formed an apparent gap between the traditional architecture (buildings a generation ago) and the contemporary (current).

In the context of attempts to develop, improve, innovate, and slide to achieve better architecture suited to the modern needs of habitants, architectural styles and patterns have emerged a quaint and separate from the environmental style, local pattern, or any other pattern architectural style. Almerbati (2016) said, "The introduction of electricity and extra wealth made it easier for modernity to take off layers of advanced vernacular architectural dwellings, which were replaced by concrete buildings".

In the contemporary residential buildings, Babsail and Al-Qawasmi (2015) stated that " it is hard to find surviving examples of traditional vernacular elements such as internal courtyards, Mashrabiyah, wind towers, small openings, and shaded passageways". Modern buildings depend on active systems, especially in lighting and ventilation, rather than utilisation of natural resources optimally, and that causes an increase in energy consumption.

According to Al Tayash (2011), modern architecture issues in Saudi Arabia can be summarised as follows: 1) Loss of architectural and urban identity in housing design. 2) Adopting architectural styles that are unsuitable for the environment, cultural, and civilised aspects of Saudi society and do not meet social life requirements and way of living. 3) misusing building materials and incompatible with the local climate and applying some construction methods are economically useless. 4) Increase the social and cultural gap between generations of a single society. Consequently, all of this negatively impacts the economy and society (Al Tayash, 2011).

2.3.2.1 Residential Buildings Typology

Residential units in Saudi Arabia can be categorised into four major types: villas, apartments, traditional houses, additional floors in villas, and a floor in traditional houses. According to the General Population and Housing Census of Saudi Arabia in 2019, the most residential units in terms of number and expansion occupied by Saudi households are apartments by about 44%. After that, the villas by 29.7%, then traditional houses by 18% subsequently the annexes and other housing units by about 9% (Figure 2-13).
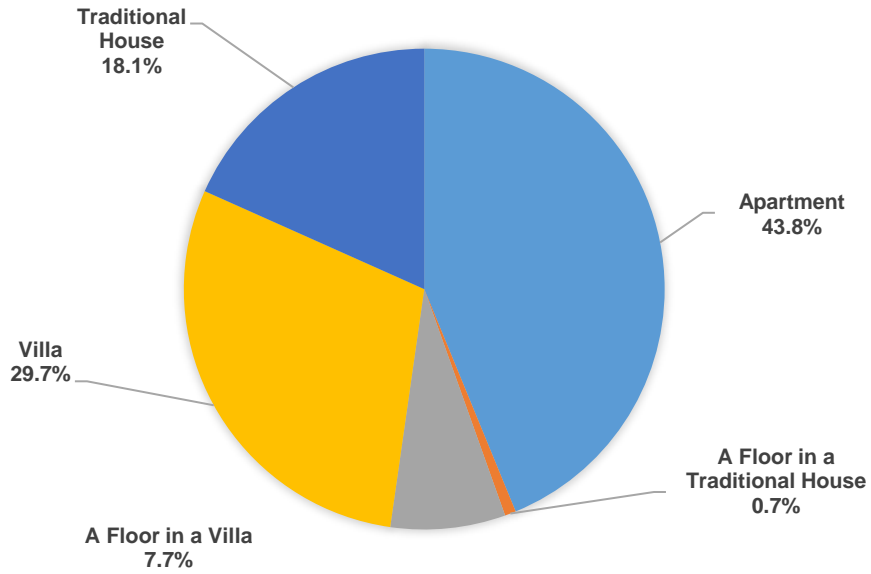
Figure 2-13 Housing Units in Saudi Arabia [Source: The General Authority for Statistics in Saudi]

As reported by the General Authority for Statistics in Saudi in 2019, the highest housing units occupied by Saudi households is Makkah province with 909228 units, then Riyadh province with 865,390 units, then in Madinah province h with 253,047units. In Makkah province, Jeddah is the largest city and the second-largest city in Saudi Arabia after the capital, Riyadh. Accordingly, it is worth noting to show some statistics about housing types in this city. Figure 2-14 shows the housing types and numbers in Jeddah, demonstrating that the apartments are the most numerous with 434,169 units (61.8%). That was mainly due to increasing land prices, rising demand for housing, and the tremendous population growth.
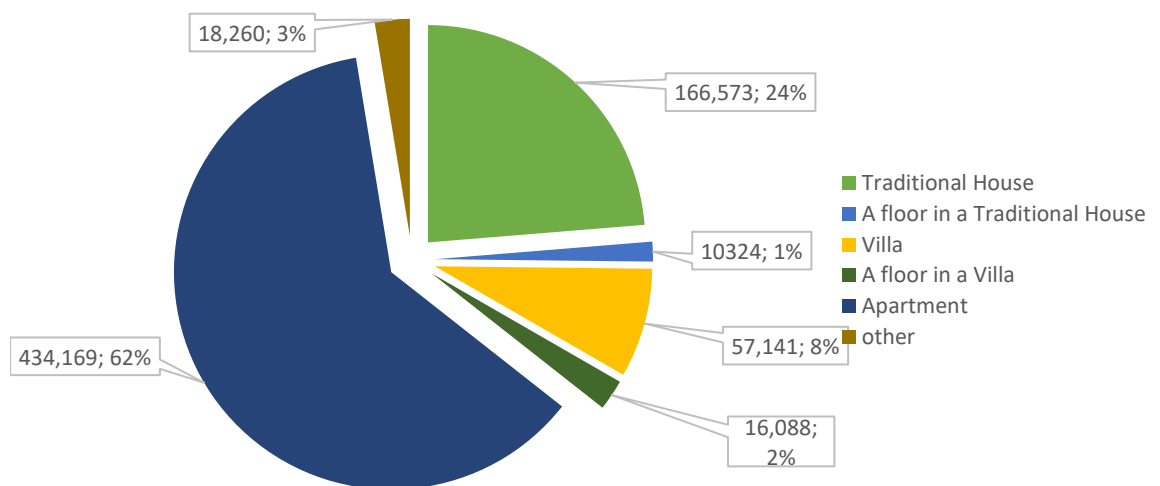
Figure 2-14 Types and numbers of housing units in Jeddah (statistics, 2019)

To summarize, most contemporary residential buildings have relied on active systems, especially in lighting, ventilation and cooling; besides the emergence of strange architectural styles that are separate from the environmental style, with the loss of the original architectural identity and the decline in the use of local architectural elements. The General Population and Housing Census of Saudi Arabia of 2019 showed that apartments are the most residential units in terms of number and expansion that Saudi families occupy. That matter requires architects to find alternatives and the most appropriate design solutions for inhabitants and the environment to utilise daylight and natural ventilation strategies to reduce energy loads.

2.4 Energy Performance and Consumption

The accelerated growth in Saudi Arabia over the previous decades has led to significant economic, social and construction changes, and the energy demand has increased significantly, where electricity demand has increased by an average of 7% per year (Dehwah et al., 2018). The high temperatures make cooling systems an urgent need for human comfort in Saudi Arabia (Rafique et al., 2016). Residential buildings in Saudi Arabia consume about 50% of total energy generated mainly because of the high outside temperatures in the summer, leading to higher use of air conditioners (Alaidroos and Krarti, 2015) (Felimban et al., 2019). Further factors contributing to high energy consumption are the lack of optimal natural resources, such as daylight and ventilation.

Saudi Arabia is the top country in the production and export of petroleum liquids for several decades. According to OPEC 2020, Saudi comprises about 17% of the world's total oil reserves. Saudi is one of the most consuming energy countries worldwide where the electricity use per capita rates based on the data from the Electricity and Cogeneration Regulatory Authority of Saudi in 2019 was around 8,434 Kilo Watt Hour (kWh). In Saudi, the local consumption of petroleum and gas materials is about 38%.

Based on the annual statical booklet for electricity and cogeneration regulatory authority, the highest energy consumption category in 2019 was the residential sector. It consumed about half of the electricity supply by 45.8%, followed by industrial 17.7%, commercial 16.4%, government 14.5, then other sectors by 5.6%.

According to Figure 2-15, residential buildings in the southern region recorded the lowest per capita electricity consumption. That is mainly due to moderate weather and the lack of reliance on air conditioners, considered among the most consuming of electricity in Saudi Arabia. According to (Muhammad Al-Dabyan and Rayan Al-Yamani 2020), different factors can lead to different electricity consumption rates between regions, such as wealth, population size, and weather.
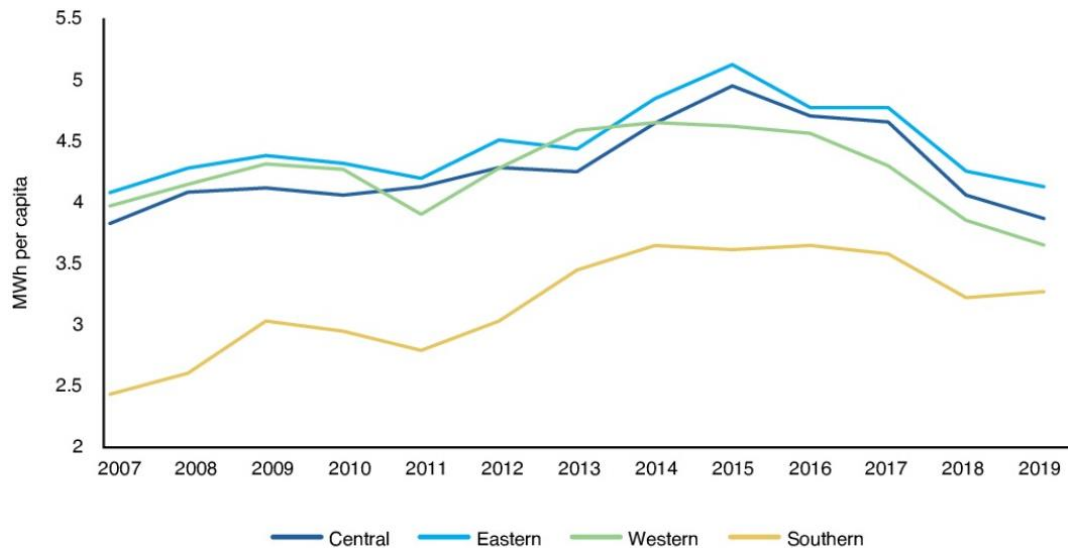
Figure 2-15 Per capita regional electricity consumption in residential buildings in Saudi Arabia. [Source: King Abdullah Petroleum Studies and Research Center]

Saudi Energy Efficiency Center (2017) states that about 80% of the electricity produced in Saudi Arabia is consumed in air conditioning, lighting, equipment and other devices in buildings, and about half this ratio is consumed in air conditioning use. That is due to high temperatures in the Kingdom, especially in the summer, resulting in high usage and increasing demand for air conditioning. Saudi Energy Efficiency Center added that electricity usage tariffs discourage investment in alternative energy use, lack of interest in thermal insulation in buildings where about 70% of buildings are not thermally insulated, and energy use habits. All these factors contributed to the energy increase. Moreover, the lack of optimal use in building designs for natural resources such as daylight and ventilation also caused a higher increase in buildings' energy consumption. (Al-Sanea and Zedan, 2008) said, "Reducing these loads is becoming increasingly important, because of an emerging shortage of electricity due to rapid population growth and the industrialisation of the kingdom". However, simple behaviour in raising the air conditioner's thermostat can lead to significant

energy savings, especially during peak electricity use(Alshahrani and Boait, 2019). A Saudi study by Al-Sanea and Zedan (2008) found that the annual thermostat setting to one more degree up can reduce the annual cooling transmission load by about 10% per year while keeping the high thermal comfort the whole year.

Said et al. (2003) said, "Escalating energy costs and increased awareness of energy conservation have created a need for codes of practice to reduce energy consumption and have resulted in several energy conservation studies."

In 2004, the Saudi Building Code approved the general framework, and the first edition for two primary building conditions and requirements categories was published. According to the Saudi Building Code, the importance of building code is to increase the quality of construction and preserve the national economy by ensuring the safety of enterprises by establishing the requirements that determine the principles of design, implementation and methods suitable for the climatic conditions, geology and nature of the Kingdom. The code also contributes to guiding engineers, architects and technicians, enabling them to implement their designs and work in safe and secure ways and eliminating the problems that result from the different points of view of the parties participating in the construction sector. Overall, the role of the code is based on protecting the environment, providing safety and a healthy environment, sustainability and energy conservation, and providing adequate lighting and ventilation. Since the mashrabiya is the main element of this work, It should be noted that mashrabiya is consistent with the principles of the Saudi code, where the code calls for providing appropriate lighting and ventilation, and these are the main functions and advantages of mashrabiya while improving mashrabiya contributes to the exploitation of natural resources and energy building saving.

In the past years, Saudi Arabia began working on several new technical considerations and studies in its plans to take advantage of renewable energy, including the Saudi Electricity Company, which launched the research in preparing a comprehensive map of sites that could produce solar energy in all regions of the Kingdom. Besides, taking advantage of the wind movement in some areas to reduce future dependence on oil and reduce environmental pollution is in line with the vision of the Kingdom of Saudi Arabia 2030.

According to the General Authority for Statistics report on renewable energy indicators in Saudi Arabia, the average number of homes that use solar energy in 2019 was about 1.6%. The Makkah region recorded a percentage close to the general average of 1.5%.

One of the axes of the 2030 vision is the development of the tourism and national heritage sector, which seeks to commercialise the Kingdom of Saudi Arabia as a tourist destination in regional and global terms, develop advanced infrastructure, prepare necessary regulations and legislation, and create institutional capacity to create different job options. In addition to reviving, preserving, promoting and classifying Islamic, Arab and national heritage in the list of internationally recognised heritage sites. During the past years, Saudi has revived and managed to register a number of historical and heritage sites on the UNESCO list, including Historic Jeddah, registered in 2014 as a heritage site. The vision also aims to improve living standards within the National Transformation Program to improve the urban landscape in Saudi for public and community spaces, impose architectural controls for buildings, and restore and beautify buildings' facades to ensure their quality and safety. In addition to minimizing unwanted scenes visually (visual pollution) and reducing environmental pollution.

The Saudi 2030 Vision mentioned:

"By preserving our environment and natural resources, we fulfill our Islamic, human and moral duties. Preservation is also our responsibility to future generations and essential to the quality of our daily lives".

The Saudi Government is taking serious steps from that point of view, starting with the Saudi Vision 2030 which intends to implement various scopes, to shift the country's economy from the oil-based to the multi-source economy (Felimban et al., 2019).

As one of the pillars of sustainable economic development of Vision 2030, the Saudi Energy Efficiency Center is keen to rationalize and increase energy efficiency in production and consumption in order to preserve the Kingdom's natural resources in several aspects. Since 2014, the SEEC has conducted several national campaigns to rationalize energy consumption and are still continuing, aiming to establish and raise the level of community awareness and change energy consumption behaviours. The SEEC also emphasized the necessity of utilising natural conditions in designing buildings by allowing natural ventilation and lighting as much as possible and taking several other considerations into the design.

According to the SEEC, the ideal shape for buildings generally is the rectangle with a longitudinal side facing north to receive the least amount of sunlight. At the same time, it is preferable to reduce windows facing direct sunlight, design projections or awnings for windows, and make double-glazed windows, to reduce heat transfer and leakage into the building.

To summarize, residential buildings in Saudi Arabia consume about 50% of the total energy generated; mainly half of this percentage is consumed in the use of air conditioning due to the high temperatures. With the population and urban growth, it became necessary to reduce these loads and find solutions. Therefore, Saudi Arabia began working on several new technical considerations and applying some standards to reduce energy consumption in residential buildings and benefit from renewable energy in the last years. As one of the pillars of sustainable economic development for Saudi's 2030 vision, the Saudi Energy Efficiency Center implemented several national energy conservation campaigns that are still ongoing. The aim of campaigns is to create and raise community awareness and change energy consumption behaviours, emphasising the need to take advantage of passive ventilation and daylight in buildings.

2.5 Conclusion

The chapter reviewed the residential buildings and climate in Saudi Arabia. The climate generally is classified as hot and dry, with high temperatures prevailing in most months of the year. Where Saudi Arabia is one of the most exposed countries to solar radiation during the year, temperatures can reach over 45°C in the hot, dry zones in summer, while in the spring and autumn, temperatures average 29° C where the average monthly relative humidity range between 30 and 58%. In comparison, the rainfall is generally very scanty, only about a few inches a year on average except in the southwest. Due to the surrounding water surfaces and the difference in the topography and the vast area, the temperature, humidity, wind direction, and precipitation rates differ from one region to another.

From Saudi Arabia's founding until the present, Saudi architecture can be divided into traditional residential architecture and contemporary residential architecture. In traditional architecture built before oil discovery, architects and designers were fully aware of the

importance of environmental and climatic factors and how to benefit from them and reflected clearly on those buildings.

The traditional architecture of each region in Saudi Arabia has been created and built based on climatic factors while catering to its population's needs and cultures' diversity from one region to another. The primary configurations that produced traditional Saudi architecture are the Hijaz architecture, upland architecture, Najd architecture, and the eastern region architecture. In general, many architectural elements common in each region acted as effective climate solutions and achieved sustainability principles in different proportions, such as mashrabiya, courtyards, wind catchers, and local material stones.

After the discovery of oil in Saudi Arabia, a clear gap has formed between traditional and modern architecture; buildings have become more dependent on active energy systems with little reliance on environmental conditions and the local climate, which contributed to raising the energy consumption issue, besides the loss of original architectural buildings and cultural identity. Saudi Arabia residential buildings consume about 50% of the total energy generated. Half of this is mainly consumed by the use of air conditioning to achieve the desired comfort level. In the next chapter, the importance of building envelopes besides thermal comfort and some passive strategies used in hot climates will be explored, which contrbuite in reduce energy consumed in buildings.

CHAPTER 3

IMPACT OF BUILDING FABRIC ON THE THERMAL ENVIRONMENT

Facades and Windows
Daylighting
Heat loss
Heat Gain
Ventilation
Thermal Comfort (Factors and Models)
Adaptive Comfort Strategies Used in Hot Climates
Thermal Comfort and Residential Buildings in Jeddah

3. IMPACT OF BUILDING FABRIC ON THE THERMAL ENVIRONMENT

The building envelope is the main link between inside and outside, whether by communicating the inside with the outside, such as viewing to outside or entering and leaving the building, and the outside linking to the inside through noise or heat and other factors that affect the indoor. Szokolay (2004) said; "The building is not just a shelter, or a barrier against unwanted influences (rain, wind, cold), but the building envelope should be considered as a selective filter: to exclude the unwanted influences, but admit the desirable and useful ones, such as daylight, solar radiation in winter or natural ventilation". Therefore, the building envelope must be designed to provide comfortable indoor environments and protect against climate (sun, wind and precipitation), cold and warm weather and noise - visual control - while offering daylight, ventilation and energy savings (Abohorlu Doğramacı, 2018).

Lechner (2014) considered and classified the thermal envelope that is the most reliable and sustainable for cooling and heating the building into three hierarchical levels, which are 1) reducing the heat flow through the building envelope, 2) passive systems, then 3) using a mechanical system. Since thermal comfort in residential buildings is considered essential, it may become a problem in many modern residential buildings, especially in hot and humid climate environments when the cooling systems or passive strategies are not afforded (Tap et al., 2011). On the other hand, traditional buildings were designed with a critical consideration of comfort through several treatments and strategies such as using the adaptive thermal mass, utilization of natural ventilation, and using various passive cooling methods.

3.1 Facades and Windows

Facades and windows are among the most critical components of buildings and play a significant role in a building's performance, affecting energy and passenger needs. The primary function of the façade is to protect the *building from the climate effects as sunlight, wind, snow, ice, and rain. The functional design of the shaded facade plays a practical impact on creating an environment that results in less energy* consumption and operation cost of the building and optimizes the building performance daylight distribution (Lee et al., 2016). As

architects and engineers, several aspects should consider in designing a facade: environmental factors, aesthetic appearance, occupant thermal comfort, social, and view (Alotaibi, 2015). Harry (2016) stated: "The design of building envelope plays a major role in determining the operational energy usage of a building during its lifetime".

The double façades in the hot climate, according to Boake (2014), can be classified into two types: 1) Facades designed as shading screens and sun protection as Mashrabiya where exterior surface coupled with a high-performance curtain wall system. The exterior shading is either steady or responsive, while the glass is not used to provide a second layer for the outer layer. 2) Facades with a more traditional approach (buffer, twin-face or extract-air) where the exterior coat is glazed.

In the last two decades, the dynamic façade has recognisable development in the concept. The dynamic façade is also called intelligent skin/façade, Kinetic, or active facade. According to Wigginton and Harris (2002), the intelligent facade is characterised as "A facade joining variable technology, which would adjust itself to give solace conditions inside the building whatever the outside natural conditions, maybe, in a specific building area". According to Ramzy and Fayed (2011), Kinetic architecture is "a design concept in contemporary architecture, which explores the physical transformation of a building to redefine traditional applications of motion through technological innovation".

In the Middle Ages, wooden shutters were installed on the openings, kept open or closed to control daylight and airflow (Phillips, 2004). According to Phillips (2004) "With the introduction of glass, used first in small panes in Roman architecture, the window as we know it today had its beginnings". Nowadays, glass windows are widely used in buildings around the world. However, windows are openings in buildings' walls or sides that perform several essential functions depending on their design cases. Windows can provide several benefits like daylight, view, heat, ventilation, or even occupants' privacy. All those functions could benefit if they are appropriately designed for the case design. In the last decades, many research, studies, and experiments demonstrated the impact of appropriate windows design on psychological and physiological needs, performance, health, and comfort. The view is another benefit of using windows in buildings. It is gained by windows that provide a visual connection between the interior and exterior environment. One key function of a window is to provide a

view of the outside, and it is an important part of the space's occupants even if the exterior environment does not seem attractive. In attempting to control the climate problems of solar heat gain and glare, the view could be disturbed by shading devices, especially in hot climate regions (Waheeb, 2006). However, windows size, position, frames, type, and other elevation elements must be considered carefully concerning building users' eye level to provide the best view and comfort (Ruck et al., 2000).

Although the outside view and communication with others are important, privacy is also important for most people. The large windows can provide a pleasant and good view but may not provide enough privacy for users of a space or room. If the desire for privacy outweighs the desire for a view, especially when windows are on the ground floor, smaller windows may be preferable (Markus, 1967). While a feeling of privacy differs with view conditions, like a view of nature and degree of overlooking, and individual personality factors, some freedom of choice is desirable (Ludlow, 1976). Curtains, blinds, and shades commonly are practical elements because they can be controlled directly by the occupants. (Markus, 1967). Another well-known traditional architectural element is "Mashrabiya," which covers openings and provides privacy and view from inside to outside and other functions.

3.2 Daylighting

"Architecture is the masterly, correct and magnificent play of volumes brought together in light…The history of architecture is the history of the struggle for light."…….. Le Corbusier. Throughout ancient civilisations and centuries, daylighting (known as natural lighting) was the main source of lighting in buildings until the late 19th century when replaced by electric light widely in buildings (Kroelinger, 2002). With global warming, oil crises, and sustainable importance, using daylighting returned to be one of the most critical processes for architects and designers in designing buildings. Using daylighting in buildings can provide many benefits; view and connection to the outside, provide comfort for users and delight in the interior spaces and minimise the total energy cost. Kroelinger (2002) said: "Good daylighting design can result in energy savings and can shift peak electrical demand during afternoon hours when daylight availability levels and utility rates are high". The exploitation of daylight is an imperative need not because it eliminates or reduces the energy use of artificial lighting,

but also reduces more cooling and heating loads. Daylighting design in buildings depends on factors and considerations such as building type, climate, orientation, and daylighting strategy. Besides, it depends on psychological and physiological needs, performance, and health. In addition to that, some research demonstrated the daylighting effect on performance, comfort, and health for buildings' occupants. Also, the importance of daylighting depends on the type and function of a building. For example, education and commercial buildings that occupy during a day will use more electrical energy if there is no daylighting thoughtfulness. The amount of daylight that penetrates a space is linked to a window space's total glazing area. Naturally, increasing the area of windows will admit more daylight into a room. Also, it can reduce the heat load and increase the cooling load.

Based on windows' physical requirements, the windows' sizes depend mainly upon Daylight factor (DF), energy use, glare control, sound effects, and ventilation. To target the appropriate daylight factor for the side window area, we can use the following equation as rules of thumb (Stein and S. Reynolds, 1992):

$$DF_{average} = 0.2 \text{ (window Area / floor area)} \qquad (3.1)$$

$$DF_{minimum} = 0.1 \text{ (window Area / floor area)} \qquad (3.2)$$

However, some recent studies and research found that the minimum window area for visual comfort is 20% of the wall area, and about 30% is the preferred window area for occupants. Besides, if the window area transcended 30-35%, the number of spaces users who think their window is so large increased (Hellinga, 2013). Daylight is one of the main benefits of setting and designing space windows. Windows can admit direct light from the sun, and diffuse light from the sky, surroundings, or surfaces, and window design plays a key role in determining the distribution of daylight into space. Therefore, choosing windows just for their architectural design properties may perform to satisfactory results in many cases.

On the other hand, some cases should use advanced daylighting systems to be advantageous such as the following cases:

- Complicated in the building's geometry, such as deep rooms, spaces, or intricate facades.

- Performing difficult tasks or sensitive works that required a high degree over the visual environment.

- Required control of thermal loads (in this case, adjustable solar shading can be an effective strategy) (Ruck et al., 2000).

The quality of daylighting is affected by solar altitude, location, orientation, weather, climate, surrounding buildings, and other factors. Furthermore, the thickness of the atmosphere layer surrounding the earth and some other factors such as the existence of a few dust particles and water vapour in the air; work on dispersal and scattering of solar radiation during the daytime when it passes into the atmosphere where this phenomenon is the basis for a skylight. The skylight intensity changes regularly, depending on the earth's rotation around the sun during the four seasons and the earth's daily rotation on its axis. Also, the light varies depending on the amount of cloud cover in the sky (Figure 3-1).

The natural lighting inside the building is an essential and critical factor in creating comfort and pleasure for building users.

Generally, positive daylighting goals introduce appropriate illumination to human needs, create an aesthetic visual environment, and reduce lighting buildings' energy costs.
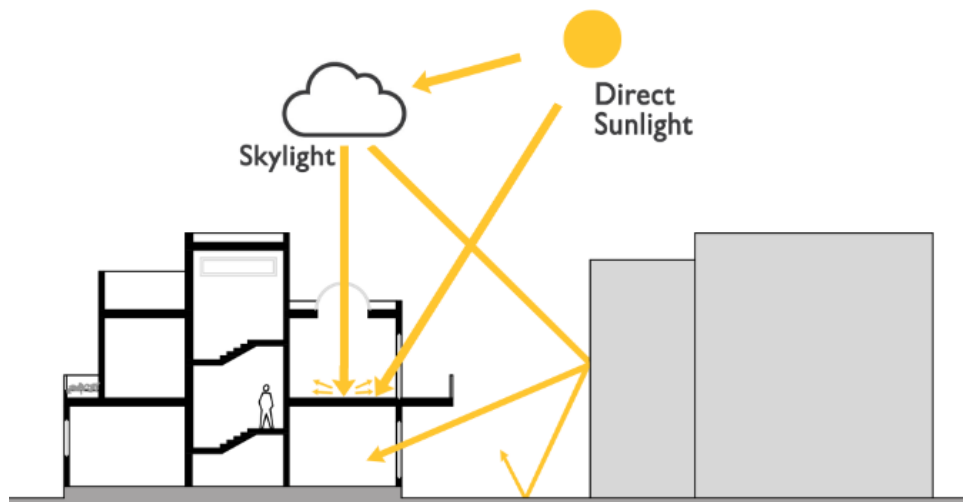
Figure 3-1 The components of daylight.

The lighting community has defined good daylighting as lighting quality which contains three primary categories:

A. **User's needs:** vision, connection with outside, performance, comfort, health, safety, communication, and aesthetic view.

B. **Architecture:** form, distribution, pattern, codes, and standards.

C. **Economics:** installation, maintenance, operating, energy use, and environment.

Therefore, architects and designers should recognise all the three previous categories for daylighting quality and be aware of the most important standards and essential requirements that help them obtain the appropriate daylight and admit it inside the buildings.

Also, they must consider five divisions of design goals to reach good daylighting with quality:

1. Create delight and comfort for the building's occupants.

2. Meet the requirements and needs of the building occupants.

3. Reduce building energy costs.

4. Improve the general architectural image.

5. Reduce the initial cost of constructing the building.

3.3 Heat Loss

The building's heat can be lost via conduction, convection, radiation, infiltration, and ventilation through ceilings, walls, floors, windows, and doors (Lechner, 2014); see Figure 3-2. Windows can be considered the most influential building component for heat gain or loss (Waheeb, 2006). The building window can allow beneficial sunlight, but it is a weak insulator and can cause a negative effect on building energy. Baker and Steemers (2005) said, "double glazing has a thermal conductance about five times that of a moderately insulated opaque wall". With the use of any element of shading, the thermal performance of the windows may be improved. The extent of the heat loss through the envelope depends on the room design, the temperature difference between inside and outside, and the envelope's thermal strength (Lechner, 2014). If the building can store heat gain during the day in the building's thermal mass, the glazing's overall energy balance can also be enhanced. The energy balance was defined by (Andersen et al., 2014) as "The balance between heat loss and solar gain for a window". Overall, elaborate design, shared walls, and strong resistance of insulators can minimize thermal loss. Rodrigues (2010) stated that "By slowly storing and releasing relatively large quantities of heat per unit volume, the thermal mass that is well implemented in a building can help to regulate the indoor temperature".
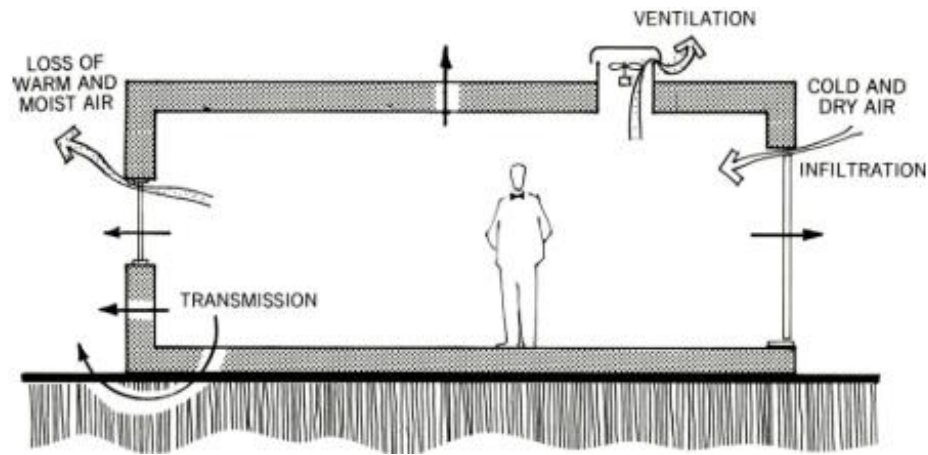
Figure 3-2 The flow of energy through a building and heat loss. Reproduced from (Lechner, 2014)

3.4 Heat Gain

The windows are closely related to solar gain due to receiving and admitting the sun's light quickly. The need to reduce active cooling systems and maximize the use of passive cooling and thus reduce energy dependence depends on how well the heat gain controls, the global radiation incidence rate (W/m^2), and the fenestration design. For example, direct solar light that falls on a window can generate about 0.5 kW/m^2 of heat into space (Baker and Steemers, 2005). Martin (1996) mentioned that the buildings' heat could be gained from different sources, through conduction via building fabric, air infiltration, heat gained from window panes, and interior gains such as lighting, equipment, and occupants.

In some design cases, adding solar gains from daylighting are desirable whereas in others, heat gain must be controlled. Ruck et al. (2000) said; "In passive systems as a function of solar architectural concepts, solar gains are controlled by the orientation and the application of shading the sun's position".

One of the primary considerations to be considered in the design is the building's direction or orientation. The greatest received amount of light from the sun is at noon on any day of a year, and this amount is received when the sun is vertically on windows (Robertson, 2003). The time and date of maximum received energy can be determined depending on the building's latitude and the wall orientation. If glass facades are needed in hot climates, their orientation should be north or east and facing west and south should be avoided if possible. Baker and Steemers (2005) stated that "Rooms facing west and south-west are particularly

vulnerable to overheating from solar gains". Fenestrations on a northern facade can provide indirect daylight with minimal heat gains and also lose heat and create comfort issues during the heating season.

In contrast, fenestrations on a southern facade can provide strong direct and indirect sunlight, but uncontrolled heat gain can be a problem during the cooling season.

When using glass windows, it is essential to know the solar heat gain coefficient (SHGC), a useful measure of a window's ability to admit solar energy. SHGC was defined by Energy (2020) as "the fraction of solar radiation admitted through a window, door, or skylight -- either transmitted directly and/or absorbed and subsequently released as heat inside a home". SHGC range between 0 to 1 where 0 indicates no solar gain "complete shading" and 1 indicates unrestrained solar gain "no shading" (Lechner, 2014). Table 3-1 shows different types of glazings and shading devices and the shading coefficient SC and SHGC. It should be noted that the SHGC was replaced the old SC, which was counter-intuitive because the SC of 0 means full shaded while 1 indicates no shading. It can be indicated that these horizontal overhangs SC range between 0.1 "excellent" and 0.7 "bad" (Lechner, 2014).

Table 3-1 Shading coefficients (SC) and solar heat gain coefficient (SHGC) for different shading devices. Amended from (Lechner, 2014)

Device	SC	SHGC
Single glazing		
Clear glass, 1/8 in (3 mm) thick	1.0	0.86
Clear glass, 1/4 in. (6 mm)	0.94	0.81
thick	0.6–0.8	0.5–0.7
Heat-absorbing or tinted	0.2–0.5	0.2–0.4
Reflective		
Double glazing	0.84	0.73
Clear	0.5–0.7	0.4–0.6
Bronze	0.6–0.8	0.5–0.7
Low-e clear	0.4–0.5	0.3–0.4
Spectrally selective	0.7–0.8	0.6–0.7
Triple-clear		
Interior shading		
Venetian blinds	0.4–0.7	
Roller shades	0.2–0.6	
Curtains	0.4–0.8	
External shading		
Eggcrate	0.1–0.3	
Horizontal overhang	0.1–0.6	
Vertical fins	0.1–0.7	
Trees	0.2–0.7	

The higher SHGC of the window will perform better as a solar collector. So, windows with a low SHGC decrease cooling loads by excluding solar energy. The pane is a sheet of glass in a window. When the number of glass layers increases, the amount of daylight transmitted through a windowpane will decrease. As a rule of thumb, double glazing with no coating will transmit about 80% of the light, while triple glazing with no coating will transmit around 70% of the light. Besides, coloured or coated glazing may reduce the visible transmittance of a windowpane to values as low as 20% and significantly modify the spectral quality of the transmitted light and the perception of surface colours in the interior (Andersen et al., 2014). Heating or cooling loads decrease depending on the daylighting efficiency. Generally, reducing cooling and heating loads is the goal of building design. Controlling solar gains from windows and facades has several ways. The most direct and effective way to reduce heat gain is to simultaneously control the shading system in both visual and thermal environments. Furthermore, advanced technologies such as assembly windows and double-skin facades will separate thermal and visual environments. Baker and Steemers(2005) classified three types of shading devices in terms of performance concerning ventilation and visibility: fixed overhang, louvres, and moveable blinds.

It is evident from Figure 3-3 that a fixed overhang may be considered the best in terms of ventilation and visibility, while louvres mode is the best in terms of privacy and effectively dealing with different sunlight angles falling on it.

As a result, it is essential to be careful when designing the building and its fabric and choose suitable control methods to reduce heat gain, especially in hot months, to minimise the consumption of cooling loads.

Louvres   Moveable Blind   Fixed Overhang
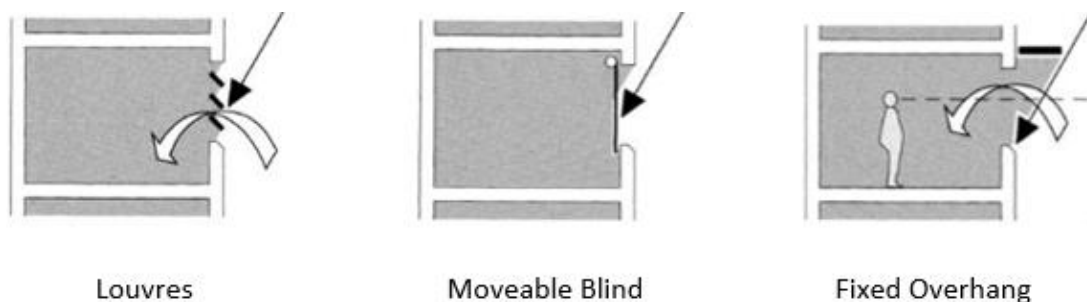
Figure 3-3 Effects of different shading devices on visibility and ventilation. Reproduced from (Baker and Steemers, 2005)

3.5 Ventilation

Ventilation is a sustainable strategy that can be the easiest and fastest way to refresh and replace the buildings' air and reduce buildings' energy loads. According to Martin (1996), "Approximately 30% of the energy delivered to buildings is dissipated in the departing ventilation and exfiltration air streams". So, ventilation helps to achieve and maintain good air quality and thermal comfort. In agreement with (Andersen et al., 2014), ventilation has important psychological aspects, illustrated by the feeling of being in control, having odour management and creating a link to nature, and the outdoor environment. Martin (1996) stated that ventilation is necessary to provide oxygen for metabolism, dilute metabolic pollutants and preserve good air quality indoors for occupants.

Good indoor air quality depends on air's purity from pollutants that cause occupants irritation, discomfort, or ill health (Andersen et al., 2014). In general, interior spaces vary in ventilation levels based on the room's function and occupants' needs. The quality of indoor air affects occupants in several aspects: comfort, health, and performance. To achieve acceptable IAQ, the three main ways are to gain minimise indoor emissions, keep the air dry, and ventilate well (Andersen et al., 2014). In our houses, three master systems can use to provide airflow; natural, mechanical or hybrid. Andersen et al. (2014) stated, " There are two ways to ventilate or cool buildings: actively or passively. Active ventilation/cooling refers to systems where mechanical components or other energy-consuming components (such as air-conditioning systems) are used. Passive ventilation/cooling is a technology or design feature used to ventilate/ cool buildings with no energy consumption (e.g. natural ventilation by openable windows)."

Passive cooling is a technique that uses natural sources with a non-reliance on the building's energy. It mainly concentrates on at least three concepts: solar shading, thermal mass, and ventilated cooling (Andersen et al., 2014).

Stavrakakis et al. (2009) stated that "Natural ventilation results from pressure differences between the indoor and the outdoor environment due to wind and buoyancy forces". Figure 3-4 illustrates the impact of height from the ground, where air velocities increase as the level rises. Also, the graph demonstrates pressure differences and shape effects on wind and

buoyancy forces. Natural ventilation employs natural energy "wind and temperature variations" to exchange the air in a building. In residential buildings, the airflow is often supplied through the side windows, then flows out and removed from selected rooms (often kitchen and bathrooms).

Further, windows must be finely adjustable to be efficient and give more impact. The design and technique of windows play a prominent role in levels of ventilation characteristics (Hausladen et al., 2008). Lechner (2014) said, "Cross ventilation is very effective because air is both pushed and pulled through the building by a positive pressure on the windward side and a negative pressure on the leeward side".
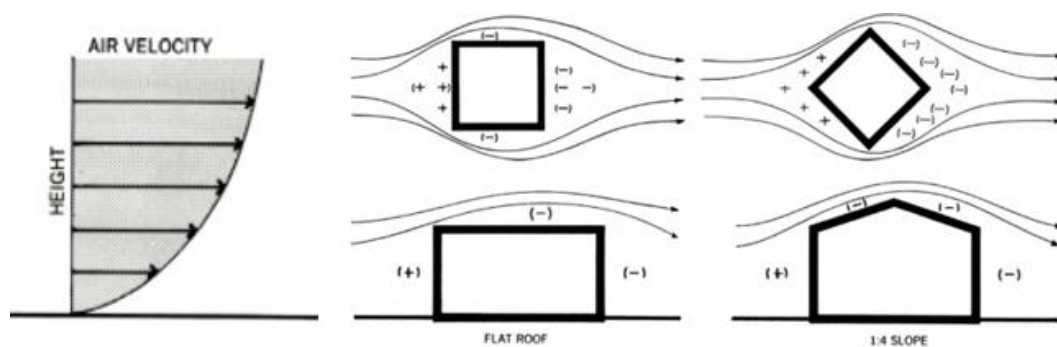
Figure 3-4 Airflow around building and pressure variations. Reproduced from (Lechner, 2014)

With the acceleration, development and technology in construction, mechanical ventilation has become one of the essential elements used in buildings to meet building users' comfort. Mechanical ventilation is a system that works by electric fans to ventilate the building. It can provide a stable air change rate separate from the external ambient conditions, but it cannot change the ventilation rate as the need changes over the day and year (Andersen et al., 2014). It is worth noting that this system negatively affects the environment in terms of energy consumption; in addition to that, if the filters are dirty and not changed, this will be a source of indoor air pollution and reduce the quality of indoor spaces, which affects the health and performance of occupants. According to Martin (1996), "The quantity of ventilation needed depends on the amount and nature of pollutant present in a space".

Another primary system that can be used for providing airflow is hybrid ventilation. This system integrates two ventilation systems: natural and mechanical ventilation. It is a new solution suitable for residential buildings, especially if roof or skylight windows facilitate the stack effect (Andersen et al., 2014).

3.6 Thermal Comfort

The building's design affects the comfort and health of occupants and energy efficiency. Therefore, architects must take into account all the influencing factors that contribute to achieving thermal comfort. Thermal comfort can be defined as "the condition of mind that expresses satisfaction with the thermal environment and is assessed by subjective evaluation" (ASHRAE, 2010b). By Autodesk (2014a), thermal comfort can be described as "the occupants' satisfaction with the surrounding thermal conditions and is essential to consider when designing a structure that people will occupy". Parsons (2014) stated, "An understanding of why a person reports thermal comfort (or discomfort) or related feelings of warmth, freshness, pleasure and so on, is complex and not known". However, thermal comfort is linked to the thermal balance between heat increase caused by the body's metabolism and heat losses to the environment (Baker and Steemers, 2005).

3.6.1 Thermal comfort factors and models

Thermal comfort is a condition that results from a combination of several factors that impact heat comfort by affecting the human body's heat dissipation (Kotbi, 2013). Several studies, such as Fanger and ASHRAE, have defined thermal comfort quality through many field measurements of both environmental and personal parameters (Elaiab, 2014). According to Autodesk (2014a), thermal comfort can be determined by the following factors:

1. Metabolic rate (met): The generated energy from a person body.

2. Clothing insulation (clo): Number and thickness of clothes the person is wearing.

3. Air temperature (TA): Temperature of the air surrounding the occupant.

4. Radiant temperature (TR): The weighted average of all the temperatures from different surfaces surrounding an occupant; walls, ceiling, floor and windows. (Andersen et al., 2014).

5. Air velocity (Av): Rate of air movement given distance over time.

6. Relative humidity (RH): Percentage of water vapour in the room air.

While thermal comfort was classified by Szokolay (2004) into three factors: 1) Environmental: air temperature, air movement, and relative humidity, 2) Personal: metabolic rate (activity),

clothing, health condition, acclimatization, and 3) Contributing: food and drink, body shape, subcutaneous fat, age and gender.

From an environmental engineering standpoint, a thermal environment surrounding a person could be classified into several layers according to the environmental control level (Nakano, 2003), as seen in Figure 3-5. Regarding the figure, the outdoor environment where no artificial adjustment is made, while the semi-outdoor environment is the layer between indoor and outdoor and is moderately controlled (Nakano, 2003).
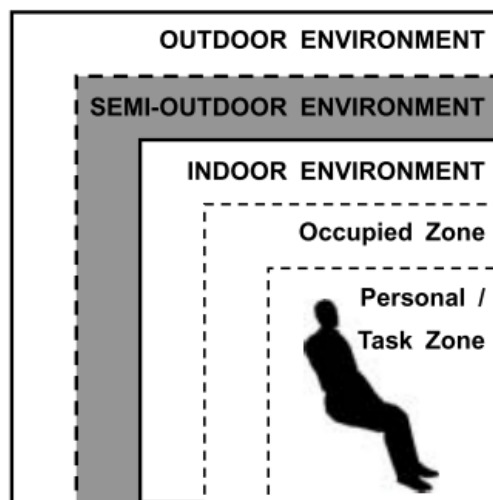
Figure 3-5 Thermal environment Layers surrounding an occupant. Reproduced from (Nakano, 2003)

Parsons (2014) mentioned that the four fundamental environmental variables affecting human response to thermal environments are air temperature, radiant temperature, humidity and air movement. The most important environmental variable is air temperature measured by dry bulb temperature (DBT).

The body's surface resistance (or clothing) is significantly decreased in the presence of air movement. The air movement velocity can affect the evaporation of moisture from the skin, thereby evaporative cooling impact. According to Szokolay (2004), subjective reactions from air movement and its effect on comfort can be described in Table 3-2. However, air velocity up to 2m/s may be desirable under hot conditions (Szokolay, 2004).

Table 3-2 Subjective reactions from different air velocities (Szokolay, 2004)

Sensation	Stuffy	unnoticed	pleasant	awareness	draughty	annoying
Air velocity (m/s)	<0.1	to 0.2	to 0.5	to 1	to 1.5	>1.5

Another primary factor that effect the evaporation ratio is humidity which can be measured by relative humidity (RH, %), absolute humidity or moisture content (AH, g/kg), or vapour pressure (p, in kPa) (Auliciems and Szokolay, 2007). The mean radiant temperature "MRT" can be defined by Martin (1996) as " a measure of the average radiation exchange between the occupant and the surrounding surfaces and is conventionally measured using a black globe thermometer to represent the occupant". It should be noted that the radiative exchange can be asymmetrical to no small extent since certain factors, such as hot windows, cause local discomfort by enhanced radiative heating. Daemei et al. (2019) mentioned that It is assumed indoors that the MRT is close to the dry-bulb temperature.

The comfort experts believe that when interior conditions in air-conditioned buildings deviate from their usual comfort zone, the occupants' condition is critical and hard to adapt to heat fluctuations (Santamouris, 2006). In contrast, people's thermal preferences in the non-air-conditioned buildings are usually broader and can adjust and customise to climatic fluctuations and thermal differences.

Due to thermal comfort variations between people in terms of their culture, season, health, fat a person carries, the clothes a person wears, and physical activity, there are no absolute limits to thermal comfort (Lechner, 2014).

Nicol and Humphreys (2002) stated that "Thermal comfort standards are required to help building designers to provide an indoor climate that building occupants will and thermally comfortable". However, one of the most critical tools for thermal performance assessment is the Psychrometric Chart in the engineering and architecture field. It is defined by Autodesk (2014b) as " " a graphical representation of the psychrometric processes of air. Psychrometric processes include physical and thermodynamic properties such as dry bulb temperature, wet bulb temperature, humidity, enthalpy, and air density" (Figure 3-6). Based on that, different zones of climate types can specify on the chart. The psychrometric chart is used by appointing multiple data points on the chart representing the air conditions at a particular moment. Then, the "comfort zone" is determined from the formatted area. The comfort zone is defined by Givoni (1992) as "The "comfort zone" is defined. as· the range of climatic conditions within which the majority of persons would not feel thermal discomfort, either of heat or of cold". According to Lechner (2014), environmental variables of air temperature,

relative humidity, air movement, and MRT lead to most people's thermal comfort. Placing the convenient combinations on a psychrometric chart determines an area known as the comfort zone, as shown below.
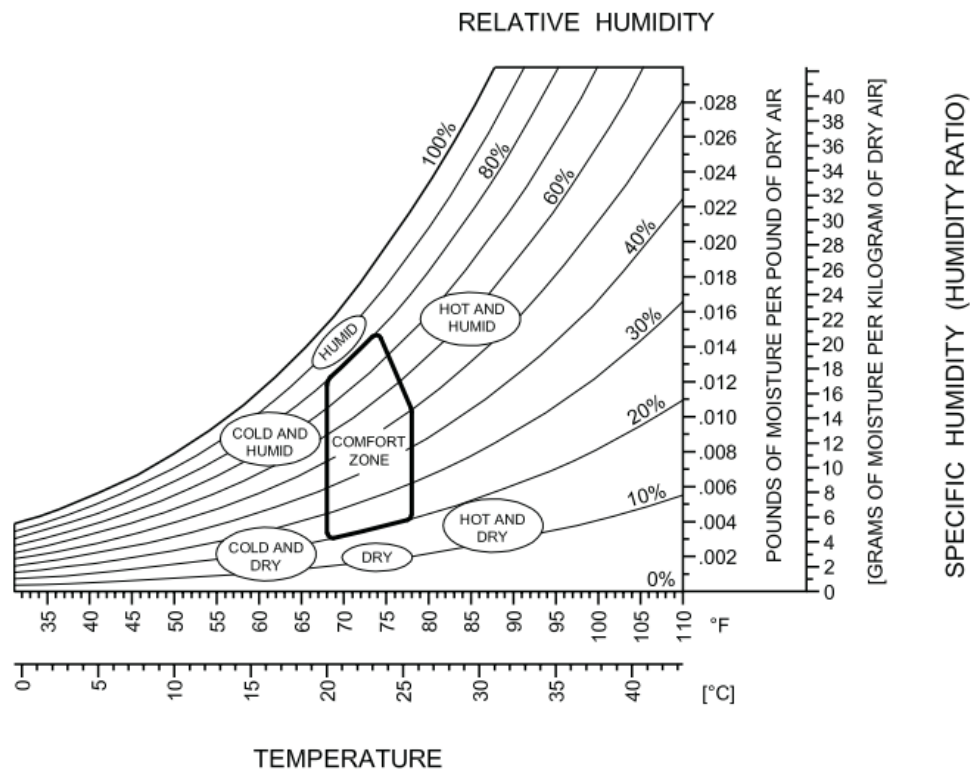
Figure 3-6 Different types of discomfort and the comfort zone. Reproduced from (Lechner, 2014)

ASHRAE (2010) states that several factors must be considered when assessing the thermal environment, including the location of the measurements, measurement periods, and measuring conditions. Measurements should be made in areas where occupants are working or expected to spend time working or sitting. For unoccupied rooms, measurements should be conducted based on the best estimate of the most used places and occupancy levels. However, if the occupancy distribution cannot be estimated, the measurement locations must be either in the centre of the room or at a one-meter distance from the largest window in rooms with windows. Air temperature and air velocity should be measured at levels of 0.1, 0.6, and 1.1m, according to ASHRAE (2010). Standing activity should be measured at 0.1, 1.1, and 1.7m, while seated occupants should be measured at 0.6 meters.

Two types can be classified as thermal comfort models: standard and adaptive (Murali, 2013). Standard models are founded on the body's heat balance and are based on a uniform thermal environment. A popular example is the predicted mean value (PMV) model developed by

Fanger (1972). Daemei et al. (2019) said, "The zone in which most people are comfortable is calculated using the PMV model".

In buildings, the thermal design should aim at the comfort zone, as 80% of the residents are satisfied with these conditions. Based on PMV-PPD, 10% is dependent on a general thermal comfort criterion (the entire body), plus an average of 10% due to local thermal discomfort (partial body) (ASHRAE, 2010b). Predicted Percentage of Dissatisfied (PPD) is defined by ASHRAE (2010b) as "an index that establishes a quantitative prediction of the percentage of thermally dissatisfied people determined from PMV. While PMV was defined by ASHRAE (2010b) as " an index that predicts the mean value of the votes of a large group of persons on the seven point thermal sensation scale".

Fanger (1970) has identified the link between the PMV index and a predicted dissatisfied percentage (PPD), as shown in Figure 3-7, through steady-state investigations. The graph shows the symmetry around the PMV of 0, where the complaints on the right "hot" side are the same as the "cold" left side. Peeters et al. (2009) said, "At the optimal condition, there is thus a balance between those sensing uncomfortably warm and those sensing uncomfortably cold". A deviation from 0 would mean an increasing percentage of dissatisfaction and an asymmetric distribution between who feels warmth and cold (Peeters et al., 2009).
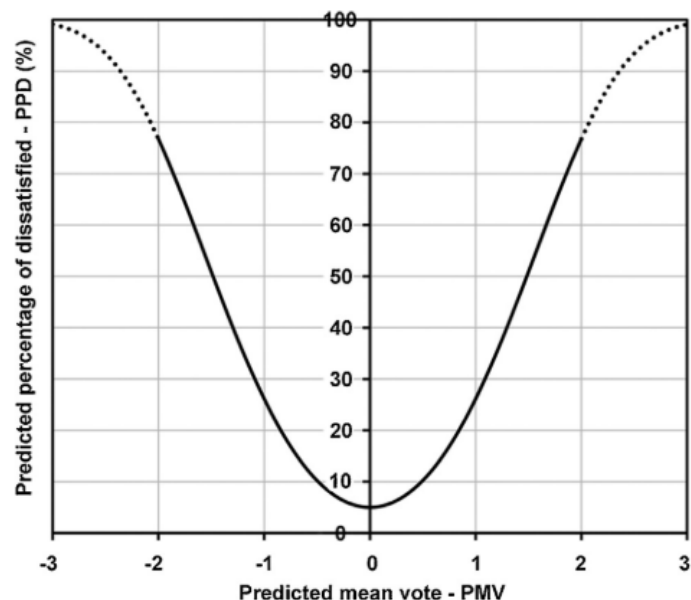
Figure 3-7 Predicted percentage of dissatisfied (PPD) as a function of the predicted mean vote (PMV). Reproduced from (Peeters et al., 2009)

According to ASHRAE (2010b), an adaptive model was defined as "a model that relates indoor design temperatures or acceptable temperature ranges to outdoor meteorological or climatological parameters". Yun (2018) stated that the adaptive comfort models originated from a black-box approach and linked the optimal indoor operating temperature to outdoor air temperature (To), by linear regression analysis with the optimum operating temperature indoor as Tc = To+b. van der Linden et al. (2006) said: "When applying models of adaptive thermal comfort, one should distinguish between different types of buildings, usage and climatic circumstances". People's natural inclination to adapt to changing conditions of their environment is expressed by the adaptive thermal comfort approach (Nicol and Humphreys, 2002).

Figure 3-8 shows an optional ASHRAE method, which can be used to determine acceptable thermal conditions in natural passive buildings. In these buildings, users can essentially regulate space's thermal conditions by opening or closing the windows. An adaptive approach to thermal comfort is based on simultaneous field surveys of people's thermal environment and thermal comfort during their daily lives in buildings (Nicol and Humphreys, 2002). This thermal comfort adaptive model was derived from a global database of 21,000 thermal measurements in office buildings. This method is confined to average outdoor temperatures between 10 and 33.5 degrees to give operating temperature limits above 17 degrees and less than 31°C. In this method, local thermal disturbance effects in buildings were not considered, nor were particular humidity or air velocity ratios specified. Besides, it is not necessary to estimate the clothing values of the space. The natural adaptation of people's clothes has been considered by linking the acceptable range of indoor temperatures to the outdoor climate. Figure 3-8 displays two groups, the grey shaded group representing 90%, the highest percentage in achieving acceptable temperature, while the acceptable limits for the second group, coloured in blue, represent 80%.

de Dear and Brager (2002) stated, "People who live or work in naturally ventilated buildings where they can open windows, become used to thermal diversity that reflects local patterns of daily and seasonal climate variability. Their thermal perceptions—both preferences as well as tolerances—are likely to extend over a wider range of temperatures than are currently reflected in the old ASHRAE Standard 55 comfort zone."
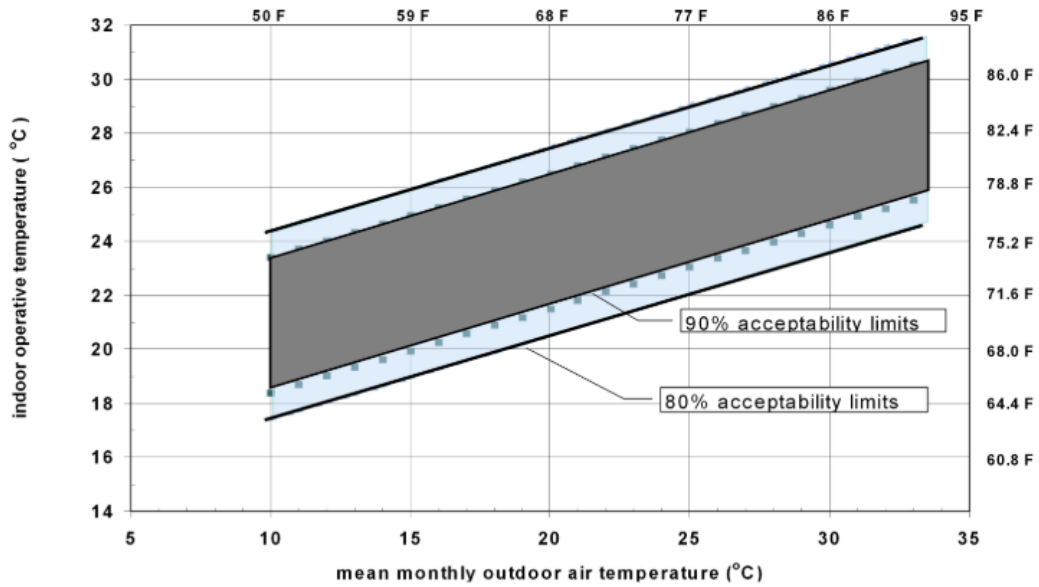
Figure 3-8 Acceptable operating temperatures for natural spaces. Reproduced from (ASHRAE, 2010b)

Another assessment used to determine the comfort temperature is the equation of Nicol and Humphreys (2002), as shown below:

$$T_c = 13.5 + 0.54 \ T_o \qquad (3.3)$$

where Tc is the comfort temperature, and To is the monthly outdoor air temperature average. This equation was derived from data field measurements of thermal comfort of more than 20,000 buildings, most of which are office worker measurements. The data used regression analysis to estimate neutral temperatures in terms of the operative temperature, the mean of the air temperature and the radiant temperature (Humphreys and Nicol, 2000).

Another method to assess the indoor comfort temperature in free-running buildings is by using the (de Dear and Brager, 2002) equation.

$$T_c = 0.31 \ T_o + 17.8 \qquad (3.4)$$

It is worth pointing out that Pakistani participants felt comfortable at indoor temperatures around 33 °C in the Nicol and Humphrey field study. The study also stated that the workers changed their clothing and used fans during the tests. Nicol and Humphreys (2002) mentioned that if no clothes or activity can be changed and air movement cannot be used, the comfort zone may be extended ±2°C. The comfort zone can also be more extensive in which these adaptive possibilities are available and suitable.

Although traditional buildings often achieve comfort without using a mechanical system, these levels do not meet today's expectations (Lotfabadi and Hançer, 2019). Nicol and Humphreys (2002) said: "People have a natural tendency to adapt to changing conditions in their environment. This natural tendency is expressed in the adaptive approach to thermal comfort".

Some studies have shown the advantage of individual thermal control systems through windows, major air-conditioning systems, or other buildings' methods. Hawkes (1982) found that energy efficiency improved when people could control their environment because their use was more consistent with their needs. Wilson and Hedge (1987) have found that the level of individual control perceived has reduced the symptoms of building-related health and increased productivity. de Dear and Brager (2002) mentioned that, although personal control is essential, further investigation is necessary to understand its impact on occupants' comfort, health, and productivity.

According to Kiamba (2016), it is recommended that the comfort zone be specified using the PMV model in air-conditioned buildings where conditions can be more controlled, while the adaptive comfort model is recommended in free-running buildings.

The human body continually generates heat from two types: biological metabolism and muscle-metabolism during work (Auliciems and Szokolay, 2007). Table 3-3 presents specific typical metabolic rates that can be expressed as a density of power (W), per body area (W/m²) or in a unit intended for thermal comfort subjects called the met where 1 meter = 58.2 W/m² (Auliciems and Szokolay, 2007).

Table 3-3 Metabolic rates at different activities. Reproduced from (Auliciems and Szokolay, 2007)

Activity	met	W/m²
Sleeping	0.7	40
Reclining, lying in bed	0.8	46
Seated, at rest	1.0	58
Standing, sedentary work	1.2	70
Very light work (shopping, cooking, light industry)	1.6	93
Medium light work (house~, machine tool ~)	2.0	116
Steady medium work (jackhammer, social dancing)	3.0	175
Heavy work (sawing, planting by hand, tennis) up to	6.0	350
Very heavy work (squash, furnace work) up to	7.0	410

Several thermal comfort scales can be used to assess the body's thermal sensation, comfort, and discomfort conditions, as shown in Table 3-4. It can be seen that most of these scales are based on a scale from +5 to -4 described with thermal sensation expressions. Markus et al. (1980) define the neutral temperature as "the state that in which people will judge the environment they stay neither too cold nor too warm, it is a kind of neutral point defined by the absence of any feeling of discomfort".

Table 3-4 Thermal sensation scales and expressions. Reproduced from (Rosenlund, 2000)

	ASHRAE	Fanger (PMV)	Rohles & Nevins	Gagge's DISC	SET (°C)
Painful			+5	+5	
Very hot			+4	+4	37.5 -
Hot	7	+3	+3	+3	34.5 - 37.5
Warm	6	+2	+2	+2	30.0 - 34.5
Slightly warm	5	+1	+1	+1	25.6 - 30.0
Neutral	4	0	0	±0.5	22.2 - 25.6
Slightly cool	3	−1	−1	−1	17.5 - 22.2
Cool	2	−2	−2	−2	14.5 - 17.5
Cold	1	−3	−3	−3	10.0 - 14.5
Very cold			−4	−4	

To make the indoor environment comfortable and more sustainable, the design should follow three stages: 1) reducing the heat flow through the building envelope, 2) passive systems, then 3) using a mechanical system (Lechner, 2014). As mentioned by ASHRAE (2010b), field experiments have shown that the thermal responses of occupants in natural buildings differ mainly from thermal responses in buildings with HVAC systems and are partly dependent on the external climate, due to different thermal experiments, changes in clothing, availability of control and, expectations of occupants. In addition to thermal comfort standards and models, some widespread and computational methods, such as computational fluid dynamics (CFD) can be used to analyze and quantify comfort depending on the building's envelope and conditions (Tap et al., 2011).

3.6.2 Adaptive Comfort Strategies Used in Hot Climates

Since residential thermal comfort is considered crucial, this can become a problem in many modern residential buildings, mainly when the cooling systems or passive strategies are not provided in hot and humid environments (Tap et al., 2011). It was mentioned by Shahzad et

al. (2020) that a large portion of energy use is consumed globally to keep the indoor air temperature of buildings within the required comfort temperature. Most residential buildings in Saudi Arabia mainly use air conditioners to provide comfort, whereas this consumes 50% of the total generated energy (SEEC, 2019). Besides, the lack of optimal utilisation of natural resources such as daylight and ventilation contributes to high energy consumption. It was noticed by CATE 19 (2019) that these energy consumption levels emphasize that saving energy strategies in buildings need to be integrated.

In general, most traditional buildings could provide better indoor comfort than modern buildings that use mechanical systems for cooling or heating (Shaeri et al., 2018). Different passive cooling methods were designed and used in traditional buildings, such as the adaptive thermal mass, and natural ventilation to provide comfort.

3.6.2.1 Thermal mass

Thermal mass was defined by Baker and Steemers (2005) as the material of the building which absorbs or releases heat from or to the interior space. Figure 3-9 illustrates the advantage of using high thermal mass compared to low thermal mass and the effect range of thermal mass stability on internal temperature. When the building has adequate thermal mass and thermal resistance, it can sustain daytime temperatures below the outdoor temperature and protects it from absorbed heat and penetrating sunlight (Givoni, 1992). The high thermal mass delays the transmit heat through walls and performs as a heat sink throughout the day (Lechner, 2014). One of the critical materials for enhancing thermal mass in modern buildings is thermal insulation. According to SEEC (2019), most Saudi Arabia buildings lack thermal insulation, which contributes significantly to increased energy consumption.

Moreover, thermal insulation can significantly reduce energy consumption by up to 40% (SEEC, 2019). It should be noted that both insulators and thermal mass are required and should be used as a combination to improve the building envelope energy efficiency (Saulles, 2015). According to Elaiab (2014), thermal mass capacity's thermal insulation application provides extremely robust control over the timing of heat input, particularly in climates with significant daily temperature fluctuations. The excess heat can be stored at once and then released at another time.

Thermal energy storage has a strong impact and relationship with the building structure and building materials quality as the utilization of materials with a high thermal mass, such as bricks, stone, or adobe, can significantly relieve daily variations in temperatures (Kienzl, 1999).
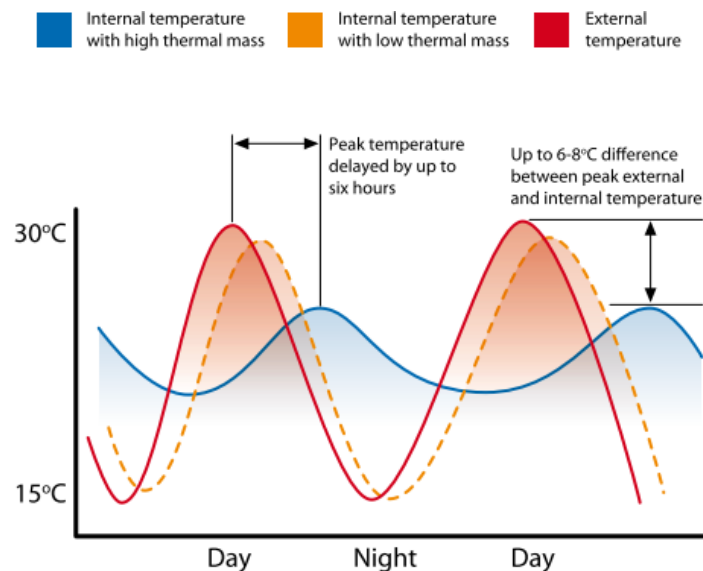
Figure 3-9 Stabilising effect of thermal mass on indoor temperature. Reproduced from (Saulles, 2015)

Saulles (2015) mentioned that a combination of three basic properties is required to provide the material with a suitable thermal mass: a high specific heat capacity, a high density, and moderate thermal conductivity. Moreover, there are two main parameters we must know related to thermal mass; thermal storage capacity and thermal diffusiveness of the used construction material. Thermal storage capacity is defined by Kienzl (1999) as "the product of the materials density, specific heat and conductivity and determines the amount of energy that can be stored within a given volume of material". Thermal diffusivity is defined by Kienzl (1999) as "the conductivity divided by the product of density and specific heat and determines the speed by which heat travels through a material and thus how fast a material reacts to temperature changes".

Table 3-5 presents some common materials in buildings and their thermal properties. To provide a beneficial thermal mass in the buildings, the construction materials should be characterized by high specific heat capacity, high density, and moderate thermal conductivity (Saulles, 2015). such as brick, stone and concrete (see Table 3-5). From the table, timber and steel have low thermal mass, whilst precast, brick, and sandstone have a high thermal

mass that allow the heat to transfer between the material's surface and its inner at a rate corresponding to the daily heating and cooling cycle of buildings (Saulles, 2015). Timber has the highest specific heat capacity among the materials in the table, which means it can store more heat per kg, whereas its thermal conductivity is relatively low due to its porosity. In contrast to timber, steel has high thermal conductivity where it absorbs and releases heat too rapidly, inconsistent with the building's natural heat flow.

Table 3-5 Thermal properties of common construction materials. Reproduced from (Saulles, 2015)

Building material	Specific heat capacity (J/kg.K)	Density (kg/m3)	Thermal conductivity (W/m.K)	Effective thermal mass
Timber	1600	500	0.13	Low
Steel	450	7800	50	Low
Lightweight aggregate block	1000	1400	0.57	Medium-high
Precast and in-situ concrete	1000	2300	1.75	High
Brick	1000	1750	0.77	High
Sandstone	1000	2300	1.8	High

In passive buildings, the entire interior mass should be equally exposed to the night ventilation in summer and direct sunlight in winter (Meir and Roaf, 2002). Figure 3-10 present different thermal mass types besides night ventilation and their impact on the indoor temperature. For example, the temperature can increase by about five °C when using a lightweight mass without ventilation than a heavyweight mass with night ventilation.
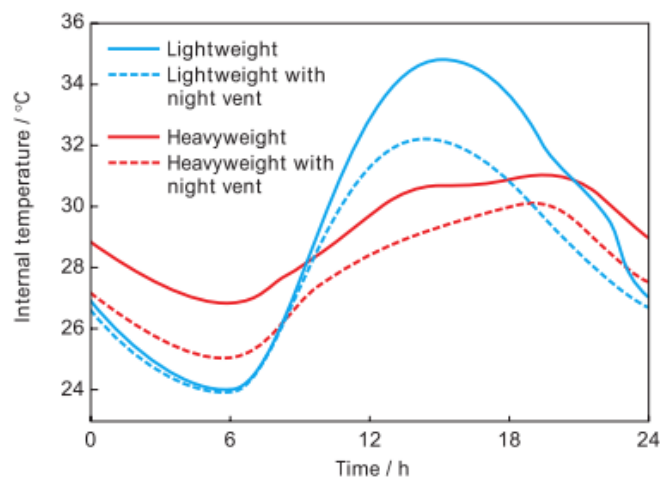
Figure 3-10 Thermal mass and ventilation impact on indoor temperature peak. Reproduced from (Irving and Clements-Croome, 2005)

Ajaj and Pugnaloni (2014) mentioned that traditional buildings were mainly constructed with local materials suitably adapted to climate conditions, providing a comfortable and natural

passive indoor environment. These buildings were compliant with one of the Islamic principles to preserve the environment, as they used thick heat-insulating walls and energy-saving and environmentally sustainable materials; recyclable and reusable (Ajaj and Pugnaloni, 2014). In summary, the thermal storage efficiency relies on various parameters such as material characteristics, surface exposition, thickness, and position and orientation of the building's storage elements (Elaiab, 2014). Therefore, in areas where there is a large change between periodic temperatures, it is advisable to build the heavy wall with adequate thermal mass, with a low surface absorption as much as possible, as this may lead to high energy savings that may reach 95% (Al-Sanea et al., 2013).

3.6.2.2 Ventilation

Natural ventilation is one of the recommended natural passive cooling approaches for hot-arid climates (Al-Hemiddi and Megren Al-Saud, 2001). This strategy is used to conserve the energy of buildings while maintaining adequate thermal comfort for occupants. It is worth noting that active ventilation contributes mainly to increasing the building energy demand. Therefore, Martin (1996) recommended relying on various energy-saving ventilation technologies where the most important described are; minimising the need for ventilation, avoiding uncontrolled air infiltration losses, and providing efficient ventilation. Efficient natural ventilation design allows adjusting occupants' situations to the changing conditions in a so-called adaptive way (Irving and Clements-Croome, 2005). According to Irving and Clements-Croome (2005), this can include the use of fixed or moving shades to eliminate direct solar radiation and enhance air movement by opening windows or using desk fans. In the vernacular architecture at hot climate, several elements were designed and used to allow air movement and circulation inside the buildings as wind towers, courtyard, and mashrabiya. According to Vefik Alp (1991), "The wind tower, or "wind catcher" harnesses the prevailing summer wind to cool it down and circulate it through the building. While one end of the tower rises from the roof, the other end goes down to the basement". The air tower's orifice usually extends a few meters above the building and faces and open to the wind (Maghrabi, 2000). In Saudi Arabia, the wind towers' forms and designs differ in several aspects: height, airway division, location and number of openings, and position of the tower concerning the building and materials (Vefik Alp, 1991).

The courtyard has proven to be one of the significant elements in response to hot dry climates, as it helps to moderate the indoor thermal environment, ventilate the spaces, and provide shading and privacy for occupants. There are two types of courtyards in Islamic architecture: an internal or an atrium-shaped courtyard surrounded by rooms; and an exterior courtyard, not surrounded by rooms but adjacent to the building. The hot climate buildings can benefit from a courtyard that admits the night air and cool spaces until mid-afternoon, while plants protect patio walls against direct solar heat gain (Vefik Alp, 1991). Moreover, courtyard filters dust and sand by utilizing water or water puddles (Vefik Alp, 1991). Another architectural element that was employed and used effectively and widely in hot climates is mashrabiya. Bagasi et al. (2021) defined mashrabiya as "a wooden frame covering a window opening and decorating the building façade". Mashrabiyas are traditionally characterised by their functions, allowing air and daylight to penetrate and providing privacy beside the aesthetic purpose. Ventilation at night through a mashrabiya can minimise the cooling load in buildings (Daemei et al., 2019). The technique "Night-flush cooling" uses cool night air to flow out the building's temperature through windows or openings while very little outside air is being brought indoors during the day to minimize the heat gain in the building (Lechner, 2014). Although night ventilation can significantly reduce the length and duration of time for the need for additional cooling systems. Lechner (2014) said, "when the indoor air temperature has risen above the comfort zone, internal circulating fans are required to maintain comfort for additional hours". Whereas, Givoni (1992) stated that "In desert regions with daytime temperatures above 36 C, night ventilation alone would not maintain the indoor daytime temperature at an acceptable level and other passive cooling systems should be applied during the hot hours, such as evaporative cooling".

3.6.2.3 Evaporative Cooling

Evaporative cooling is defined by Amer et al. (2015) as "a heat and mass transfer process that uses water evaporation for air cooling, in which a large amount of heat is transferred from air to water, and consequently, the air temperature decreases". This method is considered to be highly effective in hot, dry regions, as its performance improves and improves with increasing air temperature and low humidity. However, it can be used in humid regions by incorporating suitable drying media (Misra and Ghosh, 2018).

The strategy of water evaporation in terms of energy can be used in two different ways to cool buildings which were described by Givoni (1992) as the following:

1- Direct evaporation cooling DEC: Water is sprayed into the air entering a building, lowering the air's temperature and raising its humidity.

2- Indirect evaporative cooling IDEC: Evaporation cools the incoming air into a building without raising the indoor humidity. Alternatively, water is sprayed on the roof to cool it.

Referring to the past, the vernacular buildings in the hot regions have shown an intimate connection with the local environment and responded to multiple factors such as climate conditions and inhabitants' comfort and needs. Furthermore, passive evaporative cooling technique has been used and incorporated into most of these elements. In Saudi Arabia, traditional buildings have used different passive strategies to cool the incoming airflow into buildings by evaporative, such as wind towers and mashrabiya. A wind tower or windcatcher is a passive cooling and ventilation component designed to harness wind potential and humidify incoming air before entering a building's spaces. It may have some shutters on the top to prevent undesirable ventilation. Air towers are typically designed as a square, rectangular or three-dimensional shape and located either on or beside a building roof or as a single structure connected to the building (Kleiven, 2003). Some wind towers have porous water jars at their base, while others use fountains or water (Lechner, 2014).

Mashrabiya was described by Fathy (1986) as a space covered in cantilevers by a wooden grid, in which small jars of water were positioned to cool the air by the evaporation effects through openings. Evaporation occurs from porous jugs of water placed in the mashrabiya, which cool the jugs of water and inside the building as well, and wherever the humidity is low, evaporative cooling is more effective (Lechner, 2014).

Although evaporative cooling is one of the primary effective passive cooling strategies, it increases moisture, decreases the dry bulb temperature inside the enclosed spaces, and converts the sensible heat into latent heat (Szokolay, 2004). Therefore, the typical humidity level in a regular room should be maintained between 40 and 60 %, while higher than that may affect the occupants' comfort and health.

3.6.3 Passive Evaporative Cooling Techniques for Comfort

Passive evaporation techniques depend mainly on increasing humidity to reduce the air temperature, and therefore an increase in humidity above the acceptable limit may cause potential discomfort to the building occupants (Sajjad et al., 2021). However, integrating different passive evaporative techniques to architectural elements such as wind towers and mashrabiya in hot climates provided or improved thermal comfort for occupants (Amer, 2017). The traditional Mashrabiya has been associated with evaporative cooling through porous water jars "pots" built into them.

Evaporative cooling in the mashrabiya was conducted by placing porous water jars in front of the mashrabiya, where the airflow passes through pores while small portions of water evaporate from the surface of the jars, which led to lowering the temperature of the air passing through it, as shown in Figure 3-11. This traditional method was used to cool the water of the jar for drinking and help provide a better indoor temperature.

Samuels (2011) said, "If this process is provided for effectively, it can dramatically cool the air that enters the room and make it far more comfortable". However, to obtain a more effective impact on the evaporative cooling process, it is preferable to have high air speed with considering the maximum of about one m/s for human comfort, while taking into consideration the air velocity here depends on the sizing and porosity of the mashrabiya (Samuels, 2011).
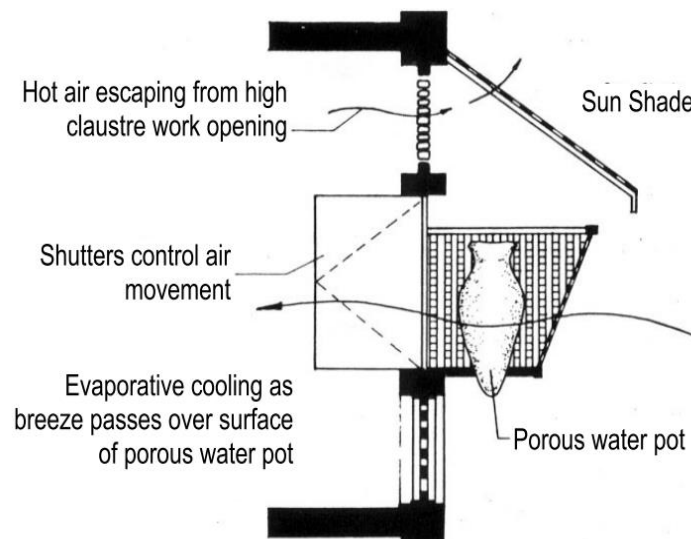
Figure 3-11 The evaporative cooling technique for a traditional mashrabiya integrated with a water Jar (Cain et al., 1976)

Porous water pots and water chutes have also been integrated into wind towers or wind catchers as passive evaporative cooling techniques that were commonly utilised in Middle Eastern and North African vernacular architecture (ElSoudani, 2016). As seen in Figure 3-12, the wind tower catches oncoming wind from the upper opening, and then the captured air passes through porous water jars, which sweat moisture (Vefik Alp, 1991). The water jars increase the humidity and hence cool down the passing air and flow it down and circulate it through the building. As the air enters the building spaces, a pond of water and maybe a fountain at the base cools the air further through evaporation.
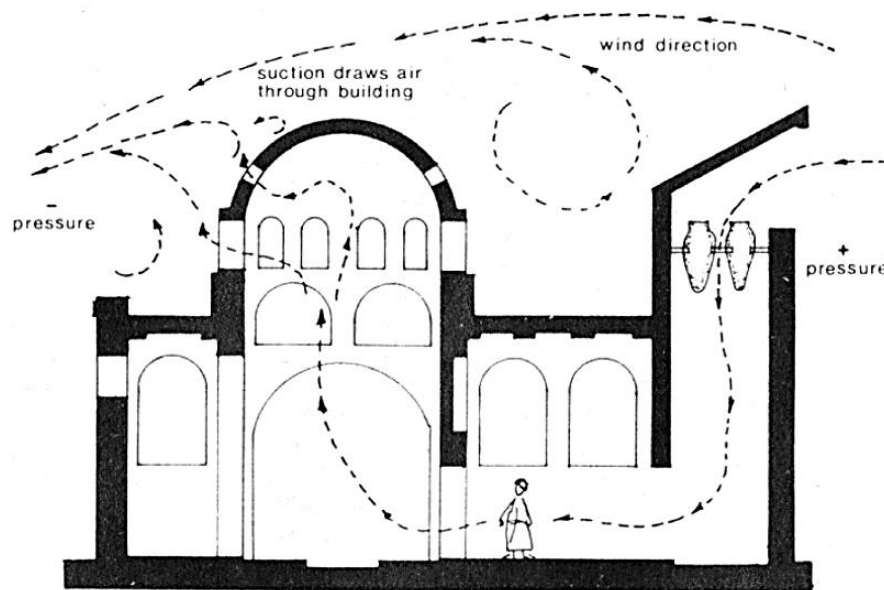
Figure 3-12 Airflow movement in a traditional building with wind catchers integrated with water pots (Cain et al., 1976)

In the last decades, several studies have been conducted to improve the cooling performance of buildings in the hot climates throughout integrated different passive evaporative cooling means with mashrabiya or wind towers. In 2010, Schiano-Phan proposed an evaporative cooling system that was derived from the mashrabiya concept using a porous ceramic medium called "Evapco system" developed by Cain et al. (1976). The study demonstrated that the system could save for the selected apartments around 3.08 MWh compared to air conditioning. Samuels (2011) proposed a new concept for a mashrabiya. The lattice screen of mashrabiya has been integrated with a water spray device for cooling the indoor spaces of a case study in the Gibson Desert of Australia. More studies about the mashrabiya and its developments will be presented and discussed in the next chapter in section 4.7.

Despite the role of wind towers in ventilation, their ability in cooling buildings is limited and providing thermal comfort standards for occupants can not be achieved (Morales et al., 2021). Therefore, some researchers have proposed novel techniques such as water-droplet spray and water wet curtains integrated into a wind tower to improve cooling performance and comfort. Bahadori et al. (2008) tested wetted curtains hung in a wind tower column in a hot climate and found that this technique performed better than the traditional wind tower and can significantly save the electrical energy consumed for summer cooling of buildings. Morales et al. (2021) stated, "Water-droplet spray can reduce the air-stream temperature at the air-inlet section to increase wind-tower effectiveness". As shown in Figure 3-13, when air enters the top opening of the tower, it is cooled, becomes denser due to the water spray, then falls and replace the hot air inside the building with cooler air (Lechner, 2014).
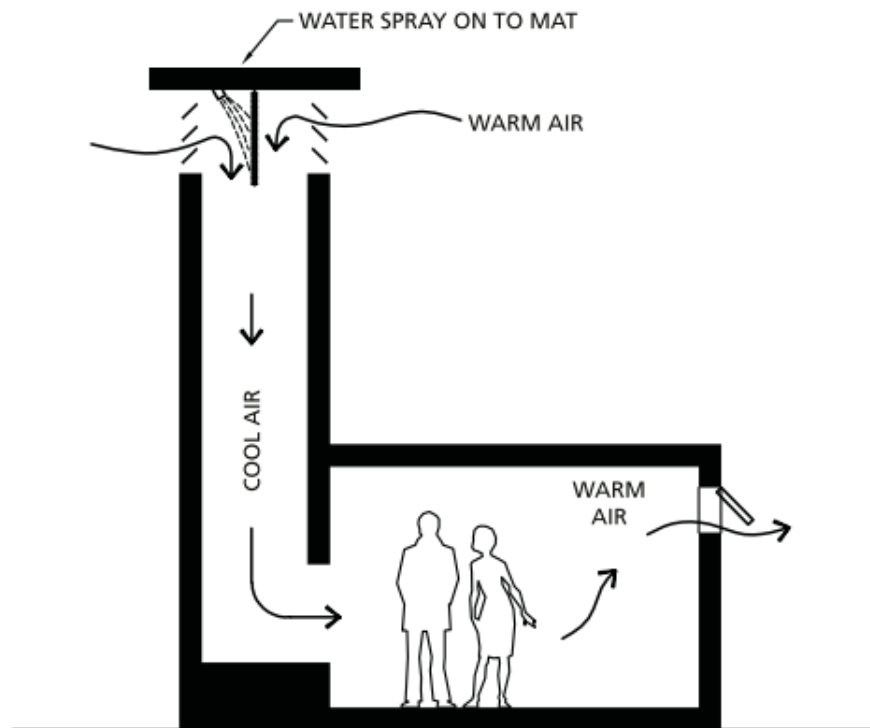
Figure 3-13 Water-droplet spray integrated into a wind tower (Lechner, 2014)

3.6.4 Thermal Comfort and Residential Buildings in Jeddah

Figure 3-14 illustrates the entire year of average temperatures showing the comfort level for each month in hours. From the graph, the best months that achieve the highest comfort levels are January, February, March, and December, where the comfort hours range between 9 and 12 hours. The comfort periods cover some hours from early morning to about 11 am then

after about 9 pm. Depending on Jeddah's climate and the standards and studies mentioned previously in Section 3.6.1, the warm zone ranges between 25 and 29 can also be considered within the comfort zone, and thus this includes January and most of February and December. On the other hand, May to October is considered beyond the comfort zone except for a few hours during the morning. Said and Al-Zaharnah (1994) said, "The thermal discomfort accounts for 61% of the total hours. The 42% of this which is considered hot requires mechanical means of active cooling".
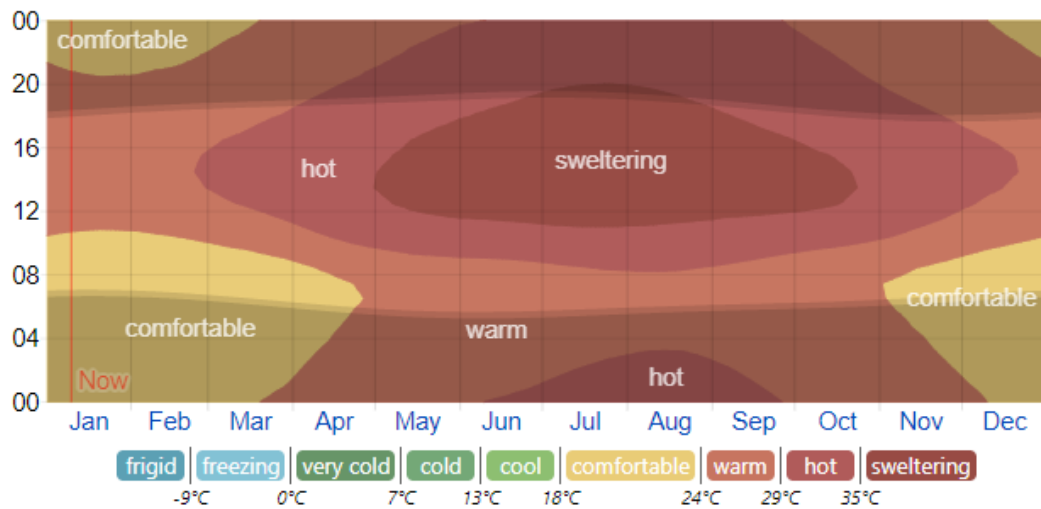
Figure 3-14 The average hourly temperature for the entire year for Jeddah and the shaded overlays indicate night and day (Spark, 2022)

Therefore, Said and Al-Zaharnah (1994) recommended several considerations and treatments in such this climate, which can be summarized as follows:

- Air conditioners should be used from May to October, particularly in the evening when other systems such as fans are ineffective.

- As a low-cost alternative, it is recommended to use fans to ventilate and circulate indoor air during harsh conditions when it is difficult to benefit from the natural ventilation where the outdoor temperature is high and the potential for dust and sandstorms.

- -Buildings should be protected by window screens, vegetation or no openings from the strong north and northwest winds.

- A building should be ventilated between 6 am and 8 am during the warm season, reducing ventilation during the remainder of the time.

- Facades and windows must be designed not to be exposed to direct sunlight during the hot period, especially on southern façades.
- Courtyard width should be designed the same as the building's height to ensure efficient shading inside a building.

Referring to the past, the vernacular buildings in the Gulf regions have shown an intimate connection with the local environment and responded to multiple factors such as climate conditions and inhabitants' comfort and needs (Oliver, 2006). In the traditional buildings of Jeddah, many architectural elements have been used as treatments and climate solutions to improve the feeling of comfort and improve the thermal performance of the building, such as mashrabiyas and heavyweight mass. Mashrabiya plays an essential role in enhancing thermal efficiency in hot climates alongside the thermal mass's role. Mashrabiyas are traditionally characterised by their functions, allowing air and daylight to penetrate and providing privacy besides the aesthetic purpose. The next chapter will cover several aspects of mashrabiya including the concept, history, functions, mashrabiya globally, and some previous studies and applications.

3.7 Conclusion

This chapter reviews one of the main components of buildings, the "building envelope", which plays an essential function in providing comfort to building occupants, increasing energy efficiency, and connecting the interior and exterior. Besides, protect the indoors from unwanted climatic influences, such as hot and cold weather, dusty winds, direct sunlight in summer, and noise. It is necessary to provide comfort for occupants and prevent or limit the heat entering the building, especially in hot climates, via building envelope and integrating negative or positive systems or all. However, the building envelope should be designed taking advantage of desirable and beneficial outdoor influences, such as daylight or solar radiation in winter or natural ventilation. Globally, a large portion of the energy is consumed to maintain indoor air temperature within the required comfort temperature. In Saudi Arabia, about 50% of building energy is consumed in cooling loads to reach users' comfort, and this is due to several reasons where the most prominent of which is the lack of use or weak thermal insulation in addition to the effect of using glass windows, which represent an additional heat burden on the buildings. That confirms the need to reduce consumption through more in-depth studies of methods and strategies to reduce this consumption while meeting building occupants' comfort needs. Most traditional Saudi buildings have adapted to climatic conditions and provide indoor comfort in a sustainable and environmentally better manner than modern buildings that use mechanical cooling systems as the primary method to achieve comfort. Generally, traditional buildings could make optimum solutions for utilising ventilation and natural lighting by incorporating many different passive elements, such as mashrabiya, courtyard, and wind tower. Therefore, architects must be aware of all influencing factors that may increase heat gain in the building and try to take advantage of sustainable passive methods to reduce energy waste while keeping in mind thermal comfort. Since mashrabiya is considered one of the traditional architectural elements in Saudi Arabia, which was representing the main element to cover openings such as windows in modern buildings, it is a traditional architectural element that performs many practical functions. Therefore, studying mashrabiya in depth and trying to develop it and integrate it into modern buildings may solve part of the problem of heat gain and energy consumption.

CHAPTER 4

Mashrabiya

What is Mashrabiya?
History of Mashrabiya
Design and Structure details
Functions & Characteristics
Previous studies and Applications

4. MASHRABIYA

For hundreds of years, several architectural elements were employed effectively and widely in the traditional housing in the Arab Gulf region, such as mashrabiyas, courtyards, and windcatchers that have been demonstrated to meet the population's needs and have strong local climate compatibility. One of the most prominent traditional architectural elements in the Middle East is the Mashrabiya which still exists in several old cities in the Middle East, such as Jeddah, Makkah, Yanbu, Baghdad, Cairo, Damascus, and Tunis. Nevertheless, Mashrabiya or "interlaced wooden screen" is not restricted to the Arabic countries, but it has also been adopted widely in different regions worldwide, from the Far East to South America, such as India, Japan, China, Portugal, and Spain. Mashrabiyas are traditionally characterised by several functions, allowing air and daylight to penetrate and providing privacy besides the aesthetic purpose. Therefore, many researchers have studied various aspects of mashrabiyas in the last decades. However, this chapter reviews most studies and applications on mashrabiya from different aspects, including the design and concept.

4.1 What is Mashrabiya?

Mashrabiya is one of the primary features of the Arab-Islamic architecture which can be found and still staunch in the old cities. Besides, mashrabiya, an "interlaced wooden screen", has been found and adopted widely in different regions around the world from the Far East to South America as India, Japan, China, Portugal, and Spain (Figure 4-1). As a result, mashrabiya has several names and variations in spelling. For example, it is named in India jali, jaali, jaalis, or jalis, which means the latticework screen. Mashrabiya as a word or term has different spellings because it is written originally from Arabic (مشربية) to different languages such as English and French. So in English, mashrabiya can be written in different spellings as mashrabia, mashrabiyya, mashrabiyah, mashrebeeyeh, meshrebiya, or mashrabiyah). It is spelt and defined by (Dictionary, 2016) "meshrebeeyeh (in Islamic countries) an oriel screened by latticework ". In French, mashrabiya is named *moucharbieh*, *moucharaby, mashrabiyyah, or mushrabiyyah,* while it called muxarabi by Portuguese, and sachnisi in Greek.

Mashrabiya is known under different names based on the region; it is known as shanasheel in Iraq and Iran, also called mushabak in Iran (Almerbati et al., 2014), Roshan in Sudan, takhrima (means full of holes) in Yemen, moucharabieh in Algeria (Almerbati, 2016). While in Saudi Arabia, it is called either mashrabiya or rowshan.

The root of the word mashrabiya is Arabic, yet there are some differences in its source interpretation. Mashrabiya in Arabic is derived mashrabah and mashrubah, which means a room (Maajim, 2013). Others said, mashrabiya linguistically is its origin from "Mashrafiya" the noun of the verb "Ashrafa" which means the place to look out or observe from the upper level (Mohamed, 2015). With time and due to the accents and effect of the non-Arab speakers, mashrafiya became uttering mashrabiya. While Fathy (1986) stated the word of mashrabiya is derived from the Arabic word called 'sharbah', meaning "drink" and initially referring to "a drinking place". He also described mashrabiya as a cantilevered space with a lattice screen where small water jars cool the air passing through the apertures.

Figure 4-1 Traditional Mashrabiya around the world and its names. (Bagasi et al., 2021)

Fathy (1986) also mentioned that now the word (Mashrabiya) is used for an opening consist of a wooden lattice screen with small wooden balusters that are circular in part and arranged at specific regular spaces, often in a decorative and complex geometric pattern. Mashrabiyas (Kamal, 2014) defined as "projecting windows with wooden latticework for natural ventilation and privacy".

Rawshan is defined by (Aljofi, 2005) as an architectural device made of a combination of wood strips and screens, which is commonly used for large external openings. Also, it is described by (Saini, 1991) as a projected bay window with decorative wooden screens as an enclosure. Al-Murahhem (2010) said Roshan plural Rawasheen or Rawāshīn", is a projected wooden screen type that covers the building's façade and protects it as a garment.

The statements differed about the source of the word Rowshan. (Salloum, 1983) stated that the origin of the word "Rowshan" from India, known as "Rushandan" means the light source or clerestory windows near the ceiling. "Rushandan" is consisting of two parts: "Rowshani" which means "light" and "Dan" which means "giving". Whereas (Al-Murahhem, 2010) states the linguistic origin of the term rowshan is Farsi, meaning a source of light which means the same in Indian. Also, the word Rowshan has an origin in Arabic under the Word "Raushun" which means; 1) balcony or 2) a hole or opening in the wall or in the ceiling that air and light enter from it (Almaany, 2017).

Mashrabiyas were described by Talib (1984) as a group of rowshans on top of one another covering a façade. Then, he described Rowshans as a projected bay window with decorative wooden screens as enclosures. According to (Batterjee, 2010) "the Roshan, or mashrabiya, is the wooden lattice work structure projected off a wide opening in facades of houses. It captures breezes from three directions and controls the penetration of daylight to the interior of the houses". Generally, mashrabiya can be defined as a wooden frame covering a window opening characterised by several functions as allowing air and daylight to penetrate and providing privacy beside decorating the building facade.

Although there are many sources of the origins and diversity of the meanings of whether the word Mashrabiya or Rowshan, the word "Mashrabiya" from the researcher's view is the most common name and has clearer indication of the meaning. So, this research used "Mashrabiya" as the primary reference.

4.2 History of Mashrabiya

Since the historical background of the mashrabiya and its development in the old centuries is not the main focus of this research. However, the main points addressed about the Mashrabiya history in previous studies will be mentioned here briefly. Due to the variation of opinions and researchers, the historical root of Mashrabiya cannot be confirmed when and where it originated. However, Khan (1986) stated that the origins of mashrabiya might back to the ancient castles or forts of the past that were built with unique bay windows and were used for defensive purposes by cast hot water or oil on the enemies through small openings in the bottom of the bay (Al-Shareef, 1996). Also, Khan (1986) added that mashrabiya during Mamluk and Ottoman eras was known and dominant in the Islamic world. Sudy (2011) mentioned, the mashrabiya was created in the thirteenth century AD, where it developed through Muslim builders during the Mamluk Era in Cairo. Abdelgelil (2006) stated the Mashrabiya appeared in Egypt (1517 ~1905) through the Mamluk and Ottoman periods. During the Mamluk rule era (1248–1516), mashrabiya was a predominant architectural element where maybe the oldest Mashrabiya in the Great Masjid at Qayrawan (Al-Murahhem, 2010). Alitany et al. (2013b) mentioned, "The term Roshan can be traced as far back as 1100 AD, and in North Africa, Egypt and Yemen has come to be known as Mashrabiya". Mashrabiya reached the height climax of its use in the Ottoman era when it was widespread almost completely in Iraq, Syria, Egypt, and the Arabian Peninsula.

In the western region of Saudi Arabia, Jeddah played a prominent role as a gateway for pilgrims due to the proximity of its seaport to the two holiest cities, Makkah and Medina. The region took advantage of its cultural exchange position with the caravans of pilgrims coming for the Hajj from different countries who brought their skills, exchanged ideas with the people, and enriched the art of architecture, including the mashrabiya in Hijaz (Talib, 1984). Although Makkah, Taif, Medina, and Yanbu have different climatic characteristics than Jeddah, the mashrabiyas have flourished similarly to mashrabiyas in Jeddah.

4.3 Mashrabiya Design and Structure Details

The design of Mashrabiya varies from region to region according to several physical variables. These variables can be size, material, patterns and ornament, and openings technique. The most effective design factor in mashrabiya design and its role in affecting the building mainly depends on the size and dimensions (height, width, length, thickness and overlap), including the opening sizes. In addition, the design varies according to the condition of mashrabiya, separate or sequential (Figure 4-2). Al-Shareef (1996) mentioned that the ratio of the opening sizes depends mainly on the humidity, as increasing the size of the openings would be helpful to provide more natural ventilation for the building and eliminate the effect of humidity as in the old Jeddah buildings. While the size of the openings is small, it contributes to reducing glare and heat gain when the humidity is low, as in some old buildings in Medina. The percentage of openings size "solid to void" of typical mashrabiyas can be ranged between 40% and 60% (Alkenaidari, 2019).

Figure 4-2 Different types of Mashrabiya in Nasseef House at Old Jeddah (Author)

The regular construction material used in the mashrabiya structure is wood. Many types of wood are used for these structures, but the most common ones used in Saudi Arabia are teak, ebony, oak and mahogany (Al-Shareef, 1996). Kamal (2014) stated, "The Rowshans were constructed entirely of cantilevered timber framework and were often installed over the openings after prefabrication with the desired decorations and finish". The terracotta material was historically used in some countries such as Iran and India for structure latticed screens (Germanà et al., 2015). In the present era, mashrabiya can be made from Aluminium, Steel, or GRC. Further, the patterns through the accuracy of the details and the woodworks and decoration affect the design and shape of mashrabiya.

The openings technique of mashrabiya can be in different methods; fixed, movable, operable, or kinetic (Figure 4-3).
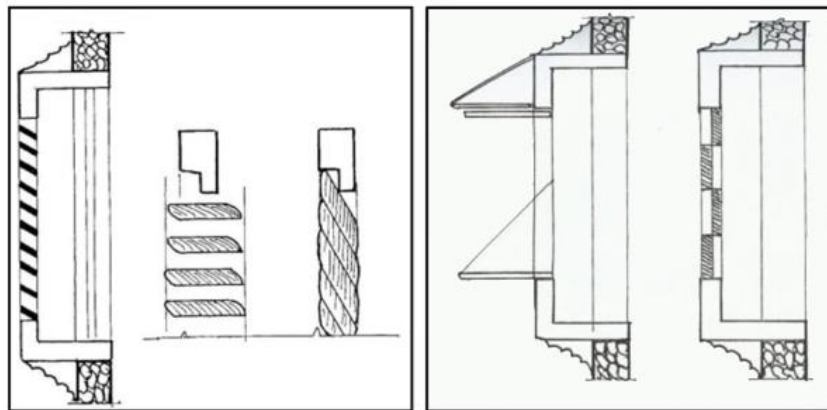
Figure 4-3 Fixed louvre on the left and different method for Shutters on the right (Aljofi, 1995)

Mostly, the structure of a mashrabiya comprises three major parts: the upper, middle, and lower parts. Each part has several components that are either functional, aesthetic or both. Alitany et al. (2013a) defined these parts as the head "crown or Tajj", the body "Suddir", and the base "Qaida" (Figure 4-4). Al-Shareef (1996) described the division of the external details of mashrabiyas into five elements: crown, first horizontal panel, opening sashes, second horizontal panel and brackets. Other elements can be adopted as additions based on the prevailing climate, such as wooden screens (sheesh) and water jars (Al-Shareef, 1996).
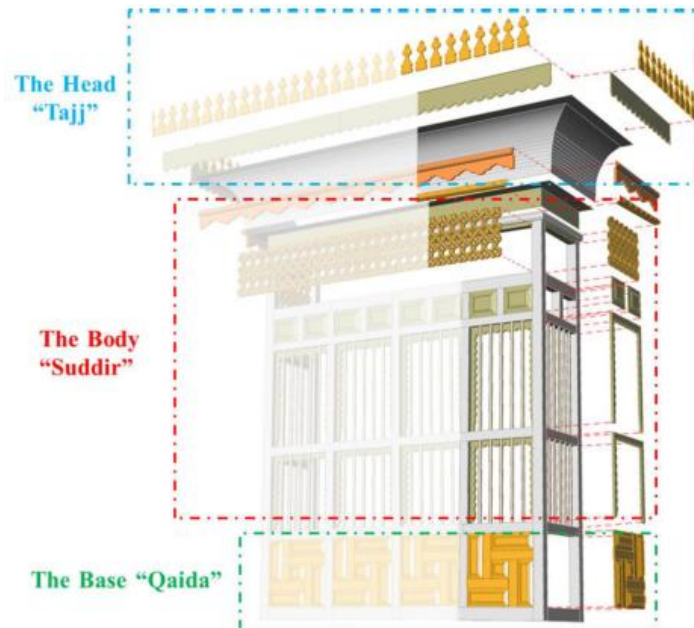
Figure 4-4 Main parts for a Mashrabiya in Jeddah. Reproduced from (Alitany et al., 2013a)

Hariri (1992) defined the mashrabiya structure into six elements: first wooden panel "Hezam Fawqani", the upper section of sashes opening, second horizontal panel, the lower section of sashes opening, the lower horizontal panel "Hezam Tahtani", and Wooden brackets. Maghrabi (2000) combined some previous research related to mashrabiya form and described it in seven main elements; crown, pearl, upper belt, sashes, lower belt, brackets, and wooden screen. Typical mashrabiya parts can be divided into three main structural components—the head, the body, and the base—each with several elements (Figure 4-5). The crown in the upper part work as a canopy for the middle part of the mashrabiya. The upper belt connects the upper part with the middle part. Under the upper belt, the sashes are in the middle part of mashrabiya that can be designed as louvres, shutters, or screens (Batterjee, 2010). The sashes are considered the essential part of mashrabiya due to their significant role in most mashrabiyas functions for allowing penetrating air and daylight and providing privacy. The sashes cover an aperture and are usually divided horizontally into two equal sections. Vertically, the middle part usually contains three to five sashes. Each sash has several horizontal sliding slats or "louvre blades" (Maghrabi, 2000).
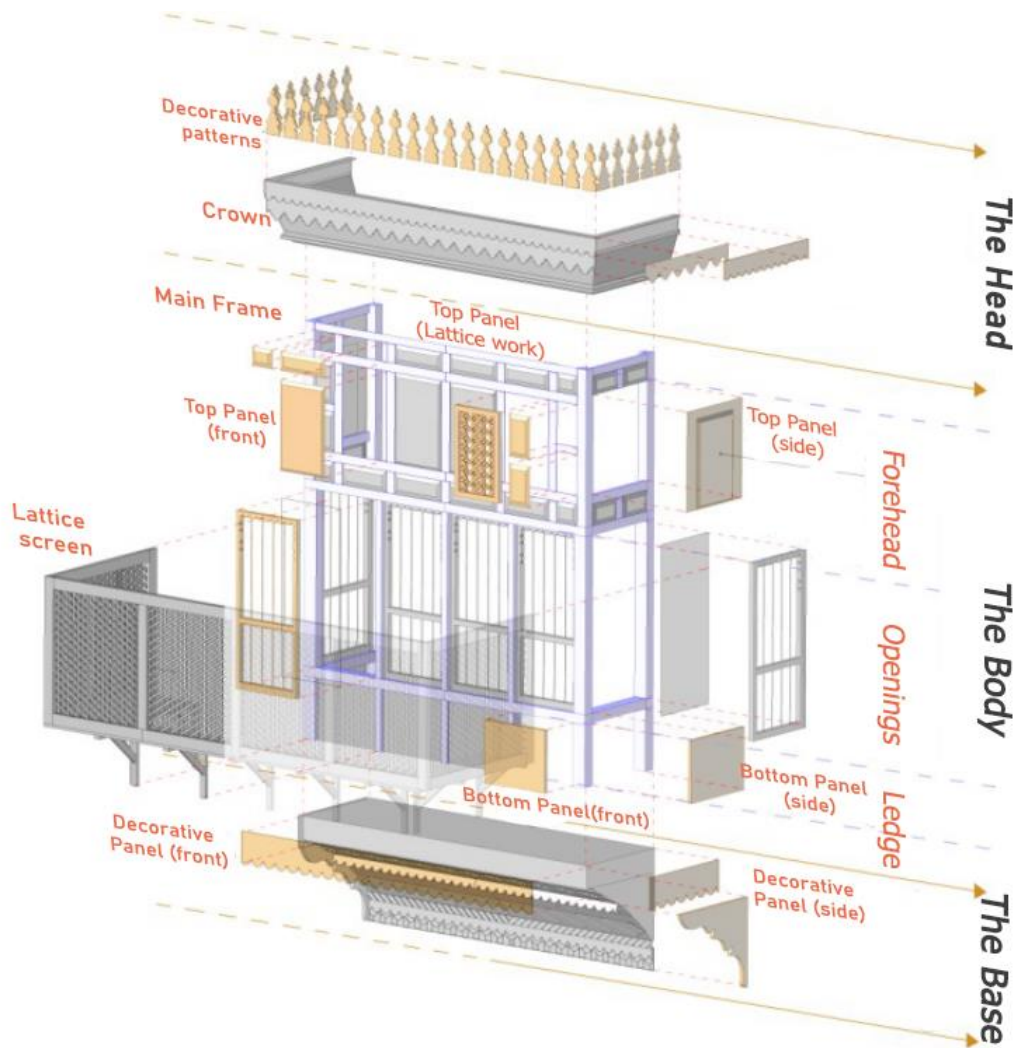
Figure 4-5 Detailed view of parts and components for a mashrabiya in Jeddah, amended from Alitany et al. (Alitany et al., 2013b)

The primary purpose of movable louvres is to control the entry of light and air into a room desired by the occupant (Al-Murahhem, 2010). Over the lower sashes with an overhang of 0.5 m from the outer part, a wooden screen locally named "sheesh" was placed in some mashrabiyas where it provides a place for water jars, which work to cool the air by evaporation (Maghrabi, 2000). The bottom part of a mashrabiya consists of two sections: the lower belt and brackets. The brackets work as the primary support of the whole mashrabiya structure.

4.4 Mashrabiya Typology

In the central concept, all mashrabiyas have the same approach. Despite this, mashrabiyas differ in their forms from one region to others according to several factors. These differences were mainly due to the climate type, the local craftsmen's skill, the accuracy of the details and the woodwork, and the client's request and financial ability. An abundance of inscriptions and an increase in detailing details and the size of a mashrabiya, and the quality of the wood used in mashrabiya construction indicate the wealth and social status of the house owner. Salloum (Salloum, 1983) divided the mashrabiya into three sorts taking into consideration the size: (1) simple wooden screens or louvres covering the openings; (2) the cantilevered mashrabiya as an expansion part of the interior spaces; (3) wooden louvres on two or three sides surrounding a room located on the uppermost floor of a property named "al mabit" where the occupants sleep during hot days. Aljofi (Aljofi, 2005) also divided the mashrabiya into three types: (1) cantilevered, (2) screen panels, (3) louvred timber walls and louvred windows. While Hariri (1992) classified mashrabiya into two main categories, each one has many types. The first category is the continuous vertical mashrabiya from the building top util the lower or ground floor. The other category is separate and covers one opening for a room. According to Alitany et al. (2013b), although mashrabiya has many differences in shapes and sizes, including the different levels of its heights on the facades, it can be divided into three types; 1) Form complexity; 2) layout configuration; and 3) height level on the façade. Mashrabiya in Jeddah come in many different shapes and sizes; the most common shapes can be classified into three groups: mashrabiyas, plain mashrabiyas, and projected mashrabiya, as shown in Figure 4-6.

4.4.1 Mashrabiya Dimensions

Due to the different shapes and sizes of mashrabiya, there is no fixed size and specific dimensions for mashrabiya. However, some researchers have outlined the typical dimensions of mashrabiya. Greenlaw (1976) described the main internal dimensions of the traditional mashrabiya by saying: "The size of a Rowshan is related to the dimensions of the human body; it is wide enough to lie down in comfortably, that is just over two meters, 2.40 m usually; high enough to stand in, about 3 m, and projecting about 60 cm into the street". Alitany et al.

(2013a) and Adas (2013) described a typical dimension of mashrabiya by; its width is 2.4-2.8m and its internal height 2.7-3.5m. It can protrude externally about 0.4–0.7 m. Adding the thickness of the external wall with the projection of the mashrabiya may result in a width that ranges up to 1.2 m, which can be conveniently used as a seating area. Al-Shareef (1996) stated, "The usual dimensions of a single traditional Rowshan unit are 3 m in height, 2.3 m in width and 1.1-1.9 m in depth, to allow sufficient space for a sleeping adult. Some Rowshans are built with a depth of 1.9 m to accommodate a man and his wife".

Hariri (1992) stated the area between the floor of the mashrabiya and the lower panels, where it can consist of horizontal panels varying in height between 40 and 50 cm suitable for sitting with a clear vision from inside to outside. The floor of mashrabiya extends the floor of the room or higher than floor level by around 0.5m.
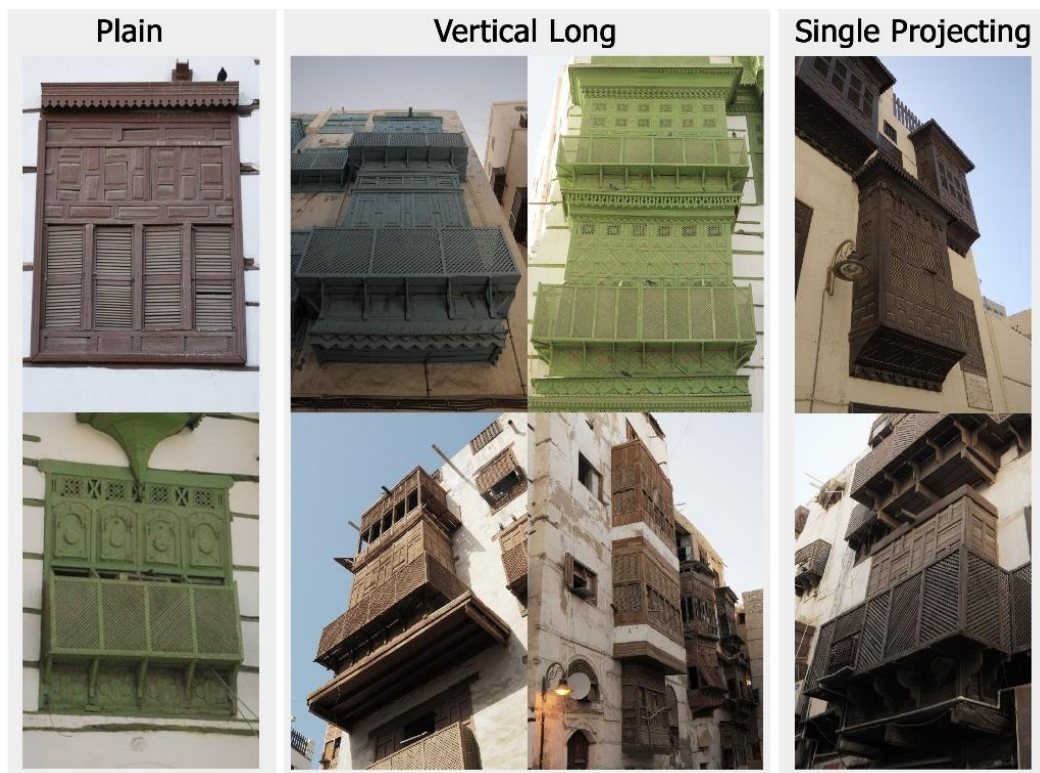
Figure 4-6 Different types of mashrabiya in Historic Jeddah

4.5 Functions of Mashrabiya

Although mashrabiya were widely used in many different countries, they generally have the same functions. Functionally, a mashrabiya is primarily focused on environmental, social and architectural factors. Mashrabiya perfectly works as a protection device from direct sunlight and effectively reduces heat gain, especially during hot seasons. Traditional mashrabiyas are durable and do not need frequent maintenance where excellent quality wood types are used in the mashrabiya, such as teak or mahogany wood, which are durable and can be used for long periods without damage and resist extreme weather conditions such as heat and humidity (Hariri, 1992). According to the architect Fathy (1986) "The mashrabiya interstices intercept the direct solar radiation and soften the uncomfortable glare. Besides, considering that the mashrabiya is made of wood, it helps regulate the humidity inside the space. It is known that wood absorbs, retains and releases water. When air passes through the interstices of the porous wooden mashrabiya, it vaporises some of the moisture gathered in the wood and carries it towards the interior" (Naciri, 2007). Sabry and Dwidar (Sabry and Dwidar, 2015) stated that "Mashrabia provide shade within the housing without complete closure of windows and allow the movement of air, which helps to reduce the temperature in the summer". Algburi and Beyhan (Algburi and Beyhan, 2019) mentioned that the lattice apertures on mashrabiya surfaces allow the passage of natural fresh air and provide thermal comfort. Mashrabiyas work perfectly for social life in houses. They provide privacy to room occupants and grants them freedom in their actions and movements. At the same time, it allows looking outward without isolation from the surrounding environment.

Aestheticism is another vital function of the mashrabiya, as its shapes and designs adorn houses' facades. Mashrabiyas generally are characterised by an aesthetic shape and precision geometric and beauty with ornamental inscriptions of different styles. Besides, mashrabiya's outline and parts are in line with the vertical extension of the façades, which directly contribute to making mashrabiya efficient. Al-Ban (2016) noted that the colours, lattice works, motifs and facades of Mashrabiyas contributed to creating a distinctive visual character in Jeddah. The mashrabiya and its carved wood openings foster a unique dialogue between the interior and the exterior while creating a beautiful and pleasant link between

privacy and publicity for the home (Al-Ban, 2016). Moreover, Ashour (2018) said: "Regarding psychological needs, one can investigate how the mashrabiya enhances the feelings of confidence, bliss, and quiet relaxation experienced by the occupants and how much it arouses and inspires creative energy". To summarise, mashrabiyas are traditionally characterised by allowing air and daylight to penetrate into a building and providing privacy beside the aesthetic purpose (Figure 4-7).
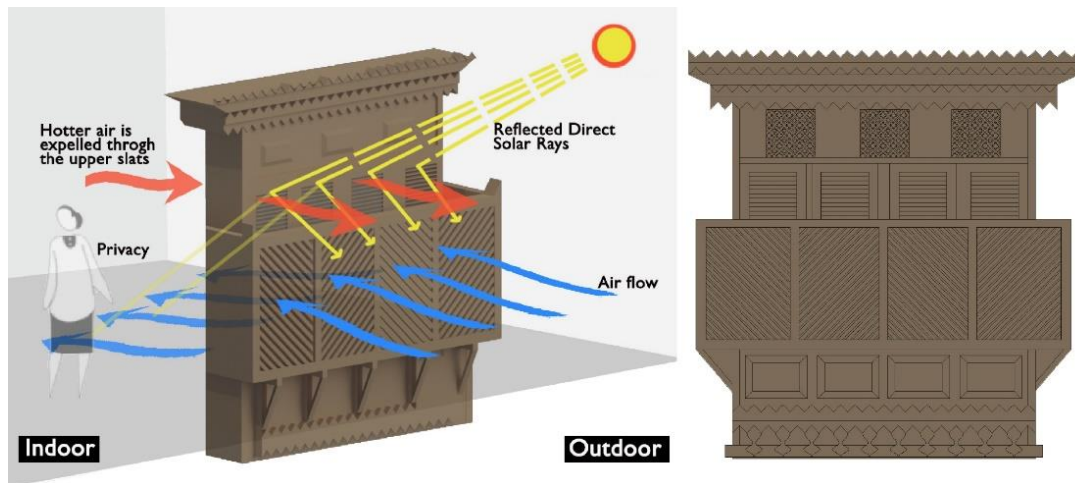
Figure 4-7 Example of Mashrabiya demonstrating the principal functions

4.6 An evaluation of Mashrabiya Characteristics

When analysing the composition and components of the mashrabiya, many environmental, aesthetic, and social advantages mashrabiya can provide and some negatives. The following is a quick review of the most prominent advantages and disadvantages of using or employing mashrabiya in modern buildings.

4.6.1 Advantages of Mashrabiya

The mashrabiya has many advantages which described by Hariri (1992) and can be summarised in the following points;

1- **Integration of the shape with function:** The mashrabiyas are generally characterized by aesthetic shape and precision geometric and beauty in ornamental inscriptions with different styles, in addition to the outline of the mashrabiya and its sections, which are in line with the vertical extension of the facades, which directly contribute to making the mashrabiya functions are effective and success

2- **Strength and durability:** Traditional mashrabiya are featured by durability and no need for frequent maintenance where the excellent quality of used wood types in mashrabiya, such as teak or mahogany wood, are durable and remain for long periods without damage and resist weather conditions such as heat and humidity.

3- **Environmental compatibility:** One of the main environmental benefits of mashrabiya is providing daylighting with control and allowing air to pass through with determined quantity and direction. Mashrabiya design achieves control of the amount of desired sunlight that emits to the room by the adjustable wooden sashes, which work as flexible louvres and can be opened to allow more sunlight to enter the room or closed and be satisfied with lighting through it. Adjustable wooden sashes allow control for each sash separately, which contributes to the elimination of glare. Furthermore, the movement flexibility of sashes allows for the benefit of outside air in moderate seasons nights and the direction of air movement towards the room either to the bottom or above as desired by the occupants.

4- **Religious and social compatibility:** Islam has emphasised the principle of privacy and stressed on respect it. The design of Mashrabiya is in line with the principles of Islam and societies, which applies the principle of privacy basically, where the latticed wooden screen prevents the detection of room occupants and grant them freedom in their actions and movements. At the same time, it allows us to look outward and non-isolation from the surrounding environment.

4.6.2 Disadvantages of Mashrabiya

With the rapid development in the past decades, climate change and increasing humanitarian needs, some issues have emerged in the use of mashrabiya. Due to the perimeter of adjustable louvres, it is not possible to close Mashrabiya tightly. The louvres need a sliding path, and as they go down, the friction with the wood increase and flipping is neither possible nor difficult. All of that can lead to dust permeability and penetration of insects, including noise disturbance (Hariri, 1992). In addition, continuous air leakage is not compatible with one of the essential needs of modern houses in Saudi Arabia (air conditioning), which depends on the isolation of external air to control the internal air temperature effectively and economically.

Moreover, the cost of the mashrabiya is several times higher than that of regular windows made of wood or aluminium. Batterjee (2010) mentioned that "Roshan is made from expensive woods such as teak, ebony, oak, and mahogany. These woods are difficult to find locally and expensive to import. That raises the cost of construction and maintenance considerably". In addition to that, the period required to implement a mashrabiya is long, where the manufacture and installation of one mashrabiya may take up to two months or more based on the size and design.

Otusanya et al. (2020) stated, "New passive cooling technologies are being discovered every day, but undeniably the internal thermal comfort of buildings cannot be attained utilising only one passive cooling method". In addition, new technologies such as fans and air conditioners provide alternative solutions that address the drawbacks of mashrabiyas. These technologies have replaced most mashrabiyas' essential functions, such as natural ventilation and cold air, with faster and more operational efficiency to meet thermal needs in hot climates.

However, because of the need to reduce greenhouse gas emissions, passive techniques should be applied in buildings and integrated with active techniques (AL-Dossary and Kim, 2020). Alothman (2017) stated that air conditioners have failed in some way compared to mashrabiyas, because they consume much energy and are expensive to run.

Therefore, it is vital to revive the local architectural elements such as the mashrabiya after studying, testing, and analyzing, then developing the mashrabiya adequately and intensive in line with the inhabitants' needs and modern building methods and technologies.

4.7 Previous studies and Applications

This part reviews most of the previous studies and researchers to explore and get an overview of mashrabiya in general with a benefit of the latest developments in some detail. Since this research consider Jeddah as a study case, the major focus is on the mashrabiya in Saudi Arabia and the most important research dealt with and developments in form and functionality. The part is divided into two sections: previous studies and applications.

4.7.1 Previous Studies

Since this research aims mainly to investigate and develop the mashrabiya performance, the following is a review and discussion of several studies that addressed either the traditional or

contemporary form by focusing on natural ventilation and daylighting and integrating some passive evaporative cooling methods with mashrabiya.

4.7.1.1 Traditional Mashrabiya

In 1989, Hariri presented his experiment about designing and developing a Mashrabiya on his house in Makkah. Hariri introduced an improved form of the traditional mashrabiya by fixing key problems such as dust permeability and insects' penetration. The exterior of mashrabiya was designed as the traditional form made by the mahogany Wood. A glass window with an aluminium frame was added to the interior at an appropriate distance from mashrabiya to place a plant pot or a water dispenser. This glassed window aims to eliminate the penetration of dust and seal the opening to not leak air condition to outside and prevent insects' penetration.

However, Hariri (1989) said that this experiment was not entirely satisfactory because the glass caused a 50% reduction in airflow control of the roshan openings area and slightly reduced the view angle due to the distance between the glass and wood. In 1992, Hariri presented another optimized mashrabiya where the glass was placed on the exterior layer of the mashrabiya and replaced the adjustable wood louvres with aluminium louvres to maintain the overall structure of the mashrabiya (Figure 4-8). The aluminium was painted a brown colour to achieve compatibility with the wood colour. Mashrabiya was divided into 12 units to control the intensity of daylight, the angle of view, and the desired air movement inside. Although this solution was characterized by easy cleaning compared to the first solution, it was not appropriate to add glass on the outside in a hot climate, where the sunlight penetrates the glass into the chamber, which necessitates a greater capacity in the air conditioning when the mashrabiya is closed (Hariri, 1992). However, field measurements and analysis or simulations in both models were not performed to determine the extent of the performance of mashrabiya and its impact on energy saving.
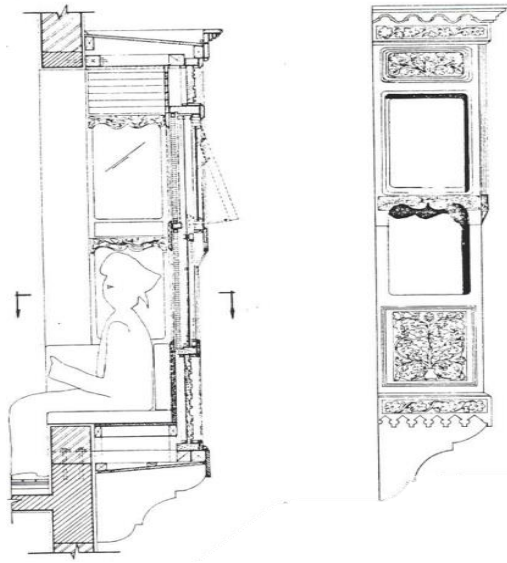
Figure 4-8 The proposed mashrabiya by (Hariri, 1992)

Al-Lyaly (1990) conducted a traditional house with mashrabiya. The study aimed to investigate and understand the use of space in Jeddah's typical house to maximise thermal comfort during summer 1987. However, due to the limited time available and limitations on borrowed equipment, Al-Lyaly stated that it was impossible to make field measurements at time intervals representative of all climatic seasons. The experimental results revealed that during that summer, the manner of room use and the family's movement from the upper to first floors at the start of the day allowed them to benefit from the temperature contrast and good thermal properties of the thick and heavy structure of the lower floors. The study showed that the outdoor air temperatures ranged from 28.5 to 39.6°C and the indoor temperatures were below outdoor temperature by 2.0 to 6.5°C during the day. During late night and early morning, indoor temperatures were higher, about 2.0°C, than outdoors. The range of indoor air velocities was between 0.2 to 1.4 m/s, where the value was affected from one space to another due to many factors such as changing wind directions and speeds, the location of the different spaces, and the number and size of the mashrabiya in each space. The study concluded that comfortable living conditions were achieved during the summer while the most significant difference to move from one space to another to take advantage of airspeeds. Although Al-Lyaly conducted field measurements on a historic building with mashrabiya, the study was limited to a short period and did not specify the actual effect of the mashrabiya on the inhabitants' comfort.

In 1996, Al-Shareef studied the mashrabiya as an element to control daylight for energy conservation in tropical architecture by considering the Hijaz architecture in the west of Saudi Arabia as a case study. The mashrabiya consists of movable horizontal louvres in eight sashes arranged in several columns and rows (Figure 4-9). Each sash was structured with a frame comprising 11 horizontal slats. The sashes were tested with declination angles of 30°, 45° and 60° slats. This study's main conclusions can be briefly summarized: the flat mashrabiya produces a very high internal illuminance than the projected one.
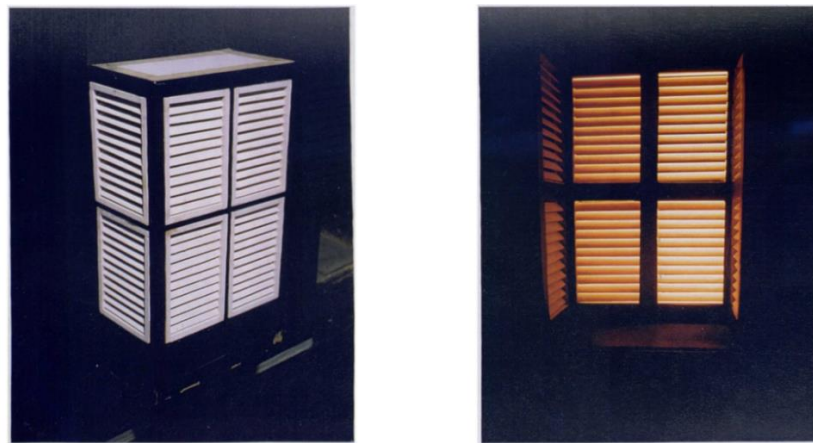
Figure 4-9 The model of mashrabiya as seen from outside "Left photo" and from inside "right photo".
Reproduced from (Al-Shareef, 1996)

As the mashrabiya size is increased, the illuminance can be more. Also, reflectance plays a significant role in the illuminance produced by the mashrabiya. As the illuminance increases, the slat reflectance increases, and adjustment of the slat declination angles plays a significant role in the level and distribution of illuminance at the work surface (Al-Shareef, 1996). Al-Shareef recommended several recommendations related to his study, which are investigating the performance of mashrabiya after considering the reflected component from internal surfaces, consider putting barrier as glass, investigate the effect of any obstacles either from outside the mashrabiya or from inside as a result of the furniture or human bodies (Al-Shareef, 1996). Although the study gave an initial understanding of some of the factors that affect the overall performance of Roshan from a brief experimental study, Al-Shareef stated that due to the limited experimental equipment available, the study did not provide sufficient data from the physical experiments.

In 2002, Maghrabi studied modulated louvre windows concerning Jeddah's mashrabiyas to examine the ventilation efficiency through modelling and simulation. The study revealed that the rooms' main reasons for poor ventilation were when the slides were adjusted in an acute inclination position. Also, the ventilation openings and free space in mashrabiya were affected with the slats tilted to ±60° resulting in a decrease in the primary pressure. Maghrabi stated that the form of the mashrabiya played a vital role in the flow pattern inside the room since the flat mashrabiya allowed more airflow in its centre compared to prominent mashrabiyas. Besides, the best option in Jeddah was to use windows near the roof, which increases airflow near the floor and makes the atmosphere at home more comfortable.

According to Aljofi (2005), "Orientation, times of the day play an important role in the amount of lighting passing the mashrabiya". In 2005, Aljofi tested six screen panels of different regular shapes (Figure 4-10). The effect of screen cells was studied in three ways; shape, size, and reflectance. The illumination values of rounded screen cells were the lowest in comparison with other screen panel types. Compared to the dark oak wood screen, the light oak contributed more light by an average DF of 17%. Besides, it was found that as the diameter of the screen cell increases, the reflected light increases too.
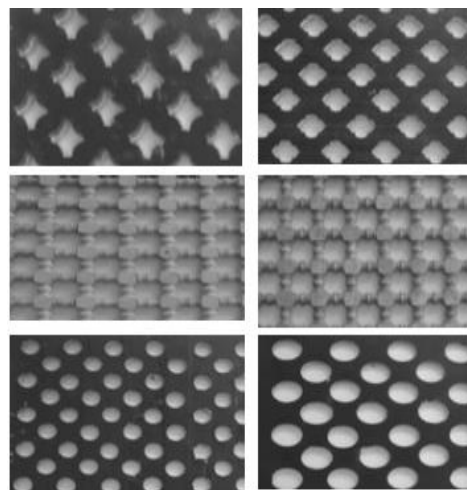
Figure 4-10 Six screen panels of different shapes (Aljofi, 2005)

Al-Hashimi and Semidor (2013) studied mashrabiyas' effects on daylight values in Jeddah's residential buildings. The study examined a room with a wooden mashrabiya, as shown in Figure 4-11. Three design cases were examined: a room with central openings closed by Venetian blinds, a room with open openings, and a room with a single glazed window facing

north during daytime (Al-Hashimi and Semidor, 2013). The study found the most massive

daylight value during daytime corresponded to a mashrabiya with an opened Venetian blind.

Although the space with a closed Venetian was dark, some small quantity of daylight (<1%)

always enters from the top of mashrabiya.
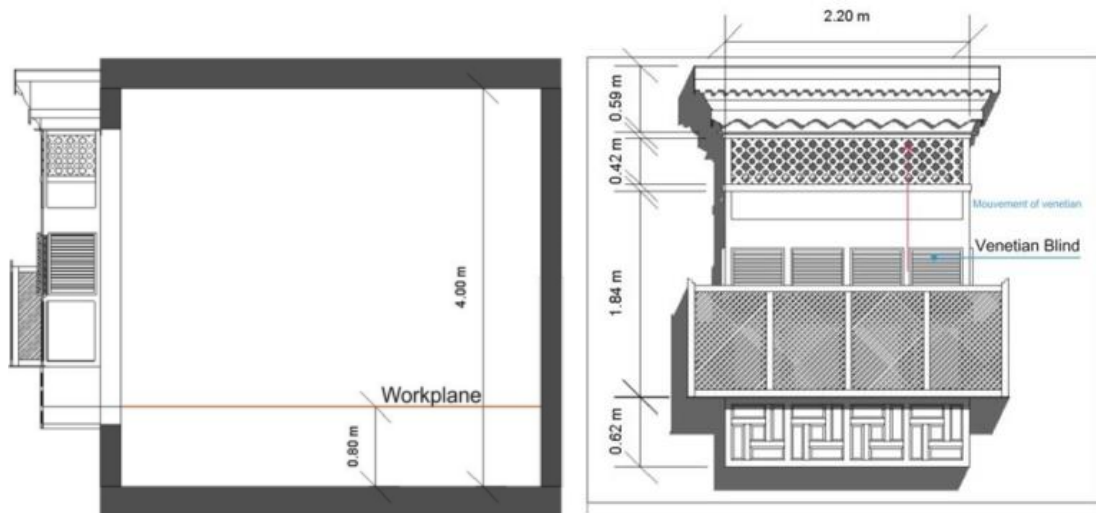
Figure 4-11 The evaluated room and mashrabiya dimensions. Reproduced from Al-Hashimi and Semidor
(2013)

In 2020, Alwetaishi et al. (2020) investigated the thermal comfort in a historical building with

mashrabiya located in Taif (Saudi Arabia). The study used an evaporative cooling technique

to enhance thermal comfort by increasing indoor airspeed. It was found that the "evaporative

cooling technique has a considerable impact on reducing indoor air temperature by 4 °C,

improving the thermal comfort sensation level" (Alwetaishi et al., 2020).

4.7.1.2 Contemporary Mashrabiya

In the current era, various shapes derived from mashrabiya can be found on the façades of

buildings in various countries worldwide. Also, several studies and applications have

submitted new designs or proposals for the development of mashrabiya either using different

materials instead of wood such as aluminium, steel, ceramic, or glass fibre reinforced

concrete (GRC), incorporating interactive techniques for opening and closing or with the

integration of evaporative cooling systems in an attempt to boost the indoor thermal and

energy consumption conditions. In 2010, Batterjee proposed a mashrabiya in Jeddah by

developing its daylight penetration performance and decreasing energy consumption.

Batterjee designed five models with different parameters and examined the daylight levels

using Ecotect and Radiance software, where the dimensions of the mashrabiya models were 2.4 m (w) × 3 m (h) × 0.4 m (prominent depth) as shown in Figure 4-12. The best case was a designed 10 cm × 10 cm opening tilted 45° upward on the interior side using stainless steel and double low-E glazing with an aluminium frame. This reduced cooling loads up to 49% and proved to be the best overall solution suggested except for the east orientation due to the sun's low position during that period.
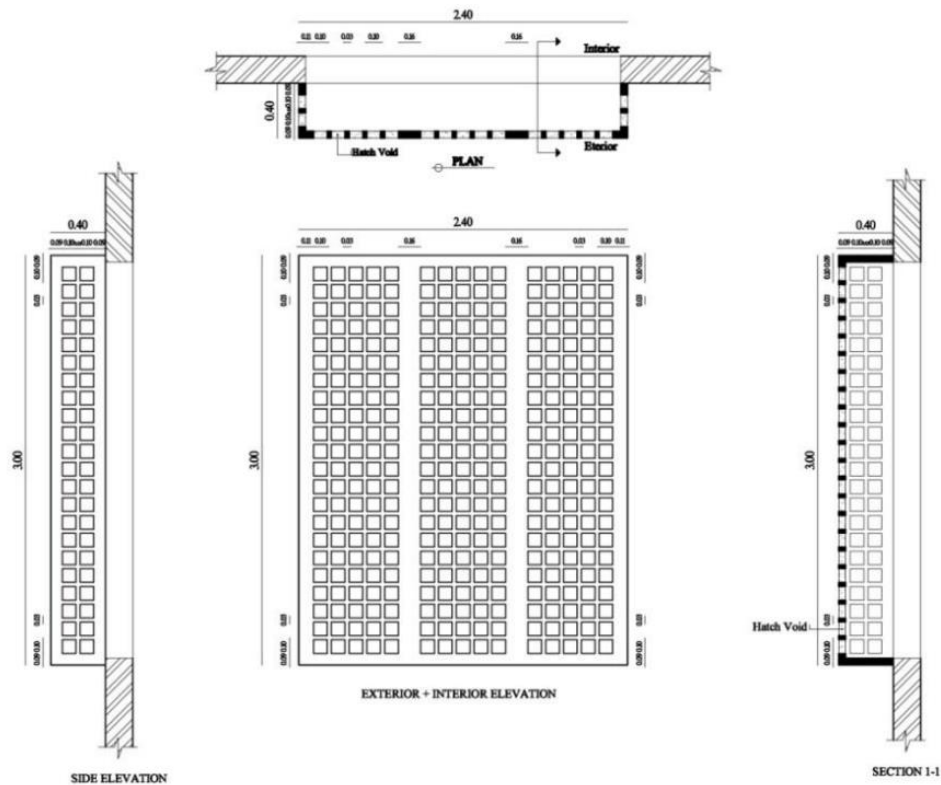
Figure 4-12 Simulation via Radiance for evaluating daylight level. Reproduced from Batterjee (2010)

Benedetti et al. (2010) investigated the evaporative cooling potential of mashrabiya screens installed in Bolzano, Italy, testing two types of local hardwoods (oak and chestnut) and two softwoods (spruce and larch) to determine their water release rate. The study recommended spruce for mashrabiya screens due to its greater cooling potential, higher permeability, and a better evaporative cooling effect. The study concluded that larch wood could be the most appropriate species for mashrabiya screens in Bolzano, given its cooling efficiency and construction features.

In the Gibson Desert of Australia, Samuels (2011) proposed a new concept for a mashrabiya, constructed as a spray device that sprays 0.2 mm diameter water droplets from the

connecting holes, as seen in Figure 4-13. The study indicated that the system established an effective and sufficient cooling technique for the structure, but no results or measurements of thermal efficiency and performance were given.
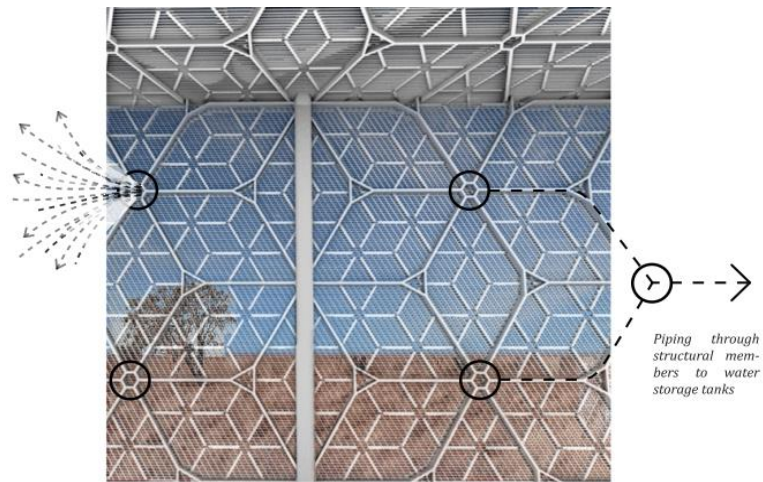
Figure 4-13 Screen and System of the Designed Mashrabiya. Reproduced from (Samuels, 2011)

Karamata et al. (2014) proposed a new system inspired by the mashrabiya concept comprising a shape variable mashrabiya (SVM) and specified Abu Dhabi as a case study. The SVM was made from three identical perforated opaque shields; the first is fixed while the second and the third one can singly move along the vertical and lateral axis. The results of annual daylight performance simulations showed that SVM provides adequate and well-balanced illumination (most of the time across the whole space). In contrast, the SVM shields decrease and scatter the amount of diffuse light.

In 2015, the SVM was studied again by (Giovannini et al., 2015) showed that the SVM minimised overheating problems and, consequently, the primary energy demand for cooling (−17.2% and −9.9% compared to selective glazing = 41% and Venetian blinds, respectively). It also minimised the primary energy required for lighting (−65.7% and −30.7% compared to reflective glazing = %16 and Venetian blinds, respectively) and the efficiency of lighting and global primary energy (−27% and −16.3% compared to RG16 and V.B., consecutively).

Sabry et al. (Sabry et al., 2014) designed several solar screens to achieve visual comfort and reduce energy use in a residential desert environment. The study assumed a residential living room space of 4.30 m × 5.20 m in Jeddah with different screen designs. It concentrated on the influence of varying the solar screen's axial rotation and the aspect ratio of its openings

beneath the clear desert sky (Figure 4-14). The study concluded that the solar screens could provide 66–97% daylit areas in the inspected spaces and reduce energy consumption to 25% compared to a standard glazed window.
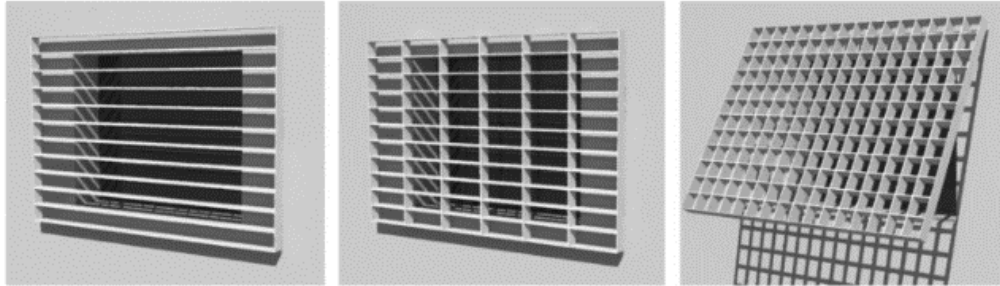
Figure 4-14 Radiance renderings of the window and the solar screens virtual model (Sabry et al., 2014)

Khadra and Chalfoun (2014) attempted to improve an integrated façade technology that interacts with and adapts to climate change in hot arid areas, specifically in Tucson, Arizona. The study aimed to optimise thermal comfort for occupants in mixed-mode office buildings using passive ventilation and evaporative cooling methods to reduce mechanical cooling energy loads. The case was a typical office space facing south by 6 m (w) × 7.6 m (d) × 2.7 m (h), and a 33% window to wall ratio. The study tested three different operating systems: a mechanical cooling system, passive ventilation and an evaporative cooling system, as shown in Figure 4-15. The proposed model demonstrated that the cooling load decreased by nearly 70 % throughout the year while the heating load increased slightly in the winter months.
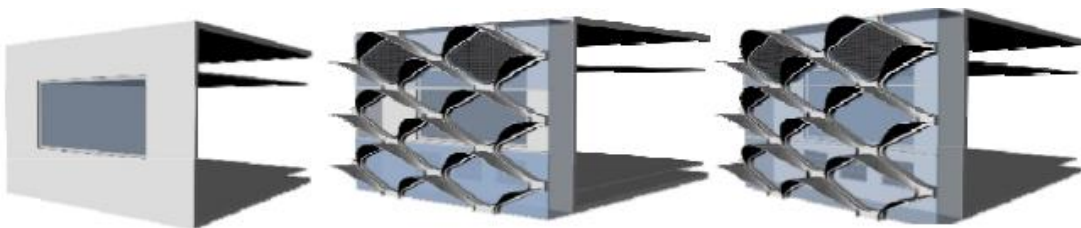
Figure 4-15 The three operating systems (left to right); mechanical cooling system, natural ventilation system, evaporative cooling system (Khadra and Chalfoun, 2014)

Batool (2014) estimated the impact of a range of perforation ratios (30%, 40% and 50%) of hexagonal jali screens on energy savings and daylight performance in a modern office building in Lahore, Pakistan. The study comprised data collection and analysis using the IES VE simulation software for the field measurements and energy modelling. The results

indicated the positive impact of jali screens on cooling loads and improved visual convenience. The 50% void ratio in windows facing south was also a better way of achieving a balanced cooling and lighting energy strategy.

Elkhatieb and Sharples (2016) studied and developed traditional mashrabiya in order to optimise daylighting performance. The study tested an office space facing south located in Cairo, integrated it with climate-adaptive building shells (CABS). Elkhatieb and Sharples (2016) explained, "The CABS system consists of 40 units each unit 1m * 1m. They were randomly divided into four groups, each with a different scale based on 30 different random distribution scenarios for a south facing façade inspired by a a traditional Egyptian pattern". The CABS were integrated with horizontal and vertical louvres. The study inspected three parameters to validate the design efficiency A) illuminance, luminous distribution and solar irradiation and B) daylight glare probability, without setting CABS (Figure 4-16). Elkhatieb and Sharples noted that the CABS system had demonstrated its ability to provide sufficient lighting efficiency that meets the requirements and can contribute towards integrating daylight algorithms to promote parametric façades and genetic daily lighting performance.
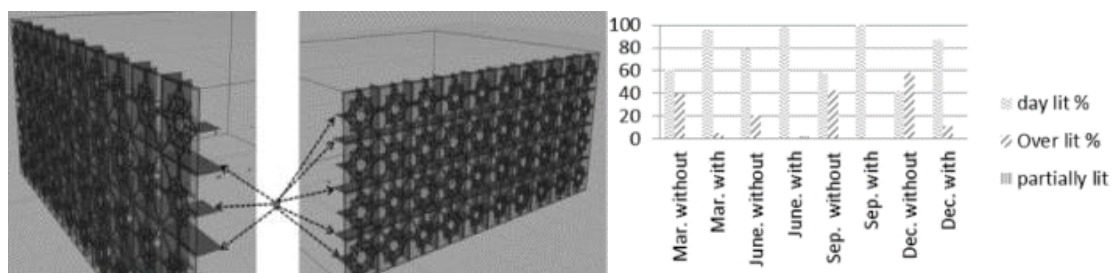
Figure 4-16 The CABS system integrates louvres with pattern "right", Daylighting performance with and without CABS "left". Reproduced from (Elkhatieb and Sharples, 2016)

A new system of wooden lattice openings was proposed by (Di Turi and Ruggiero, 2017) to control the daylight that enters a building. The study was carried out for an isolated test room using computational fluid dynamics (CFD) as a simulation tool, showing that it could provide better indoor conditions, increase airspeed, and improve the room's air change rate. Alrashed et al. (2017) integrated a mashrabiya with a simulated building in Saudi Arabia and concluded that it could sequentially reduce annual demand for electricity and maximum power need by 4% and 3%. Another study by Algburi and Beyhan (2019) simulated an air-conditioned house in Iraq with a proposed mashrabiya and demonstrated using a mashrabiya could save

12.56% of the total cooling load. Taleb and Antony (2020) simulated an office building in Dubai to evaluate the mashrabiaya performance and different chosen glazing types. The proposed mashrabiya had a hexagonal pattern with 40% coverage of the glazing unit. The study found that mashrabiya as tinted glazing could reduce cooling load by 23%.

The integration of evaporative cooling elements with mashrabiyas has been discussed or investigated in some studies. Schiano-Phan (2010) proposed an evaporative cooling system that was derived from the mashrabiya concept using a porous ceramic medium called "Evapco system" developed by Cain et al. (1976), and the aim was to address some of the cooling needs of residential buildings in hot-dry regions. Compared to air conditioning, the total annual energy savings were about 3.08 MWh for the selected apartments.

In 2015, an innovative design inspired by traditional mashrabiya and water-filled ceramic vessels was reported by Rael and Fratello (Rael and Fratello, 2015). The form consists of 3D impressed porous ceramic bricks, where each brick absorbs water and enables air to pass. The design used the evaporative cooling principle, where the air passes through the form and evaporates the water in the pores, refracting air and reducing the internal temperature.

Table 4-1 summarises most of those studies in some critical criteria for this paper. As a summary of this section, most of the studies addressed either the daylight or ventilation aspects of the mashrabiya and a few included evaporative cooling. Although Samuels (2011) considered all aspects, the study did not cover any analysis and measurements or simulation demonstrate the effectiveness of the proposed mashrabiya. As reviewed, most studies tend to focus on either the history or development of mashrabiyas without testing or considering their actual performance and influence on the indoor thermal environment.

Table 4-1 Review of some primary research on mashrabiyas and different aspects.

Author, Date	Design	Daylight	Ventilation	Evaporative Cooling	Analysis
Batterjee, 2010	T	✓	X	X	✓
Maghrabi, 2000	T	X	✓	X	✓
Aljofi, 2005	T	✓	X	X	✓
Hariri, 1990	S.T.	✓	✓	X	X
Hariri, 1992	T	✓	X	X	✓
Al-Hashimi and Semidor, 2013	T	✓	X	X	✓
Samuels, 2011	A	✓	✓	✓	X
Sabry et al., 2014	ST	✓	X	X	✓
Khadra and Chalfoun, 2014	A	X	✓	✓	✓
Schiano-Phan, 2010	ST	X	✓	✓	✓
Karamata et al., 2014	A	✓	X	X	✓
Nermine and Nancy, 2014	S.T.	✓	✓	X	✓
Faggal, 2015	A	✓	X	✓	X
Headley et al., 2015	S.T.	✓	✓	X	✓
Alsharif, 2016	A	X	✓	✓	X
Elkhatieb and Sharples, 2016	A	✓	X	X	✓
[Design: T=Traditional]		[S.T. =Semi Traditional]		[A=Advance]	

4.7.2 Applications of Developing Mashrabiya

Table 4-2 briefly highlights some of the applications from the researchers' viewpoint based on two aspects: (1) mashrabiya improvements through design and materials; (2) design of innovative mashrabiyas, which generally have an idea inspired by the design concept and functions of traditional mashrabiya.

Table 4-2 Different applications of mashrabiya

Project|Built|Location	Approach	Concept	
Arab World Institute 1987 *Paris, France	-Interactive -Kinetic	Each unit in the mashrabiya performs as a camera lens. The south facade was covered by a vast mashrabiya of 30 × 80 m size made up of hundreds of light-sensitive diaphragms that admit a certain amount of light into the building and govern cooling.	
CH2 Melbourne City Council House 2 2006 *Melbourne, Australia	-Innovative -Kinetic	The building's façade was inspired by Nature, while the micro-ventilation ducts are integrated with daylight strategies, and the walled concrete floor structure plays a central role in heating and cooling the building.	

Pearl Academy of Fashion 2008 *Jaipur, India	-New Fixed Design -Improved	The double skin is designed 4 m away from the exterior walls, acts as a thermal barrier that reduces direct heat gain through the windows. The dripping channels along the jaali internal face allow passive evaporative cooling, hence reducing the airflow temperature.	
Paul Valery High School 2009 *Menton, France	-New Fixed Design -Improved	The wooden louvres on the facade act to let daylight pass and interact with the exterior spaces. The design took into consideration visual unity while ensuring thermal comfort bound to solar protection.	
Masdar city Residential Buildings 2010 *Abu Dhabi, UAE	-New Fixed Design -Improved	The mashrabiya was built to be aesthetic and integrated with the surrounding desert by using developed GRC coloured with local sand in a sustainable way. The concept of light and shadow apertures is based on typical Islamic architectural patterns.	
The Q1 Headquarters 2010 *Essen, Germany	-Interactive -Kinetic	In response to the Sun's movement, the kinetic façade consists of about 400,000 stainless steel lamellas that allow light to be redirected without obstructing the view.	
Private house 2011 *New Delhi, India	-New Fixed Design -Improved	-The mashrabiya is structured from moulded red brick. The brick acts as a veil in the screens that shade the west facade of the building.	
Al Bahr Towers 2012 *Abu Dhabi, UAE	-Interactive -Kinetic	This adaptive mashrabiya looks like a triangle when it expands. Every six units connect from a joint point looks like the rhombus shape. It is made from stainless steel supporting frames, dynamic aluminium frames and fibreglass mesh.	

Doha Tower 2012 *Doha, Qatar	-Fixed -Interactive	The facade consists of four aluminium "butterfly" components of various sizes, which protect against direct sunlight. The shape varies depending on the orientation and the solar protection that individuals require: 25% northward, 40% southward, 60% eastward and westward.	
Vishranthi Office 2014 *Chennai, India	-New Fixed Design -Improved	The building's total façade is divided into 600 mm transparent panels with white aluminium mullions that shape the frames. Two different types of skin between the mullions were added: a lighting panel and a jali screen panel.	
Community Center 2015 *Roses, Spain	-New Fixed Design -Improved	The facade design allows the view towards the sea with respecting the environment and the privacy of the surrounding buildings. The ventilated facade consists of perforated panels in the same pattern as the original geometric mosaic covering the old floor of the building.	

To summarise, the applications in Table 4-2 illustrated that buildings focussed on daylight by innovatively utilising the mashrabiya principle and trying to take advantage of the formation of mashrabiya to reduce heat gain and thus reduce cooling loads. However, Mashrabiah needs more studies and experiments to evaluate its impact on energy loads

4.8 Conclusion

This chapter started with described different opinions on the source, names, and history of mashrabiya. Despite the presence of many sources for the origins and diversity of the meanings of mashrabiya, the researcher tends to the opinion of Fathi 1986, where the word of mashrabiya is derived from the Arabic word called 'sharbah', meaning "drink" and initially referring to "a drinking place". Mashrabiya can be defined and described as a wooden frame covering a window opening characterised by several functions. It allows air and daylight to penetrate and providing privacy besides decorating the building facade. It is not likely to confirm the historical root of the mashrabiya when and where it was created due to the

difference in opinions and researchers, but several opinions believe that it appeared in Egypt during the thirteenth century.

The chapter has reviewed mashrabiya from different aspects; design, concept, functions, advantages, and disadvantages. Typical mashrabiya parts can be split into three main structural components—the head, the body, and the base. The body is the middle part containing the sashes, which considered the essential part of mashrabiya due to their significant role in most mashrabiyas functions for allowing penetrating air and daylight and providing privacy. Functionally, a traditional mashrabiya is characterised by allowing air and daylight to enter the building and providing privacy besides the aesthetic purpose.

On the other hand, the use of traditional mashrabiyas in modern buildings as an alternative to windows is not feasible for several causes, the most important of which is the inability to close the mashrabiya tightly, which leads to the permeability of dust and the penetration of insects. In addition to the leakage of outdoor air into the building, it may increase air conditioning consumption in hot seasons. However, due to the need to reduce greenhouse gas emissions, passive technologies must be applied in buildings and combined with active technologies.

Therefore, the chapter included reviewing several studies and applications from two scopes; traditional and contemporary. It can be summarized that most of the studies addressed either the daylight or ventilation aspects of the mashrabiya, and a few included evaporative cooling. As reviewed, most studies tend to focus on the history or evolution of the mashrabiya without testing or considering their actual performance and influence on the indoor thermal environment.

It has been illustrated that mashrabiya applications in modern buildings are concentrated in daylight by innovatively implementing the concept of mashrabiya to minimise heat gain and thus reduce cooling loads. Therefore, it is necessary to revive the local architectural elements such as mashrabiya after studying, testing and analysing its impact on the indoor thermal condition, then develop its design adequately and extensively to contribute to reducing the energy consumption of the buildings and in proportion to the needs of the inhabitants and modern building methods and technologies.

CHAPTER 5

CASE STUDY (BAESHEN HOUSE)

Location and Historical Background
Local Climate
Baeshen House
Base Case "1st Field study"
Integration Passive Evaporative Cooling with Mashrabiya "2nd Field study"
Summary and Conclusions

5. CASE STUDY (BAESHEN HOUSE)

After reviewing the mashrabiya from different aspects, including several studies and applications on mashrabiya, it was found that the scope of mashrabiya research still lacks demonstrating and proving the actual performance of the mashrabiya and the extent of its influence on the indoor thermal environment, in addition to proving the effectiveness of integrating passive evaporation in improving its performance in cooling the building and provide comfort. Therefore, to practically understand the role of mashrabiya concerning the indoor thermal environment and investigate the effect of incorporating some cooling strategies with it in improving the indoor thermal environment, this work investigated its performance through two field experiments in a historic building in a hot climate. The case study is located in old Jeddah, Saudi Arabia.

This chapter started by describing and clarifying the criteria for selecting the fieldwork's case study "Baeshen House". Then, it presents an overview of Jeddah's geographic and climatic context where the case study is located. Next, section 5.4 (Base Case "Pilot Study of the existing situation" was conducted in the summer 2018. Section 5.5 presents the fieldwork of summer 2019, where several passive evaporative cooling techniques have been investigated with mashrabiya. Both sections present the aim and objectives of each field study, methodology, results and conclusions. Moreover, evaluating the indoor thermal comfort for each strategy.

The first field experiment was conducted during the summer 2018 from 4th Aug to 1st Sep for 28. The experiment used calibrated digital devices to monitor air temperature, relative humidity, air velocity, and indoor globe temperature for the courtyard and two selected rooms. Two different modes were examined; One room with open mashrabiya and another closed. The second fieldwork was conducted during summer 2019 from 30th July to 8th Aug on the same rooms and courtyard with two stages using different strategies: 1) Standard mode; one open mashrabiya and one closed, and 2) Evaporative Cooling mode; integrate pots, water spray, and cloth with mashrabiya. Finally, section 5.5 summarises the overall findings and limitations of the field experiments.

5.1 Criteria for Selection of the Case study

Old Jeddah has many buildings built with local stones with plaster and their façades decorative by different shapes and types of mashrabiyas. The case study "Baeshen House" is located among the oldest and known houses in Old Jeddah. The house represents one of the most featured historical buildings of Jeddah, in the past and present, due to the magnificence, luxury, and beauty of its facades rich with the adorable mashrabiyas.

In this study, Baeshen House was selected as a case study based on several criteria: validity, condition of mashrabiyas, functions and duration, availability of drawings, the possibility of the experiments, and access to the building. The case study results will provide a clear framework about the influence of mashrabiya in general and the extent of its actual impact on the old houses with load-bearing walls in Jeddah in particular. Thus a broader understanding of the performance and impacts of mashrabiya on the buildings.

5.1.1 Location and Historical Background

Jeddah, known as the Red Sea Bride, is the second largest city in Saudi Arabia after Riyadh's capital. It is located in the western part (Hijaz region) of Saudi Arabia and the middle of the eastern Red Sea coast exactly at Latitude 21° 29′ 25″ N and Longitude 39° 11′ 10″ E (Figure 5-1). Jeddah is the largest city in Makkah province, has the largest seaport in the Red Sea and is the main gateway to the holy cities: Makkah and Madinah.

The history of Jeddah dates back about 3000 years, but the historical transformation of the city occurred in 647 AD during the reign of the third caliph of Muslims, "Othman bin Affan" when he directed Jeddah to be transformed into a coastal city, which enabled it to receive pilgrims as nearest sea destination to Makkah (Chamber, 2018). Due to the central position of Jeddah between three continents: Asia, Africa, and Europe, it
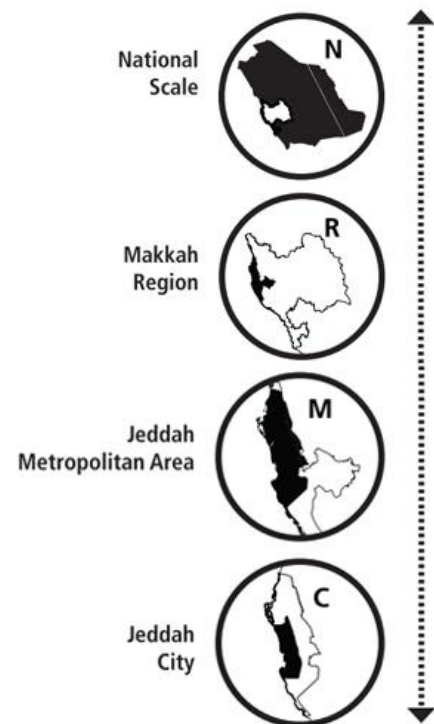
Figure 5-1 Jeddah location. Amended from (Affairs, 2019)

has simply become one of the centres of international commerce, which affected the Hejaz region's traditional architecture (Batterjee, 2010).

Jeddah has a beautiful architectural heritage district known as Old Jeddah or Al-Balad, where historical buildings. For more than 200 years, many Al-Balad buildings were established and built with Red Sea stones with lime and plaster and their façades rich in different shapes and types of mashrabiyas (Adas, 2013).

Based on what Al-Lyaly (1990) reported, the Swiss traveller Johann Burckhardt described in 1814, where Johann wrote: "The interior of Djidda is divided into different districts...The streets are unpaved but spacious and airy... Almost every house has two stories, with many small windows and wooden shutters. Some have bow windows, which exhibit a great display of joiners' or carpenters' work... There is, generally a spacious hall at the entrance, where strangers are received, and which, during the heat of the day, is cooler than any other part of the house, as its floors are kept almost constantly wet".

Greenlaw (1976) described the general character of old Jeddah buildings by "The distinguishing external features of the old houses of the Red Sea, and some other Islamic and Indian styles are the large casement-windows jutting-out into the street to catch the slightest passing breeze", where the mashrabiyas were expressed by saying casement-windows.

During the past decades, most of Jeddah's historic buildings became deserted and neglected. Despite this, Saudi has turned its attention to promoting heritage sites' preservation and restoration as part of Saudi Arabia's heritage in the last years. The development of the tourism sector and national heritage consider one of the axes of the Saudi 2030 vision, which seeks to market Saudi Arabia as a regional and global tourist destination through various aspects. As a result, the Kingdom of Saudi Arabia could revive and register many historical and heritage sites on the UNESCO list, including Historic Jeddah, which was registered in 2014 as a heritage site.

d'Avignon (2012) stated that "In the area 'protected' by UNESCO there are about 240 buildings of historical and architectural interest; There are other buildings built more or less recently totally disrespectful of the environment outside the traditional urban regulations dating back to 1980…".

Old Jeddah has well-known four traditional neighbourhoods and many heritage monuments and buildings of archaeological importance, including the Old Jeddah Wall and its open historical squares, and many mosques and various old markets. The four traditional neighbourhoods have divided the city into well-known areas and are known locally as "Hara"; Al-Sham, Al-Mazloum, Al-Yemen, and Al-Bahr, as shown in Figure 5-2. Each district is named based on its geographical location within the city or after a famous event there (Chamber, 2018). The most famous and oldest existing buildings and still in good condition mentioned by d'Avignon (2012) includes; Bayt Baeshen, Bayt Nassif, Bayt Noorwali, Bayt Nawar, Bayt Sharbatli, and Bayt ash Shafe'i.
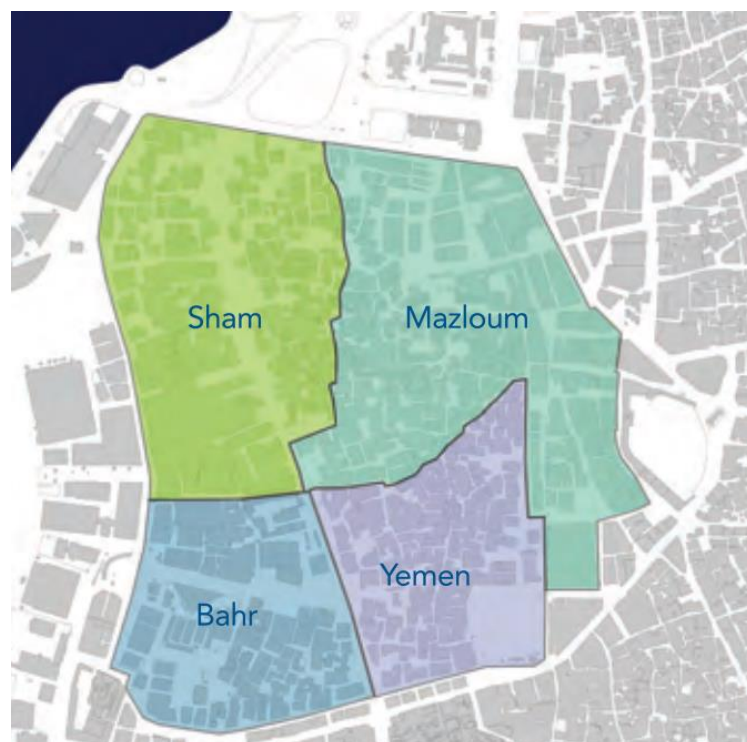
Figure 5-2 The four quarters of the old city. Reproduced from (Antiquities, 2013)

Old Jeddah's traditional buildings used several architectural solutions and climate treatments to provide thermal comfort to their residents (Bogari, 2011). The buildings structures were mainly built from local building materials where Coral stone, or what is known as "Mangabi", was the primary material in building the walls with adding some timber joints to support any gaps between the coral stone, as shown in Figure 5-3. Coral stone was extracted from the immediate vicinity of the old city. Coral stone is a porous stone with good insulation properties and is relatively light. The wood joints were used to prevent the collapse of walls that can be

diminished by high humidity and salinity in the air and soil (Batterjee, 2010). Moreover, the walls were covered with a white plaster layer to protect the stones from moisture and heat also reflect a portion of the direct solar radiation and resist the aggressive salty air of the Red Sea coast (Alsharif, 2016). The typical wall thickness of multi-storey houses ranges from about 80 cm, with a decrease of about 15 cm for each upper floor. Al-Ban (2016) stated that "the traditional buildings of Old Jeddah are tall and graceful, constructed of coral and limestone and decorated intricately with beautiful Indian or Javan teak facades that ventilated the houses as well as shaded the narrow streets". The average number of floors of the old buildings are ranging from two to four floors. Al-Ban (2016) said that "The hierarchy of rooms in Jeddah houses remained consistent: the lowest floor was used by the servants or for storage, the second floor was used for cooking, the third floor was used for bedrooms, while the uppermost floor would be for the majlis". The majlis was used for family and located on the top floor to catch the breeze as it is considered the coldest room at night (Alharbi, 1989).
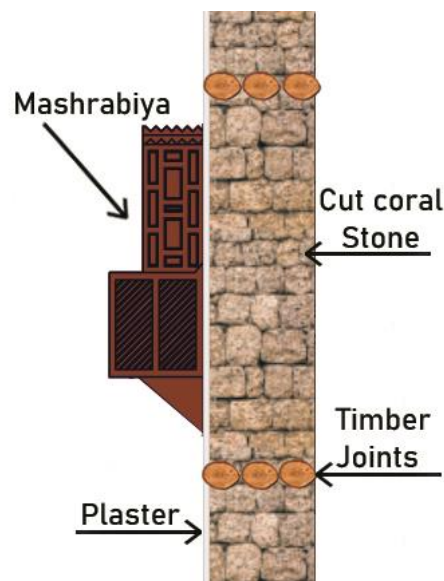
Figure 5-3 A section of a stone wall of an old building in Historic Jeddah

The old Jeddah buildings' facades were distinguished by the wooden mashrabiyas, which varied in shapes, sizes, colours, and geometric patterns. The wood of mashrabiyas mostly was imported from India and the Mediterranean (Batterjee, 2010). The colours of the mashrabiyas have varied, frequently indicated to the position of the house's owners where the light green for businessman, brown for the middle class, light brown for the poor, and light blue for the fishers (Al-Ban, 2016).

To conclude, it is clear how these buildings responded and adapted to the harsh conditions of the Jeddah climate, as the designers were keen to use several treatments and architectural solutions to reduce heat gain to provide comfort to home residents.

5.2 Local Climate

Climate is one of the most important determinants and influencing factors that must be considered when designing buildings. The case study for this research is located in Jeddah, and thus, it was necessary to study Jeddah climate to be discerning and find out the most important climatic factors affecting housing design.

According to Said and Al-Zaharnah (1994), the climate of Jeddah can be classified as hot dry with maritime desert sub-zones. Jeddah has a coastal semi-tropical climate, hot and high humidity in summer (Antiquities, 2013). Jeddah has low humidity during winter, and mild temperatures range from 16°C at night to 25 °C in the afternoon (see Figure 5-4). In summer, the mean daily temperature reaches 40°C in the afternoon and decreases to 23 °C at night. Besides the high percentages of relative humidity and direct solar radiation, these temperatures are the leading cause of thermal discomfort during the summer seasons. Generally, the coldest months are January, February, March, and December, with a maximum average of about 30°C and an average minimum of about 17°C. In comparison, the highest average air temperatures were recorded between May and September. Most of the rain is of the type of showers accompanied by thunderstorms, and it usually falls during the winter season and in the spring.
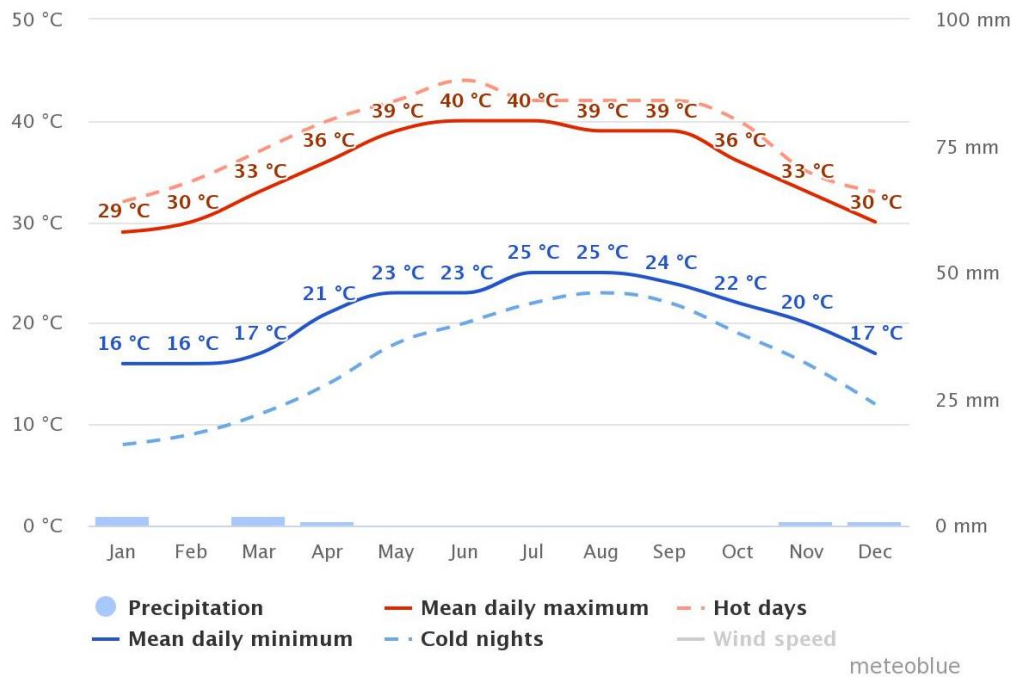
Figure 5-4 Average temperatures and precipitation for a 30-year of hourly historical weather data for Jeddah (Meteoblue, 2020)

The entire year of average temperatures related to the comfort level hourly for each month can be seen in Figure 5-5. From the graph, the best months that achieve the highest rate of comfort levels are January, February and December. Due to Jeddah's location on the Red Sea coast, high humidity is one of the most prominent characteristics of its climate. The maximum average of relative humidity is 67% in September (Figure 5-6 and the least humid month is July by 53%. The average annual percentage of relative humidity is 60%.
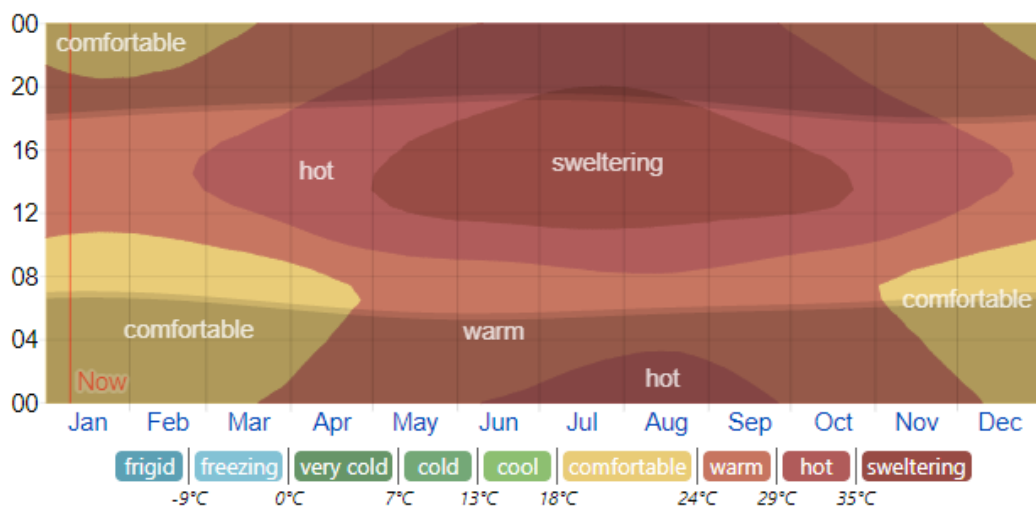
Figure 5-5 The average hourly temperature and the shaded overlays indicate night and day for Jeddah (Spark, 2022)
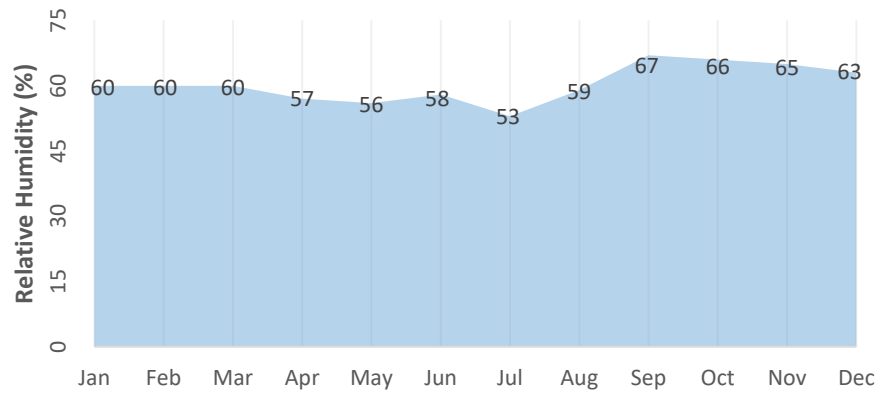
Figure 5-6 The mean monthly relative humidity from 1985 to 2010. Reproduced from (Meteorology, 2019)

Figure 5-7 below display an extreme variation of the average monthly rates for perceived humidity in Jeddah. The percentage of time spent at different humidity comfort levels is classified in the graph by dew point where dry < 13°C < comfortable < 16°C < humid < 18°C < muggy < 21°C < oppressive < 24°C < miserable.

As shown in Figure 5-7, the weather from 8 Apr to 13 Dec is mostly muggy, where the comfort level is muggy, oppressive, or miserable at least 38% of the time. Whilst the least muggy day of the year with humidity 21% of the time is 21 Jan.
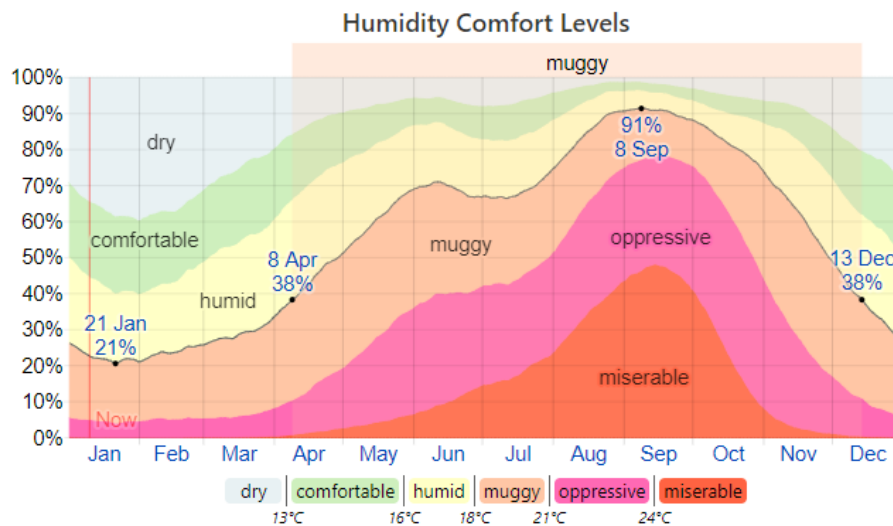
Figure 5-7 Average monthly Humidity rates in Jeddah with Humidity Comfort levels (Spark, 2022)

In Figure 5-8, the wind rose for Jeddah demonstrates the average percentages for the wind blowing from the indicated direction taken between 06/2009 and 04/2017 daily from the weather station at Jeddah King Abdulaziz Airport. The predominant average wind direction in Jeddah is from the northwest by 20.1% throughout the year. The maximum average wind

speed varies with season. The maximum average of airspeed can reach 9.2 kilometres per hour in warm seasons and decreases to 8 kilometres per hour in winter, as shown in Figure 5-9. However, the winds are light-to-medium winds for most of the year.
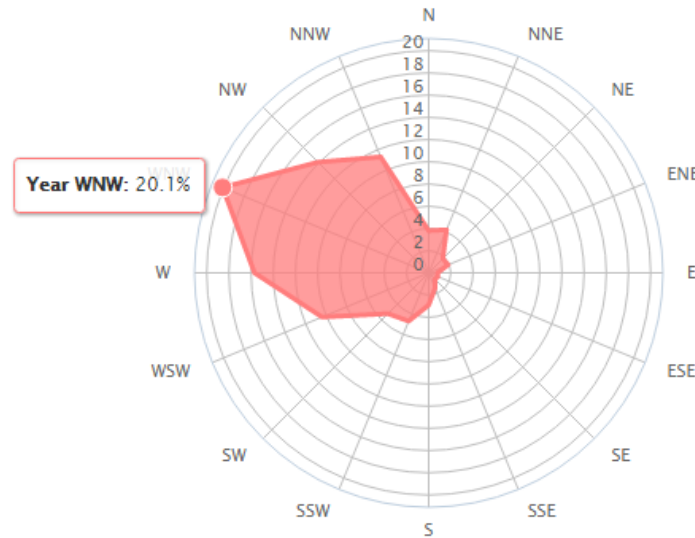
Figure 5-8 Wind direction distribution of Jeddah (Windfinder, 2017)

In Jeddah, rainfall rates are few during the year and are among the lowest rates in Saudi, with an annual average of about 60 mm. According to (Subyani and Hajjar, 2016), the rainfall during a year can be determined by three main rainy seasons: a) high rainy season (November, December, January) with an average between 26 to 10mm/month, b) low rainy season (February, March, April, October) with an average between 4 to 1mm/month, and c) dry season (May, June, July, August, September) with an average less than 0.5 mm/month.
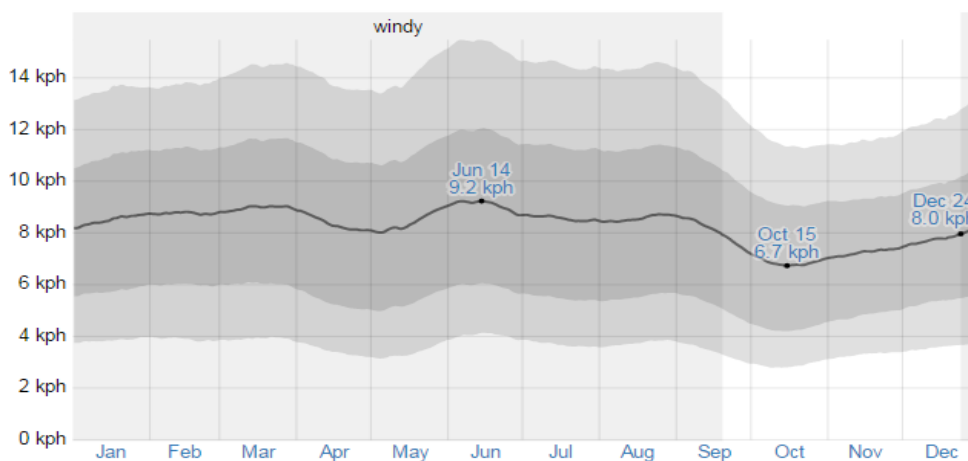
Figure 5-9 Average wind speed of Jeddah through a year (Spark, 2022)

As displayed from the sun path diagram (Figure 5-10) of Jeddah on 21 ° N latitude and 39 ° longitude, the summer solstice occurs on 21 Jun. Moreover, the Sun's azimuth is 80.3 ° at noon where the winter solstice occurs on 21 Dec and the Sun's azimuth is 80.3 ° at noon. Based on SunEarthTools.com, 21 Jun is the longest day during the year when daylight continues for about 14 hours starts from the sunrise at 06:41 am to sunset at 8.08 pm. Based on SunEarthTools.com, the 21 Jun is the longest day during the year where daylight continues about 14 hours start from the sunrise at 6:41 am to sunset at 8:08 pm. Whereas 21 Dec is the shortest day throughout the year when daylight continues for about 11.5 hours starts from 7:56 am to 6:46 pm.

According to (Maxwell et al., 1996), the average daily total Global Horizontal Irradiance "GHI" 5924 Wh/m^2, the average daily total Direct normal irradiance "DNI" 5142 (Wh/m^2), and the average daily total Diffuse horizontal irradiance "DHI" 2329 Wh/m^2. In general, Jeddah has medium levels of GHI and DNI compared to the rest regions of Saudi.
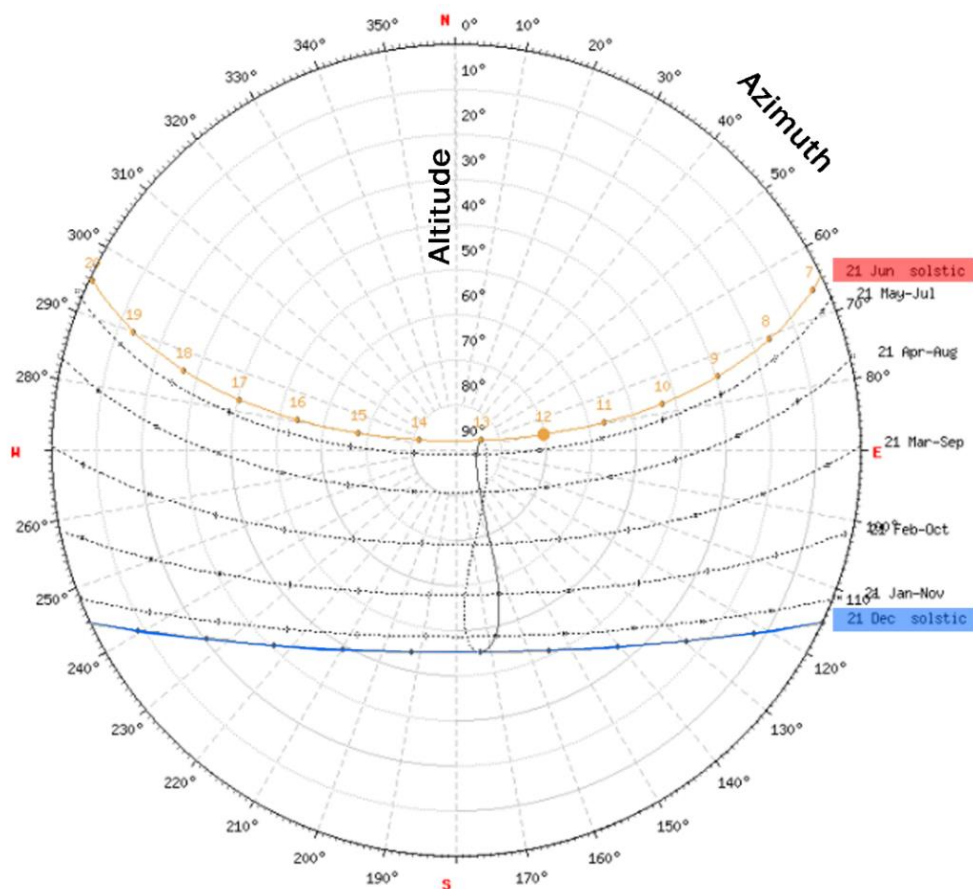
Figure 5-10 Sunpath diagram with summer and winter solstice for Jeddah (SunEarthTools, 2017)

To conclude, due to the Jeddah location in the tropical zone and the Red Sea coast, its climate, hot in summer and humid throughout the year. Jeddah temperatures reach 40°C in summer and can drop to 16°C in winter, while the average annual percentage of relative humidity is 60%. Thus these temperatures are the leading cause of thermal discomfort during the summer seasons and the high levels of relative humidity and direct solar radiation. The predominant average wind direction in Jeddah is from the northwest by 20.1% throughout the year, while the wind speed is light-to-medium winds for most of the year.

5.3 Baeshen House

The historic Jeddah "Al-Balad" has many traditional buildings built with local stones with plaster, and their façades decorative with different shapes and types of mashrabiyas. Al-Balad is one of the most important historical areas that the Saudi government has endeavoured to sponsor and support in order to preserve it as a UNESCO heritage site, as well as being one of the Vision 2030 initiatives that consider such sites as part of the heritage and civilisation of the Kingdom of Saudi Arabia. The case study for this research represents one of 240 registered buildings of historical and architectural significance by UNESCO in the preserved area. The case study is located among these traditional buildings where it is located on the latitude of 21 ° 29'12.8 " North and longitude 39 ° 11'11.5" East (Figure 5-11). This research's case study is "Baeshen House" which is one of the oldest and known houses in Al-Mazlum district (Figure 5-12). The house was constructed by Mohammed Saleh Ali Abdullah Baeshen about 200 years ago during the Ottoman era (Bagasi and Calautit, 2020). Now the current legal guardian of the house is sheikh 'Oboud Abu-Bakr Abdullah Baeshen'. The building was built from approximately 60 - 80 cm thick load-bearing walls containing three types of stones: limestone, coral, marine and coral reef (Bagasi and Calautit, 2020). As illustrated in Figure 5-13, the construction walls were protected from the humidity, heat and salinity by covering them with white plaster.

Figure 5-11 Baeshen House Location (Google Maps)

The house consists of two adjacent buildings: the main one has four floors with a height of 19.75m, and the other has five floors and 20.5m in height. The first building was built during the Ottomans' reign in 1834AD. The second building is the north-western part of the house built about 155 years ago (Al-hamid and Mohammed, 2014). Each building has internal central square stairs, which contribute to the effective ventilation of the home from the inside. Al-Ban (2016) said, "One unique feature of the house is an additional space not found in the other two houses: Bayt Ba`ishan has a private praying area for the family on the ground floor".

Figure 5-12 Three-dimensional view of the building (left)- photo of the building (right)

The main façade of the building is oriented towards the north. All facades are decorated by mashrabiyas except the southern facade, where another building adjoined Baeshen House. The building has two entrances, one of which is the main entrance and the other is private, while there is another entrance in the east for women.

The building was structured from the load-bearing wall using three types of stones: calcareous, marine, and coral. The load-bearing walls were constructed approximately 60-80 cm thick, thicker on the first floor, then less thick on the upper floors, supported by vertical wooden horizontal members spaced about one meter vertically. Figure 5-13 shows that the building walls were created from stones with mud mortar and covered by white plaster to protect the coral stones from humidity, heat and salinity's effects.

Moreover, the building was designed to allow natural ventilation and daylighting by covering the facade's openings with mashrabiyas designed in different shapes and sizes. Figure 5-14 display the building's western façade with dimensions and the tested rooms' location. The selected mashrabiyas are set on the right side of the façade as seen in Figure 5-14. The first mashrabiya (Mash1) in room1 is located on a level 5.95m from the ground, and the second mashrabiya (Mash2) is located about 9.50m from the ground. Figure 5-15 shows a section of the building showing a typical cross movement of airflow caused by opening the mashrabiyas. In recent years, most ground and first floor spaces were converted into an exhibition or gallery the building has been opened to the public.
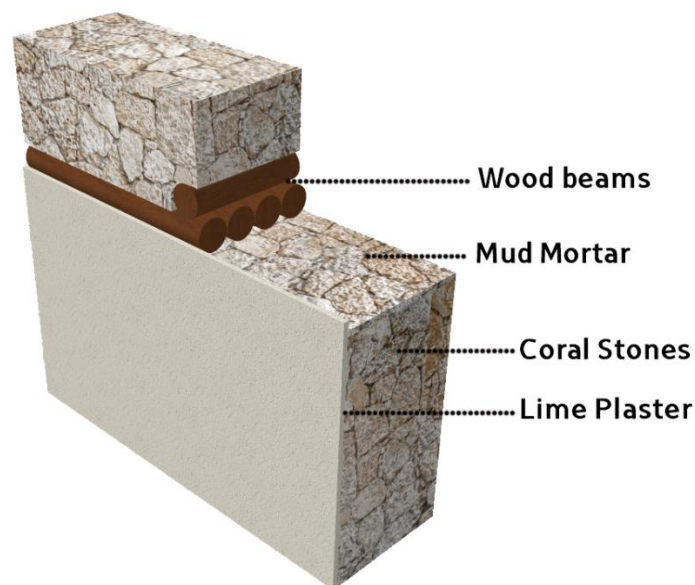
Figure 5-13 Cross-section view of the external wall.

Figure 5-14 Western façade and tested rooms locations
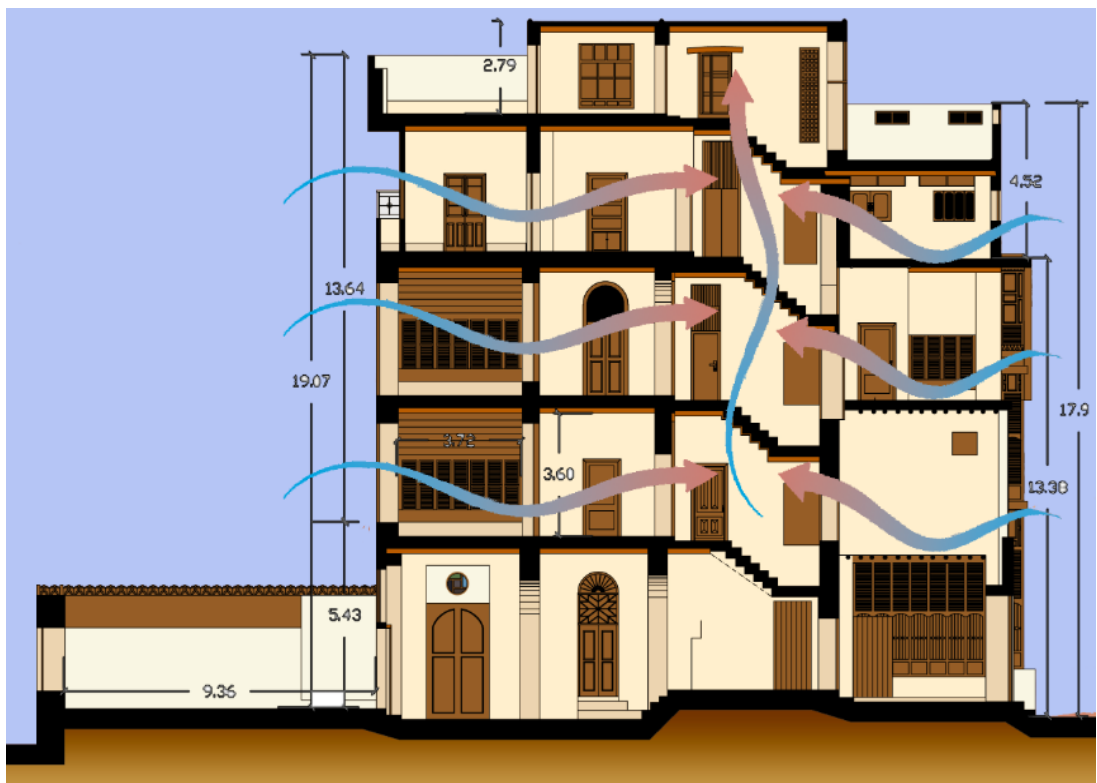
Figure 5-15 Cross-section of the building and the potential movement of the airflow

The dimensions of the structure and values of the selected test mashrabiyas are presented in Table 5-1. The mashrabiya consists of two rows of sashes in four columns (2x4). Each sash contains 16 slats, between each slat 2 cm, equivalent to twice the thickness of the slat. The opening ratio " void to solid" in each sash is 33%. The section in Figure 5-16 demonstrates materials and the internal façade of mashrabiya with dimensions. The ceiling was built from stones and timber and mashrabiya from wood. Figure 5-17 presents the internal elevation of the first mashrabiya, while Figure 5-18 presents the mashrabiya on the second floor.

Table 5-1 Dimension structure of the Mashrabiya in detail

Object	Dimension/Value	Object	Dimension/Value
Mashrabiya Frame F	(H) 331cm x(W) 241cm x (T) 11cm	Sash size with frame $SH+F$	(H) 68cm * (W) 52cm
Mashrabiya body B	(H) 139cm * (W) 241cm	Sash size without frame $SH-F$	(H) 58cm * (W) 42cm
Sill Height S_H	81cm	Space between Slats SP_{SL}	2.4cm
Total Number of sashes N_{SH}	8	Slat Thickness SL_T	1.2cm
No. of sashes rows N_{SHR}	2	Slat Depth SL_D	6cm
No. of sashes columns N_{SHC}	4	Slats Inclination Angles SL_A	0 to 70˚
No. of Slats N_{SL}	16 Slats in Each sash	No. of Tilt rod N_{TI}	8
Spaces between Sashes SP_{SH}	6-7cm	Tilt rod size TI_{sz}	(H) 64cm x (W) 2cm x (T) 2.5m
*(H): height (W): width (T): thickness			
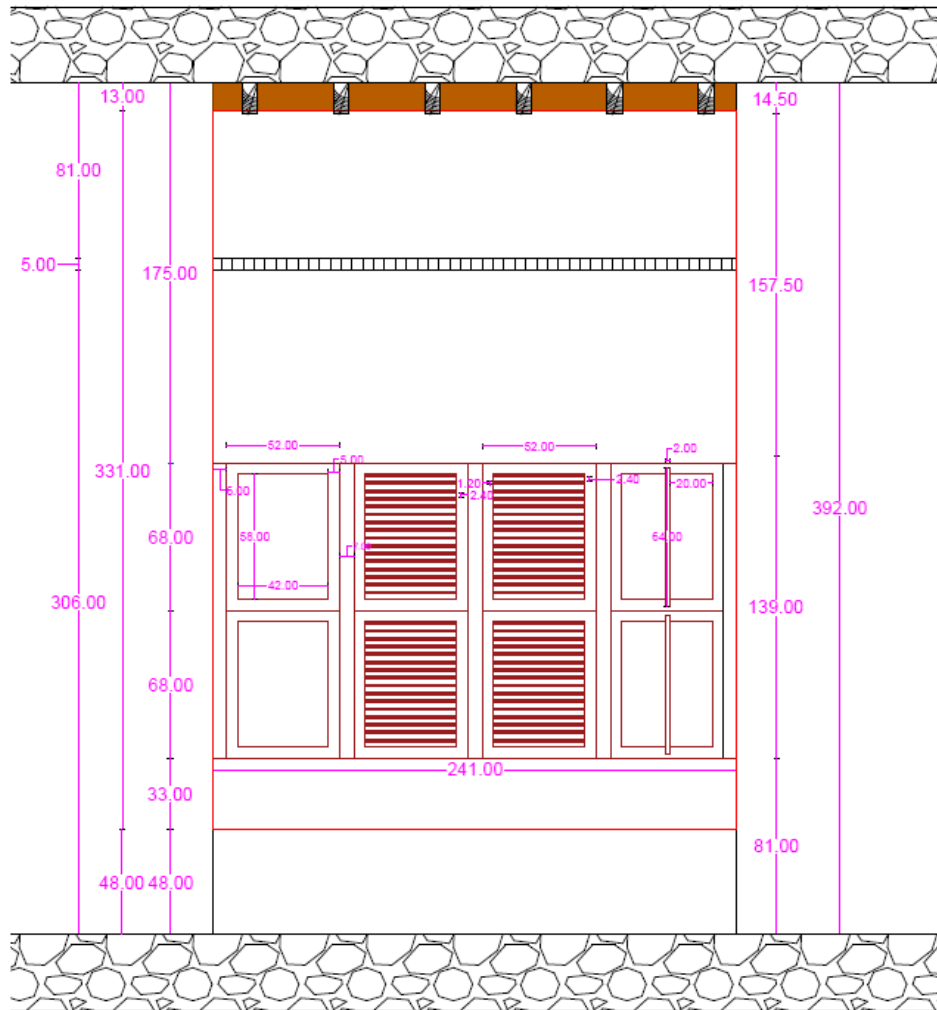
Figure 5-16 The front internal facade of the mashrabiya with dimensions
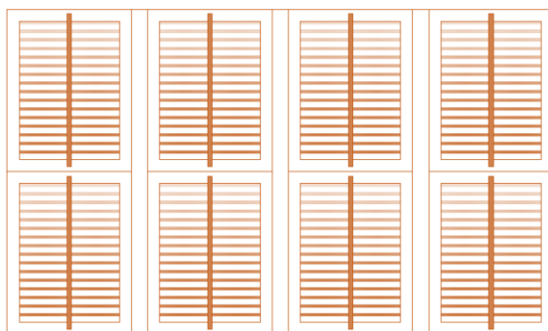
Figure 5-17 The internal elevation of the open Mash   Figure 5-18 The internal elevation of the closed Mash
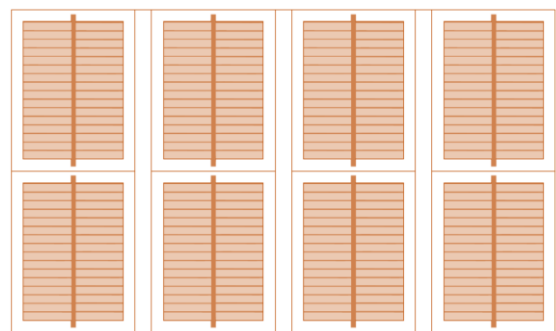
5.3.2 Fieldwork Experiments Aim and Objectives

To achieve the first part of this research aim, which is to investigate the effect of mashrabiya on the indoor thermal environment", two field experiments were conducted with different procedures and strategies. The first fieldwork aimed to investigate the effect of mashrabiya on the indoor environmental thermal comfort in a historical residential building in a hot climate in Jeddah, Saudi Arabia. The fieldwork was conducted during the summer 2018 from 4th August to 1st September, for 28 days in two similar rooms in Baeshen house.

The main objectives of this fieldwork were:

- To measure the accurate dimensions of all mashrabiya details.
- To investigate the effect of mashrabiya and the most critical factors affecting indoor thermal comfort.
- To determine the differences between indoor and courtyard based on specific measurements (air temperature, humidity, air velocity).
- To assess the performance difference and the impact between open and closed mashrabiya in terms of thermal comfort.
- To obtain data for use in calibrating the simulation model at a later stage.

After studying and analysing the fieldwork results of summer 2018 and the experience gained, it was found that mashrabiya needs to be more effective to improve the indoor thermal environment and achieve comfort. Therefore, another fieldwork was carried out to investigate the effect of mashrabiya on the indoor thermal environment and test the impact of integrating some passive evaporative cooling techniques with mashrabiya. It should be noted that despite that the climate of Jeddah is hot and humid, direct evaporative cooling with mashrabiya could be applied during the hot summer hours when the outdoor relative humidity levels were less than 50%. This fieldwork was conducted during July and August 2019. In this experiment, the field data of air temperature, relative humidity, globe temperature, and air velocity were collected for the same rooms as in the previous fieldwork 2018 during typical hot summer conditions when the outdoor temperature ranged between 40 and 41.6 °C in the afternoon. In addition, different passive evaporative cooling strategies were integrated with the mashrabiya: thermal mass, water pots, water spray, and cloth.

5.4 Base Case

5.4.1 Overview

The field study of the base case is one of the most important stages of the practical approach to achieving the aim of this research. Therefore, this field case was considered a pilot study and aimed mainly to assess the performance difference and the impact between open and closed mashrabiya on environmental thermal comfort.

5.4.2 Base Case Methodology

The fieldwork was carried out in the building in summer 2018 from 4 August to 1 September. The experimental investigations used calibrated digital instruments to monitor air temperature, relative humidity, air velocity, and globe temperature for two selected rooms and the courtyard (Table 5-2). In this study, the courtyard is an open land area adjacent to and west of the building, as shown in Figure 5-19.

All temperatures and relative humidity values were continuously monitored for 28 days from the first to the last day of the experiment, while the other measurements, air velocity, globe temperatures, and surface temperature, were taken on specific days and periods.

The devices used for monitoring the experiment are detailed in Table 5-3. Each instrument was placed in a particular position during the entire investigation period. Furthermore, the observed rooms and courtyard were not occupied, except for moments of setting the data loggers or carrying out some instantaneous measurements.

Table 5-2 Overview of the building and measurement equipment.

City | Location	Jeddah | 21° 29' 12.8" N 39° 11' 11.5" E		
Climate zone	Hot arid		
Building Type	Historical Residential Building		
Current use	Exhibition and Gallery (Ground and 1st floor)		
Instruments (Intervals)	Hot Wire Anemometer	1 min	Indoor, Out
	WBGT Data logger	1 min	Indoor
	Tinytag Plus 2 Dual Channel	1 h	Indoor, Out
	Tinytag View 2	1 h	Indoor, Out
	Dual Laser Infrared Thermometer	1 h	Indoor, Out
Measurements	Air Temperature, Globe Temperature, Relative Humidity, Air Velocity, Surface Temperature.		
Mashrabiya	Orientation: West / Mode: open-closed		
Materials	Wall: calcareous and coral stones Celling: Stones and Timber Mashrabiyas: Wood		

In the west part of the building, the selected rooms and the courtyard of this study are located. The first room (R1) with the open mashrabiya is located on the first floor, and the second room (R2) with the closed mashrabiya is on the second, as shown in Figure 5-20. Both rooms have the same conditions, except for the difference in height from ground level to each floor. The height difference between the room levels is about 3.5 m. Despite the difference in height from the ground between the rooms, which may affect the air velocity readings, it was neglected in this work because the mashrabiya was set closed in Room 2. Each room has one mashrabiya on the west wall and overlooks the courtyard, exposed to the prevalent wind and the Red Sea breeze. Besides, each room has three openings in each wall blocked to isolate and prevent adjacent rooms' influence.
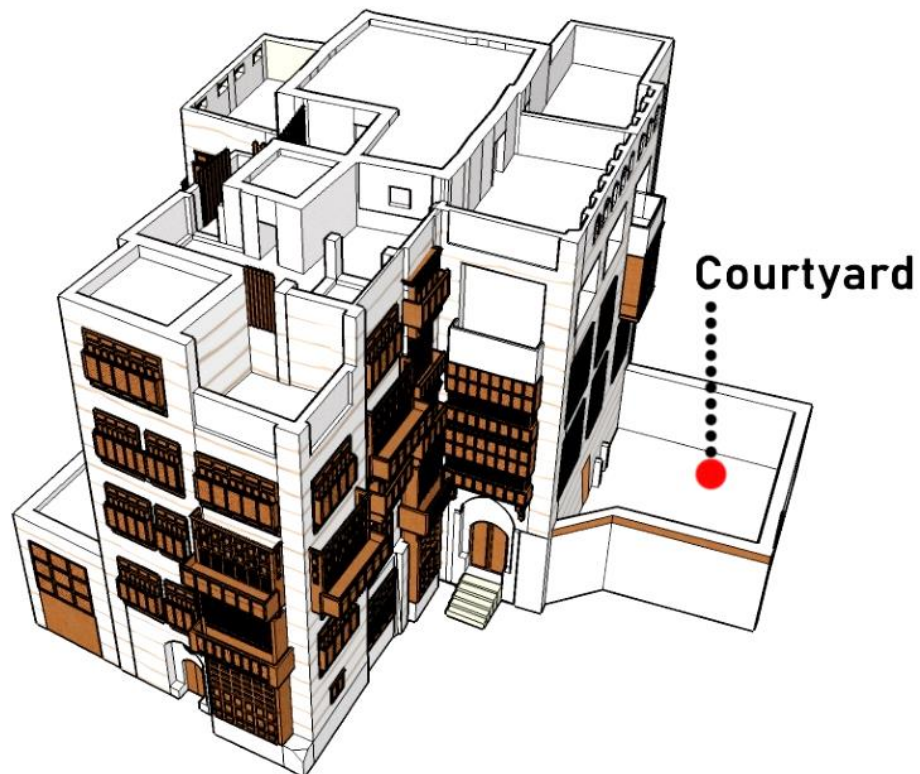
Figure 5-19 A 3D perspective of the building and the courtyard.

Table 5-3 The equipment used in the field work.

Number	Instrument	Parameters and range	Accuracy and resolution
3	Hot Wire Anemometer with Real-Time Data Logger #HHF2005HW	-Air volume and velocity -Range 0.2 to 20 m/s	±(10% + lsd) Full Scale ±0.8°C
2	WBGT Data Logger PCE-WB 20SD	- Wet Bulb Globe Temperature -Black globe temperature (TG) -Range 0 to 59°C	WBGT: ± 1 to 1.5°C TG: ± 0.6°C
2	Tinytag Plus 2 Dual Channel Temperature/Relative Humidity #TGP-4500	- Temperature range −25 to +85 C° -Relative humidity range 0 to 100%. -Suitable for outdoor use.	T: 0.01°C or better. RH: ±3.0% at 25°C
1	Tinytag View 2 Temperature/Relative Humidity Logger #TV-4500	- Temperature range from −25 to +50 C° -Relative humidity range 0 to 100%. -Suitable for indoor use	T: 0.02°C or better. RH: Better than 0.3% RH
1	Dual Laser Infrared Thermometer	-Surface Temperature -Rang − 50°C ~ 550°C temperature -Emissivity 0.10 to 1.0.	+/− 1 % of reading
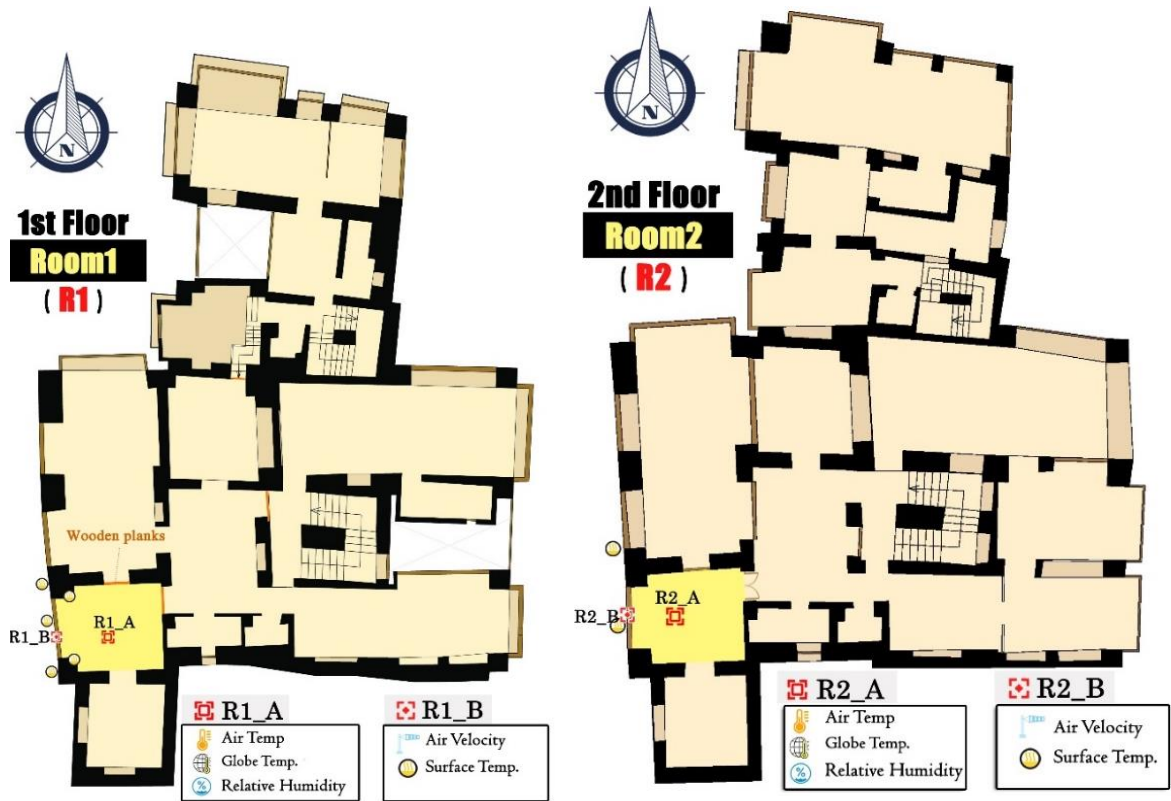
Figure 5-20 First and second-floor plans and the places of measurement.

The room dimensions are 4 m long, 3.6 m wide, and 3.9 m high, and the mashrabiya is 2.4 m wide × 3.1 m high. Four data loggers were used in each room to monitor air temperature, velocity, relative humidity, and globe temperature. In addition to that, a dual laser thermometer was used to measure the surface temperature of mashrabiyas and adjacent walls. In order to measure the surface temperature, grid points were placed in specific spots on the mashrabiya and its adjacent walls of R1, as shown in Figure 5-21.

Figure 5-21 The mashrabiya and grids in Room 1.

The data loggers for the air and globe temperatures in both rooms were at 0.6 m in height and 2 m away from mashrabiya on the basis of ASHRAE suggestions (ASHRAE, 2010b). At the internal edge of each mashrabiya at a level of about 1.1 m, airflow velocity data loggers were placed. During the test period, each room was monitored for air temperature, relative humidity, and the globe data loggers and anemometers were recorded during certain times of the day.

Three meters apart from the exterior building wall in the courtyard, two types of data loggers have been installed: Tinytag Plus and an anemometer. The Tinytag recorded outdoor Ta and RH from 4 August to 1 September 2018 at a level of around 1.7 m based on one of the levels recommended by the 2010 ASHRAE standards. The anemometer recorded specific periods of days and was placed at 0.1 m height and shaded by a table. On specific days and periods of the fieldwork, a dual laser infrared thermometer was used to measure the surface temperatures of the open mash and closed mash from inside and outside, including the adjacent wall of the mashrabiyas.

Figure 5-22 presents the experiment's timeline indicating the measurements from the first day "Set up" to the last day. The chart shows that the experiments monitored the outdoor and indoor air temperature" Ta" and relative humidity "RH" for the entire period. Also, the graph displays the monitoring days for the other measurements; air velocity "AV", globe temperature "Tg", and surface temperature "Ts".
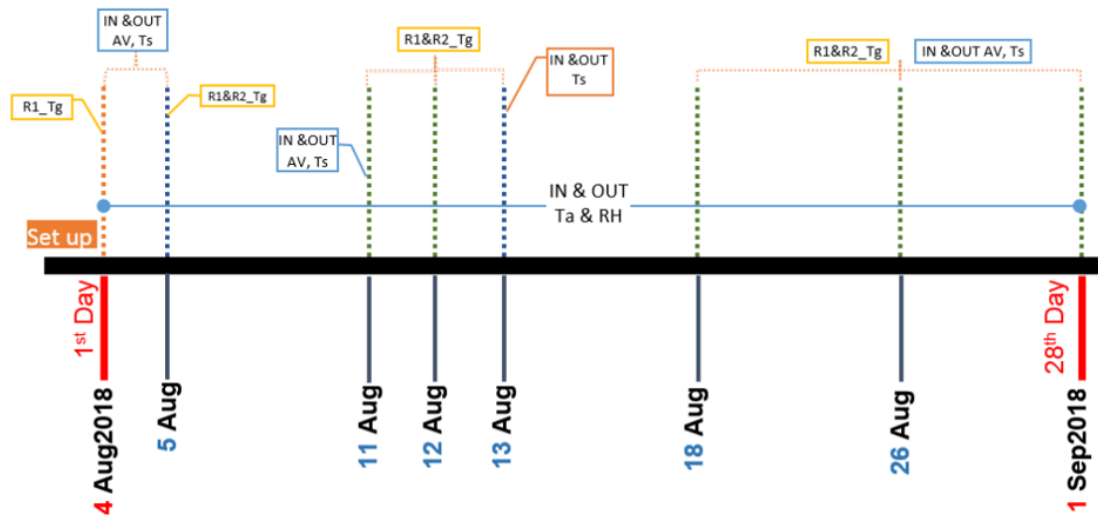
Figure 5-22 Timeline of the experiment.

5.4.3 Results and Discussion

This section presents the indoor and outdoor measurements data collected in this work. The results of the air temperature, air velocity, humidity, and surface temperatures will be presented and analysed in detail.

5.4.3.1 Indoor Air Temperature and Relative Humidity

Figure 5-23 presents the measurements of indoor and outdoor air temperature from 5 to 31 August. As observed, the thermal mass and the mashrabiya played an important role in regulating the indoor temperature during the high fluctuations where the temperature of Room 1 ranged between 32.2 and 38.5 °C, Room 2 from 32.5 to 38.4 °C, whilst there was a recorded high variation in the courtyard temperatures between 30.9 and 48.7 °C. The thermal mass and closed mashrabiya delayed the heat flux in Room 2 up to three hours per day, while the open mashrabiya in Room 1 reduced the time lag to one hour, as shown in Figure 5-24. However, the open mashrabiya allowed more airflow, which lowered the Room 1 temperature, especially during the afternoon, by up to 2.4 °C compared to Room 2. As observed in Figure 5-24, both rooms were able to keep the temperature below 38 °C when the outdoor

temperature peaked at 43.6–45.4 °C. This effect is again mainly attributed to the role of the building's total thermal mass. It can also be observed that night ventilation decreased the indoor air temperature up to 34 °C and contributed to lowering the excess heat and cooling the building fabric. Also, it helped to reduce and delay the peak time of the indoor temperatures.
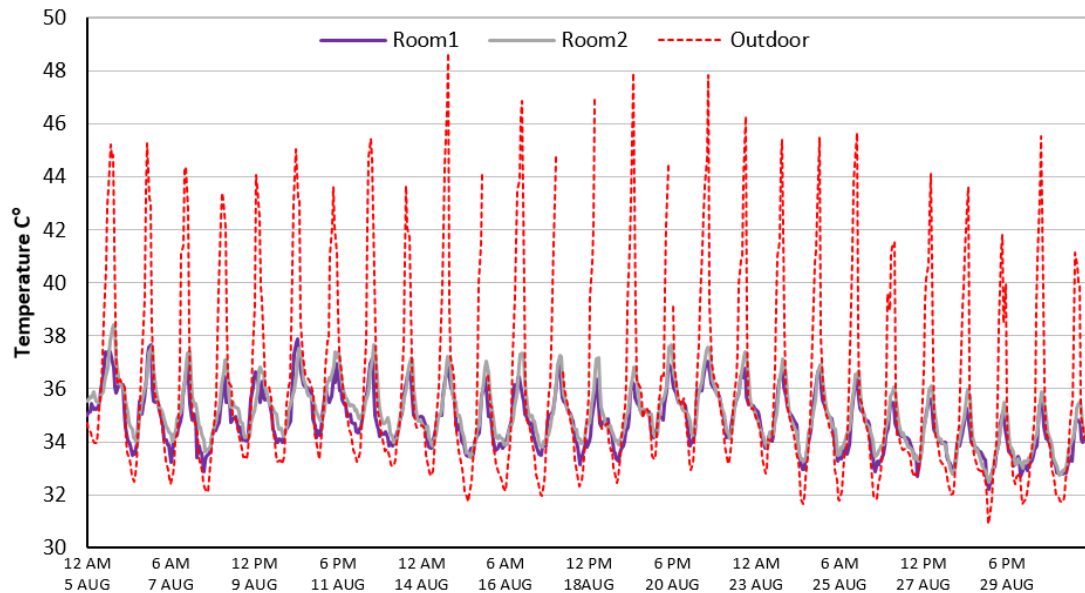
Figure 5-23 Indoor and outdoor air temperature from 5 to 31 August 2018.

The average air temperature and relative humidity results from the fieldwork measurements for the outdoor and selected rooms are shown in Table 5-4. The measurements were carried out from 4 August until 1 September 2018 for each space. All air temperature and relative humidity data were recorded for 24 h on all dates except the first and last day due to the researcher setting for the data loggers.

As shown in Table 5-4, 5 August recorded the highest average air temperature in both rooms while the outdoor recorded the hottest at 37.62 °C. In contrast, the lowest indoor air temperature averages were recorded on 29 August when the average outdoor air temperature reached the lowest at 37.62 °C. As occurred to the indoor air temperature from the outdoor air temperature, the rooms were affected by the outdoor relative humidity. The highest relative humidity in all spaces was on 31 August and the lowest on 23 August, with less than 3% variation rates. It should be noticed that opening the mashrabiya was beneficial for improving the air movement inside Room 1 and allowed more humidity and airflow, which helped relieve the heat better than Room 2 with the closed mashrabiya.
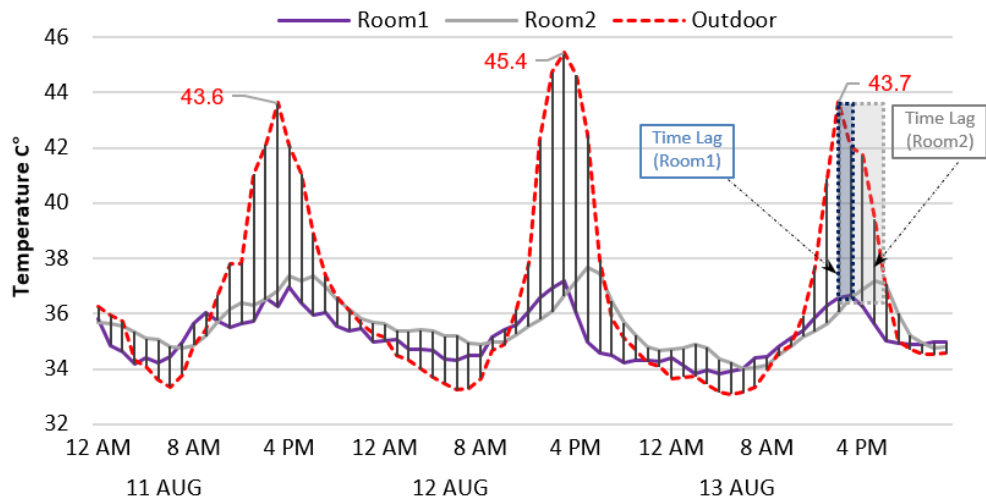
Figure 5-24 Hourly indoor and outdoor air temperature on 11, 12 & 13 August 2018.

Table 5-4 Daily average indoor and outdoor air temperature and relative humidity.

	Room1		Room2		Outdoor	
Date	Ta	RH	Ta	RH	Ta	RH
4 AUG	36.76	39.91	36.72	38.07	41.68	33.59
5 AUG	36.11	48.21	36.41	46.88	37.62	47.12
6 AUG	35.18	55.01	35.58	53.05	36.51	53.73
7 AUG	34.71	61.68	35.31	56.66	36.13	58.12
8 AUG	34.56	63.42	35.01	60.78	36.05	60.84
9 AUG	35.23	48.96	35.31	47.82	36.60	47.40
10 AUG	35.53	47.72	35.60	48.59	37.05	48.73
11 AUG	35.47	53.58	35.96	49.36	37.06	49.48
12 AUG	35.08	58.99	35.65	55.28	36.68	56.83
13 AUG	34.96	56.63	35.19	55.98	35.93	56.79
14 AUG	35.04	51.91	35.18	49.75	36.88	48.80
15 AUG	34.43	53.02	34.81	50.21	34.82	53.49
16 AUG	34.90	52.71	35.15	50.44	36.48	49.79
17 AUG	34.95	48.90	35.10	48.42	35.55	50.68
18 AUG	34.50	57.04	35.02	53.94	35.51	54.90
19 AUG	34.64	59.51	35.03	56.43	36.50	55.63
20 AUG	35.35	49.92	35.61	49.92	36.37	48.91
21 AUG	35.61	48.96	35.78	47.60	37.46	46.07
22 AUG	35.38	46.19	35.58	45.18	36.66	46.06
23 AUG	35.01	43.53	35.07	42.87	36.26	43.02
24 AUG	34.76	45.34	34.87	44.01	35.84	44.85
25 AUG	34.55	54.93	34.84	52.70	35.93	53.13
26 AUG	34.11	62.43	34.53	59.14	35.06	61.65
27 AUG	34.20	55.75	34.34	54.40	35.44	54.77
28 AUG	33.92	53.80	34.09	52.42	35.06	53.23
29 AUG	33.54	56.04	33.68	53.63	34.41	55.17
30 AUG	33.77	63.50	34.04	60.91	35.19	61.36
31 AUG	33.66	67.42	33.91	64.97	34.71	65.95
1 SEP	34.29	63.17	34.33	61.54	35.84	60.07

● Maximum Average Relative Humidity ● Maximum Average Air temperature
● Minimum Average Relative Humidity ● Minimum Average Air temperature

Figure 5-25a shows the relationship between average air temperature (Ta) and relative humidity (RH) in Room 1, Room 2 and the courtyard between 5 and 31 August 2018. As expected, the relative humidity decreases as the air temperature in both rooms increases and vice versa. The highest relative humidity was recorded on 31 August with a range of about 65 and 67.4% while the lowest was 43% on 23 August. Due to airflow into Room 1 through the open mashrabiya, R1 reduced more heat and allowed more relative humidity than R2.

The average daily indoor and outdoor absolute humidity from 5 to 31 August 2018 are presented in Figure 5-25b. The graph demonstrates that the absolute humidity rates in the rooms were affected by the outdoor absolute humidity. The rooms' averages of absolute humidity ranged between 16.8 and 25 g of moisture per cubic meter of air (g/m³) and in the courtyard from 18 to 25.5 g/m³.
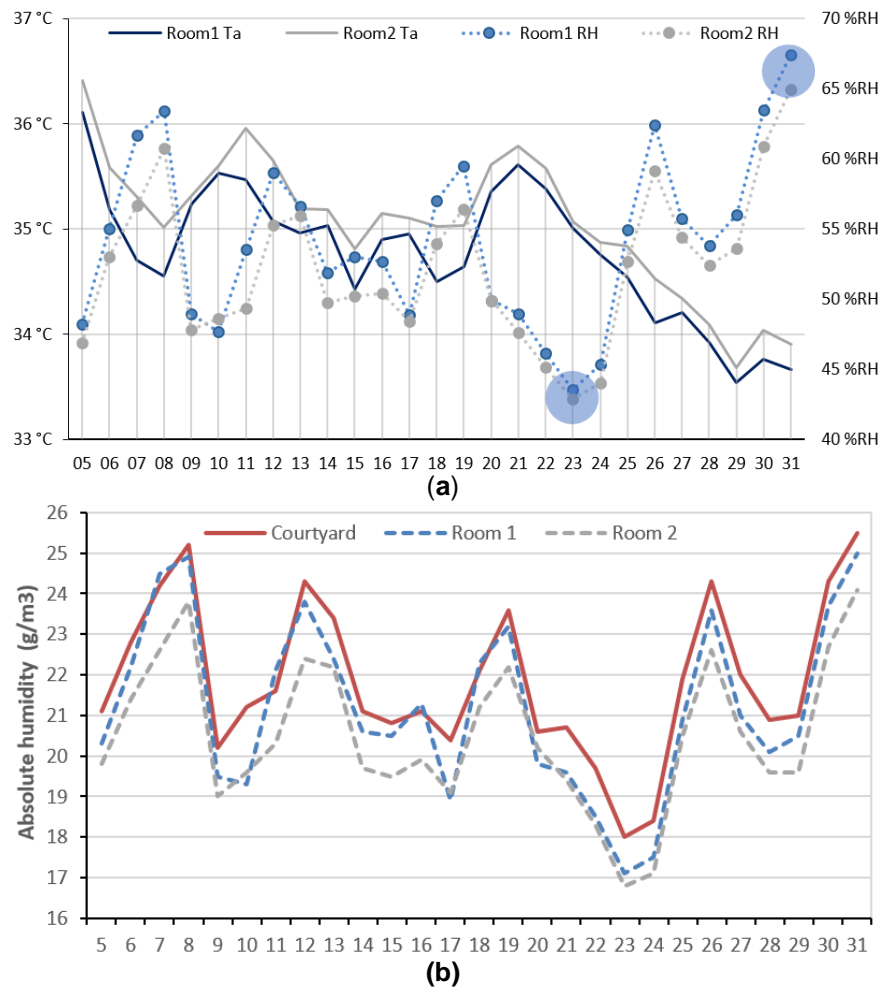
Figure 5-25 (a). Average air temperature and relative humidity for R1 and R2 from 5 to 31 August 2018; (b). The daily absolute humidity for each room and courtyard from 5 to 31 August 2018.

5.4.3.2 Indoor Air Velocity Results

Figure 5-26 demonstrates the frequency percentages and maximum indoor and outdoor air velocity during a specific period of days. The monitoring days included 4–5,11–12, 18, 26 August and 1 September during the afternoon hours. It should be pointed out that the room's airflow velocities were measured at a specific point at each mashrabiya, as mentioned earlier in the method part. Moreover, the mashrabiya for Room 2 was not completely closed due to the difficulty of moving the tilting rods, which caused the amount of natural daylight to pass and the airflow through the openings of the semi-open mashrabiya slats. As for the courtyard air velocity, readings may havbeen influenced by several factors such as the anemometer's position, proximity to ground level, and some surrounding obstacles.

Figure 5-26 displays the ranges of indoor and outdoor air velocity that vary from 0 to 8.1 m/s in the courtyard, 0 to 6.9 m/s in Room 1, and 0 to 1.1 m/s in Room 2. According to the chart, the highest frequency value of air velocity was in Room 1 with a speed of 2 m/s (18.27%), courtyard 0.5 m/s (28.9%) and in Room 2 by 0 m/s (90.44%). In general, the air velocity rates through the mashrabiya of Room 1 were greater than courtyard and Room 2 due to the opening the mashrabiya, which admitted more airflow without being affected by obstacles as in the courtyard or when been closed as the mashrabiya of Room 2.
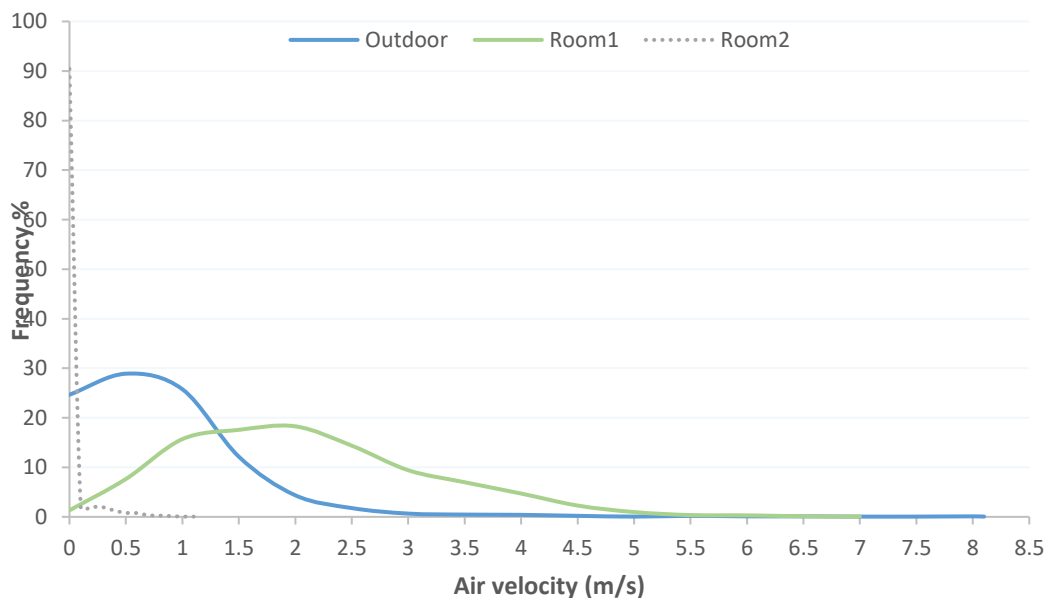
Figure 5-26 Frequency of indoor and outdoor air velocity measurements.

5.4.3.3 Statistical Analysis of Indoor and Outdoor Measurements

Table 5-5 presents a brief statistical comparisons between the air velocity (Av) and air temperature (Ta) for; the open mashrabiya in R1, the closed mashrabiya in R2, and the courtyard. Dates included in this table were only restricted to days that covered the same period for monitoring both air temperature and velocity. The measurement times of each day covered the period from noon to 3:30 p.m. The maximum air velocity values of the R1 range from 4.50 to 6.90 m/s, courtyard from 1.60 to 5.20 m/s, and R2 from 0 to 1.10 m/s. This indicates that the room with open mashrabiya has higher air velocity than the courtyard, which is the benchmark, and the room with closed mashrabiya. The lowest standard deviation values were calculated in R2 and the highest in R1, which mean that there is inconsistency in R1 in air velocity compared to R2 and the courtyard. This may be due to the low air velocity in R2 and the courtyard, which is equivalent to zero for some periods.

The maximum Room 1 air temperature ranges from 36.1 to 39.3 °C, R2 from 40 to 43.4 °C, and the courtyard from 43.2 to 48.3 °C. The average air temperature measurements of the R1 range from 33.8 to 37 °C, R2 from 37 to 40.9 °C, and courtyard from 37 to 41.8 °C. The lowest value of minimum air temperature was monitored in R1 at 32.7 °C. From this, it can elicit that a higher air velocity can improve the air temperature. For example, the lowest standard deviation values have been calculated in R1 and the highest in the courtyard. The lowest standard deviation values have been calculated in R1 and the highest in the courtyard. This means R1 have more consistency in air temperature and the lowest in fluctuations. However, the room with open mashrabiya shows better air velocity and air temperature than the courtyard and Room 2.

Table 5-5 Statistical comparisons between indoor and outdoor air velocity and temperature.

Space	Date	Air velocity (m/s)				Air Temperature (C°)			
		Max	Avg	Min	S.D.	Max	Avg	Min	S.D.
Room1	04-Aug-18	5.20	2.37	0.30	0.97	39.3	37.0	35	1.0
	05-Aug-18	4.50	2.03	0.00	0.89	38.1	37.0	35.8	0.5
	11-Aug-18	6.90	1.71	0.00	1.14	38.4	35.4	33.1	0.8
	18-Aug-18	6.40	2.63	0.10	1.13	36.6	34.1	32.7	0.7
	26-Aug-18	5.30	2.08	0.20	0.76	36.1	34.6	33.1	0.6
	01-Sep-18	4.80	2.17	0.00	1.03	36.7	34.8	33.1	0.8
Room2	04-Aug-18	1.10	0.27	0.00	0.26	41.8	39.3	36.9	1.6
	05-Aug-18	0.10	0.00	0.00	0.01	43.4	40.9	38.4	1.1
	11-Aug-18	0.00	0.00	0.00	0.00	41.6	38.1	35.8	1.7
	18-Aug-18	0.20	0.01	0.00	0.03	40.2	37.0	34.6	1.5
	26-Aug-18	0.00	0.00	0.00	0.00	40	37.5	35.0	1.3
	01-Sep-18	0.70	0.06	0.00	0.12	40	37.8	36.3	1.0
Courtyard	04-Aug-18	2.80	0.78	0.00	0.63	48.3	41.8	36.8	2.2
	05-Aug-18	3.20	0.71	0.00	0.58	46	40.7	37.7	1.4
	11-Aug-18	3.70	0.45	0.00	0.50	43.2	37.0	34.3	1.6
	18-Aug-18	3.40	0.80	0.00	0.63	46.4	38.9	34.9	2.4
	26-Aug-18	1.60	0.51	0.00	0.38	46.1	39.6	35.9	1.8
	01-Sep-18	5.20	1.02	0.00	1.06	45	38.4	33.4	2.5

Table 5-6 presents the air temperature (Ta) and air velocity (Av) correlation coefficient for Room 1 and the courtyard on specific dates during the same period, from 12 p.m. to 3:30 p.m. The coefficient correlation was used here to determine the strength of the relationship between the relative movements of air temperature and air velocity where -1 expresses a strong negative correlation whilst 0 there is no linear relationship or weak correlation between the variables. It can be noticed from the table that the relationships between the variables Av and Ta in both spaces have a negative correlation. In Room 1, the correlation coefficient ranges from −0.19 to −0.54, which can be evaluated as a weak to moderate correlation. In comparison, the correlation coefficient in the courtyard ranges from −0.10 to −0.68, which can be evaluated as a weak to strong correlation. It may be concluded from this table that as air velocity increases, the indoor air temperature may decrease.

Table 5-6 The correlation between the air temperature and air velocity for Room 1 and the courtyard.

	4 Aug	5 Aug	11Aug	18 Aug	26 Aug	1 Sep
Room 1	− 0.19	− 0.45	− 0.5	− 0.05	− 0.19	− 0.54
Courtyard	− 0.59	− 0.68	− 0.62	− 0.69	− 0.1	− 0.67

Table 5-7 provides a statistical summary of indoor and outdoor averages and ranges of air temperature, relative humidity, air velocity, and indoor globe temperatures. The range (RNG)

values in the table refer to the difference between each space's maximum and minimum readings for a day. The table only displays the days when all thermal measurements were taken for all observed spaces. It should be noted that globe temperature (Tg) readings in R2 on 4&5 August were not listed due to an issue in the inserted SD card memory.

The highest outdoor temperature average was recorded at 41.7 °C on 4 August with a range of 19.6 degrees, as can be observed from the table. It is worth noting that some of the readings may have been affected somewhat because the data logger was not shaded properly during some periods of the day. However, the outdoor temperature range for 4 August was reflected in the indoor values as both rooms recorded the highest average and range on the same day. On average, the indoor air temperature, Room 1 was lower by 0.5°C than Room 2.

The average globe temperature values (Tg) for both rooms were close to the average air temperature, indicating the absence of low thermal radiation. Furthermore, the variations between indoor air temperature and globe temperature measurements have not exceeded two degrees.

The highest relative humidity range was 45% in the courtyard on 12 August, while the highest average relative humidity was recorded on the last day of the experiment at 63.2% in Room 1, 61.5% in Room 2, and 60.1% in the courtyard. Despite the higher relative humidity ranges in the courtyard, the relative humidity in the rooms on average was higher than the courtyard, beneficial for thermal comfort. This behaviour was attributed to the building envelope that reduced temperature fluctuations, thus leading to more moisture stability inside the building.

The highest averages and ranges for air velocity were primarily recorded in Room 1 due to the open mashrabiya facing air directly without being affected by obstacles or closure. Surface temperature values were measured for the open mashrabiya and closed mashrabiya from inside and outside in addition to the surrounding surfaces of the open mashrabiya, as shown in the subsequent tables. All averages of measuring points at various positions, days and times are displayed in Table 5-8, Table 5-9, Table 5-10. The points represent the averages of measurement areas for the open mashrabiya (Mash1), closed mashrabiya (Mash2) and walls beside each mashrabiya from inside and outside (Figure 5-27 and Figure 5-28).

The measurements were monitored on 4 August at about 1:00, 2:00, 3:00 p.m. also at noon on 5, 11, 18, 26 August and 1 September, while monitored at about 6:00 p.m. on 13 August 2018. As shown in the tables, surface temperature measurements increased and reached the highest values, usually at 3 p.m., while the entire facade was exposed to direct sunlight.

Table 5-7 Summary of thermal conditions during different days of the experiment.

Date	DESC	T (°C)			Globe Temperature (°C)		RH (%)			Av (m/s)		
		R1	R2	Out	R1	R2	R1	R2	Out	R1	R2	Out
4 AUG	AVG	36.8	36.7	41.7	37.0	n/a	39.9	38.1	33.6	2.4	0.3	0.8
	RNG	3.8	3.9	19.6	3.9	n/a	27.7	13.8	29.1	4.9	1.1	2.8
5 AUG	AVG	36.1	36.4	37.6	36.8	n/a	48.2	46.9	47.1	2.0	0	0.7
	RNG	2.3	3	11.3	2.9	n/a	23.1	17.5	29.3	4.5	0.1	3.2
11 AUG	AVG	35.5	36.0	37.1	35.0	35.9	53.6	49.4	49.5	1.7	0	0.4
	RNG	2.8	2.6	10.3	3.6	3.2	31.3	28.3	37	6.9	0	3.7
12 AUG	AVG	35.1	35.7	36.7	34.9	35.7	59.0	55.3	56.8	0.8	0	0.9
	RNG	2.9	3	12.2	3.4	3.2	23.9	19.6	45	2.7	0	8.1
18 AUG	AVG	34.5	35.0	35.5	34.4	35.5	57.0	53.9	54.9	2.6	0	0.8
	RNG	3.2	3.3	14.6	7.3	2.2	34.7	30.9	37.4	6.3	0.2	3.4
26 AUG	AVG	34.1	34.5	35.1	34.7	35.3	62.4	59.1	61.7	2.1	0	0.5
	RNG	2.6	2.6	9.7	1.7	1.6	28.3	28.8	35.1	5.1	0	1.6
1 SEP	AVG	34.3	34.3	35.8	35.0	35.4	63.2	61.5	60.1	2.2	0.1	1.0
	RNG	3.4	2.8	9.4	1.2	1.6	16.2	9.4	25.5	4.8	0.7	5.2

Table 5-8 Surface temperature measurements of Room 1, Room 2, and the external surfaces of Mash 1 and its surroundings on 4 and 5 August 2018.

			4 Aug			5 Aug			
		Time	1 p.m.	2 p.m.	3 p.m.	Noon.	1 p.m.	2 p.m.	3 p.m.
Room 1	Above Mash1	A M1	38.0	38.9	39.8	38.2	38.2	38.1	38.6
	Middle Mash1	B M1	38.1	39.2	40.2	39.2	38.4	38.8	39.8
	Bottom Mash1	C M1	37.3	37.5	38.8	37.8	37.7	38.0	38.4
	Right Wall Mash1	WA M1	36.9	36.7	38.3	38.4	37.7	37.3	37.9
Room 2	Left Wall Mash1	WB M1	36.7	36.7	38.1	38.3	37.8	37.2	37.7
	Above Mash2	A M2	39.0	39.4	41.0	42.0	41.0	40.6	41.5
	Middle Mash2	B M2	40.0	41.5	44.0	43.0	41.5	42.0	43.8
	Bottom Mash2	C M2	37.0	39.0	45.8	42.0	40.5	40.2	41.2
	Right Wall Mash2	WA M2							
	Left Wall Mash2	WB M2							
External Surfaces	O Above Mash1	A O	47.0	49.0	51.0	49.0	47.0	49.5	53.0
	O Middle Mash1	B O	49.0	50.0	55.0	47.0	49.0	47.0	50.0
	O Bottom Mash1	C O	43.0	43.0	45.0	46.0	47.0	49.0	49.0
	O Below Mash1	W O				43.0	42.0	44.0	44.0	45.0
	Out Right Wall Mash1	OWR M1							
	Out Left Wall Mash1	OWL M1							
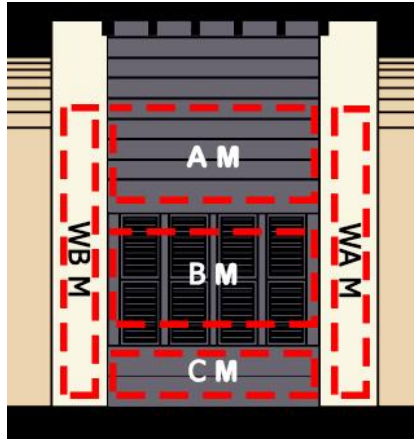
Temperature °C
36
55

Figure 5-27 Interior measurement zones on the mashrabiya and abbreviated names.
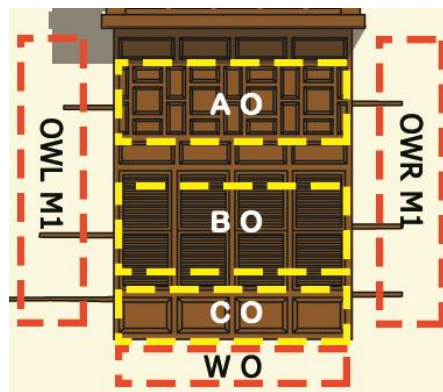
Figure 5-28 Measurement zones and abbreviated on the Mash1 from outside.

Table 5-9 Surface temperatures of Room 1, Room 2, and the external surfaces of Mash 1 and its surroundings on 11, 13 and 18 August 2018.

		11 Aug				13 Aug		18 Aug		
	Time	Noon.	1 p.m.	2 p.m.	3 p.m.	6 p.m.	Noon.	1 p.m.	2 p.m.	3 p.m.
Room 1	A M1	36.5	36.1	35.4	35.9	36.9	35.0	35.1	35.2	36.3
	B M1	36.4	35.9	35.7	36.5	35.9	34.4	35.1	36.3	37.1
	C M1	33.7	36.6	37.1	36.2	37.2	35.4	35.5	35.7	36.0
	WA M1	36.5	36.0	36.4	35.2	36.0	35.5	35.4	35.6	35.6
	WB M1	36.5	36.2	36.5	35.2	36.0	35.6	35.5	35.6	35.6
Room 2	A M2	38.0	37.3	41.3	41.4	35.9	36.0	36.0	39.0	40.4
	B M2	38.4	37.5	40.8	43.4	40.0	36.0	36.3	40.0	42.0
	C M2	37.7	37.1	40.5	40.8	39.2	35.8	35.8	38.4	39.3
	WA M2			40.0	39.2	38.0	36.2	35.9	37.8	38.0
	WB M2			40.0	39.2	38.0	36.1	35.8	37.7	37.9
External Surfaces	A O	42.0	43.0	49.0	52.0	41.0	39.5	46.0	49.0	57.0
	B O	40.0	43.5	46.5	50.0	38.0	40.8	47.0	47.0	50.0
	C O	38.0	41.0	44.0	46.0	40.0	41.0	44.0	43.0	52.0
	W O	37.0	39.9	42.5	43.0	38.0	39.0	41.0	41.0	42.0
	OWR M1	38.75	39.9	43.75	44.35	37.65	38.65	39.7	41.95	44
	OWL M1	39.4	39.35	43	44.25	37.6	38.5	39.8	41.95	43.8

Table 5-10 Surface temperatures of Room 1, Room 2, and the external surfaces of Mash 1 and its surroundings on 26 August and 1 September 2018.

	Time	26 Aug				1 Sep			
		Noon.	1 p.m.	2 p.m.	3 p.m.	Noon.	1 p.m.	2 p.m.	3 p.m.
Room 1	A M1	34.8	35.9	36.4	36.0	36.7	35.7	34.7	35.8
	B M1	34.7	36.4	36.7	37.3	37.6	36.0	35.9	37.5
	C M1	35.1	35.7	36.1	35.5	36.1	35.2	35.4	36.3
	WA M1	35.3	35.4	35.7	35.1	35.9	34.8	35.6	36.1
	WB M1	35.2	35.5	35.8	35.1	36.0	34.9	35.3	36.1
Room 2	A M2	35.5	36.3	37.3	39.2	37.2	36.9	39.9	40.5
	B M2	36.0	37.0	39.7	41.0	37.9	37.5	40.8	42.8
	C M2	35.4	36.1	37.1	38.5	36.7	36.5	39.0	39.7
	WA M2	35.8	35.8	36.2	37.2	36.3	35.7	38.6	38.3
	WB M2	35.5	35.7	36.3	37.1	36.2	35.8	38.6	38.1
External Surfaces	A O	42.7	43.5	49.0	52.0	43.9	45.5	49.8	51.0
	B O	41.0	42.0	44.0	50.0	42.0	43.8	47.0	48.0
	C O	40.0	45.0	49.0	53.0	43.0	46.0	48.5	52.0
	W O	39.0	39.5	39.3	41.0	38.5	39.0	41.0	40.7
	OWR M1	39.5	39.5	41	42	40.2	40.7	42	42.5
	OWL M1	39.5	39.3	41	41.8	40.6	41	41.7	41.5

Temperature °C
34
53

Moreover, Figure 5-29 shows the inside and outside average surface temperature in the middle area of the open mashrabiya and adjacent sidewalls on different days. It is important to clarify that the western facade, which includes the exterior frames of the tested mashrabiyas, is not exposed to direct sunlight during the measurement times until about 12.30 p.m. 55 °C the maximum value was recorded on the external surface of the open mashrabiya at 3:00 p.m. on 4 August while the minimum was 34.3 °C on the internal surface of mashrabiya at noon on 18 August. It can be noticed that surface temperatures of the exterior wall around the open mashrabiya absorbed less heat than the exterior surface of the mashrabiya, indicating the benefit of the properties and colour of the plaster. Although the outside wall surface temperature was between 37 °C to 45 °C, the heat gain in the rooms was reduced by the building's thermal mass, where the temperatures ranged from 34.8 to 38.4 °C on the internal surface of the wall. From Figure 5-29, it can be noticed that the outside surface temperature of the wall and the mashrabiyas' external surface become equal during the sunset with a temperature of around 38 °C.
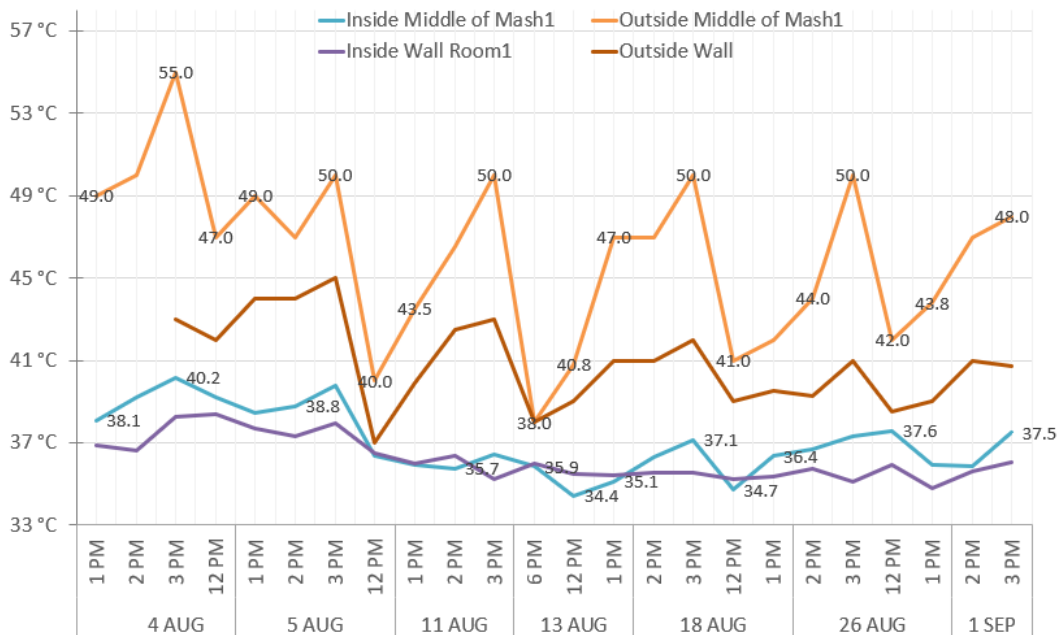
Figure 5-29 The surface temperatures of the open mashrabiya and wall surface inside and outside.

5.4.4 Thermal Comfort Assessment

As part of the study of the performance of the mashrabiya, it was important to assess the impact of the mashrabiya on indoor thermal comfort. Multiple methods and equations can be used to calculate the temperature of indoor comfort. Although ASHRAE 55 is considered a master guide, the outdoor temperature averages of less than 10 °C or higher than 33.5 °C are not considered. As the average outdoor temperature of this building was above this range, another method was used to evaluate the comfort temperature for passive buildings with the equation of Nicol and Humphreys (Nicol and Humphreys, 2002) to estimate comfort temperature in free-running buildings as described below:

$$Tc = 13.5 + 0.54T_o \quad (3.3)$$

where Tc is the comfort temperature, and T_o is the monthly outdoor air temperature average. This study considered the average outdoor temperature measured during the experiment only, which was 36.2 °C. Therefore, the comfort temperature for this case is 33 °C, depending on the equation. It is worth pointing out that Pakistani participants felt comfortable at indoor temperatures around 33 °C in the Nicol and Humphrey field study. The paper also stated that the workers changed their clothing during the tests and used fans of air movement.

Figure 5-30 shows the rooms' level of comfort based on the calculated comfort temperatures and total measurements for both rooms. Each bar represents measurements of the complete

room temperature for each day and the required degree to achieve comfort. The left-axis 0 value in the graph is equivalent to the calculated comfort temperature of 33 °C, which means the values equal or above 0 are considered within the comfort zone, while the values below 0 have not achieved this.

It is clear from the chart that the temperatures inside the R1 typically were closer to the level of comfort and better than R2 by 0.3 degrees on average. In any case, the decrease in outdoor temperatures to below 33 °C, contributed to improving the indoor temperatures and reaching the moderate temperature in some of the experiment days.
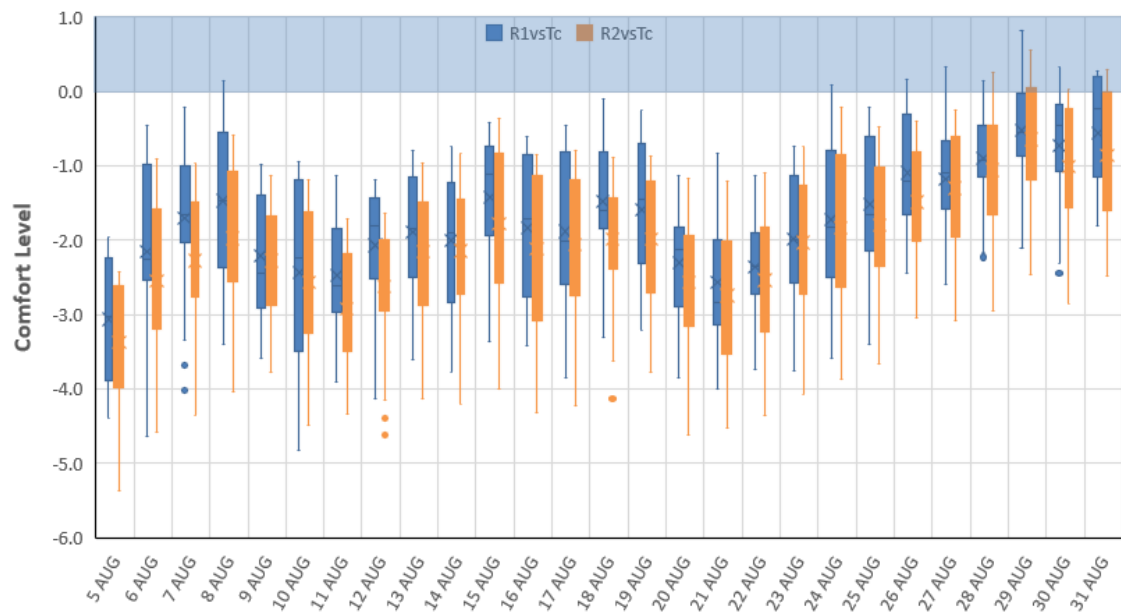
Figure 5-30 Rooms temperatures as compared to comfort temperature over the experiment days.

As shown in Figure 5-31, when the outdoor air temperature in the courtyard was below 32 °C, both rooms achieved comfort between 4 and 8:30 a.m. on 29 August. Overall, the rooms were able to achieve comfort between 3 and 7 a.m. during experiment days with the effect of night ventilation and the lower outdoor temperatures. It is important to note that the experiment was conducted in the worst climate situations, where August represents the highest temperature average of the year. Consequently, the effect of opening up the mashrabiya or applying other passive cooling methods will often provide better impacts in the mild seasons.
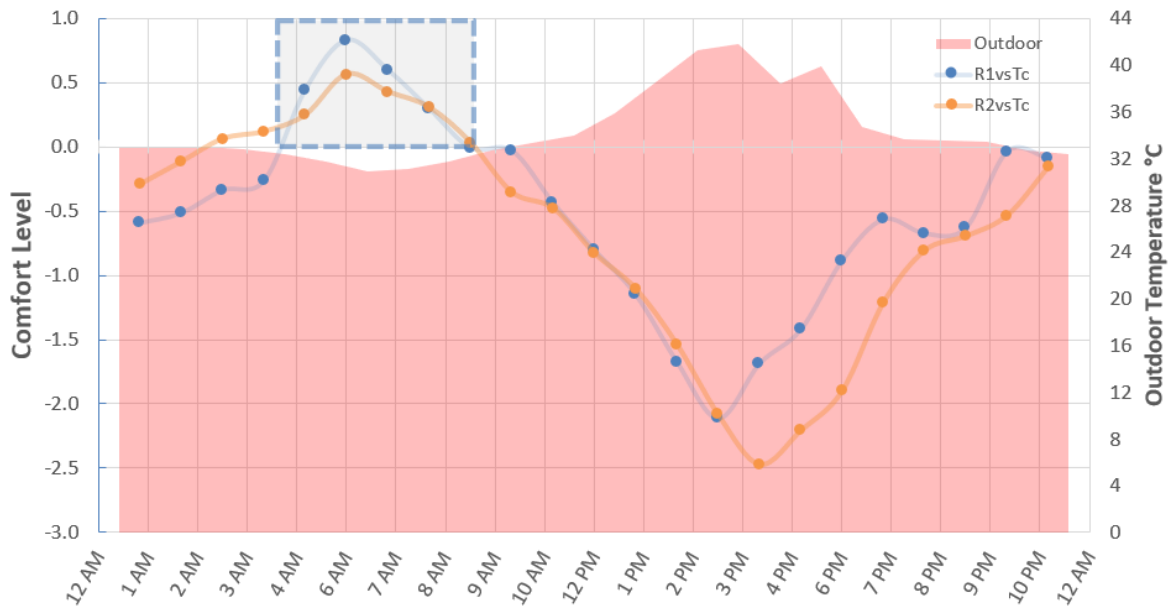
Figure 5-31 The hourly outdoor temperature on 29 August and the comfort rates of each room.

5.4.5 Limitations

Although the open mashrabiya has shown some positive effects on Room 1 compared to Room 2, there was a need to use some passive cooling methods to improve comfort during this hot weather. The study evaluated thermal comfort based on environmental factors only, without covering personal factors. That is because the building is currently not inhabited, and the difficulty of engaging people in this type of experiment in these climatic and spatial conditions. Due to the limited time and the available equipment, the indoor air velocity in the rooms was measured at one specific point in each mashrabiya. It should also be noted that the outdoor air velocity may have been affected by several factors, such as the position of the anemometer, its height above ground level, and some surrounding obstacles.

5.4.6 Summary

The field study was conducted during a typical hot summer month with two different modes: open and closed mashrabiya. This field study demonstrated that opening the mashrabiya allowed more airflow into the room during the day and reduced the indoor temperature by up to 2.4 °C as compared to the closed mashrabiya. Besides, the building envelope played an important role in preventing the high fluctuation of the indoor air temperature, where the fluctuation of the rooms air temperature ranged between 2.1 °C and 4.2 °C compared to the outdoor temperature, which recorded a fluctuation between 9.4 °C and 16 °C. The indoor

thermal comfort evaluation demonstrated that Room 1 typically were near to the temperature comfort of 33 °C and better than Room 2 by 0.3 degrees on average, where opening the mashrabiya allowed more airflow into Room 1 during the day, which helped reduce the room air temperature better than the performance of the closed mashrabiya in Room 2.

These data provided a better general understanding and conclusion of the mashrabiya concept and its effectiveness on thermal performance and thermal comfort under these hot conditions. However, more studies and tests were needed on the mashrabiya by combining it with various passive strategies to improve its thermal performance, which will be explained in the next section.

5.5 Integration of Passive Evaporative Cooling with Mashrabiya

5.5.1 Overview

After the first field study and analysing the results, it was necessary to carry out another test to evaluate and validate the performance of the mashrabiya to gather more data for two different conditions under the standard mode: a) both mashrabiyas closed, b) one mashrabiya open and other closed. After that, passive evaporative cooling strategies" have been integrated with mashrabiya to improve the effect of mashrabiya performance on the indoor thermal environment and comfort. It This evaporative cooling mode included three different techniques integrated with mashrabiya; water pots or jars, water spray, and wetted cloths. Along with the results of each stage, this field study includes an assessment of thermal comfort, limitations and an overview summary of this chapter.

5.5.2 Standard Mode

In this phase, the monitoring started on 30 July 2019 after closing the mashrabiya in both rooms and setting the measurement devices. The study aimed to set the same conditions of the mashrabiya to ensure that a valid comparison can be made in the second part of this study. This part of the experiment includes two periods: 1) closing mashrabiya in both rooms from 30 July to 1 August 2019 and 2) the mashrabiya in R1 was open while the mashrabiya in R2 was left closed until the end of the fieldwork.

It is essential to clarify that the mashrabiya in both rooms during the "close mode", were not fully closed due to the difficulty in moving the tilt rod of some panels. Table 5-11 shows the opening and closing of each panel in the mashrabiyas. It is shown that the mashrabiya mainly was fully closed, and some would be semi-open during the close configuration. While the configuration of the R1 Mash was fully open by approximately 62.5% and 12.5% semi-open.

Table 5-11 Configurations of the mashrabiyas in close and open mode

O: Open
Semi-open
•: Closed

R1 Mash (Closed)

O: Open
Semi-open
•: Closed

R1 Mash (Open)
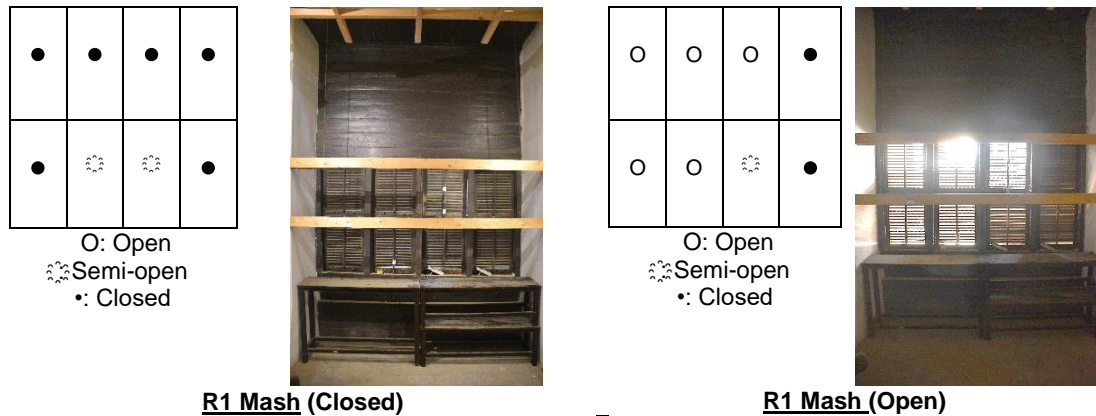
Since the building's thermal mass plays a significant role in influencing the thermal performance inside the building, it was taken into account in this study and thus determined the actual level of influence on interior spaces in the first stage of the experiment. In this experiment, the external walls are the main thermal mass component, as the rooms are not exposed to any direct sunlight except the western wall, including the mashrabiyas.

5.5.3 Evaporative Cooling Mode

In this work stage, selected passive evaporative cooling techniques were integrated into mashrabiya to improve the indoor thermal environment and enhance comfort. This stage of the evaporative cooling technique can be divided into three phases: water pots, water spray, and wetted curtains or cloth. Each stage represents a different method of integrating passive evaporative cooling into mashrabiya.

The use and applying the water pots in this work were based on its connection to the mashrabiya, where it was known in the past to place small jars in front or behind the lattice screen of a mashrabiya to cool the air through the evaporation effects. Schiano-Phan (2004) mentioned that the use of clay and porous jars in passive evaporative cooling is an ancient system known in the vernacular architecture of hot regions. Evaporation occurs from porous pots of water placed in the mashrabiya, which cool the jars' water inside the building as well,

and wherever the humidity is low, evaporative cooling is more effective (Lechner, 2014). Figure 5-32 illustrates that some air passes through the mashrabiya slats to the inside while the (A) pots are placed behind the mashrabiya. The water seeps through the jar filled with water and keeps the outside of the jar permanently moist. When air passes over the surfaces of jars, the water evaporates and absorbs heat energy, cooling the passing air.
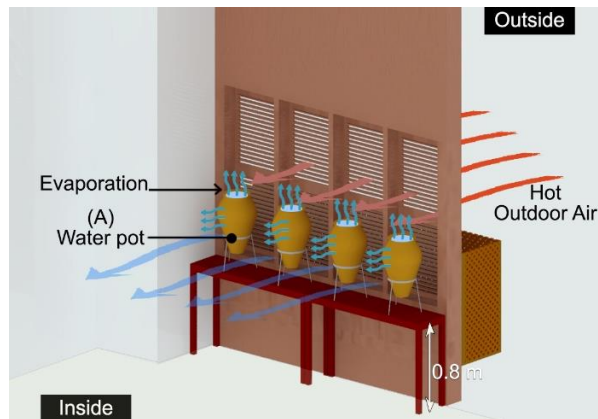
Figure 5-32 The water pots and the potential effect on air flow heat

The second evaporative cooling strategy integrated into mashrabiya was water spray. This strategy of direct evaporative cooling depends on spraying water on the mashrabiya panels; the wooden slats of the mashrabiya absorb some water, while some portion is volatile in the air (. This strategy has been used widely in several studies, such as Kang and Strand (2018), Morales et al. (2021) Alwetaishi et al. (2020), Del Rio et al. (2019), and has proven its efficiency. Accordingly, this technique was selected to be incorporated with mashrabiya and test its effect on the indoor thermal environment in this case. For the third evaporative cooling strategy, the researcher was aspired to target the same target as the previous strategies but in a different method. Although hanging wet clothes are usually used to dry them, some researchers have integrated them with wind catchers such as Noroozi and Veneris (2018), Bahadori et al. (2008), and it demonstrated its advantage in improving the indoor thermal environment compared to the traditional wind towers. Generally, this technique depends on dipping the cloth or fabric in cold water and then hanging it in front of the open mashrabiya. When the hot breeze passes through the wet cloth, the water of the cloth will evaporate. This will help reduce the air temperature of the breeze and thus improve the room temperature.

Figure 5-33 presents the actual test setup for each technique and the 3D schematics. During all phases, the R1 Mash was open while the R2 Mash remained closed. Hence, the configuration of the mashrabiya in R1 and R2, as illustrated previously in Table 5-11. The monitoring of this stage started at 12:10 p.m. on 5 August to 4:30 p.m. on 8 August 2019. The pots or jars were placed on a table 80 cm high facing the bottom panels of R1 Mash. Each pot was filled with 15 litres of water, and the water temperatures were maintained and ranged between 25 to 27 °C. The two left pots were exposed directly to the airflow by approximately 80%. The pot placed in front of the semi-open mashrabiya was exposed by approximately 50%, while the right pot that faced the closed slats was not exposed to any direct airflow from outside.

Figure 5-33 Passive evaporative cooling techniques used with the mashrabiya in R1 on the site: Pots (left), Water spray (middle) and, Cloth (right), and (below) the techniques in and 3D views

On 7 August, (A) hand pressure pump was used to (B) spray water on R1 Mash at several specified intervals systemically (Table 5-12**Error! Reference source not found.**) (Figure 5-34). The consumption of the water sprays on mashrabiya for the entire test period (2.4 hrs) was 4.9 litres, and the water was kept at temperatures ranging between 13 to 20 °C. It can be observed that each spray moment had a specific amount of water to wet the mashrabiya while it has been reduced due to the increase in the number of sprays.
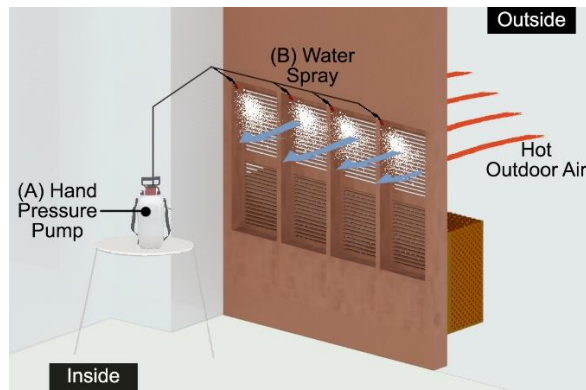
Figure 5-34 The water spray strategy and the potential effect on air flow heat

It should be noted that direct spraying on the mashrabiya with water frequently and over a long period may cause damage to it because the wood will absorb the water and expand and warp, which will require treatment or replacement. Hence future designs of mashrabiya which will incorporate direct evaporative cooling should consider employing different materials or adding a water-resistant coating to the surface.

Table 5-12 Strategies of water sprays for Mash1 during 7 Aug 2019

nterval (min)	Number	From	To	Spray amount (ml)		Water Temperature average (°C)
				Each	All	
10	4	11:32 AM	12:02 PM	180	720	13 to 16
8	6	12:25 PM	1:05 PM	150	900	13 to 20
6	6	1:29 PM	1:59 PM	130	780	15 to 18
4	9	2:20 PM	2:52 PM	140	1260	17 to 20
2	16	3:00 PM	3:30 PM	80	1280	16 to 18

On 8 August, the wet cloth strategy integrated with the mashrabiya where the (A) cloth was hanging on (B) crystal wires were installed 80 cm from the mashrabiya at R1 (Figure 5-35). In this study, two fabrics were used: cotton and voile, at different times. The cotton cloth was made of 100% cotton, while the voile was made of cotton blended with linen.
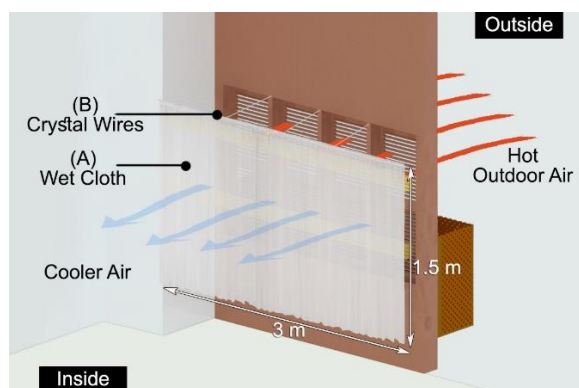
Figure 5-35 The wet cloth strategy and the potential effect on air flow heat

The fabrics were used after adding water at 16 and 19 °C (Table 5-13). At 12:20 p.m., four pieces of wetted cotton cloth (each having a dimension of 1.5 m x 0.45 m) were initially at 23 °C when hanged vertically. The effect of not using any wet cloth on the indoor thermal performance of R1 was determined from 2 to 2:40 p.m. From 2:40 p.m., one large piece of voile cloth (1.5 m x 3 m) was dipped in cold water from16 to19 °C initially at 25 °C when hanged horizontally facing the mashrabiya. At 3:30 p.m., the voile cloth was removed, and another piece of cotton cloth (1.5 m x 3 m) was initially at 28° C when it was hung.

Table 5-13 Strategies of water cloth for Mash1 during 8 Aug 2019

Fabric	From	To	Cloth temperature (°C)
Cotton	12:20 PM	02:00 PM	23
None	02:00 PM	02:40 PM	-
Voile	02:40 PM	3:30 PM	25
Cotton	3:30 PM	4:15PM	28

5.5.4 Results and Discussion

This section presents the analysis of the field data divided into two main subsections. First, the "Base Case" includes two strategies: a) Mashrabiya closed in both rooms and b) Mashrabiya open in R1 and closed in R2. Second, the "Mashrabiya and Evaporative Cooling Strategies", which comprise of three strategies: 1) Mashrabiya and water pots, 2) Evaporative cooling sprays, and 3) Mashrabiya and Cloths. The results include the indoor and outdoor field measurements of air temperature, air velocity, and relative humidity.

5.5.4.1 Base Case

Closed Mashrabiyas

Figure 5-36 illustrates the indoor and outdoor air temperatures when the mashrabiya was closed in both rooms from the noon of 30 July to 8 p.m. of 1 August 2019. During this stage, the maximum outdoor air temperature was 47.2 °C at 2 p.m. on 1 August, while the lowest was 31.4 °C at 6 a.m. on the same day. The indoor air temperatures in both rooms recorded the highest temperatures from 2 p.m. to 6:30 p.m. due to the facade of the rooms facing the west being exposed to direct sunlight during these periods. The outdoor air temperature reached its peak between 1 p.m. and 4 p.m., while the room's air temperatures peaked from 4 to 6 p.m. as shown in Figure 5-36.

Despite the difference between the outdoor and indoor temperatures that ranged between 8 and 11 °C during afternoon periods, closing the mashrabiya contributed to reducing the solar gain, where the indoor temperatures just increased from 1 to 3 °C in the same period. Moreover, the thermal mass played an essential role in delaying the passage of heat into the rooms for up to 3 hours, in addition to maintaining temperatures between 33.3 and 37.8 °C. As observed during the night, the outdoor temperature dropped from 35 to 31.4 °C, and the indoor temperature was maintained between 34.5 and 33.3 °C. Opening the mashrabiya during this period will help further cool down space and the thermal mass.
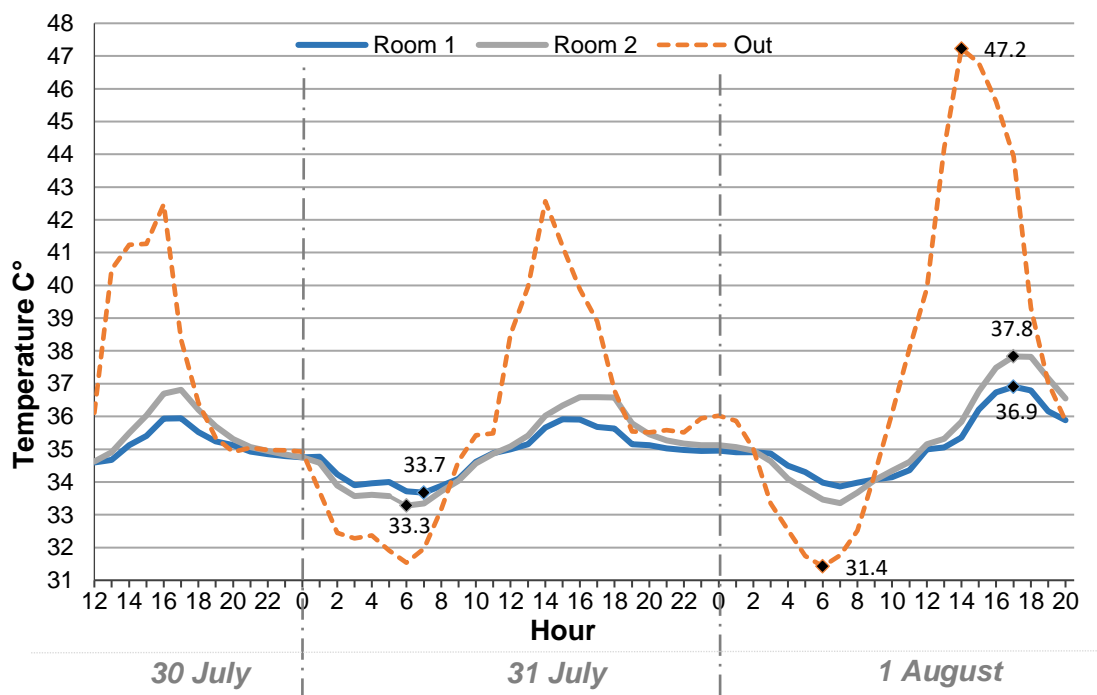
Figure 5-36 Indoor and outdoor air temperatures from 30 July to 1 August 2019 during the closed mode of the mashrabiyas

The air temperature and relative humidity measurements in both rooms (closed Mashrabiya) from noon 30 July to 8 p.m. 1 August are shown in Figure 5-37. The difference in air temperature measurements between the tested rooms did not exceed 1.1 °C, where the calculated correlation coefficient was 0.98, referring to the strong positive relationship between the air temperatures of the rooms. From this result, we were able to verify that the selected rooms were valid for the comparison for the following tests.

As illustrated, the highest air temperature inside the rooms was recorded at 5:30 p.m. on 1 August and the lowest at 6:30 a.m. on 31 July. While the highest measured relative humidity

was around 7 a.m. on 1 August and the lowest at 1:30 p.m. on the same day. The relative

humidity is typically below 40% during the afternoon hours when cooling is required the most.
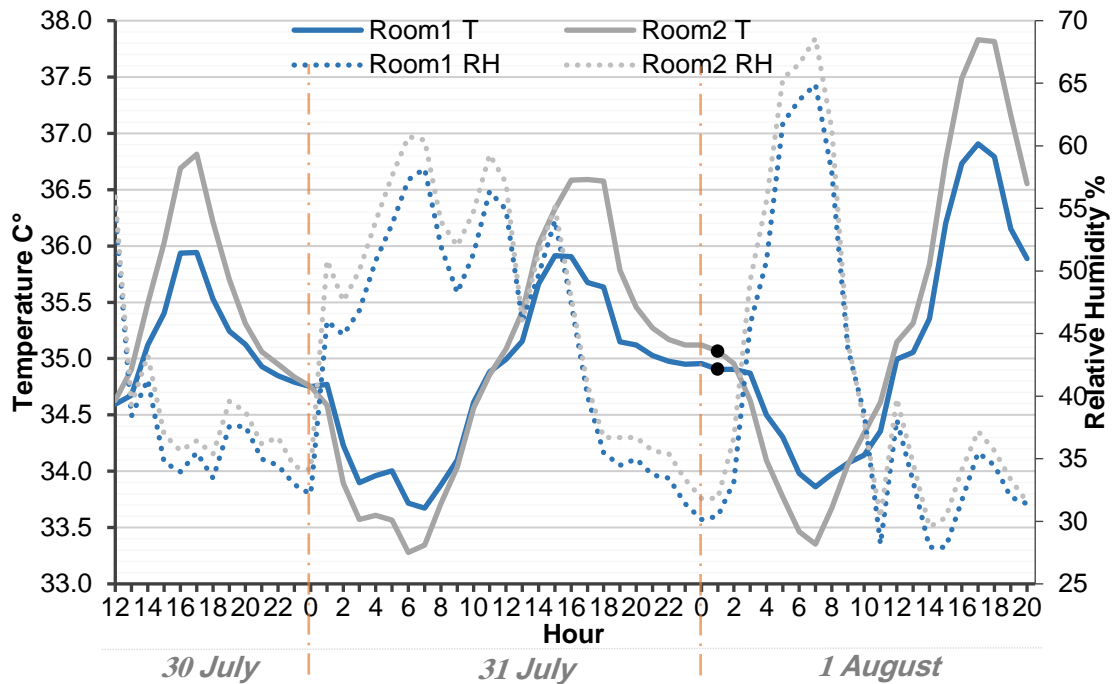
Figure 5-37 Air temperature and relative humidity measurements in Rooms 1 and 2 from 30 July to 1 August 2019

Generally, from noon until midnight, the temperature of R1 was lower as compared to R2, due

to the higher rates of airflow entering R1, which contributed to the reduction of heat gain

during the afternoons. While from around midnight to early morning, R2 recorded lower

temperatures and higher relative humidity than R1. This case occurred due to the ratio of

semi-open area of mashrabiya in R2 was about twice the semi-open area of the mashrabiya

in R1. Thus, it led to a more significant effect of night cooling and decreased the room

temperature more than R1.

As mentioned earlier, the mashrabiya was not completely closed due to the difficulty of

moving the tilt rod, which allowed a portion of natural daylight and outside air to pass through

the semi-open mashrabiya panels to the rooms. However, closing the mashrabiyas generally

reduced the entry of natural daylight and minimised the outside air flowing into the rooms. On

31 July, the average air velocity in the courtyard was 0.7m/s, in R1 0.3m/s and 0.1 m/s in R2.

Closed Mashrabiya vs Open Mashrabiya

Figure 5-38 shows the air temperature and relative humidity measurements in the courtyard

and tested rooms from 11:30 a.m. of 3 August until the end of the day when the mashrabiya

was open in R1 and closed in R2. The graph shows that the outdoor temperature peaked at 3p.m. (42.1 °C) and 5:45 p.m. for R1 (36.3 °C) and at 6 p.m. for R2 (37 °C). The outdoor relative humidity peaked at 6:30 p.m., reaching up to 54.8%, and reached its lowest value after 10 p.m. The relative humidity was typically below 45% during the afternoon hours, which could be advantageous when incorporating evaporative cooling strategies in the afternoon to alleviate the excessive heat.

The thermal mass delayed the passage of heat into space by 2.4 hours for R1 and 3 hours for R2. As a result of opening the mashrabiya in R1, the increased airflow rate led to a slight improvement in the thermal environment as compared to R2. Accordingly, the R1 recorded temperatures lower than R2, ranging from 0.5 to 1.3 ° C.
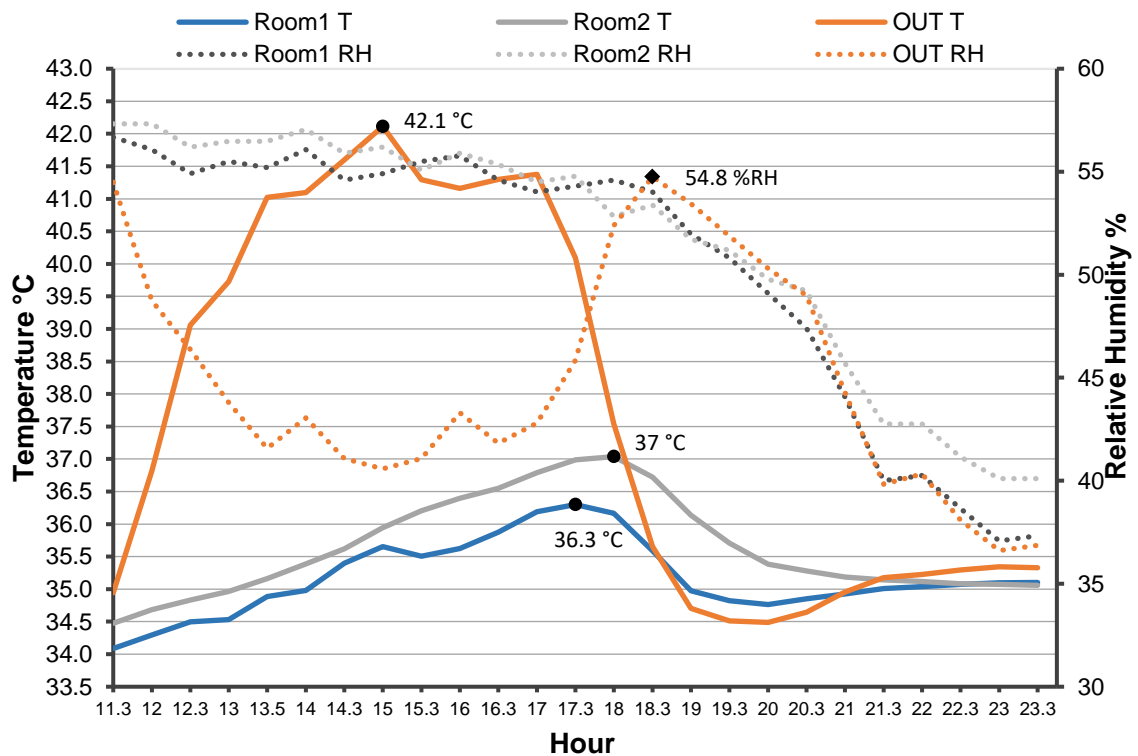
Figure 5-38 Outdoor and indoor temperatures when the mashrabiya in R1 was open and closed in R2 on 3 August 2019

It was found that the air velocity through the open mashrabiya in R1 recorded higher values than the courtyard, while the average outdoor air velocity in the courtyard was 0.9m/s and in R1 was 1.2m/s. That can be due to the positions of the data loggers in the open mashrabiya, which was facing the predominant wind with less obstacles.

In general, although the open mashrabiya provided some positive effect on the air temperature levels in R1, only a small improvement was observed and adding other cooling strategies is still required during these conditions. However, it would be useful during less extreme periods, and the benefit could be higher from using the open mashrabiya to improve the room temperature and thus reach the level of comfort without using any strategies or adding cooling systems.

5.5.4.2 Mashrabiya and Evaporative Cooling Strategies

Mashrabiya and water pots

In this experiment, four pots were placed along the inlet of the mashrabiya panels in R1 from 12:10 p.m. to the end of the day. The estimated direct exposure of the surfaces of the pots from the airflow passing through the mashrabiya was 53%, as detailed in Section 5.4.3. From 12:10 p.m., the temperature of water in the pots was kept between 25 to 27 °C by continuously replacing the pots' water with colder water. After 4 p.m., the pots' water was kept without refilling with low-temperature water. It was observed that the small pores of the pots allowed water to seep toward their exterior surfaces and became wet, while the airflow passing the pots accelerated the water evaporation process. The average wind speed for the day in R1 was 0.7 m/s and 0.3 m/s. in R2. Figure 5-39 shows the variation between the air temperature and relative humidity in the courtyard and the rooms on 5 August. It can be seen that the outdoor temperature was slightly lower than the rooms' temperature from the beginning of the day until 10:15 a.m. At 4 p.m., the courtyard recorded the highest air temperature of 44.6°C, while the highest air temperature was recorded in R1 (36.2°C) and in R2 (36.9°C) at 4:30 p.m.
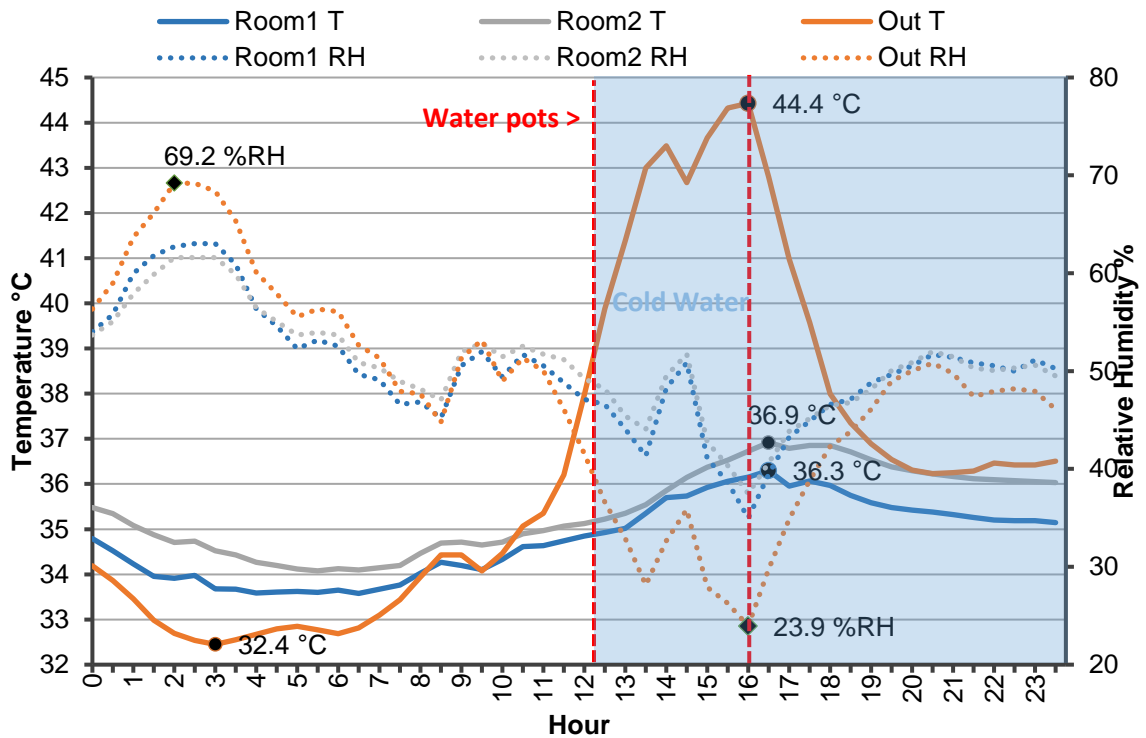
Figure 5-39 Outdoor and indoor air temperature and relative humidity on 5 August 2019

The air temperature in R1 was below R2 with a difference of up to 1 ° C. It should be noted that the weather after 3:45 p.m. has become partly cloudy, which led to raising the relative humidity and decreasing the outdoor temperature. An inverse relationship between air temperature and relative humidity can be observed from the graph, especially in relation to the outdoor air temperature and relative humidity. The outdoor relative humidity peaked (69.2 %) at 2 a.m. then at around 3 a.m., the outdoor temperature decreased up to the minimum of 32.4 °C. And with the humidity dropping to the lowest level of 21.4% at 4 p.m., the outdoor recorded the highest temperature for the day at 44.6°C. Despite the concept of using porous clay pots as a promising solution to cool the airflow passing through the mashrabiya and the surface of the jar, the water pots, in this case, did not provide the desired cooling for the indoor space, particularly during the afternoon period when cooling was required the most. However, further experimental investigations are needed to evaluate the impact of integrating the pots with mashrabiya either by changing the pots' placement and sizes or carrying out tests in moderate conditions.

Evaporative cooling sprays

Figure 5-40 presents the measurements of outdoor and indoor air temperature and relative humidity on 7 August 2019. Evaporative cooling water spray was used with Mash1 from 11.30 a.m. to 3:30 p.m. The sets and intervals of this technique are detailed in Table 5-12. As seen in the graph, the outdoor temperature was lower than the indoor temperatures until 10 a.m. The indoor temperature of R2 was slightly lower than R1 from 7:45 a.m. until 10:15 a.m. As the outdoor humidity level dropped at noon, the outdoor temperature increased sharply and peaked at 43.6 °C at 3:30 p.m. The lowest air temperatures were recorded during the night at 11:30 p.m.; 32°C in the courtyard, 33.3°C in R1, and 34.6°C in R2.

From the graph, the effect of water spraying on Mash1 can be observed, contributing to an increase in the relative humidity of the room and a slight decrease in air temperature (up to 1.2°C as compared to R2). The largest temperature difference between R1 and outdoor was recorded during the end of the last spray period at 3:30 p.m., up to 8.6 °C lower in R1 as compared to the outdoor. In this day, the average airflow velocity was 0.9 m/s in R1 and 0.2 m/s in R2.
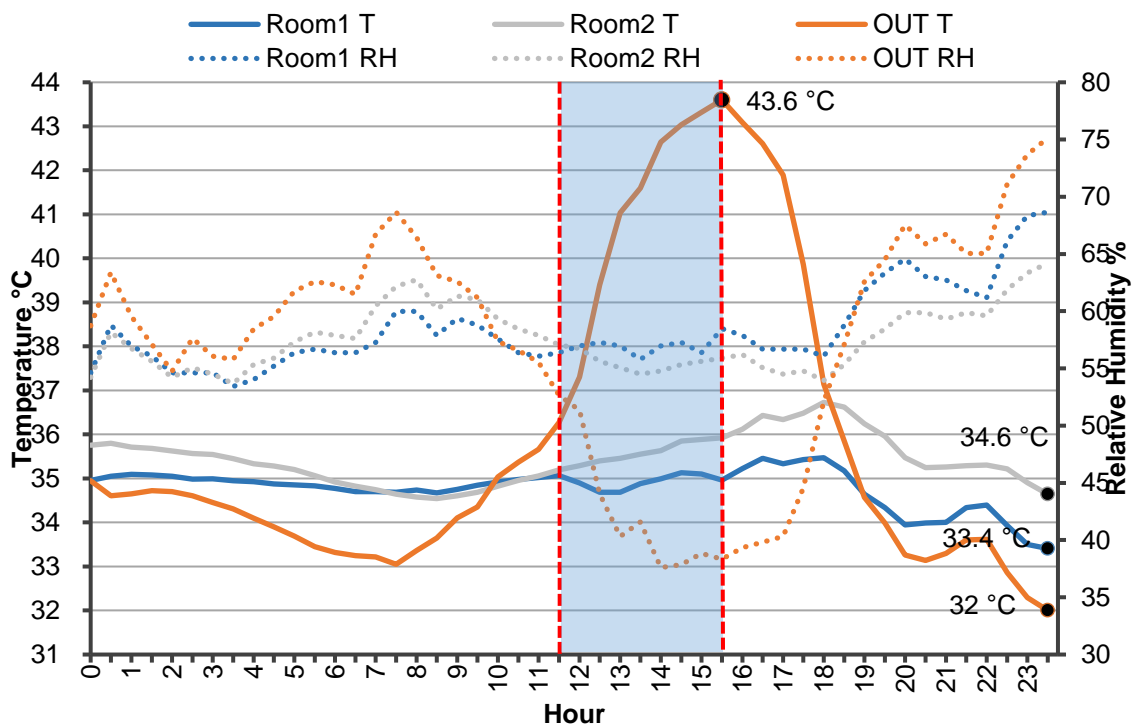
Figure 5-40 Outdoor and indoor air temperature and relative humidity on 7 August 2019

Mashrabiya and Cloths

Figure 5-41 shows the outdoor and indoor air temperature and relative humidity on 8 August when wet fabrics were hanged in R1 facing the mashrabiya from 12:30 to 2 p.m. then from 2:40 to 4:15 p.m. The outdoor temperature peaked at 43.9 °C at 2:15 p.m. We can observe that the highest variation between the outdoor and room temperature was at 2 p.m. when the outdoor temperature was 8.9 °C higher than R1 and 8.2 °C as compared to R2. The graph shows that the minimum relative outdoor humidity was 23.5%, and the maximum was 39.3% at 4:15 p.m. While using the wet fabric, the R1 temperature was 0.8 to 1.8 °C lower than R2. In this strategy, the average air velocity in Mash1 was 1.2 m/s, 0.9 m/s in the courtyard, and 0.5 m/s in Mash2.

After 2:40 p.m., a more significant temperature difference was observed between the rooms when using the wetted cloth. It is noteworthy that the voile cloth had a higher porosity after being moistened with water and increased air permeability compared to cotton fabric. Although the placement of the fabric facing the mashrabiya impeded the natural light and the air movement towards the room and restricted the view, it contributed to the spread and reflection of natural light entering the mashrabiya and reducing glare. Further data collection would be needed to test different materials. Also, the influence of the arrangement of the cloth should be further investigated.
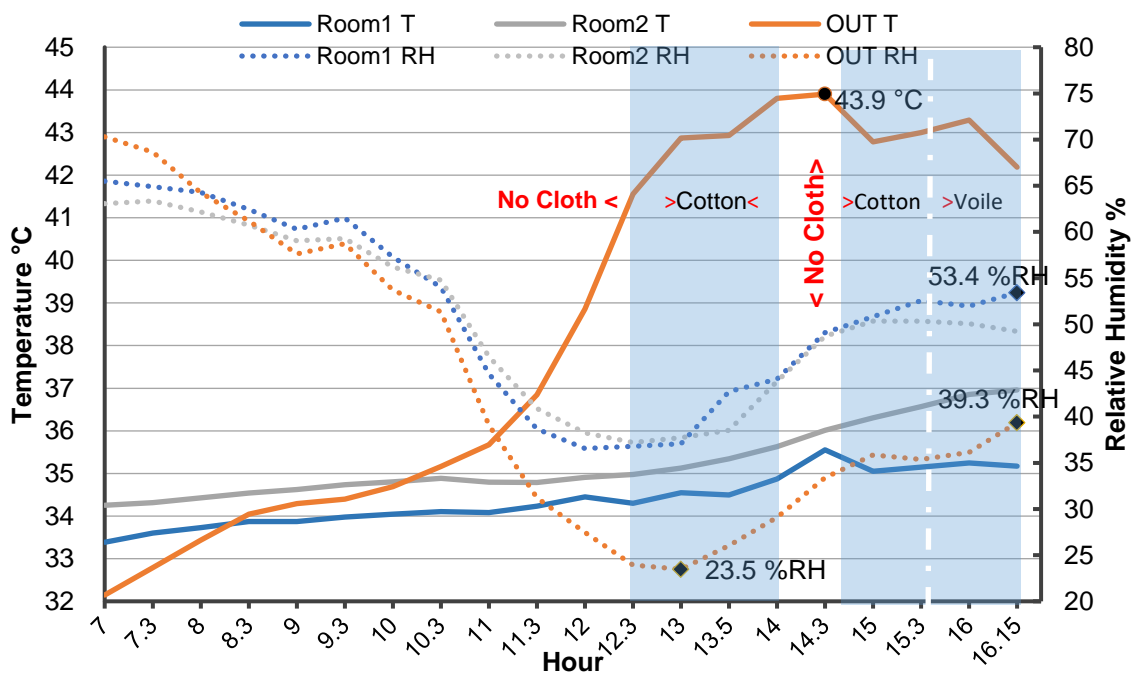
Figure 5-41 Outdoor and indoor air temperature and relative humidity on 8 August 2019

Table 5-14 summarises the fieldwork results between 11 a.m. and 4:30 p.m. for each day in this experiment. It summarises the impact of different strategies used in each room on indoor conditions, particularly temperature, air velocity, and relative humidity. Opening the mashrabiya of R1 while keeping the mashrabiya in R2 closed, contributed to increased air movement and circulation and resulted in a decrease in temperature in R1 by 0.4 ° C compared to the base case. Different evaporative cooling techniques were assessed, the water pot and spray strategies employed in R1 showed a limited reduction in temperature. Overall, the most effective strategy to reduce the air temperature of R1 was "Wet Cloth".

Table 5-14 Summary of the field test velocity and temperature results between 11am-4:30 pm

Strategy	Avg. Out T (°C)	Room	Avg. Air velocity (m/s)	Avg. Relative humidity (%)	Avg. Temperature (°C)	Avg. Reduction (°C)	Avg. Reduction (%)
Closed Mashrabiyas 31/7/2019	40.4	R1	0.5	49.5	35.5	4.9	13.5
		R2	0.2	51.1	35.8	4.6	12.4
Open Mash1 3/8/2019	40.1	R1	1.5	55.4	35.0	5.1	14.0
		R2	0.7	56.3	35.5	4.6	12.5
Pots 5/8/2019	41.5	R1	1.1	44.6	35.4	6.1	17.1
		R2	0.5	46.4	35.9	5.6	15.9
Water spray 7/8/2019	40.9	R1	1.0	57.1	35.0	5.9	17.0
		R2	0.2	55.8	35.6	5.3	14.8
Wet cloth 8/8/2019	41.6	R1	1.2	44.2	34.8	6.8	19.3
		R2	0.5	43.7	35.7	5.9	16.5

Figure 5-42 summarises the average outdoor and indoor temperatures for the period between 11 a.m. and 4:30 p.m. for each strategy. The average temperature ranged between 40 °C and 41.6 °C in the courtyard, 33.8 to 35.4 °C in R1, and 34.7 to 35.8 °C in R2. The least effective strategy in terms of temperature reduction was the "closed Mashrabiya" where R1 was 4.8 ° and R2 4.4°C lower than the outdoor temperature. Besides, closing the mashrabiya limited the airflow and blocked the daylight and view. From the graph, it can be observed that the use of pots showed the minimal indoor temperature decrease may be due to the contact time between the airflow and the surface of the pots and the obstruction of some panels to the passage of air. In addition, it might be better to use water at a lower temperature to be more effective. Regarding the use of water spray on mashrabiya slats, the strategy provided a slight reduction, probably due to the limited surface area of the wet slats that the air passes through. In future works, spraying water on both sides of the panel should be explored.

The wet cloth strategy was the most effective in reducing the indoor air temperature due to the air passing through the fabric, which contributed to the enhanced cooling of airflow. The average indoor temperature in R1 from 11 to 4 p.m. was 33.8 °C, 6.8 degrees lower than the outdoor temperature. Besides the mashrabiya and the evaporative cooling strategies used in this study, the thermal mass played a significant role in the reduction of thermal swings, and the indoor air temperatures remained lower than the outdoor by 4.6 °C to 6.8 °C. In addition, the thermal mass and closed mashrabiya delayed the heat flux into the room during the day up to 4 hours, while opening the mashrabiya decreased the time lag to 3 hours.
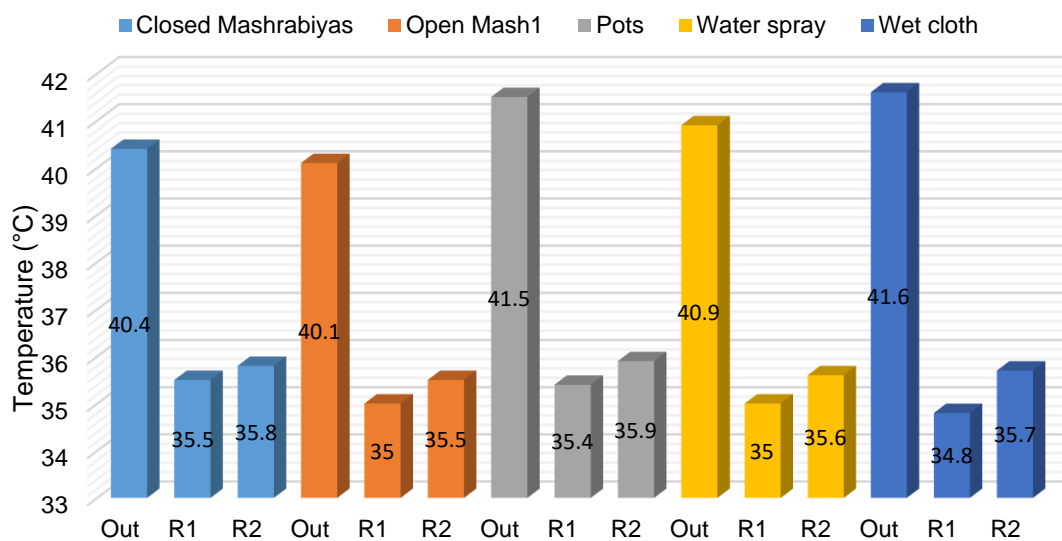
igure 5-42 The average outdoor temperature and the reduction in the rooms' temperature for the strategies assessed in the study

5.5.5 Thermal Comfort Assessment

To evaluate the acceptability of indoor thermal conditions in naturally ventilated buildings, ASHRAE Standard 55 can be considered as a prime guide. However, it is noteworthy that ASHRAE 55 did not cover or consider the average external temperature below 10 ° C or above 33.5 °C (ASHRAE, 2010a). Moreover, since the average external temperature of this work was 36.6°C which exceeded the range of ASHRAE, it was not applicable to this study, and other methods were applied. de Dear and Brager (2002) stated, "People who live or work in naturally ventilated buildings where they can open windows, become used to thermal diversity that reflects local patterns of daily and seasonal climate variability. Their thermal

perceptions—both preferences as well as tolerances—are likely to extend over a wider range of temperatures than are currently reflected in the old ASHRAE Standard 55 comfort zone." However, two different equations were used to assess the indoor comfort temperature in this study to perform a more comprehensive assessment of comfort ranges. First, the equation (5.1) of comfort temperature by de Dear and Brager (2002) in free-running buildings was used as indicated below:

$$T_{comf} = 0.31\ T_o + 17.8 \qquad (5.1)$$

Where, T_{comf} is the indoor comfort temperature, and To is the monthly mean of the outdoor air temperature. In this work, the mean of outdoor temperature for all the periods was 36.6°C. Hence based on the equation, the calculated comfort temperature is 29.2°C. The second assessment that was used to determine the comfort temperature was the equation (5.2) of Nicol and Humphreys (2002), as shown below:

$$T_{comf} = 13.5 + 0.54\ T_o \qquad (5.2)$$

In Nicol and Humphrey's field study, the Pakistani participants felt comfortable at indoor temperatures close to 33 °C. In addition, the paper indicated that the workers changed their clothing and using air movement fans during the tests.

Although traditional buildings often achieve comfort without using a mechanical system, these levels do not meet today's expectations (Lotfabadi and Hançer, 2019). Nicol and Humphreys (2002) said, "People have a natural tendency to adapt to changing conditions in their environment. This natural tendency is expressed in the adaptive approach to thermal comfort".

However, in this study, the comfort temperature was calculated to be 33.3 °C. This equation gives more flexibility in extending the acceptable comfort level inside spaces to outdoor temperatures.

Figure 5-43 illustrates the difference between the room temperature and the estimated comfort temperature for each strategy. Each bar represents all room temperature readings for a day and the difference between them for achieving the temperature comfort based on the comfort temperature calculated from the equations of de Dear and Brager (2002) and Nicol and Humphreys (2002). In the graph, 0 represent comfort temperature equivalent to 29.2°C

according to the equation (1), and equal to 33.3°C according to the equation (2), so the values from zero and above consider within the range of thermal comfort zone while the values lower than 0 are outside the range of comfort zone. As can be seen in the graph and according to '33.3 °C' the comfort temperature, the R1 temperature in the "closed Mashrabiyas" strategy needs to be lower by 3 degrees to reach the comfort level R2 requires 3.8. During the selected periods, the temperatures of R2 did not reach comfort level except for the period from 6 to 6:40 a.m. on 31 July due to the decrease in the outdoor temperature to 31.5 ° C and the role of the thermal mass. Also, the drop in the outdoor temperatures to around 31.7 °C, led to reaching the comfort temperature in R1 in the early morning hours on 8 August. From the figure, it can be seen that the R1 temperature required a decrease of 1.8 to 6.5 ° C in a "wet cloth" strategy, while R2 required a reduction of 4.6 to 7.8 ° C to achieve the temperature comfort.
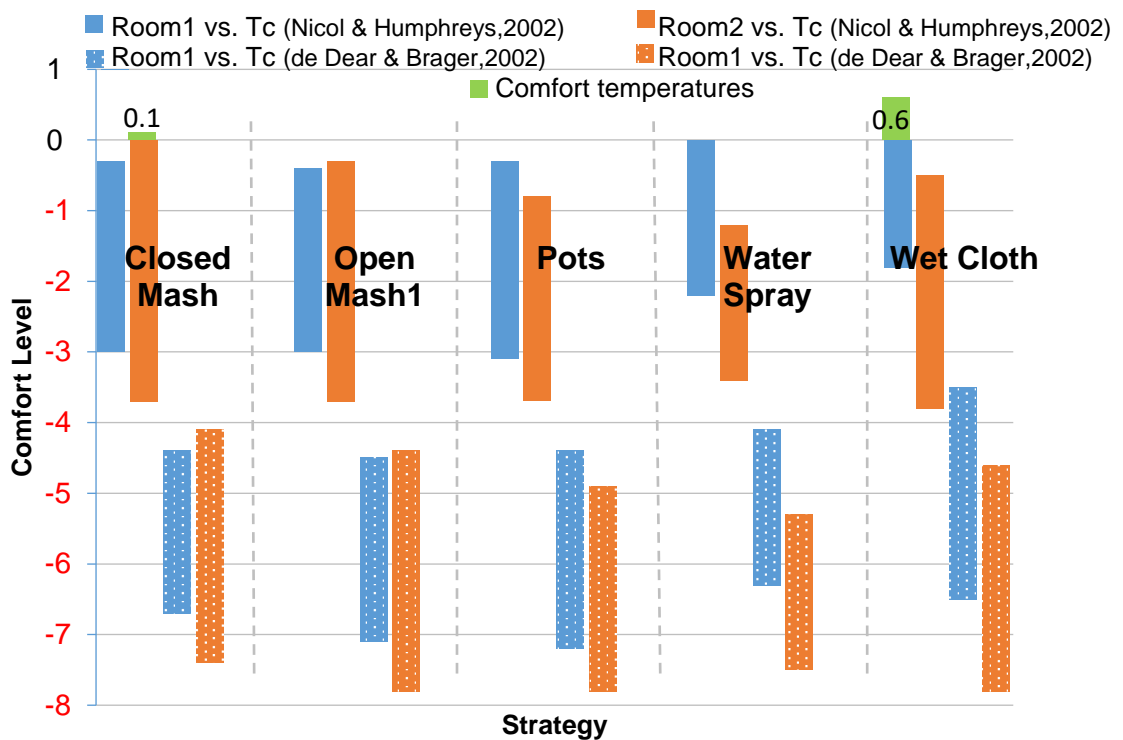
Figure 5-43 Rooms temperatures as compared to comfort temperature based on de Dear and Brager (2002) and Nicol and Humphreys (2002)

The hourly indoor and outdoor temperatures for all the strategies are compared with the comfort zone in Figure 5-44. All measurements were out of the comfort range when the 29.2°C was used as the acceptable comfort temperature. The closest temperature to

achieving thermal comfort was 32.9°C at 5 a.m. in R1 on 8 August, when the outdoor

temperature was 31.8°C. In contrast, R1 recorded the highest temperature difference from

the comfort level at 6 p.m. on 1 August when the mashrabiya was closed.

Based on the comfort temperature of 33.3°C, the temperature in R1 was within the comfort

zone on 8 August between 12 and 7 a.m. and represented 18.4% of the total measurements

of this day. Also, there were a few hours during the morning of 31 July when the R2

temperature reached the comfort zone due to the drop in the outdoor temperature to 31.6 °C.

Generally, the period between 1 to 9 a.m. can be considered the closest period to achieve the

comfort level in the rooms due to the decrease in the outdoor temperatures and night

ventilation. It is essential to clarify that the experiment was carried out in the worst conditions

during the summer as August's highest average temperature in the year. Therefore, opening

the mashrabiya or using these strategies will often give better results during the moderate

seasons. However, the addition of air moving equipment, such as a fan, can increase the

acceptance level of indoor temperature.
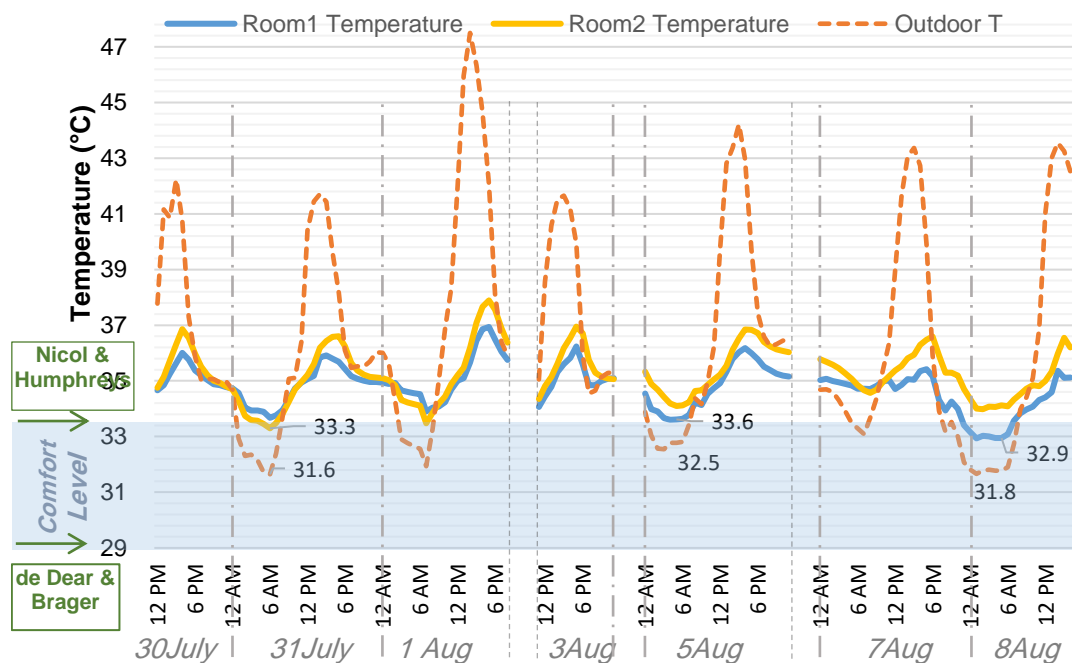
Figure 5-44 Comparing the indoor and outdoor hourly temperature with the comfort temperature

5.5.6 Limitations

As the base case, this field study evaluated thermal comfort based on environmental factors

only, without covering personal factors. That is because the building is currently not inhabited,

and the difficulty of engaging people in this type of experiment in these climatic and spatial conditions. Due to the limited time and the available equipment, the indoor air velocity in the rooms was measured at one specific point in each mashrabiya. It should also be noted that the outdoor air velocity may have been affected by several factors, such as the position of the anemometer, its height above ground level, and some surrounding obstacles. Due to the lack of time, the study was limited to specific periods during summer, so more studies are needed to conduct tests in temperate conditions and climates. The impact of different configurations of mashrabiya on indoor thermal conditions is not considered in this study and can be focused on in future.

5.6 Summary and Conclusions

The fieldwork investigated the effect of mashrabiya on the indoor thermal environment by monitoring indoor and outdoor air temperature, relative humidity, and air velocity during two separate summers in a historical building in Jeddah. The fieldwork were carried out in Baeshen House, located in the historical area of Jeddah, known for its traditional buildings and the most abundant area in terms of traditional mashrabiya in Saudi Arabia. Two fieldworks were conducted in two selected rooms and the courtyard of the building.

First, the mashrabiya in both rooms was closed from 30 July to 1 August 2019, then setting the mashrabiya in R1 open, and the mashrabiya in R2 closed until the last day of the experiment. Second, using three different passive evaporative cooling techniques with the mashrabiya in R1: pots, water spray, and fabrics.

The first fieldwork demonstrated that opening the mashrabiya allowed more airflow into the room during the day and reduced the indoor temperature by up to 2.4 °C as compared to the closed mashrabiya. Besides, the building envelope played an important role in preventing the high fluctuation of the indoor air temperature, where the fluctuation of the rooms air temperature ranged between 2.1 °C and 4.2 °C compared to the outdoor temperature, which recorded a fluctuation between 9.4 °C and 16 °C. The indoor thermal comfort evaluation demonstrated that Room 1 typically were near to the temperature comfort of 33 °C and better than Room 2 by 0.3 degrees on average.

The second fieldwork result showed that the two rooms with closed mashrabiyas had similar conditions, verifying that the selected rooms were valid for comparing the following tests. Although closing the mashrabiya limited airflow entry, it also blocked the direct sunlight during noon times. Also, the thermal mass contributed to delaying the heat into the room for up to 4 hours which helped maintain the temperatures between 33.2 and 38°C, while opening the mashrabiya delayed the heat into the room for up to 3 hours. The open mashrabiya allowed in the sea breeze during the day, which increased air movement and circulation inside the room and resulted in a slight reduction of the room's air temperature. Although the open mashrabiya provided some reduction in the heat in R1, adding some cooling strategies during those hot outdoor conditions were required. By integrating different passive evaporative cooling techniques with mashrabiya, the most effective approach to improving the room air temperature was hanging a wet cloth facing the mashrabiya. This strategy reduced the R1 average temperature by up to 6.8°C. Otherwise, integrating the pots with the mashrabiya showed minimal effect on the temperature inside the room. Also, the use of water sprays on mashrabiya slats contributed to a slight reduction in temperature. Moreover, it was demonstrated that the period between 1 and 9 a.m. could be considered the closest period to achieve comfort in the rooms due to the decrease in the outdoor temperatures and night ventilation. The results also showed that along with the mashrabiya and the evaporative cooling strategies, the thermal mass played a significant role in reducing indoor air temperatures' thermal swings.

Despite achieving the objectives of these field experiments, they were limited to certain points in the measurements, especially the air velocity measurements, due to reasons discussed previously, and thus caused a lack of a detailed perception of the air movement and directions inside the room. As a part of evaluating the performance of the mashrabiya in detail and its effect on the airflow into the room, the simulation tool, "Computational Fluid Dynamics (CFD)" will be used to create a base case and prepare for development.

To achieve better results and temperature reduction more than evaporative cooling strategies that were used in the experiment, an inspired heat transfer device technique from Calautit et al. (2015) and Shen and Li (2016) was utilized and integrated with the mashrabiya, which will be presented in Chapter 7.

CHAPTER 6

SIMULATION AND THE BENCHMARK MODEL

Introduction
The Study of Fluids
CFD Fundamentals and Models
CFD and Natural Ventilation
Modelling and Simulation Procedures
Validation Model
Summary and Conclusions

6. SIMULATION AND THE BENCHMARK MODEL

6.1 Introduction

The field experiments of this work have contributed to increasing knowledge and awareness about the role of the traditional mashrabiya by comprehensively investigating and evaluating its performance and impact on the indoor environment and thermal comfort. On the other hand, for reasons discussed in section 5.5.6, there were some limitations in the measurements, especially air velocity measurements which caused a lack of a detailed inspection of the movement and velocity of the air inside the room. Therefore, as part of evaluating the performance of mashrabiya in detail, its impact on room airflow and cost savings, and having more flexibility in development, a simulation program specialised in Computational Fluid dynamic CFD was used. Simulation is one of those technologies that progress rapidly and are increasingly used in many fields, including the architectural field. "Modelling and simulations are powerful design-tools, today, albeit their validation and verification often obliges the user to resort back to experimental results" (Eissa, 2005). Validation was defined by AIAA (1998) as "the process of determining the degree to which a model is an accurate representation of the real world from the perspective of the intended uses of the model".

Generally, this chapter presents a brief overview of the theoretical basics behind computer fluid dynamics and the process and method of modelling this work. In order to extend our scope in studying and investigating mashrabiya, a selected valid CFD model with actual results will be used as a reference and, thus, the reliability of the results extracted later from the improvements conducted to the model. In terms of natural ventilation, (CFD) is a critical tool that makes it possible for designers to use a building design to analyse air movement and evaluate various potential designs. Nevertheless, the uninformed use of this tool can be more detrimental and can result in the effect that natural ventilation forces have on a design is misleading (Allocca, 2001). Therefore, the CFD validation for this study model is necessary to indicate that the expected outcome accurately reflects the physical situation and the actual impact on the model in the optimisation phase.

6.2 The Study of Fluids

During most of the 19th and 20th centuries, two conventional methods were used to study any fluid motion: the theoretical and experimental (McDonough, 2009). The theoretical or analytical approach can solve the governing equations for simple cases and provide the exact solution with no error. Passe and Battaglia (2015) stated that "Experiments are a necessary tool to help determine the physics of airflow and provide measurements in terms of velocity and pressure". However, analytical and experimental methods are often impractical in solving real-life industrial issues due to cost, time or difficulty.

With the development of technologies in recent decades, a new method has been utilised on computers by using specific programs dedicated to fluid calculations, and the method has become known as Computational Fluid Dynamics (CFD). Haredy (2016) said, "Fluid flow and heat transfer are the most critical phenomena that need to be analysed for the airflow windows in order to achieve design optimisation". It should be mentioned that the experimental approach is a quantitative description of flow phenomena using measurements, while the simulation approach is a quantitative prediction of flow phenomena using CFD software. However, the most beneficial approach to saving time and cost compared with the corresponding experiments is a numerical method for calculating airflow and heat transfer efficiency. Numerical simulation by CFD software can generate detailed data regarding air temperature, airflow, pressure drop and turbulence intensity in the modelling domain (Li, 2015).

A fluid was defined by McDonough (2009) as "any substance that deforms continuously when subjected to a shear stress, no matter how small", from this definition, there are some main physical properties to consider as an introduction and clarification before reviewing the basics of fluid flow equations.

Viscosity (μ) is defined by Addington and Schodek (2005) as the ability of a fluid to resist flow. The units of μ is (lb/ft-hr, kg/m-hr).

Density (ρ) is described as the mass per unit volume of a fluid.

$$\rho = \text{mass of fluid (kg) / volume of fluid (m}^3)$$

Pressure (P) is the force on a surface object or fluid per unit area.

Thermal conductivity (k or λ) is the property of a material to transport or conduct heat through a substance in a manner, and it is the constant of proportionality in Fourier's Law (McDonough, 2009).

6.3 CFD Fundamentals and Models

"Computational fluid dynamics (CFD) was defined by Versteeg and Malalasekera (1995a) as "the analysis of systems involving fluid flow, heat transfer and associated phenomena such as chemical reactions by means of computer-based simulation". Another description of the term CFD by Etheridge and Sandberg (1996) referred to numerical solutions of partial differential equations that govern a flow field, allowing the prediction of velocities, temperatures, and other variables at all points in the field.

This technology is potent and covers a large number of industrial and non-industrial fields. Although CFD provides solution capabilities for partial differential equations that relate to different aspects of incompressible, compressible, laminar, and turbulent fluids (ANSYS, 2017), it is essential to understand and review the main fundamentals of flow and the equations that underpin them.

Computational fluid dynamics is based fundamentally on governing equations derived from mass, momentum, and energy conservation principles. In CFD, the governing equations of fluid dynamics can be solved using some numerical techniques such as the Finite Difference Method (FDM), Finite Element Method (FEM) or Finite Volume Method (FVM), where FVM considers the most used method (ANSYS, 2017). Mohd Nasir (2017) stated that "FVM is a technique based on discretisation equation which the resulting solution satisfies the conservation of quantities (i.e. energy, species, momentum and mass)". It should be mentioned that CFD uses widely to solve the Navier–Stokes equations "the Finite Volume Method (FVM) with the Semi Implicit Method for Pressure Linked Equations (SIMPLE) velocity-pressure coupling algorithm"(Calautit et al., 2015). In FEM, the flow field is divided into a group of non-overlapping cells covering the entire field, while in FVM, used the cell is used instead of the element and conservation laws are applied to define flow variables at separate points of cells, which are named nodes (Figure 6-1). These nodes can be triangular

cells, quadrilaterals, etc. and form a structured mesh or an unstructured network or a hybrid mesh (Anderson, 2009).

By employing CFD techniques, the system admits no analytical solution, and a numerical solution can be approached in two steps; space discretisation and equation discretisation (Sofotasiou, 2017).
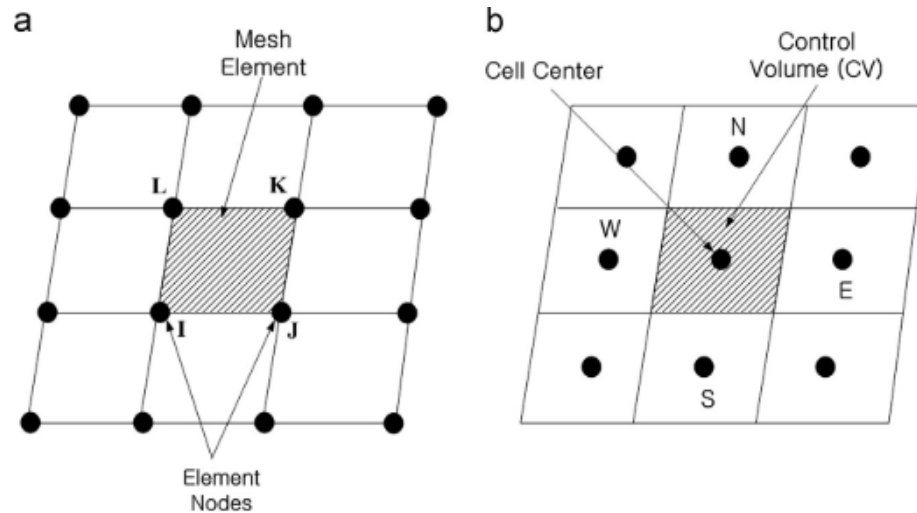
Figure 6-1 An example of structured mesh (a) the finite element method, and (b) The finite volume method (Jeong and Seong, 2014).

6.3.1 Governing Equations

Versteeg and Malalasekera (1995b) described that "The governing equations of fluid flow represent mathematical statements of the conservation laws of physics:

• The mass of fluid is conserved

•The rate of change of momentum equals the sum of the forces on a fluid particle (Newton's second law):

$$\vec{F} = m\vec{a} \qquad (6.1)$$

• The rate of change of energy is equal to the sum of the rate of heat added to and the rate of work done on a fluid particle (first law of thermodynamics)". According to Newton's second law is "the rate of change of momentum of a fluid particle equals the sum of the forces on the particle"(Versteeg and Malalasekera, 1995b). Figure 6-2 shows that when applying Newton's second law to the moving fluid element, a vector equation, a moving fluid element can be split into three scalar relations along the x, y, and z-axes.
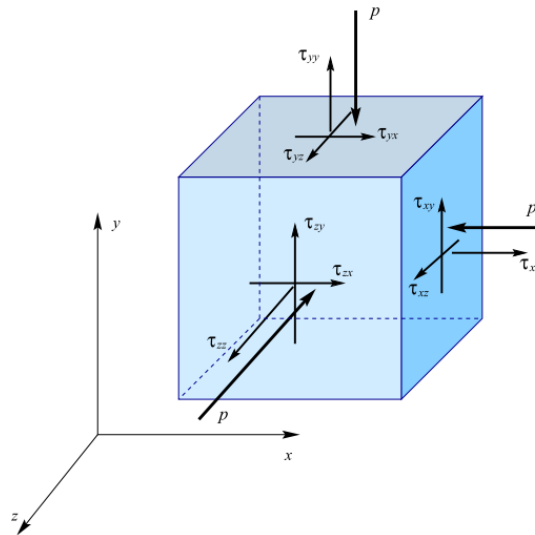
Figure 6-2 Schematic of pressure and viscous stresses acting on a fluid element (McDonough, 2009)

Under the first law in thermodynamics, the rate of energy change on a fluid particle equals the work done by the particle plus the rate of heat. Thus, mass fluid is maintained in the meantime (Li, 2015).

These three partial differential equations can be written in the general form as follows:

$$\frac{\partial(\rho\bar{\phi})}{\partial t} + \nabla(\rho\vec{u}\bar{\phi} - \Gamma_e\nabla\bar{\phi}) = S_{\bar{\phi}} \ (6.2)$$

Where is:

∂ Partial derivative

ρ Density

$\bar{\phi}$ Variable (changing property)

t Time

Γ_e diffusion coefficient

$\vec{u}$ velocity vector

S Source

In addition, $\bar{\phi}$ is changing property which includes pressure (P), velocity ($\bar{u}, \bar{v}, \bar{w}$) temperature ($\bar{T}$) Concentration Turbulence (k; turbulent kinetic energy and $\varepsilon;$ dissipation rate of k). Furthermore, φ in the continuity equation equal to 1, for the instantaneous fluid velocity components of the Navier-Stokes equations equals u, v, w, and for the energy equation equals to temperature (T) or enthalpy (h) (Sofotasiou, 2017).

Conservation of Mass

The equation for mass conservation or continuity can be valid for both incompressible and compressible flows, which be as follows:

$$\frac{\partial \rho}{\partial t} + \nabla \cdot (\rho \vec{u}) = S_m \qquad (6.3)$$

Where "S_m is the mass added to the continuous phase from the dispersed second phase (for example, due to vaporisation of liquid droplets) and ∇ represents the partial derivative of a quantity with respect to all directions in the Cartesian coordinate system. t is time, ρ is the fluid density, and $\vec{u}$ is the fluid velocity (ANSYS, 2017), (Vallejo, 2018).

Momentum Conservation

$$\frac{\partial}{\partial t}(\rho \vec{v}) + \nabla \cdot (\rho \vec{v}\vec{v}) = -\nabla p + \nabla(\bar{\bar{\tau}}) + \rho \vec{g} + \vec{F} \qquad (6.4)$$

where p is the static pressure, $\rho \vec{g}$ the gravitational body force, and $\vec{F}$ external body forces. $\bar{\bar{\tau}}$ is the stress tensor which can be described as follow;

$$\bar{\bar{\tau}} = \mu \left[(\nabla \vec{v} + \nabla \vec{v}^T) - \frac{2}{3} \nabla \cdot \vec{v} I \right] \qquad (6.5)$$

Where μ is the molecular viscosity, is the unit tensor, and the effect of volume dilation in the second term on the right-hand side (ANSYS, 2017).

Energy Conservation

From the first law of thermodynamics, the energy equation is derived where the law provides that "the rate of change of energy of a fluid particle is equal to the rate of heat addition to the fluid particle plus the rate of work done on the particle"(Versteeg and Malalasekera, 1995b). The energy conservation equation is given in the following form:

$$\frac{\partial}{\partial t}(\rho E) + \nabla \cdot (\vec{v}(\rho E + p)) = -\nabla \cdot \left(K_{eff} \nabla T - \sum_j h_j \vec{J}_j + (\bar{\bar{\tau}}_{eff} \cdot \vec{v}) \right) + S_h \qquad (6.6)$$

$K_{eff} \nabla T$ represent conduction energy transfer where K_{eff} is the effective conductivity. $h_j \vec{J}_j$ is the diffusion flux of species j and $\bar{\bar{\tau}}_{eff} \cdot \vec{v}$ represent viscous dissipation energy transfer. The first three terms represent energy transfer due to conduction, species diffusion, and viscous dissipation on the right side of the equation. Since the total enthalpy calculation already included enthalpy, S_h represents volumetric heat sources, not the heat sources generated by finite-rate volumetric or surface reactions (ANSYS, 2017).

To find E from Equation 6.6, it can be defined in the following way:

$$E = h - \frac{p}{\rho} + \frac{v^2}{2} \qquad (6.7)$$

where sensible enthalpy is defined for ideal gases as

$$h = \sum_j Y_j \, h_j \qquad (6.8)$$

and for incompressible flows as

$$h = \sum_j Y_j \, h_j + \frac{p}{\rho} \qquad (6.9)$$

h_j is the mass fraction of species j :

$$h_j = \int_{T_{ref}}^{T} c_{p,j} dT \qquad (6.10)$$

The value of T_{ref} is based on the solver and models used in the sensitive enthalpy

calculation. Where heat capacity c_p of species j and T is temperature.

The energy equation in three dimensions can be list as followed:

$$\rho \frac{DE}{D_t} = div(pu) + \left[\begin{matrix} \frac{\partial(u\tau_{xx})}{\partial x} + \frac{\partial(u\tau_{yx})}{\partial y} + \frac{\partial(u\tau_{zx})}{\partial z} + \frac{\partial(v\tau_{xy})}{\partial x} + \frac{\partial(v\tau_{yy})}{\partial y} + \frac{\partial(v\tau_{zy})}{\partial z} \\ + \frac{\partial(w\tau_{xz})}{\partial x} + \frac{\partial(w\tau_{yz})}{\partial y} + \frac{\partial(w\tau_{zz})}{\partial z} \end{matrix} \right] + div(k \, \nabla \, T) + S_E$$

$$(6.11)$$

6.3.2 Turbulence

Understanding the turbulent flow is essential to define the difference between it and laminar
flow, and perhaps water flow from the tap is the most common way to find this difference.
Figure 6-3 (a) shows a relatively low-velocity and (steady) laminar flow in which the paths
followed by fluid parcels are very regular and smooth; moreover, there is no indication that
these pathways may exhibit drastic changes in direction. In (b), the water from the tap flows
more than in the previous state, the flow is still laminar, but the water stream surface begins
to show waves depending on time but does not show clear interference of paths. In part (c) of
the figure, as the flow velocity increased, the flow became turbulent, and the paths followed
by the fluid parcels became very complex and intertwined, indicating a high degree of
momentum. McDonough (2009) concluded that "as flow speed increases, details of the flow
become more complicated and ultimately there is a "transition" from laminar to turbulent flow".
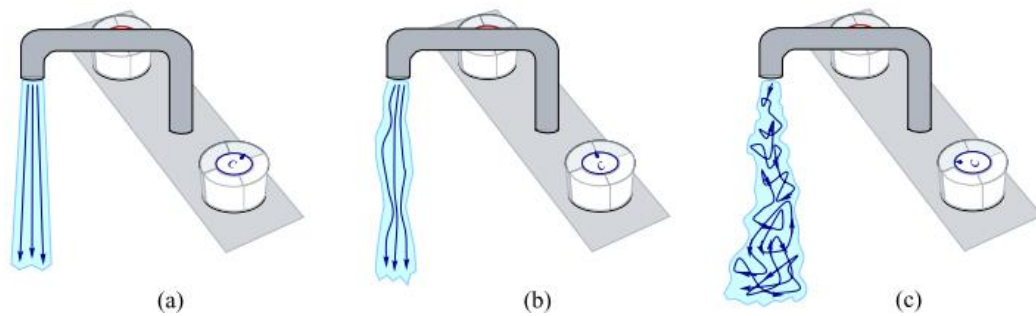
Figure 6-3 Laminar and turbulent flow of water from a faucet; (a) steady laminar, (b) periodic, wavy laminar, (c) turbulent. (McDonough, 2009)

6.3.2.1 Different choices of turbulence models

Due to the turbulent nature of most indoor and outdoor airflows, CFD modelling is used in this study. The Reynolds average navigation-stocks (RANS) equation and Large Eddy Simulation (LES) equation are the most commonly used in CFD models. O'Connor (2016) explained that the differences among CFD models concern the methodology and the size of the calculated vortices. The method and size of the calculated vortices is the main variation between RANS and LES where LES has less turbulence and a larger size mesh than RANS, whereas LES solves more and have more accurate result than RANS but requires highly efficient computers and consume more computing time (Anderson, 2009).

Since the simulation is based on the RANS model, a quick overview of the essential points is presented. The Reynolds number can be defined as "an indicator for the ratio of inertial forces to viscous forces"(Passe and Battaglia, 2015) and used to characterise different flow regimes, such as laminar or turbulent flow.

Allocca (2001) stated that modelling turbulences links the undetermined stresses of Reynold with the mean flow variable by approximations, and this kind of turbulence modelling is called Reynolds-averaged Navier-Stokes (RANS). Under RANS, there are several turbulence models where the most common model is the standard k-ε (Allocca, 2001) (Passe and Battaglia, 2015). In the k-ε model, there are three types; standard, RNG, and realisable. The standard k-ε model is the simplest two-equation turbulence model. The RNG k-ε model is used for rapidly strained and swirling flows to improve the accuracy in electronic transport equations but is more time-consuming. The realisable k-ε model is used to satisfy certain mathematical constraints on the Reynolds stresses (Passe and Battaglia, 2015). In general,

RANS depends on two equations; "the turbulent dissipation rate equation of the cinematic energy within the turbulent flow and the flow dissipation rate" (Passe and Battaglia, 2015). Both equations below demonstrate the Reynolds-averaged Navier-Stokes equations:

$$\frac{\partial \rho}{\partial t} + \frac{\partial}{\partial x_i}(\rho \mu_i) = 0$$

$$\frac{\partial}{\partial t}(\rho u_i) + \frac{\partial}{\partial x_j}(\rho u_i u_j) = -\frac{\partial}{\partial x_i} + \frac{\partial}{\partial x_j}\left[\mu\left(\frac{\partial u_i}{\partial x_j} + \frac{\partial u_j}{\partial x_i} - \frac{2}{3}\delta_{ij}\frac{\partial u_l}{\partial x_l}\right)\right] + \frac{\partial}{\partial x_j}(-\rho\overline{\acute{u}_i\acute{u}_j}) \qquad (6.12)$$

Where $(-\rho\overline{\acute{u}_i\acute{u}_j})$ is the apparent stress due to the fluctuating velocity field, indicated as the Reynolds stress (ANSYS, 2017). $-\rho\overline{\acute{u}_i\acute{u}_j}$ can be find by using this equation:

$$-\rho\overline{\acute{u}_i\acute{u}_j} = \mu_t\left(\frac{\partial u_i}{\partial x_j} + \frac{\partial u_j}{\partial x_i}\right) - \frac{2}{3}\rho k\delta_{ij} \qquad (6.13)$$

The standard k-ε model is a semi-empirical model, which was assumed to be fully turbulent, and to have negligible effects on molecular viscosity, thus valid only with thoroughly turbulent flows. The model is based on the two typical transfer equations for the kinetic energy of the perturbation k and dissipation rate ε (Versteeg and Malalasekera, 1995b), where the equations are as follows:

$$\frac{\partial}{\partial t}(\rho k) + div(\rho k \mathrm{U}) = div\left[\frac{\mu_t}{\sigma_k}grad\ k\right] + 2\mu_t S_{ij}.S_{ij} - \rho\varepsilon \qquad (6.14)$$

$$\frac{\partial(\rho\varepsilon)}{\partial t} + div(\rho\varepsilon\mathrm{U}) = div\left[\frac{\mu_t}{\sigma_\varepsilon}grad\ \varepsilon\right] + C_{1\varepsilon}\frac{\varepsilon}{k}2\mu_t S_{ij}.S_{ij} - C_{2\varepsilon}\rho\frac{\varepsilon^2}{k} \qquad (6.15)$$

The equations were simplified in expression by Versteeg and Malalasekera (1995a) as follow;

The change + Transport of k or ε = Transport of k or ε + Production - Destruction
rate of k or ε by= convection   by= diffusion   rate of k or ε rate of k or ε

Where μ_t is the eddy viscosity, S_{ij} is deformation rate, and $\sigma_k, \sigma_\varepsilon, C_{1\varepsilon}$, and $C_{2\varepsilon}$ are adjustable constants. σ_k and σ_ε are Prandtl numbers that link the diffusions of k and ε with the eddy viscosity μt while the $C_{1\varepsilon}$, and $C_{2\varepsilon}$ constants give the proper proportionality between the k and ε equations. In CFD Ansys, $\sigma_k, \sigma_\varepsilon, C_{1\varepsilon}, C_{2\varepsilon}$, and C_μ are set to default values as shown below:

$$C_\mu = 0.09, \ \ C_{1\varepsilon} = 1.44, \ \ C_{2\varepsilon} = 1.92, \ \ \sigma_k = 1.0\ , \ \ \sigma_\varepsilon = 1.3$$

The RNG is another type of model under k-ε model used in this work. RNG model is similar to the standard k-ε model but more accurate and reliable and used for rapid strained and swirling flows. The RNG k-ε model equation can be defined as shown below:

$$\frac{\partial}{\partial t}(\rho k) + \frac{\partial}{\partial x_i}(\rho k u_i) = \frac{\partial}{\partial x_j}\left(\alpha_k \mu_{eff} \frac{\partial k}{\partial x_j}\right) + G_k + G_b + \rho\varepsilon - Y_M + S_k \qquad (6.16)$$

And

$$\frac{\delta}{\delta t}(\rho\varepsilon) + \frac{\partial}{\partial x_i}(\rho\varepsilon u_i) = \frac{\partial}{\partial x_i}\left(\alpha_\varepsilon \mu_{eff} \frac{\partial \varepsilon}{\partial x_j}\right) + C_{1\varepsilon}\frac{\varepsilon}{k}(G_k + C_{3\varepsilon}G_b) - C_{2\varepsilon}\rho\frac{\varepsilon^2}{k} - R_\varepsilon + S_\varepsilon \qquad (16.17)$$

The generation of turbulence kinetic energy due to the mean velocity gradients is indicated by G_k and due to buoyancy by G_b(ANSYS, 2017). The contribution to the overall dissipation rate of the fluctuation in the compressible turbulence represents in Y_M. In CFD Ansys, $C_\mu, C_{1\varepsilon}$, and $C_{2\varepsilon}$ are set to default values as shown below:

$$C_\mu = 0.0845, \quad C_{1\varepsilon} = 1.42, \quad C_{2\varepsilon} = 1.68$$

6.3.3 CFD Procedures

CFD is designed with the integration of numerical algorithms that can predict and analyse fluid flow. The conservation is handled by the equations interacting with each cell via meshing procedures within the computational domain (Haredy, 2016), (O'Connor, 2016). Therefore, CFD codes include three main elements: a pre-processor, a solver, and a post-processor (Versteeg and Malalasekera, 1995b). This study used one of the most commonly used CFD software, which is ANSYS Fluent. Generally, the main stages of building modelling are three, begin with creating or importing the shape into the geometry, after that define the appropriate mesh of the model and boundary conditions, then preparing the model in Fluent by selecting the type of turbulence model and iterations and other inputs to get the results (Figure 6-4). Pre-processor is a procedure that involves entering a flow problem into a CFD programme by defining the geometry of the region of interest: the computational domain, and transforming it into an appropriate solver-friendly form (Versteeg and Malalasekera, 1995b). Grid generation is one of the critical tasks in the pre-processor where the domain is divided into much smaller, non-overlapping sub-domains generated by a grid (or mesh) of cells (or control volumes or elements). Each cell will be solved a flow issue such as airflow, temperature, etc., by the Fluent solution, so the number of cells plays a significant role in the accuracy of results. Also, the physical and chemical properties and properties in the pre-processor need to be defined and selected to prepare for modelling. Then, specify suitable boundary conditions in cells that coincide or affect the domain boundary (Versteeg and Malalasekera, 1995b).
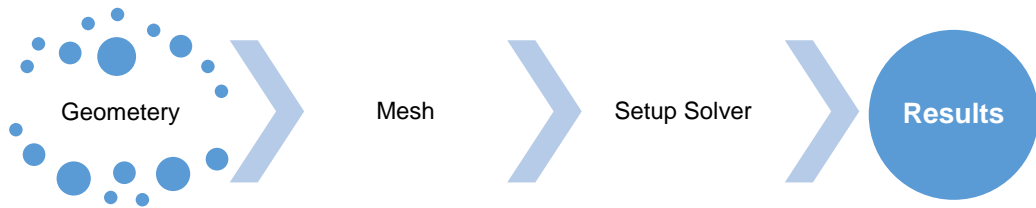
Figure 6-4 Main stages of CFD modelling

In 3D flow calculations, a tetrahedral or hexahedral mesh is widely used. Hybrid mesh combines both meshes and comes up with better resolution (Versteeg and Malalasekera, 1995b), see (Figure 6-5). According to Sofotasiou (2017), several factors affect selecting mesh density as geometry, computational time and memory availability, achieving a mesh-independent solution, numerical accuracy, and simulation errors. Therefore, to obtain high-reliability simulation results and accurate and converged solutions, a grid type and structure is essential. So, it must be taken into account when configuring the mesh several points as mesh type and size, cells numbers. In addtion, skewness, smoothness, and aspect ratios must be check for defined the mesh quality (Table 6-1).
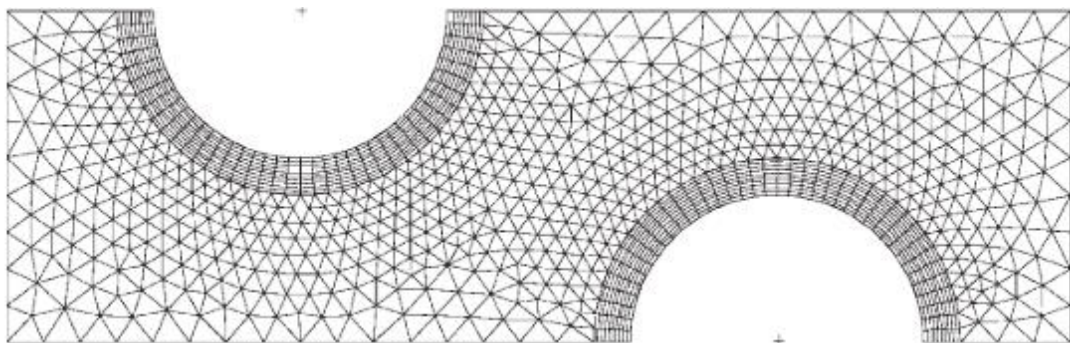
Figure 6-5 An example of hybrid mesh (Versteeg and Malalasekera, 1995b)

Table 6-1 The criterion of measuring the mesh quality

Criterion	description
Skewness	It measures the asymmetry from the normal distribution of a set of data.

Value of Skewness	0 to 0.25	0.25 to 0.5	0.5 to 0.8	0.8 to 95	0.95 to 0.99	0.99 to 1
Cell Quality	Excellent	Good	Acceptable	Poor	Sliver	Degenerate

Criterion	description
Smoothness	Measured by the number of continuous derivatives where some cases, change in cell/element size should be gradual.

$$\frac{\Delta x_{i+1}}{\Delta x_i} \leq 1.2$$

Criterion	description
Aspect ratio	A measure of the stretching of a cell which is the ratio of longest edge length to shortest edge length. The aspect ratio of most cases that use quadrilateral/hexahedral cells can be stretched up to 10:1 and can be higher in the stability of the flow solution and below 35:1

aspect ratio = 1   high-aspect-ratio quad

aspect ratio = 1   high-aspect-ratio triangle

6.4 CFD and Natural Ventilation

Computational fluid dynamics (CFD) modelling allows for improvements to be made at the design stage; by contrast, experimental methods are limited to the evaluation and analysis of existing structures after the design and building process has been completed (Allocca, 2001). When deciding on the optimal design and airflow areas for a specific building, the use of CFD is critical in terms of saving time and costs where computational costs decrease while labour and material costs for experiments increase (Allocca, 2001). With the development of computing power, using CFD has increased in the engineering field, where it provides an alternative predictive and analytical tool for problems in the field that other measuring methods cannot readily trace. Therefore, using CFD correctly and thoughtfully facilitates analysing designs before implementation and allows us to carry out pre-investigation of design effects such as predicting the movement of natural airflow around and inside buildings to obtain the optimal benefit from natural ventilation.

In 2002, Maghrabi studied modulated louvre windows concerning Jeddah's mashrabiyas to examine the ventilation efficiency through modelling and simulation. The study revealed that the leading causes of poor ventilation inside the room were when the slides were adjusted in

an acute inclination position to ±60°. Maghrabi stated that the form of the mashrabiya played a vital role in the flow pattern inside the room since the flat mashrabiya allowed more airflow in its centre compared to prominent mashrabiyas. (Allocca, 2001) investigated the impact of one-sided natural ventilation strategies in a residential room and found that CFD results differed about 10% from semi-analytical.

Chiang et al. (2005) simulated a room with horizontal louvres and tested different air velocities to improve ventilation and comfort. It was demonstrated that louvres could be used to improve indoor air quality by increasing air change rate. In contrast, the airflow rate cannot be increased, and hot air will not be transferred effectively when the depth of the louvre is less than 4 cm. Nakanishi et al. (2007) studied a CFD model that include louvres validated with wind tunnel measurements. It illustrated the relation between pressure and louvre angle and concluded that by changing the louvre angle to 20°, pressure losses could be kept to below half. Another research by Di Turi and Ruggiero (2017) used CFD DesignBuilder to study airflow on four standard window and mashrabiya with three various size patterns. The study stated that the mashrabiya system works more effectively than the standard window, especially during the hot hours of summer.

Research conducted by Shen and Li (2016) integrated cooling tubes into the metal blinds of the double-skinned glazing to reduce heat transfer to the envelope in summer. The findings showed that the venetian blinds decrease their average temperature from around 57°C to 25.4 ° C, while overall cavity temperature drops to around 29°C. A study conducted by Kosutova et al. (2019) evaluated four different configurations of openings with and without louvres, and the slats were tilted at ±15°. It was found that the efficiency of air exchange on tilt angle -15° with louvres was 9.1% higher than the case without louvres. Another study was conducted by (Salem, 2019), which tested a room with mashrabiya using evaporative cooling in CFD software. The study found that this method decreased indoor air temperature by up to 4 degrees, whereas it reduced the supply of air entering. Table 6-2 refers to a review of some previous CFD studies on the study of ventilation, either single-sided or cross ventilation, including pointing out some factors; if the model was validated and if the models used mashrabiya or louvre with integrated some cooling method in design. It should be mention that most of these studies were conducted CFD model for a domain with an isolated building

or room. Although Ramponi and Blocken (2012) model was designed as an isolated building with two openings without mashrabiya or evaporative cooling, it presented a simplified and accurate model similar to experimental results through extensive study of many parameters and variables in CFD. As a result, Ramponi and Blocken (2012) model was adapted as a reference case for this study, while the studies of (Maghrabi, 2000, Chiang et al., 2005, Nakanishi et al., 2007, Calautit et al., 2015, Shen and Li, 2016, Kosutova et al., 2019, Fallahtafti and Mahdavinejad, 2020), were taken advantage of, specifically in identifying some variables or methods of analysis used.

Table 6-2 Some previous CFD studies related to ventilation

Authors (year)	Validation	Mash /Louver	Ventilation	Integrate technique
(Maghrabi, 2000)	Y	Y	Single-sided	N
(Allocca, 2001)	Y	N	Single-sided	N
(Bartzanas et al., 2002)	N	N	Cross-vent	N
(Chiang et al., 2005)	N	Y	Single-sided	N
(Maghrabi and Shehata, 2005)	N	Y	Single-sided	N
(Nakanishi et al., 2007)	Y	Y	Single-sided	N
(Stavrakakis et al., 2008)	Y	N	Cross-vent	N
(Meroney, 2009)	Y	N	Cross-vent	N
(Gan, 2010)	Y	N	Cross-vent	N
(Nikas et al., 2010)	Y	N	Cross-vent	N
(Cheung and Liu, 2011)	Y	N	Cross-vent	N
(Ramponi and Blocken, 2012)	Y	N	Cross-vent	N
(Calautit et al., 2015)	Y	N	Single-sided	Y
(Prakash and Ravikumar, 2015)	Y	N	Cross-vent	N
(Perén et al., 2015)	Y	N	Cross-vent	N
(Shen and Li, 2016)	Y	Y	Single-sided	Y
(Haredy, 2016)	Y	N	Single-sided	N
(Di Turi and Ruggiero, 2017)	N	Y	Single-sided	N
(van Hooff et al., 2017)	Y	N	Cross-vent	N
(Ibraheem, 2018)	Y	N	Cross-vent	Y
(Kosutova et al., 2019)	Y	Y	Cross-vent	N
(Salem, 2019)	N	Y	Single-sided	Y
(Elwan, 2020)	N	Y	Single-sided	N
(Fallahtafti and Mahdavinejad, 2020)	Y	Y	Cross-vent	N

6.5 Modelling and Simulation Procedures

Simulation is the second masterwork part of this research which include several procedures and cases. The primary purpose of this modelling phase is to create a valid base case, and then use different parameters, including an evaporative cooling technique to enhance the performance of mashrabiya and improve indoor thermal comfort. For this purpose, the objectives of this simulation are the following:

- ➢ Select an accurate CFD model that evaluates coupled outdoor wind flow, indoor airflow, and natural cross-ventilation validated with detailed wind tunnel experiments.
- ➢ Simulate the benchmark model by applying the same available inputs of the CFD ref model.
- ➢ Test different turbulence models and iterations compared to the CFD ref and PIV experiments to assign the most adequate and similar cases.
- ➢ Add a plain mashrabiya to the benchmark model to obtain the base case.
- ➢ Test different angles of mashrabiya slats to find the effect of slats angle on airflow into the room.
- ➢ Integrate inspired heat transfer devices with the plain mashrabiya to improve indoor thermal comfort in accordance with specific parameters such as slat declination angle, Inlet and operative temperature, air velocities, etc.
- ➢ Analysis of the mashrabiya design response to improving thermal comfort and to which extent was efficient compared to the base case.

6.5.1 Simulation Plan

Two prime stages of the simulation, preparation and development, were followed to achieve the objectives of this research, as shown in Figure 6-6. First, several procedures were carried out as preparation for the simulation process, starting with selecting a validated model with an actual experiment. After the validation model, three sets were conducted sequentially through a group of configurations and strategies representing the base case and development stage (Figure 6-7), which will be presented and discussed in the next chapter.
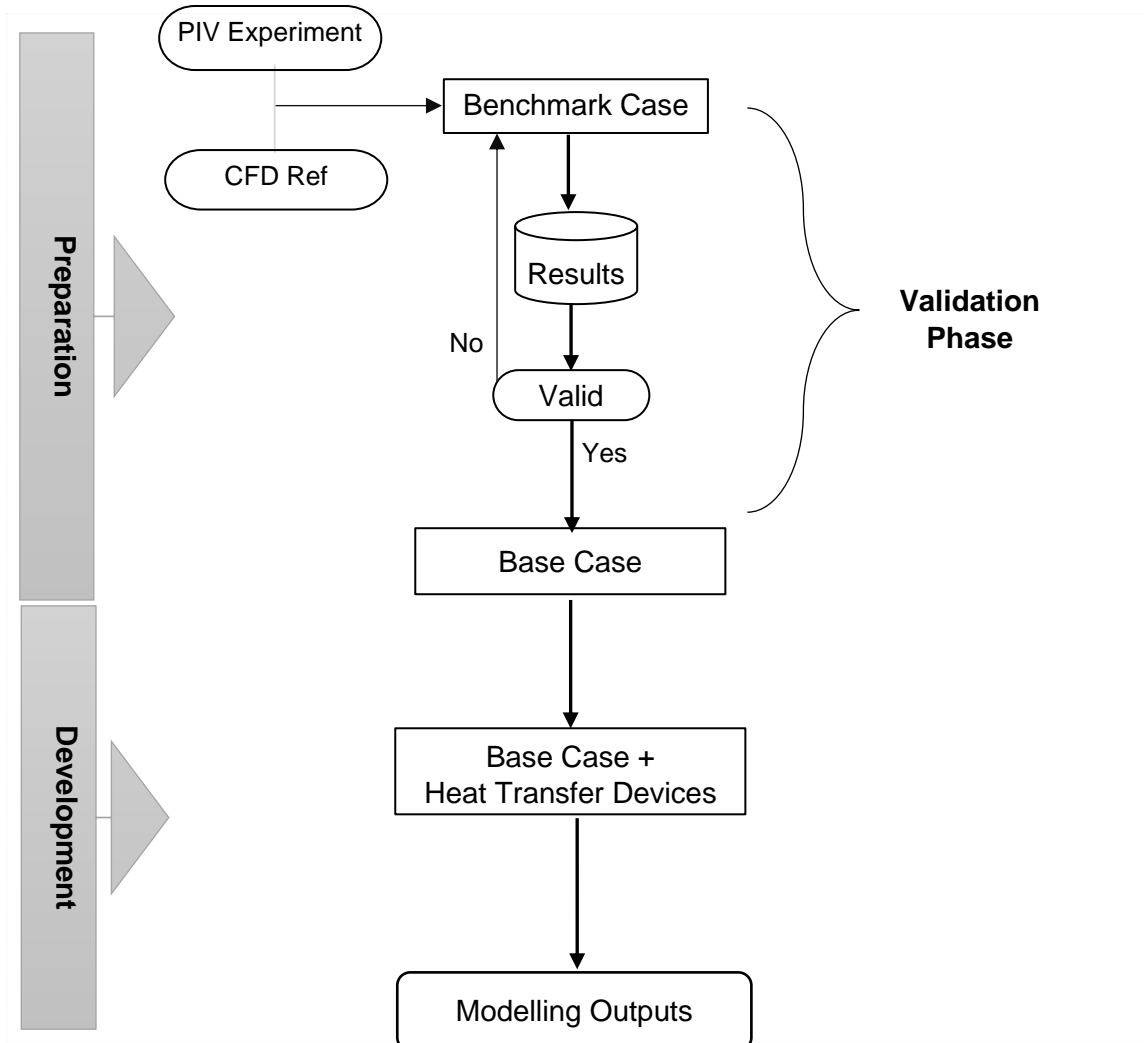
Figure 6-6 A brief diagram of simulation procedures
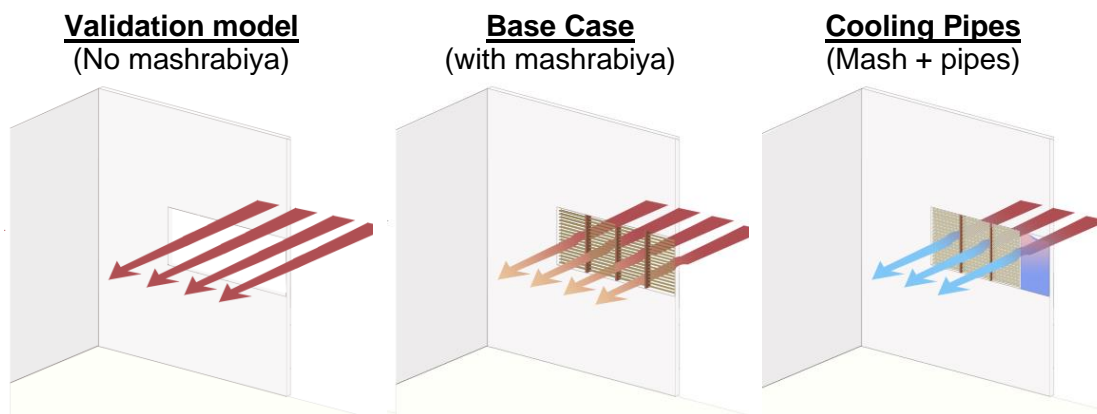
Figure 6-7 The The three main stages of the simulation

6.6 Validation Model

For the purpose of having more data than fieldwork and expansion of our understanding of mashrabiya, simulation was taking a significant part in achieving the aim of this research. After the on-site monitoring and measurements were conducted and presented with the analysis and result in chapter 5 in detail, a benchmark case was generated from a validated model that included detailed wind tunnel data of the Particle Image Velocimetry velocity measurement PIV and CFD reference with actual experiment results.

The main aim of this phase was to have a validated model which can allow more investigation of the performance of mashrabiya and development, which will be presented in the next chapter, chapter 7. The model was created as the CFD model presented by Ramponi and Blocken (2012) validated based on detailed wind tunnel experiments by Karava et al. (2011). Therefore, the reference CFD model has been selected as a benchmark based on their validation with a real experiment, including testing several computational parameters. In the reference CFD model (RCM), a wide range of computational parameters was examined, including domain size, grid resolution, turbulence model, order of the discretisation schemes, and iterative convergence criteria to reach similar results to the actual experiment.

In this work, all simulations cases were conducted using ANSYS 18.1 workbench. Ansys considers one of the most known and robust software in engineering simulation in Computational Fluid Dynamics (CFD). So, this study used ANSYS as a CFD tool for this work based on several factors such as; accuracy, prevalence, availability of guides and tutorials, technical considerations and compatibility, interfaces and integration. To recap, the next part of the simulation aimed to obtain the same or similar to CFD or PIV experiment thus that the bench case could be valid for the subsequent phases.

6.6.1 Model Setup

6.6.1.1 Design Geometry

Based on the selected CFD reference case "RCM" by (Ramponi and Blocken, 2012), which relied on the best practice guidelines by Franke et al. (2007) and Tominaga et al. (2008), the computational domain and room position of this work was created as shown in Figure 6-8.

The fluid volume was separated into the macroclimate (surrounding the test chamber) and the microclimate (the test chamber).

The macro-climate was created to simulate the airflow around the room and the micro-climate to simulate the airflow inside the room. The airflow inlet of the computational domain at a distance of 3H from the room and the boundary downstream of the building on 15 from the room, while the top and both domain's sides at an equal distance 5H from the room (Figure 6-8). The domain dimensions in full scale are 180 x 308 x 96 m^3 (W_D x L_D x H_D), and the room is 20 x 20 x 16 m^3 (W_R x L_R x H_R).

For simulation purposes, scale 1: 200 was used for this model as recommended in RCM, which means 1 mm equivalent to 200 mm in the actual model; thus, the domain in reduced scale became equal to 0.9 x 1.54 x 0.48 m^3 or 900 x 1540 x 480 mm^3, while the room's dimensions represent 100 x 100 x 80 mm^3 corresponding to 20 x 20 x 16 m^3 in full scale (Figure 6-9).
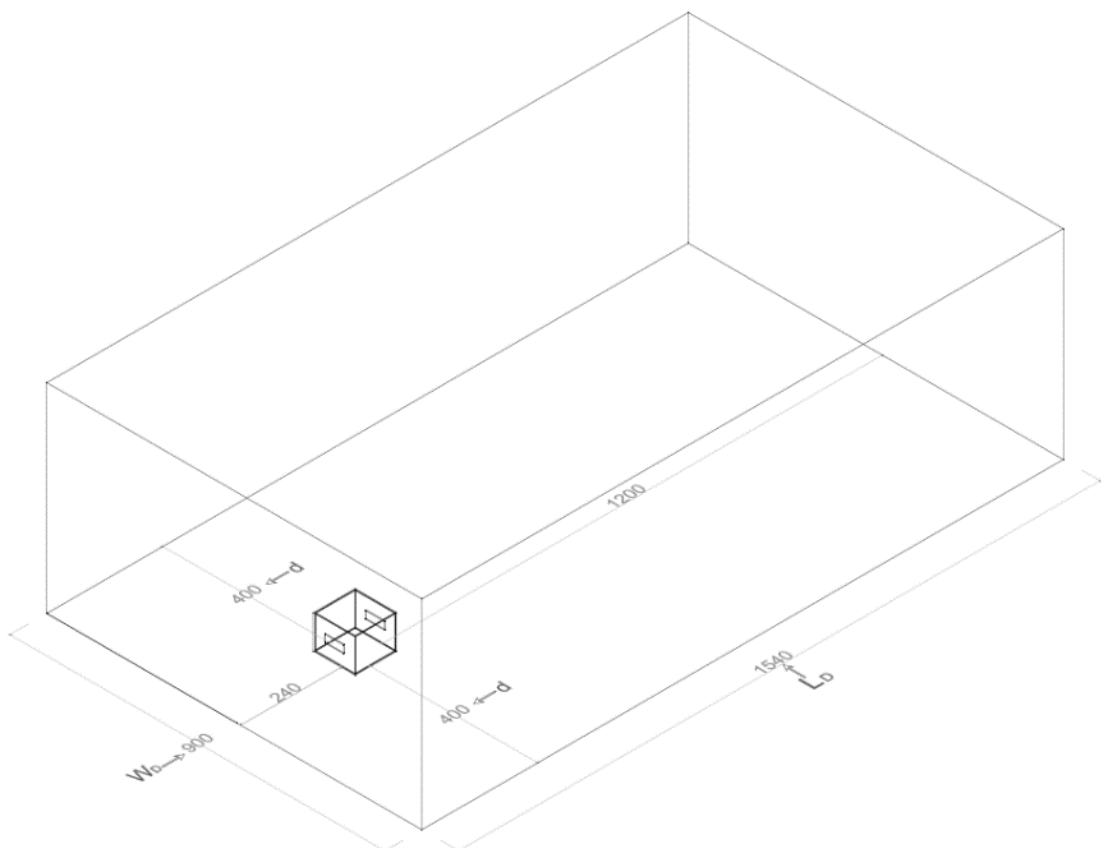
Figure 6-8 The dimensions of CFD domain and room in mm
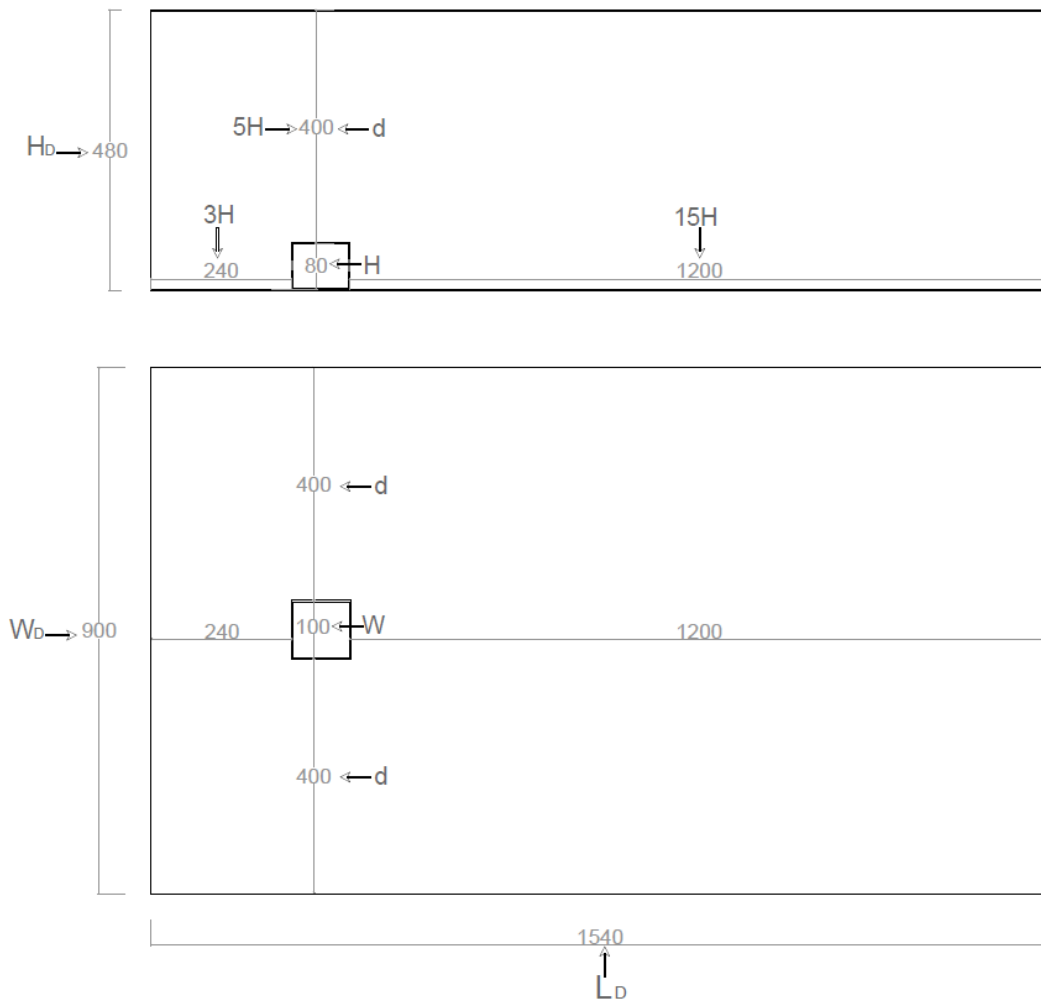
Figure 6-9 Computational domain section and plan

The wall, ceiling, and ground are designed as in RCM with a thickness of 2 mm. Table 6-3 shows the dimensions of the domain and room in full scale and reduced scale. The room has two opposite openings, one facing the windward and the other the leeward facade, as seen in Figure 6-10. The opening dimensions are 46 x 18 mm at the height of 31 mm, corresponding to 9.2 x 3.6 m^3 in full scale.

Table 6-3 Domain and room dimensions

Description	Symbols	Full Scale	Reduced scale
Domain dimensions	$D_{dim} = W_D \times L_D \times H_D$	180 x 308 x 96 m^3	0.9 x 1.54 x 0.48 m^3
Domain width	$W_D = W_R + 2d$	20 + 160 m	100 + 800 mm
Domain Length	$L_D = L_R + (3H_R + 15H_R)$	20 + (48+240) m	100 + (240+1200) mm
Domain height	$H_D = H_R + d$	16 + 80 m	80 + 400 mm
Room dimensions	$R_{dim} = W_R \times L_R \times H_R$	20 x 20 x 16 m^3	0.1 x 0.1 x 0.08 m^3
Room openings	$R_o = W_o \times H_o$	9.2 x 3.6 m	46 x 18 mm
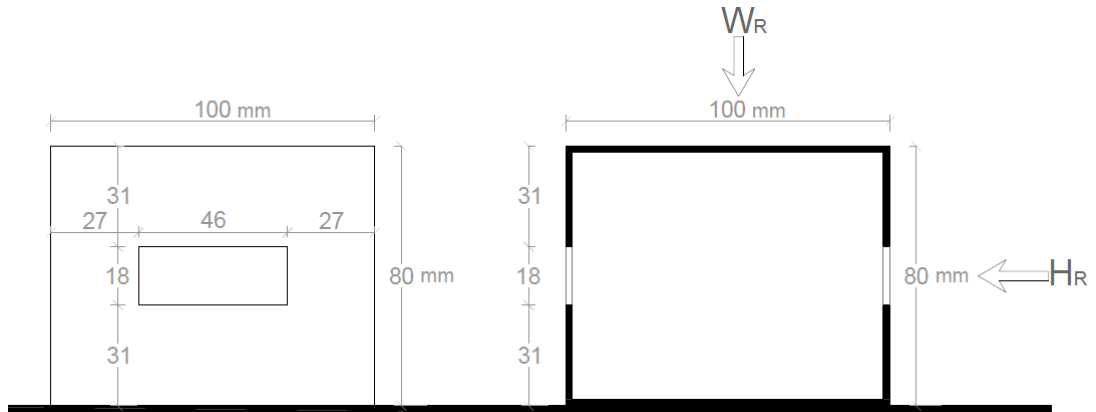
Figure 6-10 Elevation and section perspective of the computational room

6.6.1.2 Meshing

In this phase, two types of mesh have been used: hexahedral mesh and tetrahedral mesh. Figure 6-11 display both mesh on the computational domain and room. Although the RCM indicated that the hexahedral mesh provided more similar results for PIV than the tetra one, this work covered both types based on the inputs specified in Table 6-4, which have more cell elements. Due to the different handling of the used meshes, the domain was configured differently and then used different ANSYS mesh inputs. For the hexahedral mesh, the volume was prepared by applying the slicing technique explained in detail by Mohd Nasir (2017). The domain was cut into 48 volume parts before edge sizing was calculated to enable a wholly formed structured mesh for the macro domain (Mohd Nasir, 2017), as shown in Figure 6-12. On the other hand, the volume for tetra mesh was kept whole without any slicing, but the volume mesh size was determined at 0.015 m and set the facing size at 0.0007m for the room with defining hard as behavior.
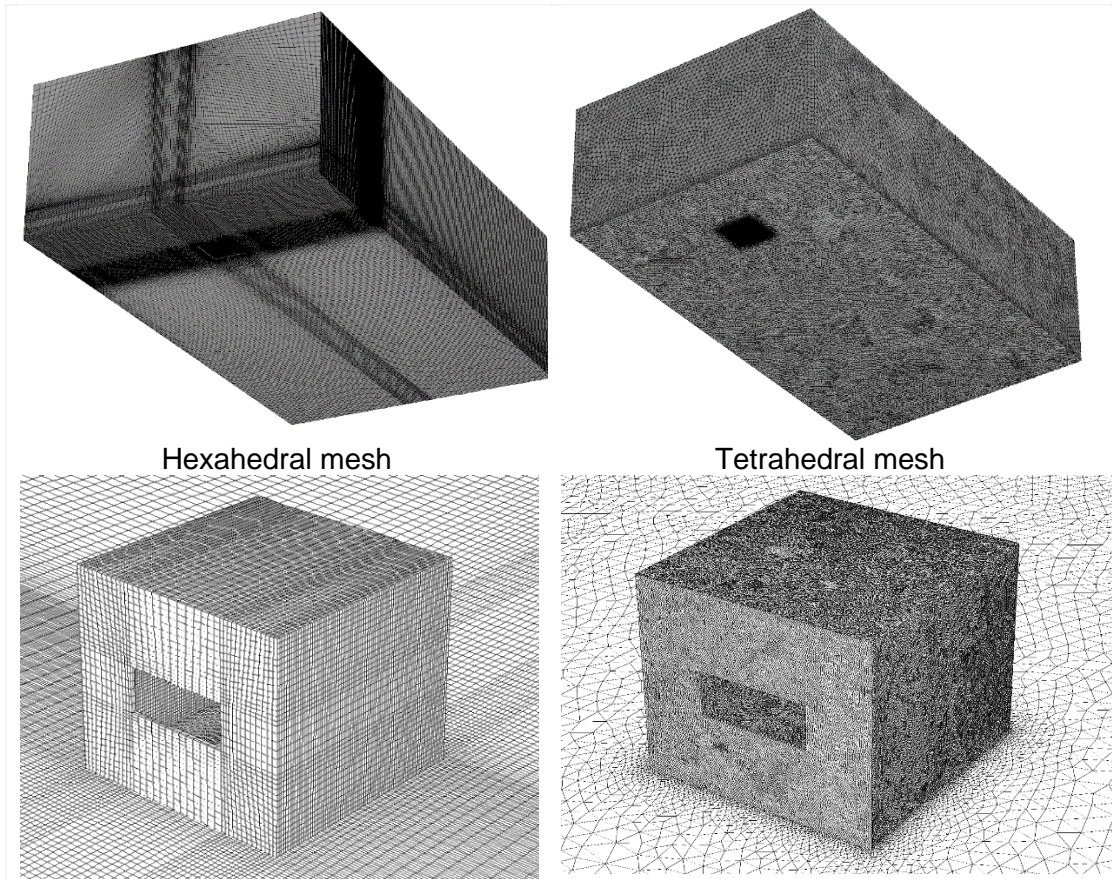
Figure 6-11 Plan, sectional elevation and 3D view of Hexa mesh vs tetra mesh

Accordingly, the cell elements amounted to 4,968,878 with nodes 5,083,972 in the hexahedral mesh with an average skewness and aspect ratio of 0.8 and 8.2, respectively. While in the tetrahedral mesh, the cell elements are 6,836,946 with 1,256,350 nodes and skewness average of 0.2 and an aspect ratio average of 1.8.

Table 6-4 Inputs and output of hexahedral tetrahedral mesh

	Physics/ Solver preference	Element order	Mesh Size Function	Relevance Center	Quality	Growth Rate
Mesh Inputs						
Hexahedral	CFD, Fluent	Quadratic	Proximity	Fine	High	1.05
Tetrahedral	CFD, Fluent	Linear	Curvature	Fine	High	1.2
Mesh Ouputs						
	Nodes	**Cell Elements**	**Skewness (Avg)**	**Aspect ratio (Avg)**	**Smoothing**	
Hexahedral	5,083,972	4,968,878	0.811	8.188	High	
Tetrahedral	1,256,350	6,836,946	0.224	1.838	High	
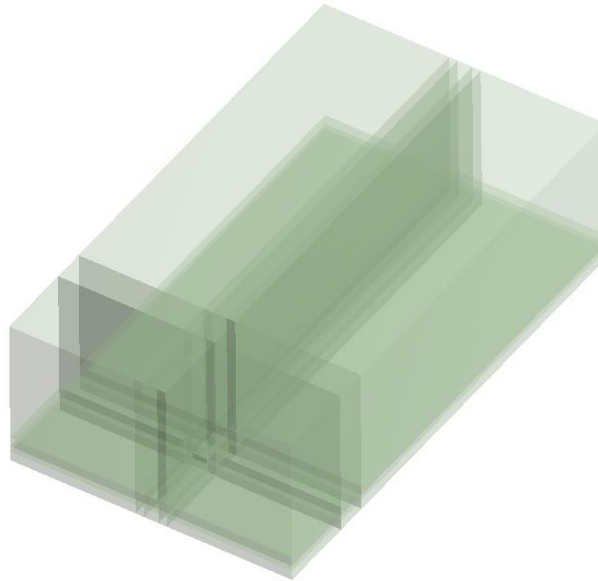
Figure 6-12 Mesh generation using Automatic Meshing Method with sliced volumes

6.6.1.3 Boundary conditions

The boundary conditions used in the simulations were based on Ramponi and Blocken (2012) data of the vertical profile of mean wind speed, as seen in Figure 6-13. It was mentioned by Ramponi and Blocken (2012) that "A reference mean U_{ref} wind speed of 6.97 m/s and a reference turbulence intensity of 10% was measured at building height", where the dashed line shows the height level of the building or room. Although the researcher attempted to redraw the exact curve of the mean wind speed profile by matching the same wind speed profile to calibrate the model and reuse it in this work, some slight differences in the curve readings might affect the results.

(A)   (B)
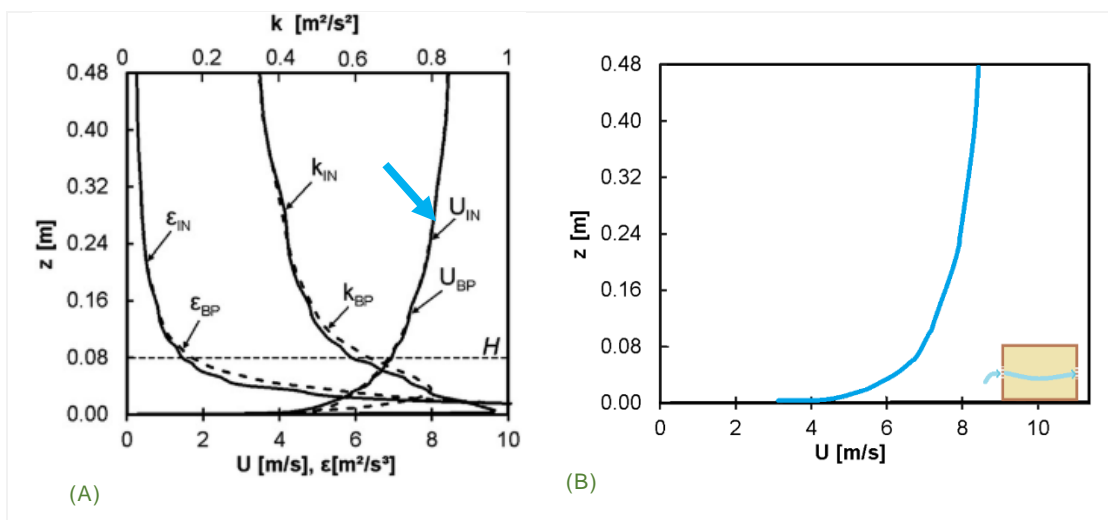
Figure 6-13 (a) Profiles of the mean wind speed (U) from RCM and the U_{ref} applied in this simulation

Thus, the velocity input varied between 0 and 8.45 m/s. Since the primary purpose of this stage was to validate the model, it followed the RCM, and any other uncovered parameters in RCM such as thermal heat transfer or heat gain were neglected at this phase. Shows

At the outlet plane, the static pressure of the outlet and symmetry conditions was set to zero, and the symmetry conditions domain means that zero normal velocity and zero normal gradients of all variables at symmetry planes (Ramponi and Blocken, 2012). Figure 6-14 illustrates the flow domain of the computational model showing the boundary conditions (inlet, outlet, ground, Symmetry) and their positions concerning the axes. Table 6-5 shows the overall boundary conditions of the validation model.
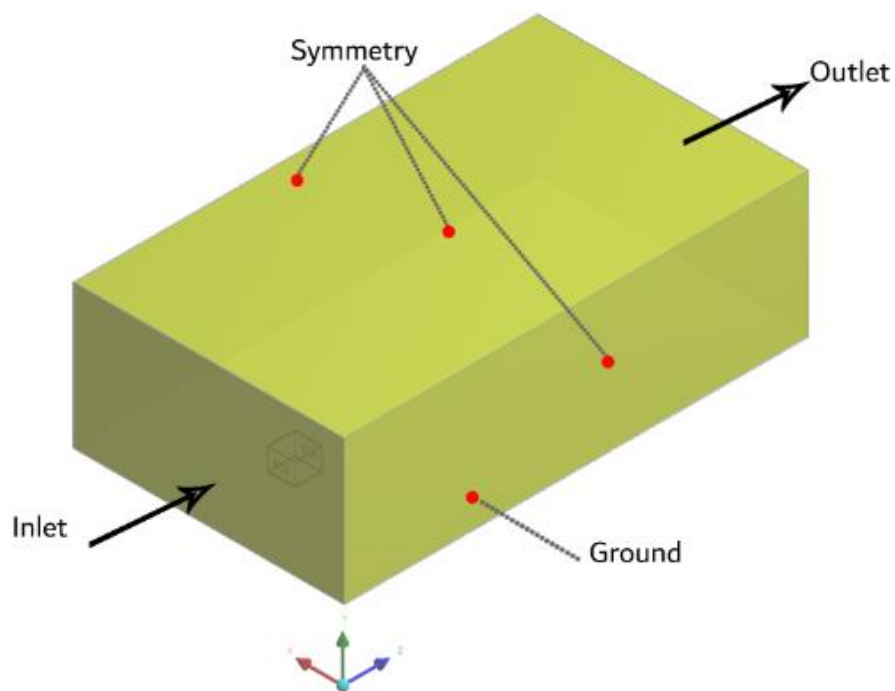
Figure 6-14 The boundary conditions in the flow domain of the computational model.

Table 6-5 The Applied boundary conditions for the numerical simulation

Property	Value
Micro–macroclimate	Fluid (air)
Uref wind speed	6.97 m/s
Velocity inlet	Uref
Pressure outlet	Zero
Temperature	–
Relative humidity	–

6.6.1.4 Solver settings

The simulations were conducted with the commercial CFD code ANSYS FLUENT to simulate the airflow inside the domain and into the room. Convergence is considered a critical factor in any CFD model, defined by (Calautit et al., 2015) as " the term for a numerical method using iterations to solve the grid, whereby the error approaches zero". The ANSYS guide mentioned that for most cases, the default convergence criterion in FLUENT is adequate. For all equations, the scaled residuals should be reduced to 10-3, whereas in the energy equations, up to 10-6. Because of that, different iterations were applied 1000, 2000, and 10000 to obtain the best convergence and lowest residuals. All iterations of each case were run and completed without errors.

In addition, the SIMPLE algorithm was used with the default setups of ANSYS, where the pressure and momentum were specified second-order.

The 3D steady RANS equations are solved in combination with three turbulence models; (1) Shear Stress Transport (SST k- ω) model, standard k-epsilon (k- ε) model,(3) RNG k-epsilon (RNG k-ε)model;(4) K-omega (k- ω) model, see Table 6-6.

For each simulation, 14 processes on a node were used (AMD Ryzen 7 2700X Eight-Core Processor @ 3.70 GHz) with 32 GB of system memory accessible.

Table 6-6 Turbulence models used with the implemented iterations and the name of each case based on the mesh
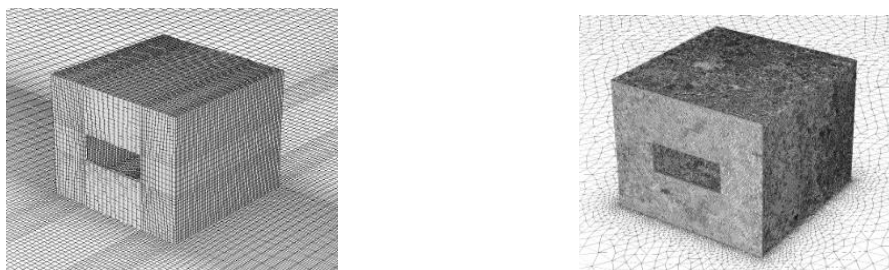
Hexa	Turbulence model	Iterations	Tetra	Turbulence model	Iterations
1-1H	Transition SST	1000	1-1T	Transition SST	1000
1-2H	Transition SST	2000	1-2T	Transition SST	2000
1-3H	Transition SST	10000	1-3T	Transition SST	10000
1-4H	k-epsilon standard	1000	1-4T	k-epsilon standard	1000
1-5H	k-epsilon standard	2000	1-5T	k-epsilon standard	2000
1-6H	k-epsilon standard	10000	1-6T	k-epsilon standard	10000
1-7H	k-epsilon RNG	2000	1-7T	k-epsilon RNG	2000
1-8H	k-omega	2000	1-8T	k-epsilon RNG	10000
			1-9T	k-omega	2000
			1-10T	k-omega	10000

It is worth noting that several points in two different levels have been specified to measure the average airflow velocity inside the room has been shown in Figure 6-15. One midpoint and two different levels were taken as the averages of indoor airflow; One is 34mm high, and the other is 12mm off the floor. Each level contains 25 points with an equal distance of 17.5 mm around each point. Besides that, the middle line is the main measurement reference for comparing the results with wind tunnel data of the Particle Image Velocimetry velocity measurement "PIV" and CFD reference case "RCM", while the plane was a section measurement for air velocity and pressure.
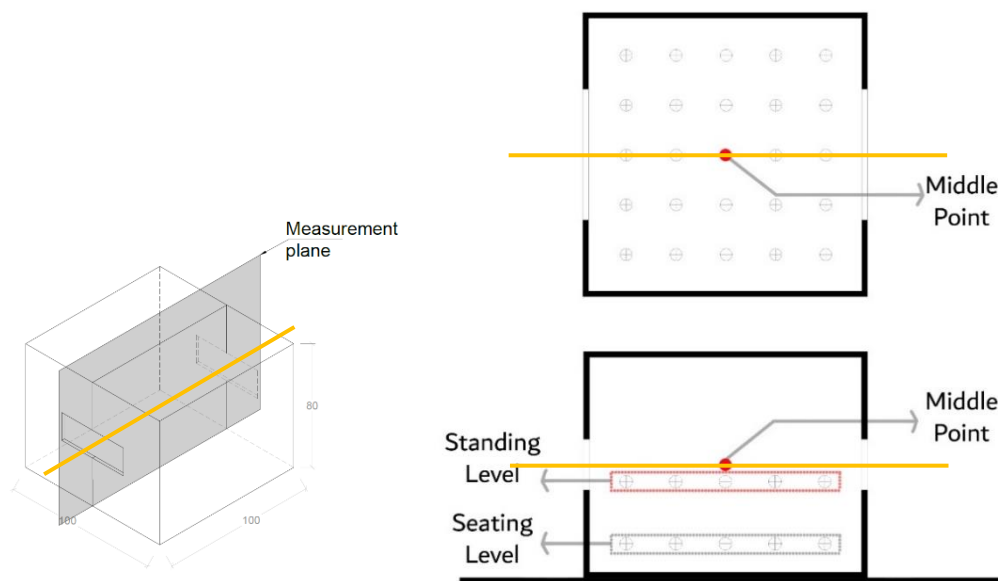
Figure 6-15 CFD measurements levels and points

6.6.2 Results and Discussion

6.6.2.1 Hexahedral mesh cases

Table 6-7 presents the agreement between the hexa cases and the PIV, including residuals ratings. By applying the hexa mesh to geometry and then testing different turbulence models, the 1-6H case " K-epsilon standard 10000" is the first model compatible with PIV measurement where its solution provides fluctuations constant, as shown in Figure 6-16. The second closest case to PIV, the 1-3H, used the SST turbulence model with 10000 iterations. Although 1-6H and 1-3h monitored the closest data match with PIV data, the high residuals in low iterations 1000 caused the decreasing agreement to PIV compared to the rest of the cases, Figure 6-17.

Table 6-7 The agreement between PIV measurement data and hexa mesh cases.

	Case	Turbulence	Iterations	Error (%)	Similarity to PIV chart	Residuals
1	1-6H	K-epsilon standard	10000	23.4	5	-3
2	1-3H	SST	10000	28.8	3	-3
3	1-8H	K-omega	2000	36.4	2	-2
4	1-7H	K-epsilon RNG	2000	29.1	1	-2
5	1-5H	K-epsilon standard	2000	28	4	-3
6	1-2H	SST	2000	20.8	7	-3
7	1-4H	K-epsilon standard	1000	35.6	6	0
8	1-1H	SST	1000	25.8	8	0
Residuals: (3 to -3, where 3 means high residuals and -3 high)						

As displayed, Figure 6-18 shows the numerical results of turbulence models using hexa mesh compared to experimental PIV results in one graph, whereas Figure 6-19 represents each case in a separate chart for a clearer view.
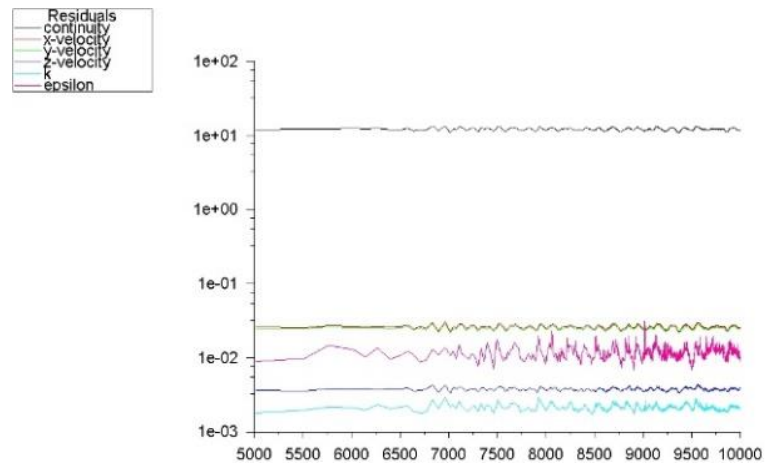
Figure 6-16 Convergence behaviour of K-epsilon standard "1-6H" Solution monitored over 10000
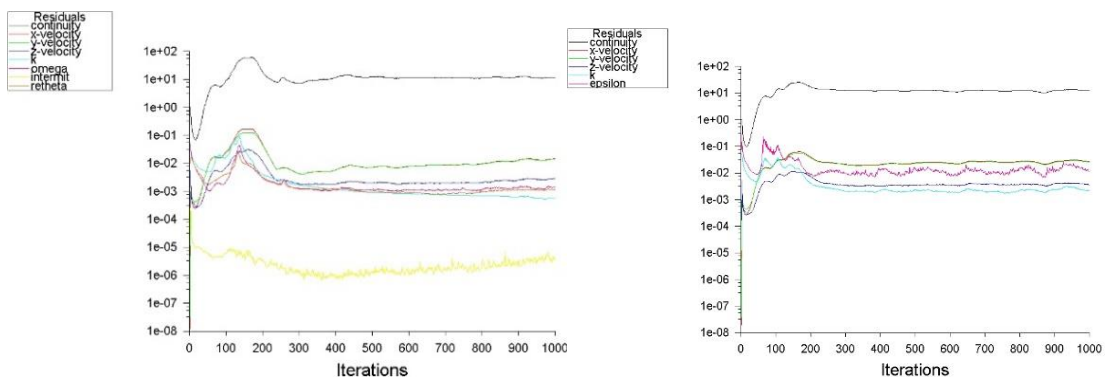
Figure 6-17 The convergence behaviour of the solution (left)SST and (right) K-epsilon standard monitored 1000

On the x-axis of Figure 6-19, -0.05 to 0.05 represents the room depth, while the values above 0.05 and less than -0.05 demonstrate the defined distance from windward and leeward of the

room. The added grey areas to the graph represent data positions ignored by the PIV experiment due to some errors.

Based on the grey areas, RNG k-ε model and k-omega are most compatible with PIV, but air velocity results in the middle of the room were affected by the solver of these turbulence models and recorded significantly higher values compared to the rest of the cases. Therefore, it can be indicated that the k-ε 10000 model is superior, followed by the SST 10000 model concerning the agreement to PIV; however, the other cases still provide acceptable results.
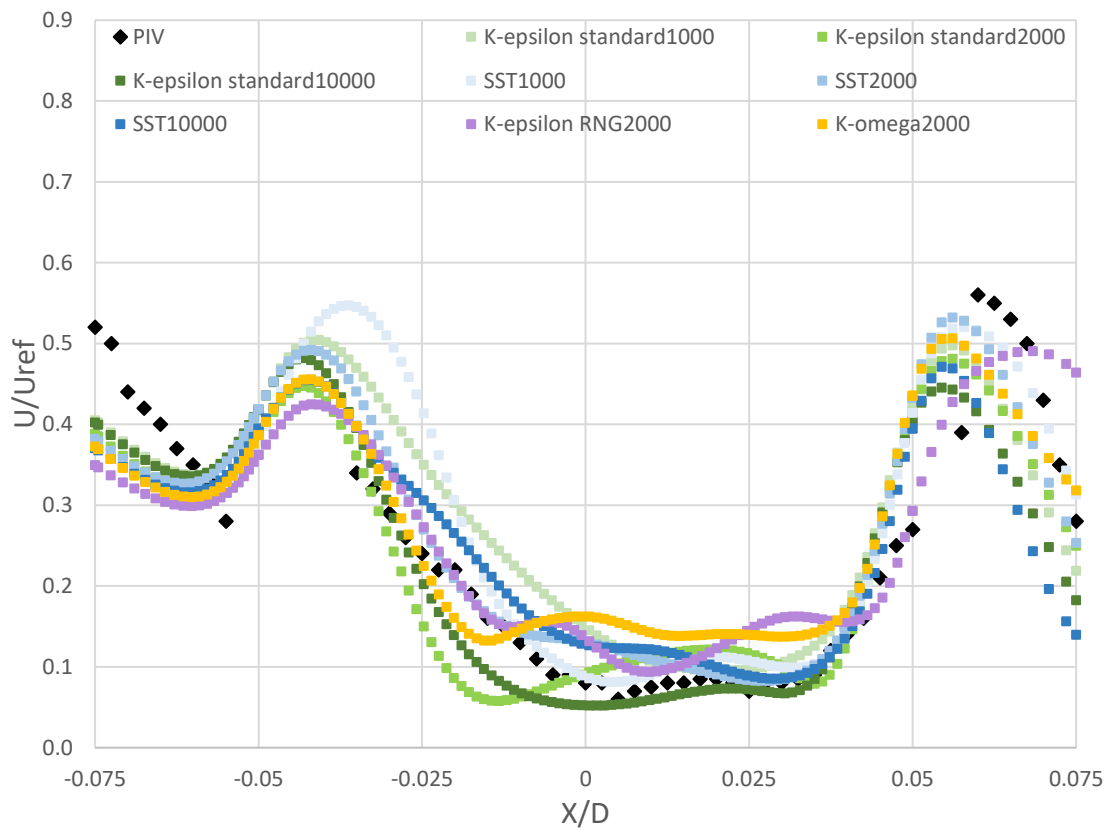
Figure 6-18 The airflow results of hexa mesh cases compared to PIV measurement
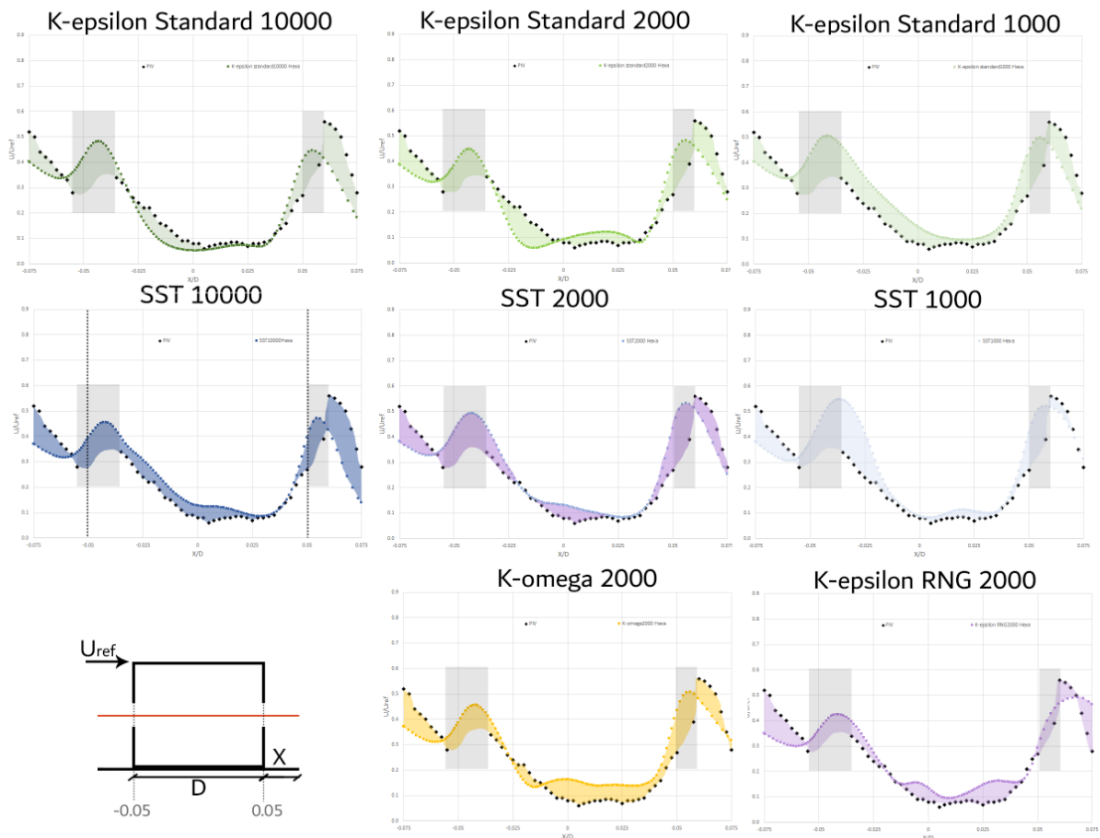
Figure 6-19 The airflow results of hexa mesh cases compared to PIV measurement along a horizontal line going through the middle of the room openings

Table 6-8 displays the cross-sectional plot of the air velocity contours in the room and the iterative convergences of turbulence models using hexa mesh. The 1000 iterations caused some less resolution of the data specified in the leeward area. It is apparent from this table, that the angle of airflow contours from the windward opening until before the opposite opening for the cases 1-1 to 1-3H, 1-7H, and 1-8H are higher inclined compared to the k-epsilon standard turbulence model.

Table 6-8 The cross-sectional plot of the air velocity contours in the room and iterations of the hexa mesh cases

1-1H		Transition SST 1000	
1-2H		Transition SST 2000	
1-3H		Transition SST 10000	
1-4H		k-epsilon standard 1000	

Velocity Magnitude [m/s]   0   1.4   2.7   4.1   5.4   6.8   8.1   9
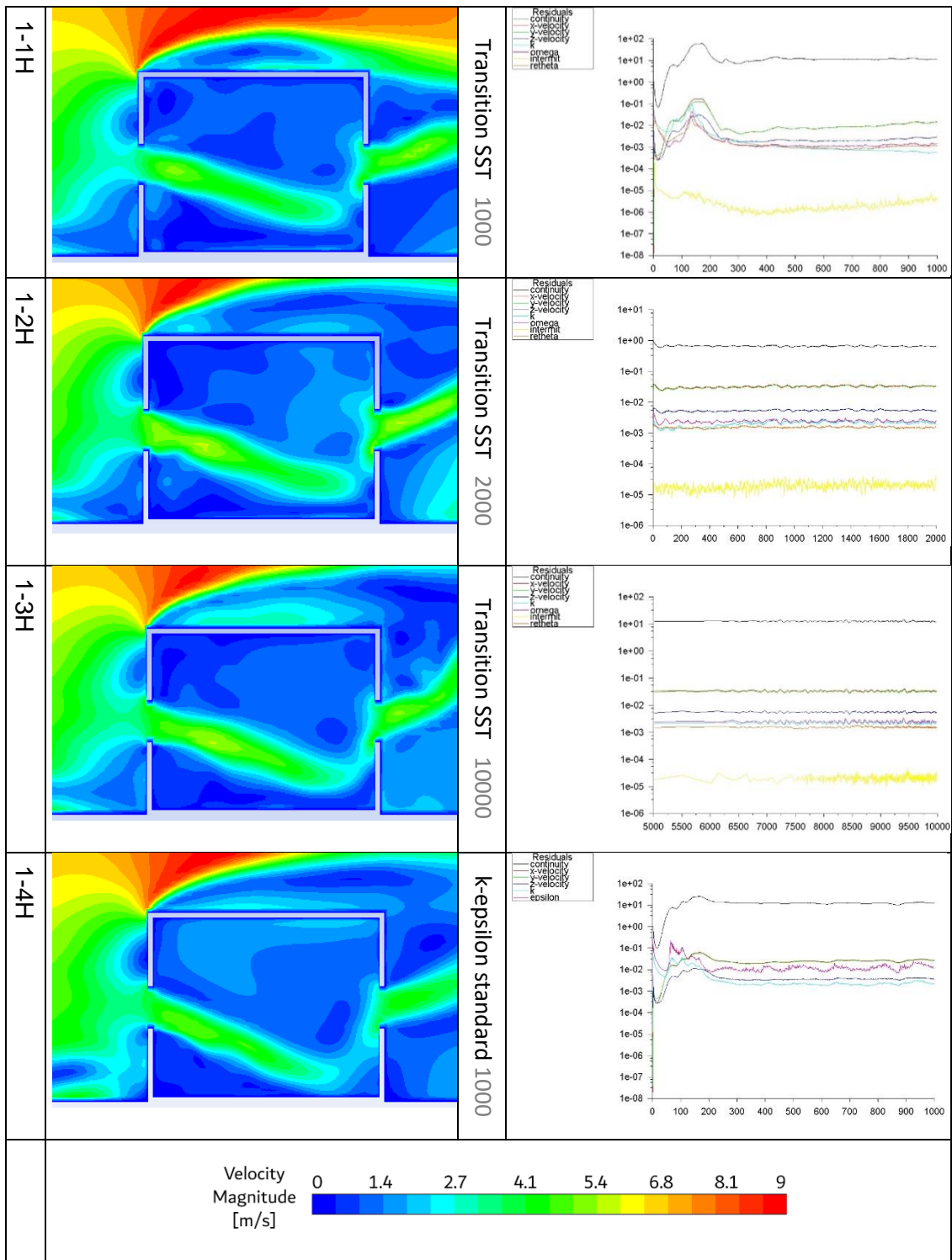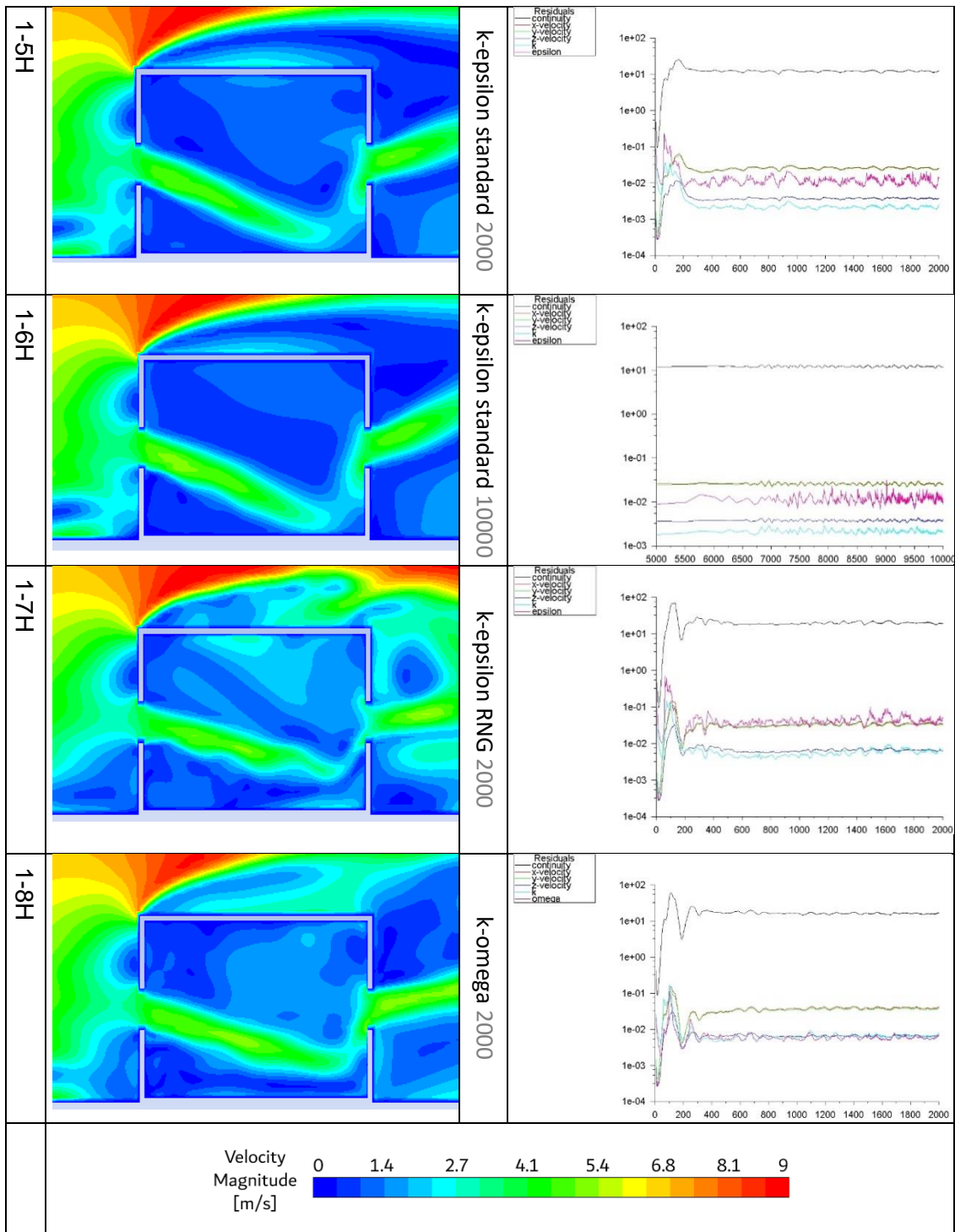
To obtain more data and understanding of these cases, the middle point of the room and several points were taken to check the average airflow on different levels. As shown in Table 6-9, there is a significant impact on the average of the air velocity when a model runs only 1000 iterations while running 2000 iterations could provide a similar result to 10000 iterations. Moreover, it can be concluded that each type of turbulence model has a different sensitivity which can lead to somewhat different results.

Table 6-9 The air velocity averages in the middle of the room and two different levels for each case

	Turbulence model / Iterations	Midpoint	Level 0.034 m	Level 0.012m
1-1H	Transition SST / 1000	0.96	2.41	1.13
1-2H	Transition SST / 2000	1.34	2.06	1.43
1-3H	Transition SST / 10000	1.40	2.16	1.46
1-4H	k-epsilon standard / 1000	1.88	2.07	1.05
1-5H	k-epsilon standard / 2000	0.87	1.59	1.45
1-6H	k-epsilon standard / 10000	0.48	1.69	1.45
1-7H	k-epsilon RNG / 2000	1.49	2.19	1.08
1-8H	k-omega / 2000	1.6	2.1	1.5

To conclude this section, the best agreement of the hexa mesh cases was able to provide a high similarity to the velocity vector fields of PIV measurements, as it can be observed in Figure 6-20.

Figure 6-20 Comparison of the velocity vector fields obtained with the PIV measurements and the Reference CFD model and the best agreement case that used hexa mesh (1-6H).

6.6.2.2 Tetrahedral mesh cases

Table 6-10 below presents the cases after replacing the hexa mesh with tetra mesh. This table presents in order the most compatible cases with PIV to the least. Also, the other criteria used to define the best cases were the error rate and the fulfilment of iterative convergence. Case 1-4T was somewhat closer to the PIV based on the grey area in Figure 6-21; a lack of repeated convergence affected the increase in airflow values in the middle of the room whilst

increasing the iterations contributed to more similar results with the PIV. At the same time, it

is clear that the low iterations, 1000 and 2000 with high residues in the other models, affected

their agreement and correlation with PIV. However, according to the considerations made in

the table and charts, 1-6T "K-ε standard model" had the best agreement with PIV

measurements, followed by 1-8T "K-ε RNG".

Table 6-10 The agreement between PIV measurement data and tetra mesh cases.

	Case (Tetra)		Iterations	Error (%)	Similarity to PIV chart	Residuals
1	1-6T	K-epsilon standard	10000	29.3	2	-3
2	1-8T	K-epsilon RNG	10000	31.4	10	-3
3	1-3T	SST	10000	33.8	8	-3
4	1-10T	K-omega	10000	31.6	5	-2
5	1-5T	K-epsilon standard	2000	31.9	3	0
6	1-2T	SST	2000	33.2	7	-2
7	1-9T	K-omega	2000	31.6	6	0
8	1-4T	K-epsilon standard	1000	35.3	1	3
9	1-7T	K-epsilon RNG	2000	38.3	9	0
10	1-1T	SST	1000	31.2	4	2

Residuals: (3 to -3, where 3 means high residuals and -3 high)

Figure 6-25 shows the comparison between the K-ε standard model while using tetra as mesh

and the RCM and PIV. Based on the cases that used tetra mesh in this work, the k-ε

standard model with 10000 iterative convergence was the most accurate and close to PIV.

However, the standard k-model with 2,000 iterative convergences remains similar to the

10,000 iterative convergences while saving more computing time by about 30%.
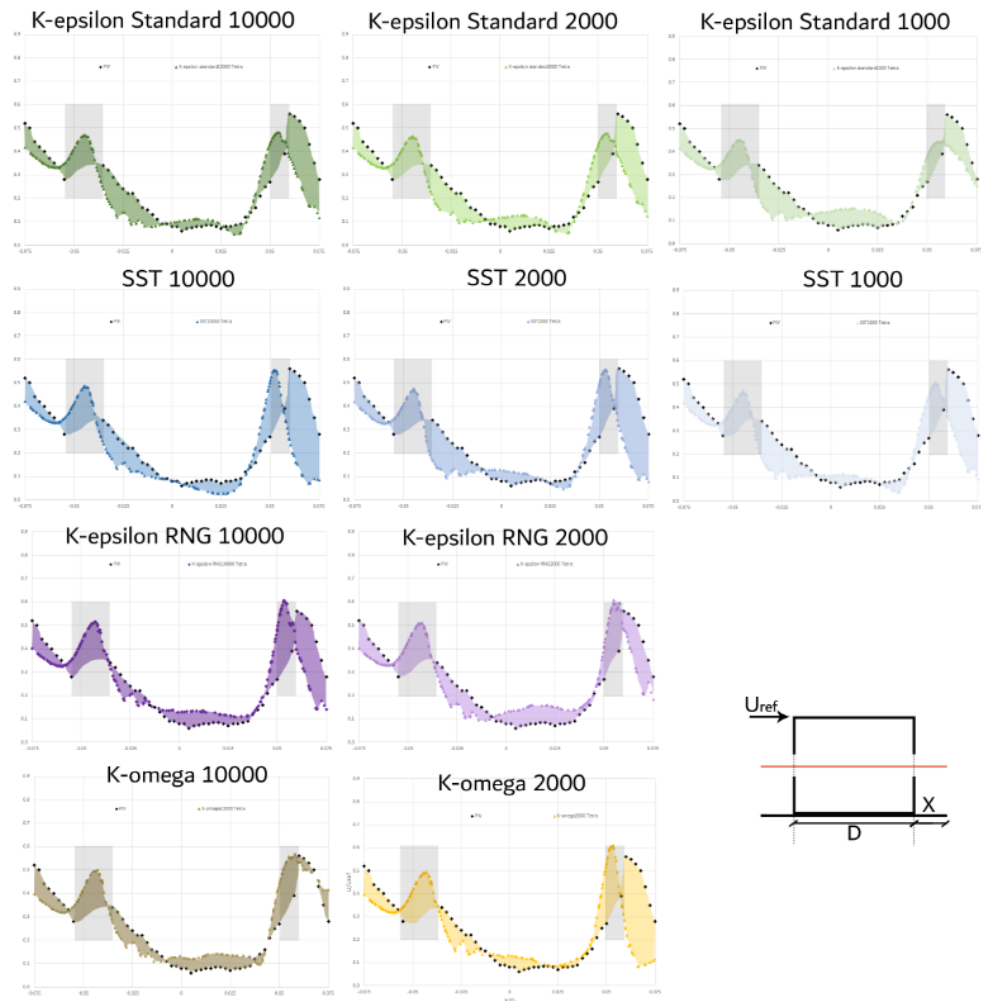
Figure 6-21 The airflow measurements of Tetra mesh cases compared to PIV measurement
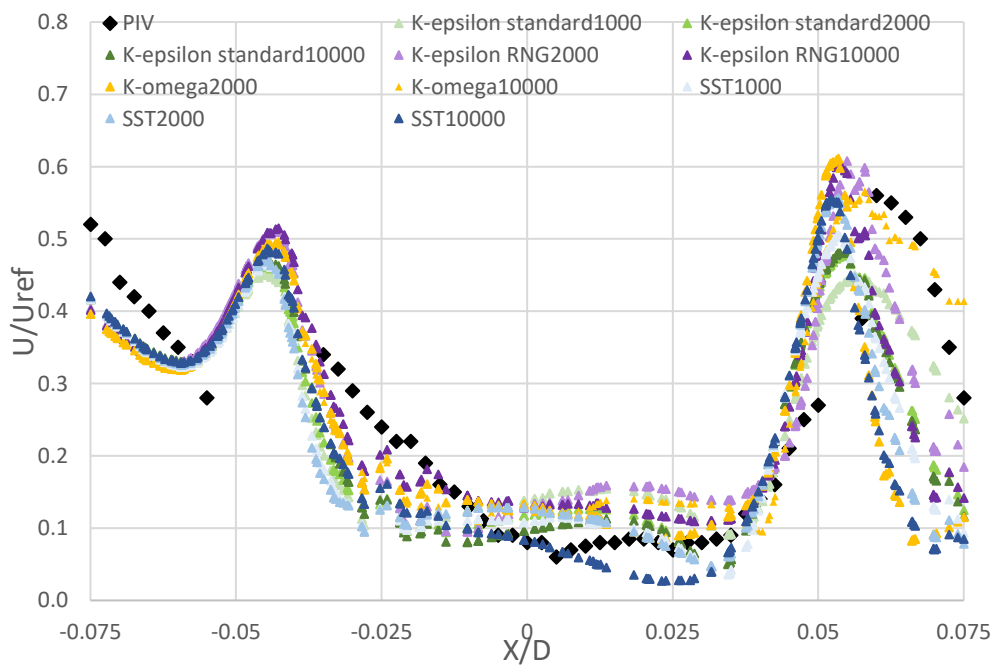
Figure 6-22 The airflow results of tetra mesh cases comparing to PIV measurement

Table 6-11 illustrates a cross-sectional plot of the velocity contours in the room and part of the surrounding areas for the tetra mesh cases. The scale of airflow velocity contours (m/s) ranging by CFD colour map from 0 to 9 m/s is shown on the bottom. It is apparent from this table, that the airflow inside the room of the cases generally is similar while it differs somewhat on the right opening and the leeward side, especially on the last case in the table; 1-10T.

Table 6-11 The cross-sectional of the airspeed contours in the room and iterations for tetra mesh cases

1-5T		k-epsilon standard 2000
1-6T		k-epsilon standard 10000
1-7T		k-epsilon RNG 2000
1-8T		k-epsilon RNG 10000
1-9T		k-omega 2000

Velocity Magnitude [m/s]

0   1.4   2.7   4.1   5.4   6.8   8.1   9

| 1-10T | | k-omega 10000 | |

| | Velocity Magnitude [m/s] | 0 1.4 2.7 4.1 5.4 6.8 8.1 9 |
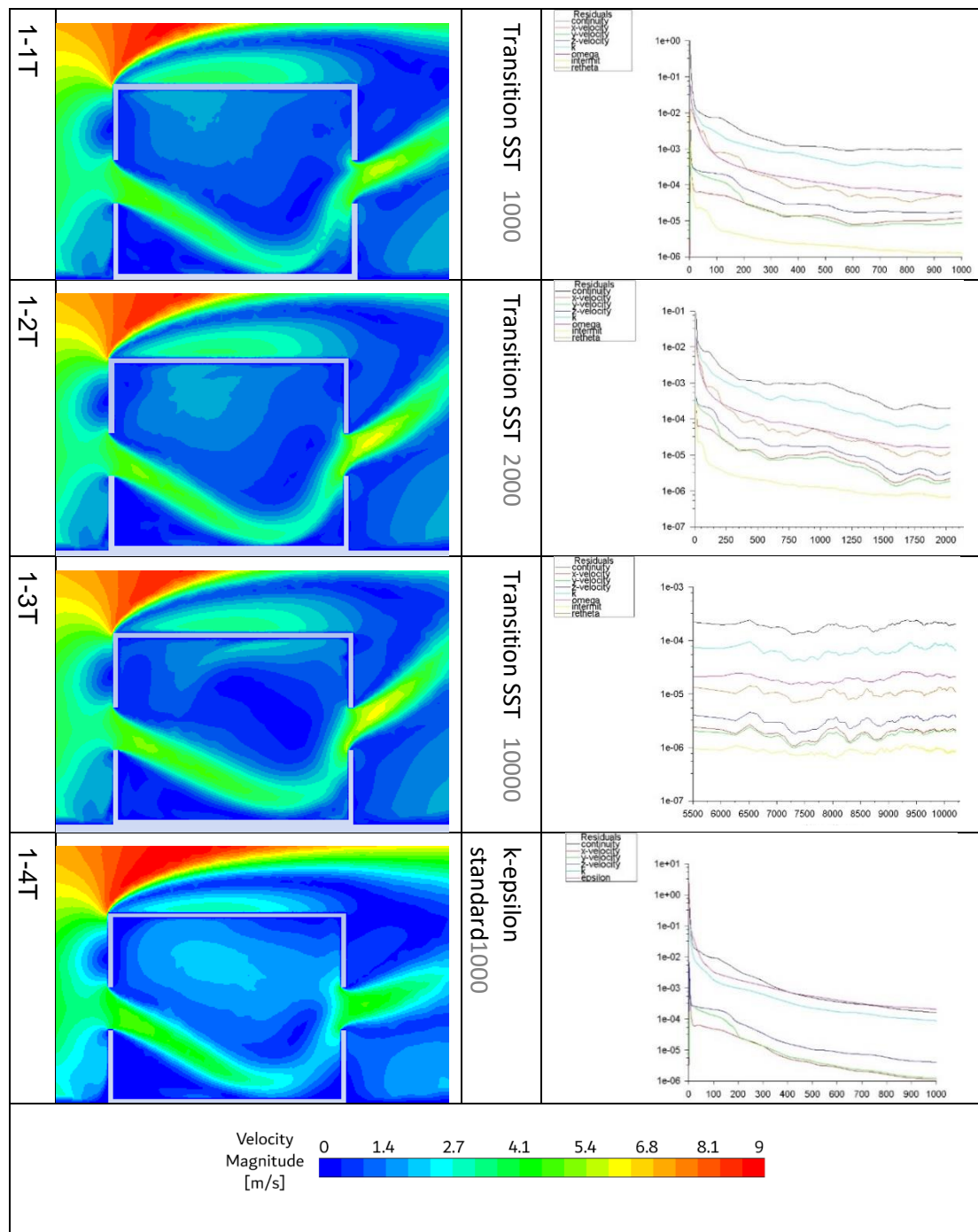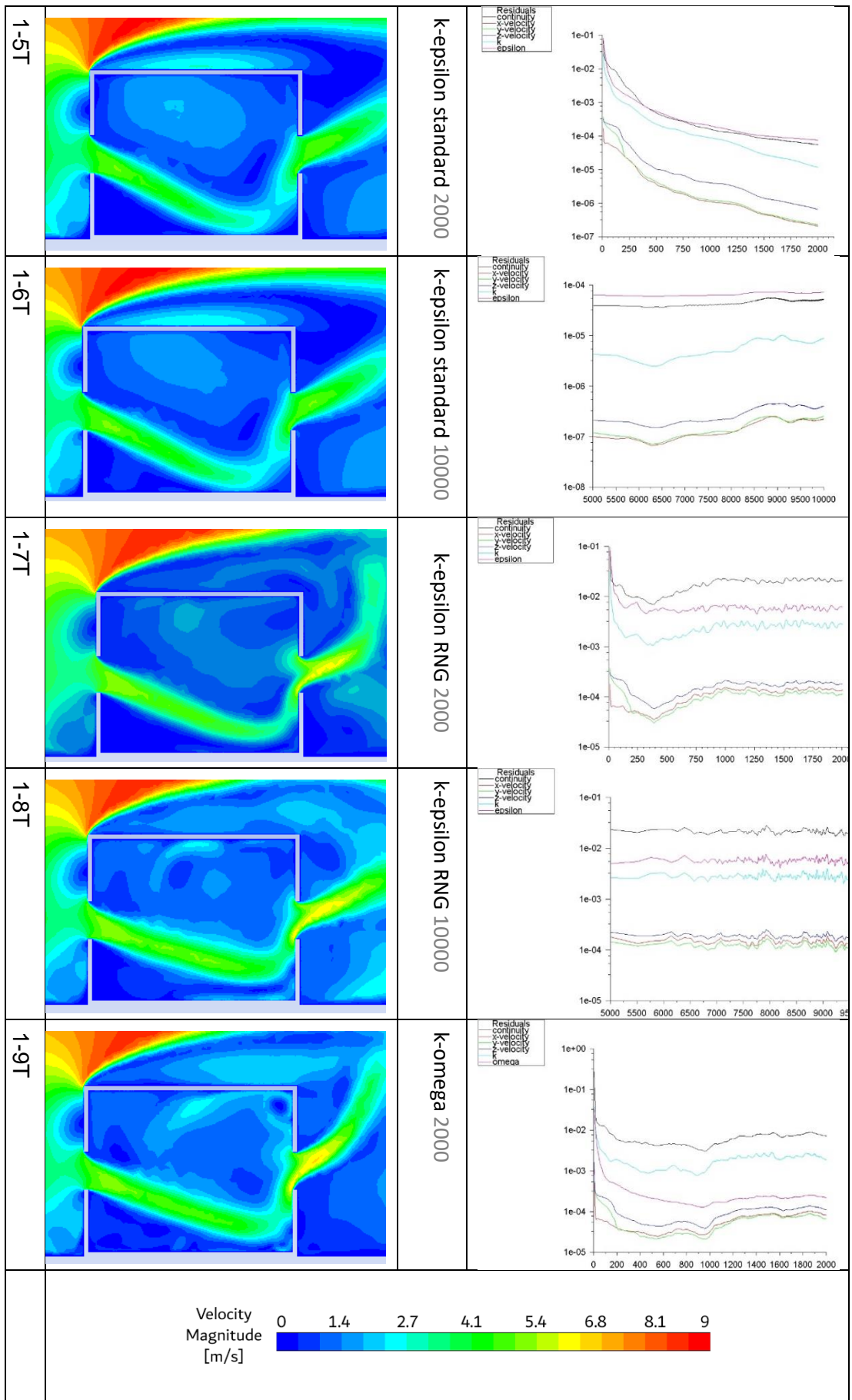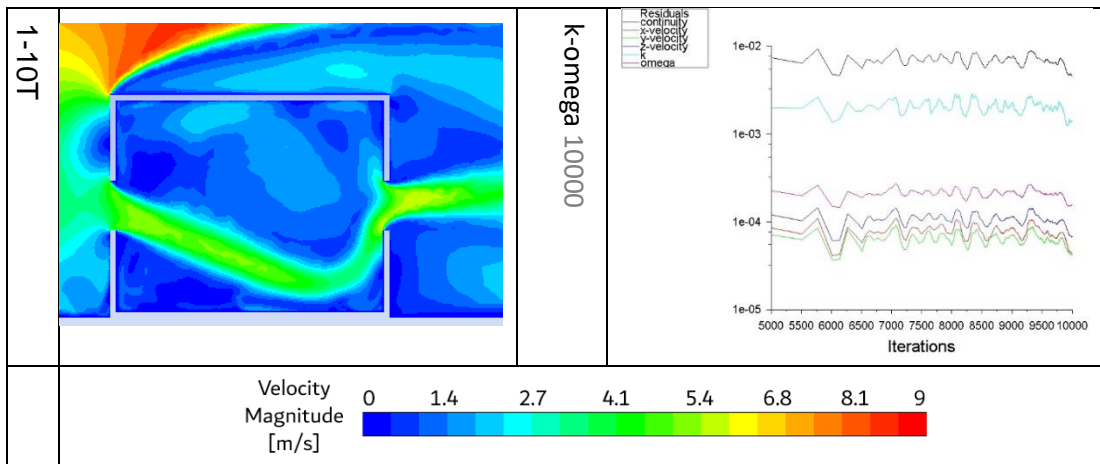
Figure 6-23 shows two different iterations where the convergence was monitored by examining the air velocity of the middle point to check the convergence of the solution. The graph shows a clear trend of increasing the convergence of the 2000 iterations compared to 1000.
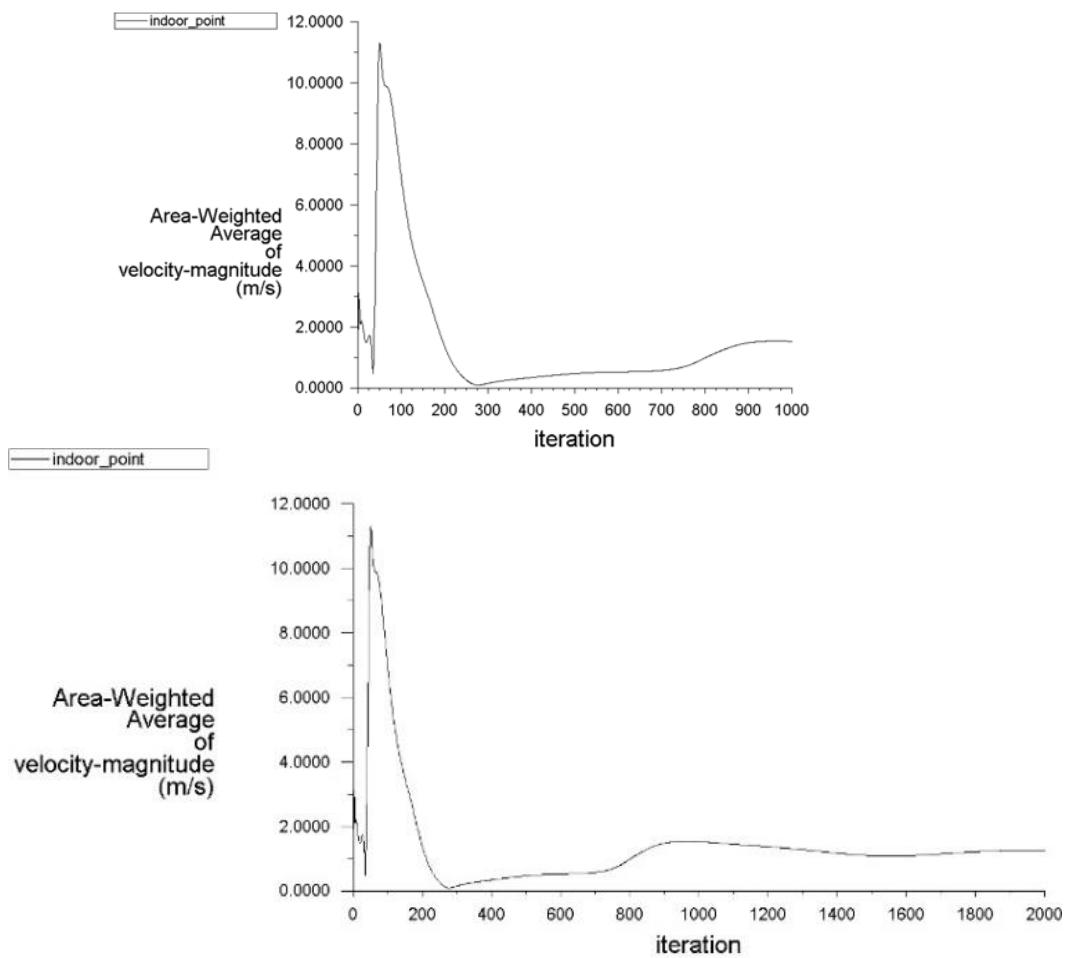
Figure 6-23 The airflow convergence of the middle point in k-epsilon standard with 1000 and 2000 iterations

The average airflow on different levels was measured at the centre of the room and two different levels to get additional data and better understand these cases.

It is apparent from Table 6-12 that the airflow averages of all cases on level 0.012m around 1.39 to 1.8 m/s and one level 0.034m in a range of 1.45 and 2.04m/s.

Table 6-12 The air velocity averages in the middle of the room and at two different levels for each case

	Turbulence model / Iterations	Midpoint	Level 0.034 m	Level 0.012m
1-1T	Transition SST / 1000	1.23	1.45	1.72
1-2T	Transition SST / 2000	1.25	1.59	1.80
1-3T	Transition SST / 10000	0.74	1.76	1.75
1-4T	k-epsilon standard / 1000	1.53	1.74	1.39
1-5T	k-epsilon standard / 2000	1.26	1.62	1.44
1-6T	k-epsilon standard / 10000	0.96	1.61	1.53
1-7T	k-epsilon RNG / 2000	1.35	1.81	1.65
1-8T	k-epsilon RNG / 10000	1.29	2.04	1.63
1-9T	k-omega / 2000	1.42	1.81	1.52
1-10T	k-omega / 10000	1.26	1.73	1.78

To conclude this section, 1-6T was the best agreement of the PIV measurements between the Tetra mesh cases. Case 1-6T resulted in a high similarity to the velocity vector fields of PIV measurements, as shown in Figure 6-24.
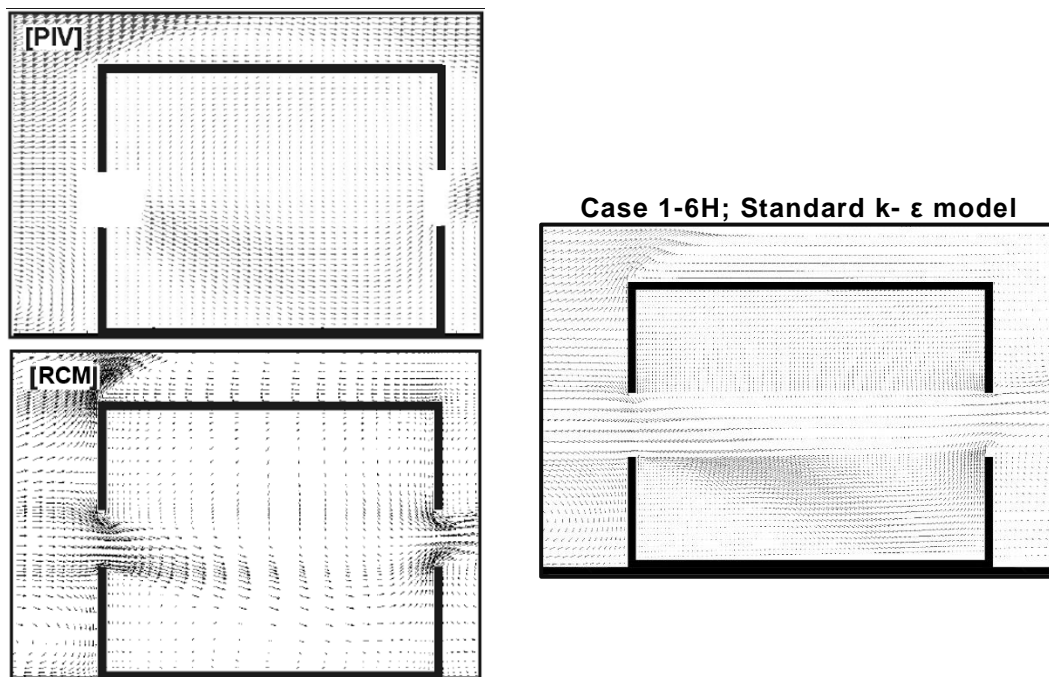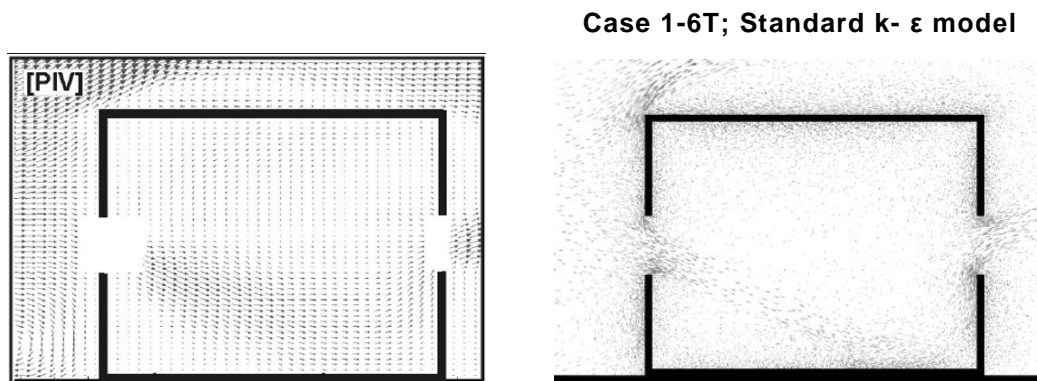

Figure 6-24 Comparison of the velocity vector fields obtained with the PIV measurements and the best agreement case that used tetra mesh (1-6T)

6.6.2.3 Conclusion

This simulation phase had been tested two different types of meshes: Hexa mesh and tetra mesh. Mainly, the hexa mesh was applied to gain the same outputs of the PIV and RCM results. More processes were applied to the geometry of the hexa mesh as slicing the volume into 48 parts, and defining the edges of these parts in a complex way, which consumed longer

time than tetra, especially on the meshing procedure and completing the computing iterations. The slicing method used in the geometry of hexa mesh cases has contributed to an increase in the nodes numbers and thus improved the accuracy of the solutions. On the other hand, using this method in non-simplified shapes and splitting the domain into many elements may cause some errors in the solution if the mesh properties are not selected and defined correctly.

Based on the data for both meshes cases, the k- ε standard model with 10000 iterations afforded the most similar numerical data to PIV measurements. However, the discrepancy percentages of the hexa mesh cases from the PIV measurements ranged from 20.8 to 36.4%, while in the tetra were 29.3 and 38.3%. It is worth noting that the percentage discrepancies or error rates may have been affected by the accuracy of estimating the points recorded in the chart of the velocity profile of PIV data.

Although the hexa mesh cases provided better results and more correlation to PIV measurements, tetra has been proven effective in saving time and achieving good and compatible results to the PIV results. It has been proven that the k- ε standard model results with iterations of 2000 1-5T gave identical results to 1-6T with an error rate of 1.6% higher, see Figure 6-25. In contrast, 1-5T could save computing time by about 30%. Therefore, the used turbulence model with 2000 iterations was selected as a constant setup for the Fluent in the next phases.
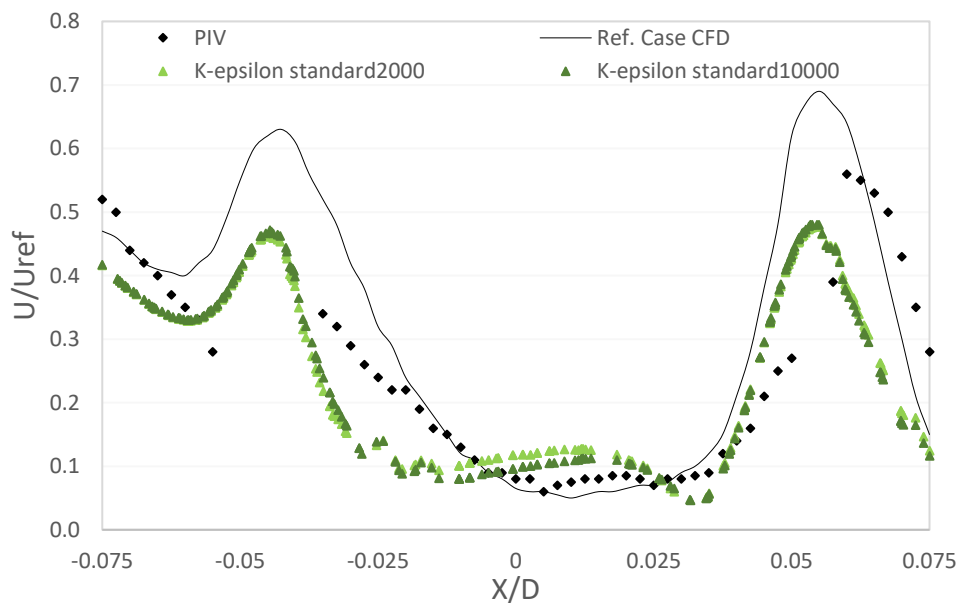
Figure 6-25 The PIV and RCM curves with a comparison of the best similar tetra mesh cases

6.7 Summary and Conclusions

In order to have more data and analyses than fieldwork and broaden our understanding of mashrabiya, simulation was taking a significant part in achieving the aim of this research. One of the most essential and powerful tools that assist in evaluating and predicting design problems with more flexibility in testing designs, analysis and development, saving cost and time compared to field experiments is CFD. Many recent studies such as Allocca (2001), Nakanishi et al. (2007), Tominaga et al. (2008), McDonough (2009), Kanaan and Chahine (2018), and Lukiantchuki et al. (2020) have proven the effectiveness and validity of CFD results with airflow or temperature with those of similar field experiments. Since the validation for this study model is necessary to indicate that the expected outcome reflects the physical situation accurately and can reflect the actual impact on the model in the optimisation phase, a validated CFD model was used as a reference.

The study selected a CFD model of Ramponi and Blocken (2012) validated based on detailed wind tunnel experiments by Karava et al. (2011). The simulations were conducted with the commercial CFD code ANSYS FLUENT to simulate the airflow inside the domain and into the room, and the SIMPLE algorithm was used with the default setups of ANSYS, where the pressure and momentum were specified second-order. In this phase, two types of mesh were used: hexahedral mesh and tetrahedral mesh, while the 3D steady RANS equations were solved in combination with three turbulence models; (1) Shear Stress Transport (SST k- ω) model, standard k-epsilon (k- ε) model,(3) RNG k-epsilon (RNG k-ε) model;(4) K-omega (k-ω) model.

It was observed that using the hexahedral mesh to geometry provided a better agreement to PIV compared to the tetrahedral mesh. That was due to slicing the domain volume into 48 parts which consumed a long time to complete the simulations and get the solution results. However, tetra mesh has been proven effective in saving time and also could provide good and compatible results to the PIV data.

It was found that from both hexa and tetra mesh cases, K-epsilon standard 10000" was the best model compatible with PIV measurement, and its solution provides fluctuations constant. While increasing the iterations contributed to more similar results with the PIV, a lack of

iterations or repeated convergence influenced the accuracy, especially in the middle of the room, where the air flow values were higher compared to the PIV values. However, the standard k-model with 2,000 iterative convergences remains similar to the 10,000 iterative convergences while saving approximately 30% of computing time.

Overall, the validation phase resulted in a strong agreement between PIV and CFD solutions; the air velocity contours and curves showed that the CFD cases of this work were comparable to experimental data.

Based on the comparison of the selected simulation model (k- ε standard model with 2000) with the best case and PIV data, the simulation model was validated and adopted as a constant setup for Fluent in the phases of the next chapter.

It should be mentioned here that despite providing some reduction in indoor thermal conditions by integrating passive evaporative cooling techniques into mashrabiya in the field experiments, the indoor thermal comfort level has not been achieved. Therefore, in an attempt to gain better results and achieve thermal comfort level, another passive cooling technique "heat transfer device" was adopted and integrated with the mashrabiya, which will be presented in Chapter 7.

CHAPTER 7

Design and Integration of Heat Transfer Devices with Mashrabiya

Introduction
Simulation Plan
Models setup
Results and discussions
The Base Case
Single row of pipes integrated with mashrabiya
Double row of pipes integrated with mashrabiya
A comprehensive comparison of the simulation Phases
Summary and Conclusions

7. DESIGN AND INTEGRATION OF HEAT TRANSFER DEVICES WITH MASHRABIYA

7.1 Introduction

Despite the positive effect on the internal thermal environment from integrating the selected means of passive evaporative cooling to mashrabiya in the field experiments and achieving their objectives, the researcher sought to explore and adopt a different technique and more effective to extend the integration efficiency of the mashrabiya. An inspired heat transfer devices technique from Calautit et al. (2015) and Shen and Li (2016) was utilized and applied integrated with mashrabiya.

Consequently, this requires a validation model, which has been presented in the previous chapter. After creating a validation model, three sets sequentially were carried out through a group of configurations and strategies: a) the base case, b) single row pipe, and c) double rows of pipe combined with mashrabiya. The base case was created as the benchmark case, with included mashrabiya on both openings of the room. In the development stage, the pipes were added behind the mashrabiya facing the wind. The applied method adopted a system that uses heat transfer devices to provide a continuous cooling cycle, which lowers internal temperatures during hot conditions (Calautit et al., 2013).

Each set was evaluated to identify the most significant elements and parameters in improving either airflow inside the room or air temperature, while the indoor thermal comfort was evaluated in the pipes phase.

Since the simulation stages have had some additions and modifications to create the base case of the mashrabiya and develop it, this chapter will include an overview of the simulation plan with each stage's variables and evaluation factors. In addition, the models' setup: design geometry, meshing, boundary conditions, and solver settings will include the changes for each phase. Finally, the chapter will include the results of each case and a comprehensive comparison of the simulation phases. From these results, the objectives of the simulation work were achieved, and the optimal solution for this work was determined.

7.2 Heat Transfer Device

The heat pipe is a passive heat-transfer device that employs phase transition to transfer heat between two interfaces. The heat transfer device is a "closed evaporator-condenser" device consisting of a pipe or tube filled with a fluid for heat transfer. It can be made of (Alharbi, 2014). A heat pipe is made up of three major components: evaporator, adiabatic section, and condenser (Figure 7-1). As illustrated in this vacuum pipe, heat enters through the evaporator and exits through the condenser. Heat enters the evaporator, causing the fluid to vaporise. The vapour quickly travels from the hot end (high pressure) to the cooler end (low pressure). The heat is released when the vapour condenses back into a fluid. The fluid is absorbed by the wick, which transports it back to the hot end, where it absorbs heat and re-evaporates (Maldonado et al., 2020). Addington and Schodek (2005) stated that a heat pipe is a very efficient device for transferring heat from one location to another. Calautit et al. (2013) mentioned "the sensible effectiveness of heat pipes is approximately between 45% and 65%".
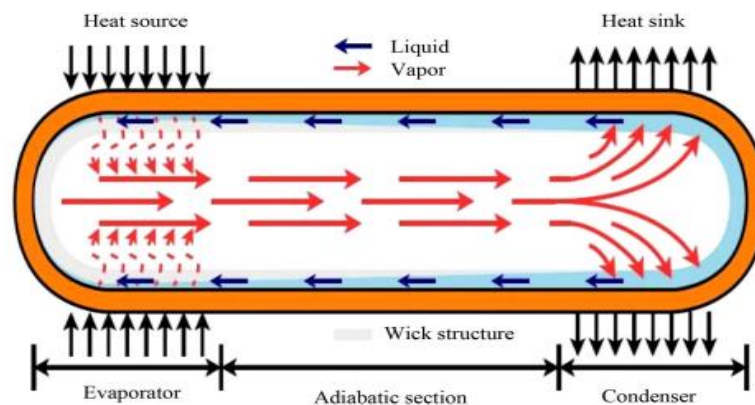
Figure 7-1 Heat pipe structure and operating cycle (Shukla, 2015)

The heat transfer device used in this study consists of a solid pipe instead of a vacuum pipe to simplify the system and lower costs. Figure 7-2 illustrates the operating cycle of the pipes that were used in this work. When the pipe is exposed to the heat of the incoming outside air, the pipe absorbs this heat and lowers the airflow temperature, as it is transmitted through the pipe by conduction from the hot part to the cold part (water tank), which in turn keeps the pipes cool by releasing the heat to it. Nevertheless, heat pipes (with phase transition) can also be used for better heat transfer.
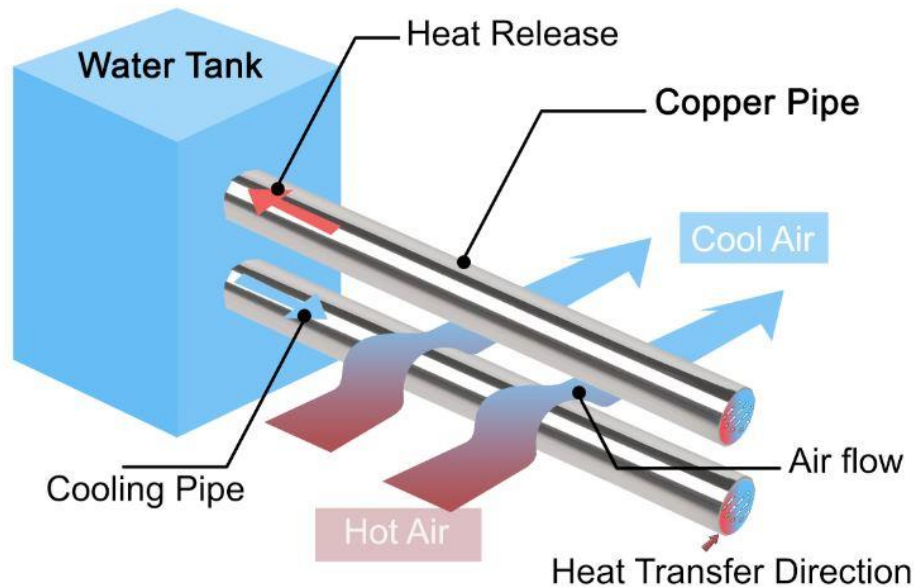
Figure 7-2 The heat flow of the heat pipes linked to a water tank

Several researchers have studied and tested heat pipes as a passive evaporative means to cool buildings. Riffat and Zhu (2004) used a system that incorporates heat pipes embedded in phase change material. The results showed that the combination of the system and night cooling offered a rate of heat storage sufficient to keep a room from overheating in typical UK summer circumstances. He and Hoyano (2011) invented and used a porous ceramic-based passive evaporative cooling wall. According to the study, the air passing through the system was cooled, and the air temperature could be decreased during the summer afternoon by roughly 2 °C. Boukhanouf et al. (2015) studied the thermal performance of an indirect porous ceramic evaporative cooler with an integrated heat transfer heat pipe. Although the study noted that the effectiveness of the technique was moderate, it lowered the dry bulb temperature of the airflow in the dry channel by 5°C. It also mentioned that the system can be an environmentally friendly and energy-saving cooling system. Calautit et al. (2015) tested the integration of heat transfer devices with a wind tower by using CFD modelling. The study aimed to cool the incoming air into the wind tower, thus eliminating reliance on mechanical cooling systems. It was found that at lower wind speeds (1–2 m/s), the temperature decreased by up to 9.5–12 K. Moreover, the effect of altering the horizontal spacing between the heat transfer devices on the supplied air temperature was shown to be more important than the effect on the airflow velocity were reducing the gap from 100 mm to 50 mm improved

the temperature drop by 3.48 K.Shen and Li (2016) integrated cooling pipes into the metal blinds of the double-skinned glazing to reduce heat transfer to the envelope in summer (Figure 7-3). The findings showed that the technique decreased their average temperature from about 57°C to 25.4 ° C, while overall cavity temperature dropped to about 29° and improved thermal comfort.
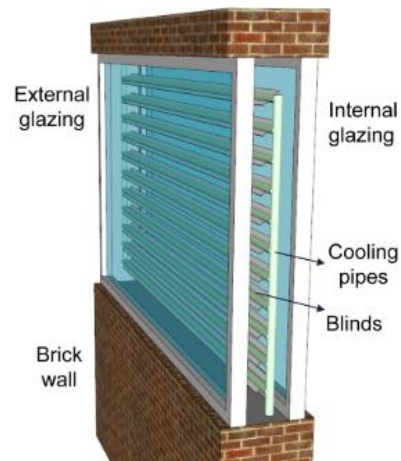
Figure 7-3 Configuration of cooling pipes integrated with double glazing window (Shen and Li, 2016)

Alharbi et al. (2019) investigated and tested a sub wet bulb evaporative cooling system for space air conditioning in buildings. The prototype was created using integrated finned heat pipes and water-filled hollow porous ceramic cuboids. It was observed that the technique was efficient where the supply air dry bulb temperature was 22.3 °C under typical dry climatic circumstances (while ambient air dry bulb temperature of 35°C and relative humidity of 35%). A study by Abdullah et al. (2019) investigated the integrated radiator pipes with clay cylinders covered by two layers of jute fibre and installed in a wind tower and examined in one of the desert cities in Yemen. The study confirmed the effectiveness of the system, as it was able to decrease the air temperature by an average of 14.6 °C.

According to what was mentioned about the effectiveness of the system in the studies that were reviewed and according to the researcher's knowledge, the researcher strained to take advantage of this system and integrate it with the mashrabiya to increase its efficiency performance and thus improve the interior temperature and reach thermal comfort. To the best of the researcher's knowledge, it should be noted that this system has never been applied with the mashrabiya testing and evaluation of its effect on improving the indoor thermal environment.

7.2 Simulation Plan

Table 7-1 demonstrates the phases of this simulation part; 1) the base case, 2) a single row of cooling pipes, and 3) double rows of cooling pipes incorporated with a mashrabiya. In this parametric study, each phase included specific parameters and variables that resulted in 23 cases. The base case was created based on the benchmark case. Moreover, all phases used the same settings in the benchmark case as the volume, room size and position, mesh type, turbulence model, air velocity profile, and iterations numbers. However, a plain mashrabiya on both room openings was added in all configurations, while some pipes were integrated in the second and third phases. Due to these additions, the meshing was increased to produce better accuracy. To the best of our knowledge, few studies covered the mashrabiya performance regarding investigating its effect on the airflow via CFD. However, the cross ventilation with mashrabiya in CFD has not been studied or explored.

Therefore, the base case aimed to investigate the effect of cross ventilation in a room with two opposite mashrabiyas. Moreover, define the most effective inclination angle in the mashrabiya of airflow into the room. While the other phases principally aimed to investigate the effect of integration cooling pipes with mashrabiya to decrease the indoor temperature and improve comfort.

Table 7-1 The main parameters and variables of the simulations

	Cases No.	Fixed Parameters	Variables	Evaluation
Base Case (Benchmark case + Mashrabiya)	5	-Design and size (Volume, "room", Mashrabiya size) -Mesh properties (CFD, Sizing, Quality) -Turbulence model, Iterations Air velocity profile 6.3 m/s	Slats Angel (Horizontal, -20°, +20, -30°, +30°)	Veloicty
One row of pipes	8	The parameters of this phase as the base case parameters except for one-row pipes were added to the geometry	Slat angle (Horizontal, -20°) Inlet Temp Pips Temp (17,22° C)	Velocity Temperature
Double rows of pipes	10	As the One row of pipes phase with adding parallel row pips Set temperutre of Inlet 40°C, and Pips 22°	Slat angle (Horizontal, -20°) Air velocity Profile (0.5, 1, 2, 4, 5 m/s)	Velocity Temperature Comfort

7.3 Models Setup

7.3.1 Design Geometry

This work's computational domain and room position were created as the benchmark model was presented in section 6.6.1 and added elements in the room openings, as shown in Figure 7-4. The dimensions of the room and the mashrabiya are shown in detail in Figure 7-5.
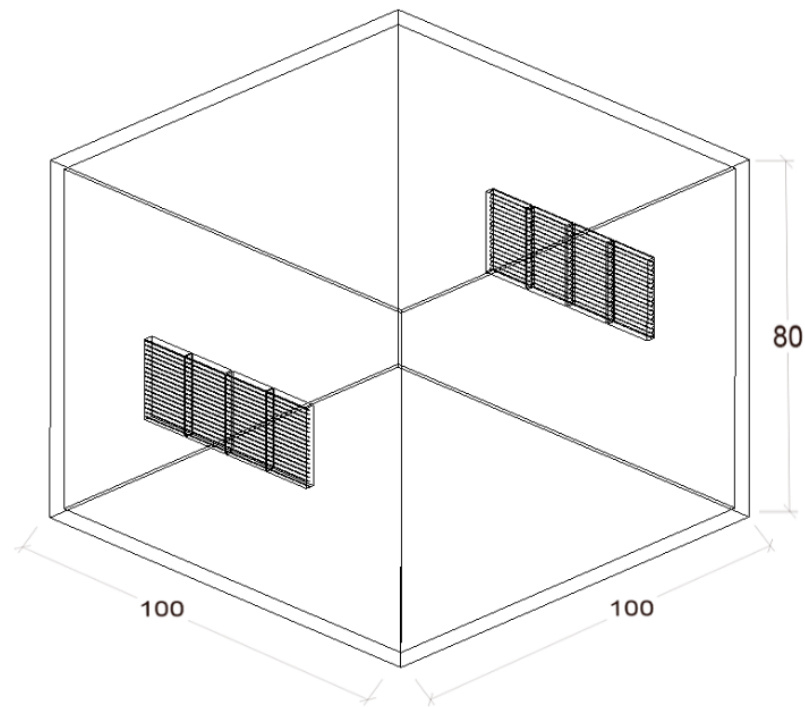
Figure 7-4 The computational room with mashrabiya design

Besides the geometry of the benchmark model, a plain mashrabiya was added, whose ratios were derived from the sizes of the mashrabiya slats and sashes tested in the field experiment, while it benefited from Maghrabi (2000) to determine the angles of the slats. In order to improve the results of the mashrabiya and increase its effectiveness concerning thermal comfort, an adopted cooling strategy was applied, which was either one or two rows of pipes behind the mashrabiya slats.

The domain dimensions in full scale are 180 x 308 x 96 m^3 (W_D x L_D x H_D), and the room is 20 x 20 x 16 m^3 (W_R x L_R x H_R). The base case used a scale of 1:200, as been applied in the benchmark; thus, the domain in reduced scale became equal to 0.9 x 1.54 x 0.48 m^3 or 900 x 1540 x 480 mm^3, while the room's dimensions represent 100 x 100 x 80 mm^3 corresponding to 20 x 20 x 16 m^3 in full scale.

Two plain mashrabiyas were added to the room's openings, one facing the windward and the other the leeward facade, as seen in Figure 7-5. The mashrabiya dimensions are 46 x 18 mm at the height of 31 mm, corresponding to 9.2 x 3.6m^3 in full scale.
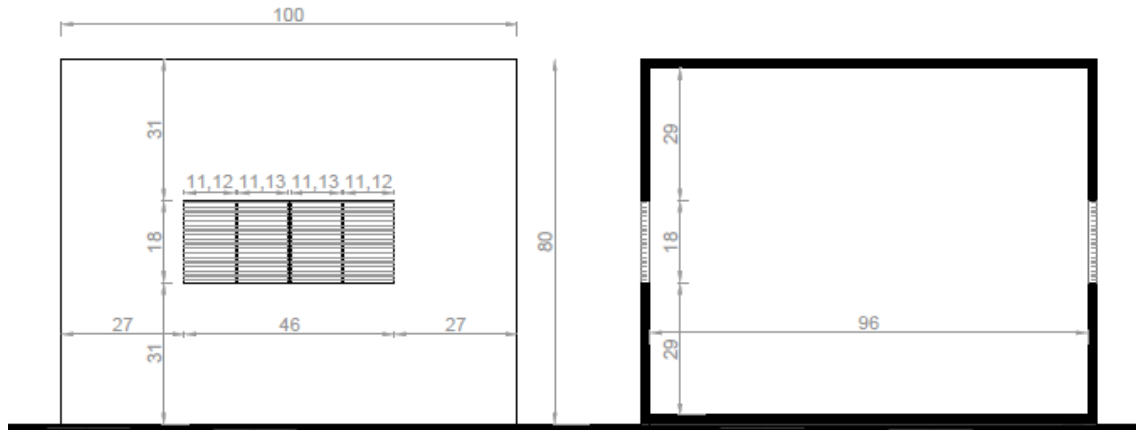
Figure 7-5 The computational room in the base case

In the pipes cases, the domain a scale of 1:50 in Fluent to get more appropriate room dimensions and then apply the ASHRAE standard of measurement levels.

Table 7-2 presents the number of cases and main configurations of the geometry for each phase. Each mashrabiya in the base case consists of 4 sashes while 18 slats in each sash. The sash dimensions are 11.1 x 18 mm (W x H), and the slat dimensions are 11.1 x 1 (W x H) with a thickness of 0.1mm corresponding to 2.2 x 20 x 0.02 m in full scale.

In the pipes phases, one sash was removed to add space for the water tank in the windward mashrabiya. Also, one sash was removed in the opposite mashrabiya as well to have equal size of mashrabiya on both sides.

Figure 7-6 shows the five configurations of slats inclination angles in the base case. The slats inclination angles in the pipes phase either were set as horizontal or -20°.

Table 7-2 The main configurations of the geometry of each phase.

Phase	Cases No.	Slats Angel	Sashes No.	Additions
Base Case	5	Horizontal +30°, -30° +20°, -20°	4	non
One row of pipes	8	Horizontal -20°	3	88 pipes
Double rows of pipes	10	Horizontal -20°	3	175 pipes
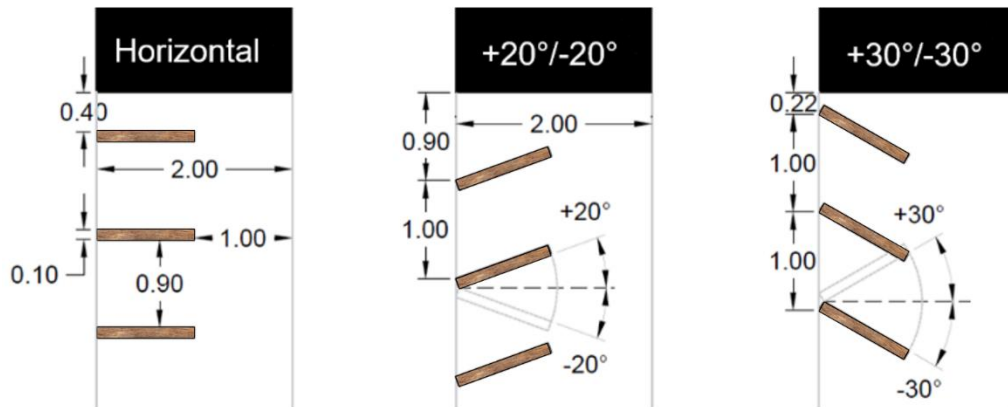
Figure 7-6 The configurations of slats inclination angles for the base case

Figure 7-7 presents the façade of the room, illustrating the place of a water tank. Figure 7-8 shows the design and dimensions of a single row or two rows of pipes on a 1:50 scale. The pipes in both phases were added only on the windward side. The pipes were designed as solid pipes and defined in CFD Fluent as a copper material. The pipe diameter is 7.5mm, and the length is 1.71mm. Figure 7-9 illustrates a perspective of the water tank and mashrabiya integrated with pipes. The mashrabiya lay a key role in protecting the pipes from direct sunlight. However, pipes were exposed to the outside airflow, which affected the temperature of the external surfaces of pipes. So, the water tank was placed on maintaining the set temperature of pipes and not release the absorbed heat into the room.
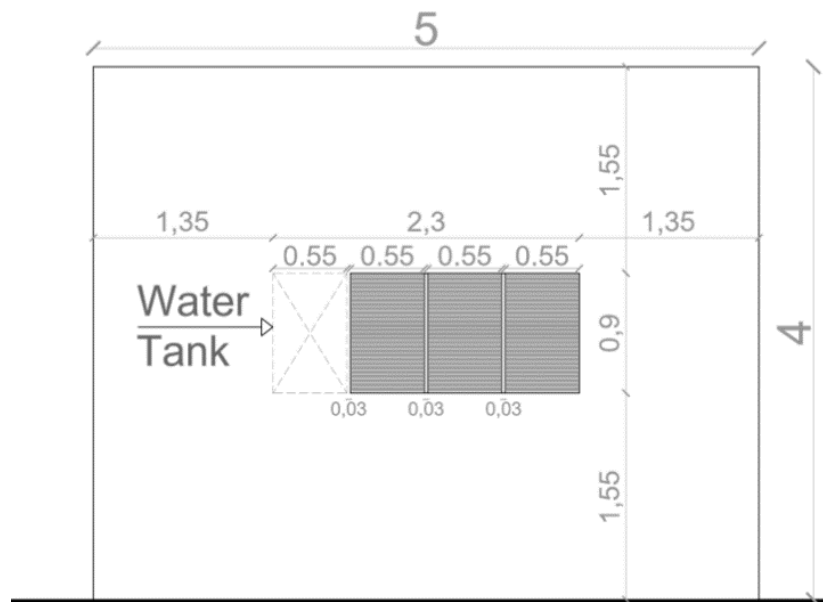
Figure 7-7 The facade of the computational room in 1:50 scale and metric unit showing the three sashes and water tank space.
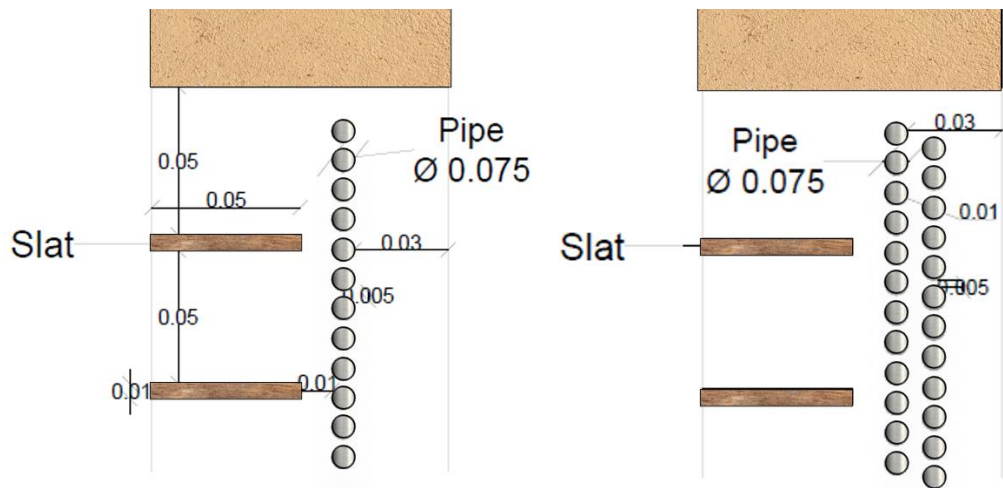
Figure 7-8 The mashrabiya slats and the pipes
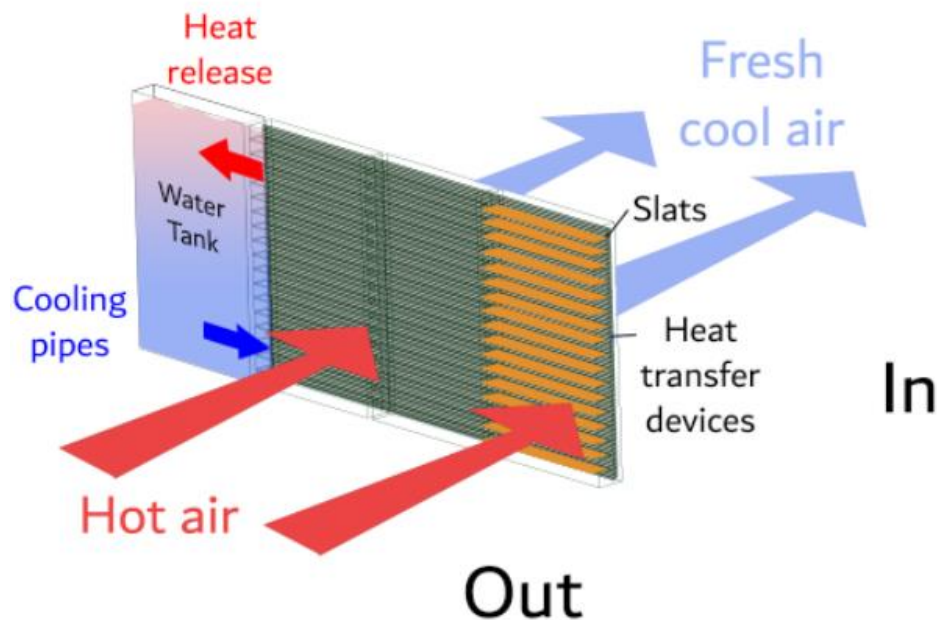
Figure 7-9 Mashrabiya integrated with pipes and water tank

7.3.2 Meshing

The tetra mesh has been generated in the same way in the benchmark case. However, the

mesh elements were increased due to the addition of mashrabiya in the base case (Figure 7-

7). Table 7-3 shows the mesh inputs and mesh output for each phase. It can be observed that

the effect of adding parts in each phase on the cell elements and nodes. Referring to the

benchmark case presented in the prevous chapter, the cell elements amounted to 6,836,946

with 1,256,350 nodes. After adding the mashrabiya to the room, the cell elements increased

about 7% from the benchmark case, where it became 7,341,339 with 1,370,881 nodes.

Due to the small size of the pipes, this was required to increase the mesh size and enable the model to run in the solution, Figure 7-11. This resulted in an increase of cells about 35% from the base case. As a result, the skewness and aspect ratio averages were excellent, and orthogonal Quality was very good based on the ANSYS guide.

Table 7-3 Inputs and output of the generated mesh

Mesh Inputs						
Type	Physics/ Solver preference	Element order	Mesh Size Function	Relevance Center	Quality	Growth Rate
Tetrahedral	CFD, Flunet	Linear	Curvature	Fine	High	1.2
Mesh Ouputs						
Phase	Nodes	Cell Elements	Skewness (Avg)	Aspect ratio (Avg)	Smoothing	Orthogonal Quality
Base Case	1,370,881	7,341,339	0.231	1.861	High	0.768
1 row Pipes	2,113,953	11,233,810	0.236	1.868	High	0.762
2 rows Pipes	2,290,709	11,809,618	0.237	1.867	High	0.760
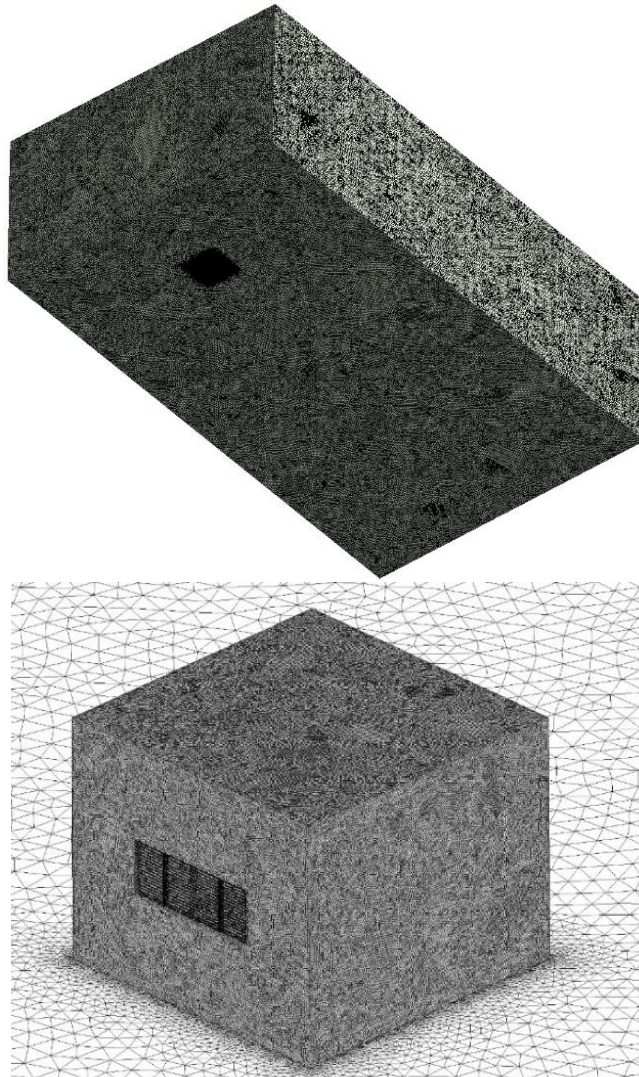
Figure 7-10 3D view of the computational domain and room in the base case
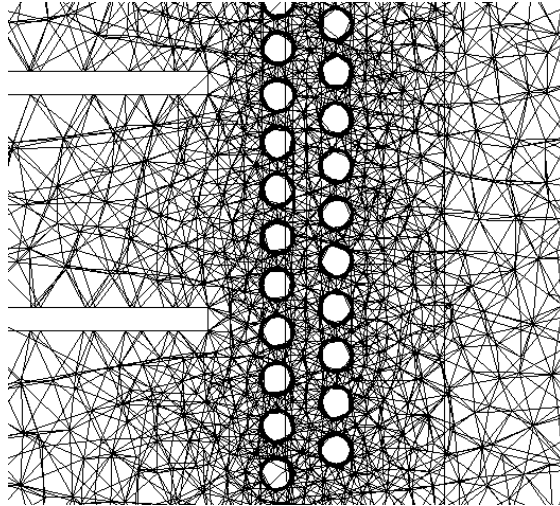
Figure 7-11 The configurations of mesh around the double rows pipes

7.3.3 Boundary Conditions

The boundary conditions used in the simulations are the same as those used in the base case. In addition, apply the same vertical profile of mean wind speed on the base case and the first phase of pipes (see Figure 7-12). On the second design of pipes and after scaling the model to 1:50, five different U profiles of the mean wind speed were tested; 5, 4, 2, 1, and 0.5 m/s, Figure 7-12. The value of 0.5 m/s was determined as the minimum wind speed profile, based on the sensation and air velocities that, according to Szokolay (2004), 0.5 is considered pleasant.
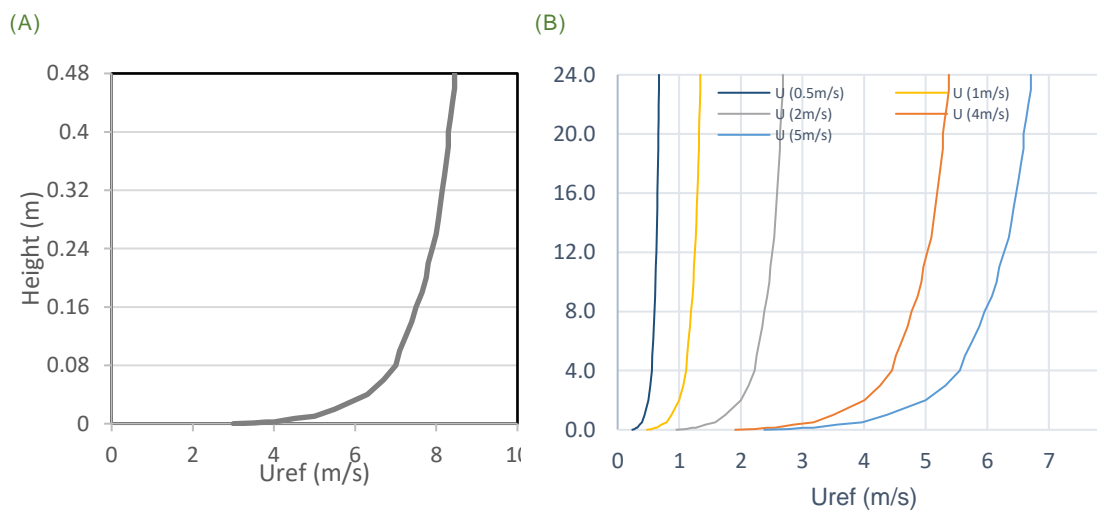
Figure 7-12 (a) The profile of the mean wind speed for the base case and one-row pipes phase (b) The profiles of the mean wind speed for the double rows pipes

In order to study the temperature with airflow, the energy equation in the pipes phases was turned ON by specifying different temperatures. Also, the materials for some parts were defined. Table 7-4 shows the materials that have been used and their properties. The temperatures of the inlet and outlet were set at 40 or 30 C°, while the temperature of the pipes was set at 22 or 17 C°.

The inlet temperature of 40 C° was set based on the average outdoor temperatures monitored from field experiment measurements and 30 C° as an imitation of moderate climatic conditions in Jeddah.

The pipe temperature of 22 C° was set based on the average water temperature from the fieldwork of this study. The pipe temperature was also set at 17 C° to compare and evaluate the impact on indoor air temperature.

Table 7-4 The materials of the pipes phase

Part	Material	Material properties		
		ρ (Kg/m3)	Cp (j/kg.k)	Λ (w/m.k)
Ground	Calcium-carbonate	2800	856	2.25
Room				
Slats	Wood	700	2310	0.173
Pipes	Copper	8978	381	387.6

7.3.4 Solver Settings

The simulations were conducted with the commercial CFD code ANSYS FLUENT 18.1 to simulate the airflow inside the domain and into the room. The cases ran 2000 iterations as the numbers of iterations applied in the benchmark case. All iterations of each case were run and completed without errors.

In addition, the SIMPLE algorithm was used with the default setups of ANSYS, where the pressure and momentum were specified second-order.

All cases were solved with the turbulence model; standard k-epsilon (k- ε) model. Table 7-5 shows the case names and the fixed and variable parameters for each simulation model.

Table 7-5 The parameters of each case of the phases of the simulation

Base Case	Fixed parameters	Slat angel		
2-1		0°		
2-2		+30°		
2-3		-30°		
2-4		+20°		
2-5		-20°		
Single row pipes		**Slat angel**	**Inlet (°C)**	**Pips (°C)**
3-1	k-epsilon standard, tetra mesh, Iterations 2000, U_{ref} 6.3m/s	0°	40	22
3-2		0°	40	17
3-3		0°	30	22
3-4		0°	30	17
3-5		-20°	40	22
3-6		-20°	40	17
3-7		-20°	30	22
3-8		-20°	30	17
Double rows pipes	**Fixed parameters**	**Slat angel**	**U_{ref} velocity (m/s)**	
4-1		0°	0.5	
4-2		0°	1	
4-3	k-epsilon standard, Iterations 2000, Inlet and outlet T 40°C, Pips T 22°C	0°	2	
4-4		0°	4	
4-5		0°	5	
4-6		-20°	0.5	
4-7		-20°	1	
4-8		-20°	2	
4-9		-20°	4	
4-10		-20°	5	

It is worth noting that several points representing either level of standing or seated have been specified based on the ASHRAE standards. These points aimed to find the average airflow inside the room, as shown in Figure 7-13. One midpoint and two different levels were taken as the averages of indoor airflow; One is 1.7m high, and the other is 0.6 off the floor. Each level contains 25 points with an equal distance of 0.875m around each point. Besides that, the middle line was set to compare the results of phases, while the plane was a section measurement for air velocity and temperature.
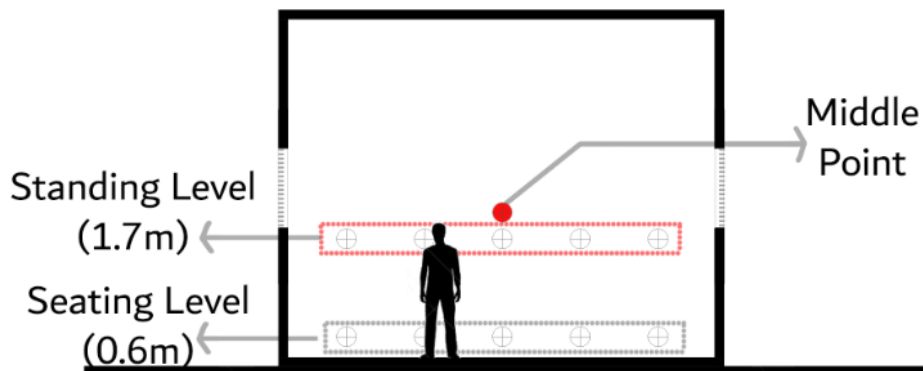
Figure 7-13 CFD measurements levels and points

7.4 Results and Discussion

7.4.1 The Base Case

Under this phase, five different slat angles were tested to investigate the effect of cross ventilation with a room with two opposite mashrabiya and define the most effective inclination angle of mashrabiya. The only difference between the models' inputs is the angle of inclination of the mashrabiya slats, designed at horizontal, +-30, and +-20°.

7.4.1.1 Velocity Distribution

Table 7-6 presents the cross-sectional plots of the air velocity contours in the room of each model in the base case. The greater the angle of inclination towards the top or the bottom, the less the airflow rate in the middle of the room and the sharper the airflow angle towards the ceiling or floor of the room, and this is evident in both cases 2-2 and 2-3. On contract, the first case 2-1 represents the best case in terms of airflow in the middle of the room at the standing level, while the best at the sitting level are both cases 2-3 and 2-5.

Figure 7-14 presents the averages of air velocity in the base case for different cases based on the inclination angle of slats of mashrabiya. The graph shows the effect of applying five different inclination angles on the averages of air velocity in three different positions: middle point (MP), standing level (STL), and seated level (SEL). The air velocity was monitored on STL at 1.7 m, SEL at 0.6 m above ground, while air velocity was measured for levels of 87.5 cm from mashrabiya and room walls.

Based on the monitored data in the middle of the room and standing level, the highest airspeed was in the case 2-1. On the air velocities mean in the standing and sitting levels, 2-5 represents the best condition.

In general, in terms of velocity distribution efficiency inside the room, the best cases were 2-1 and 2-5 (Figure 7-15), selected for the next stage.

Table 7-6 The cross-sectional plot of the air velocity contours in the room for models in the base case

2-1

2-2

2-3

2-4

2-5

Velocity Magnitude [m/s]

0   1.4   2.7   4.1   5.4   6.8   8.1   9
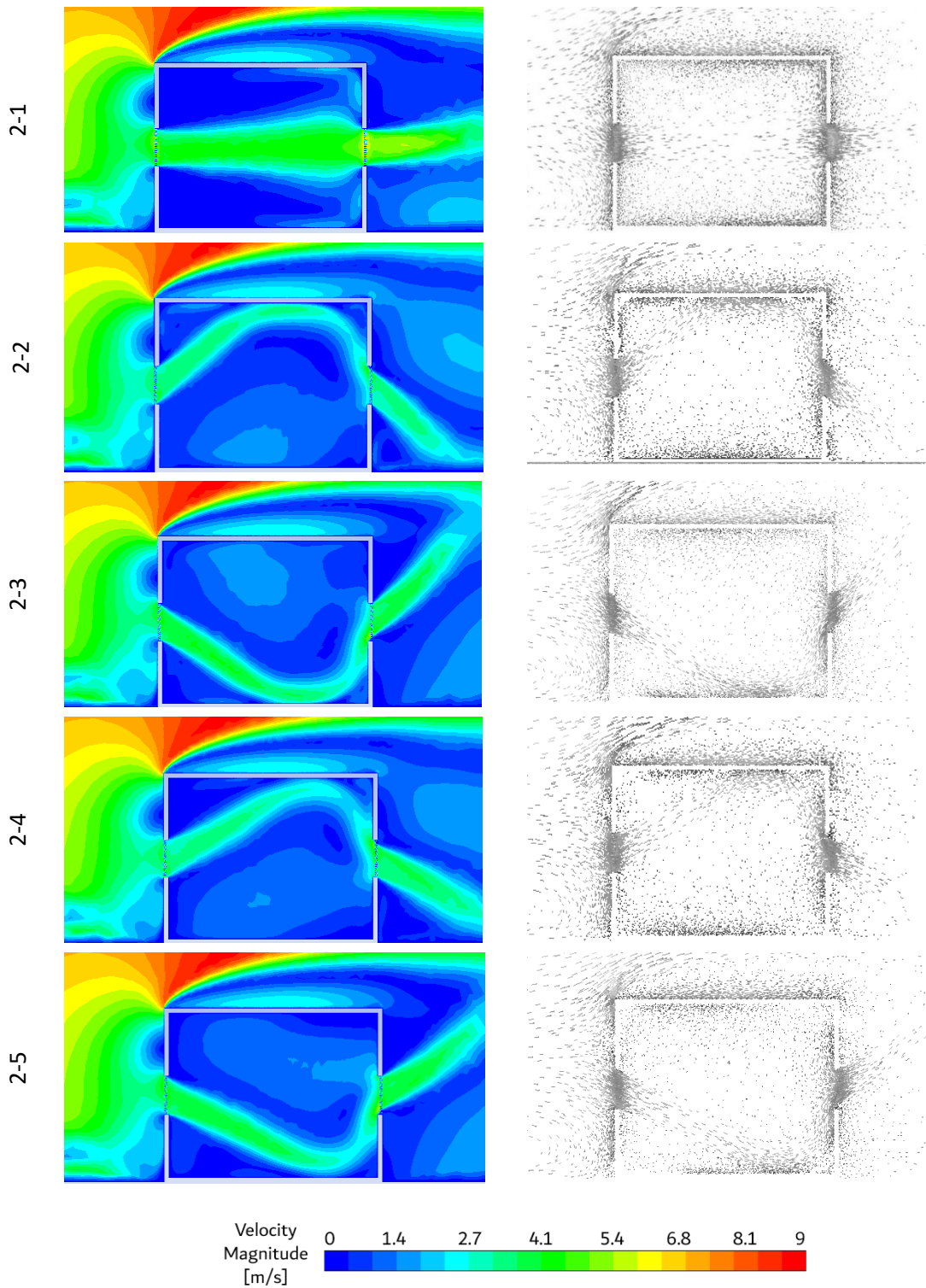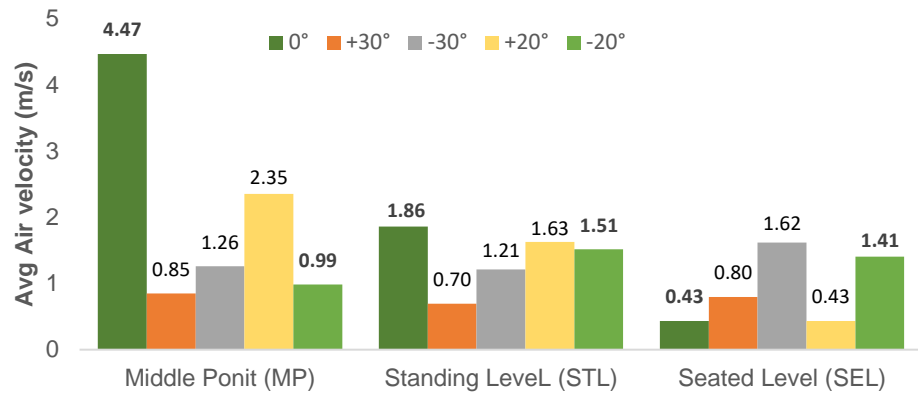
Figure 7-14 The averages of airspeed in the base case for different conditions
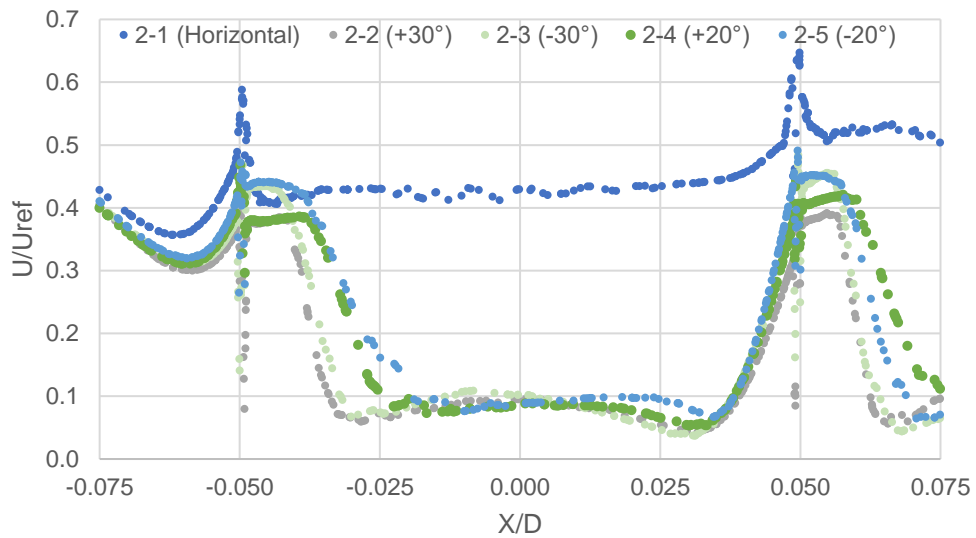
Figure 7-15 The airflow results for each case based on the angle of inclination

7.4.2 Single Row of Pipes Integrated with Mashrabiya

The applied method adopted a system that uses heat transfer devices to provide a continuous cooling cycle, which lowers internal temperatures and reduces heat gain efficiently during hot conditions (Calautit et al., 2013).

In this phase, two main designs were evaluated that differs in inclination angle of the slats (A) horizontal (B) -20°. Each design was tested at two different inlet temperatures; 40° or 30°. Also, a single row of pipes was integrated with the windward mashrabiya with set different temperatures: 22° or 17°, aimed to reduce the indoor temperature. In addition, one sash was removed to make space for a water tank. In the following, the velocity and temperature distribution results will be presented for each case in this phase.

7.4.2.1 Velocity Distribution

Since the air velocity profile is the same in all cases, adding a separate airflow chart for each case was no advantage. Figure 7-16 represents the air velocity contours for cases designed with horizontal slats (3-1 to 3-4) and cases with an inclination angle of -20° (3-5 to 3-8). The cases with horizontal slats show more airflow next to the windward mashrabiya and the standing level (Figure 7-17), whilst the airflow in the opposite mashrabiya and seating zone show a slight increase when the inclination -20°. However, despite the change in the angle of inclination of the slats, the effect of adding the pipes on the similarity of the airflow patterns can be observable (Figure 7-16).

(A)   (B)

| Velocity Magnitude [m/s] | 0 | 1.4 | 2.7 | 4.1 | 5.4 | 6.8 | 8.1 | 9 |
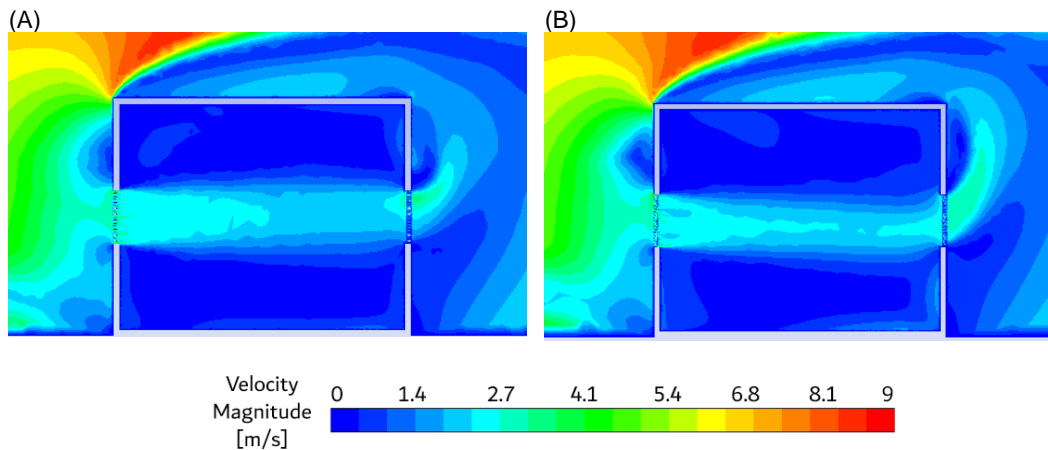
Figure 7-16 Airflow velocity contours at the measurement plane of the room (A) the model designed with horizontal slats and (B) with an inclination angle -20°
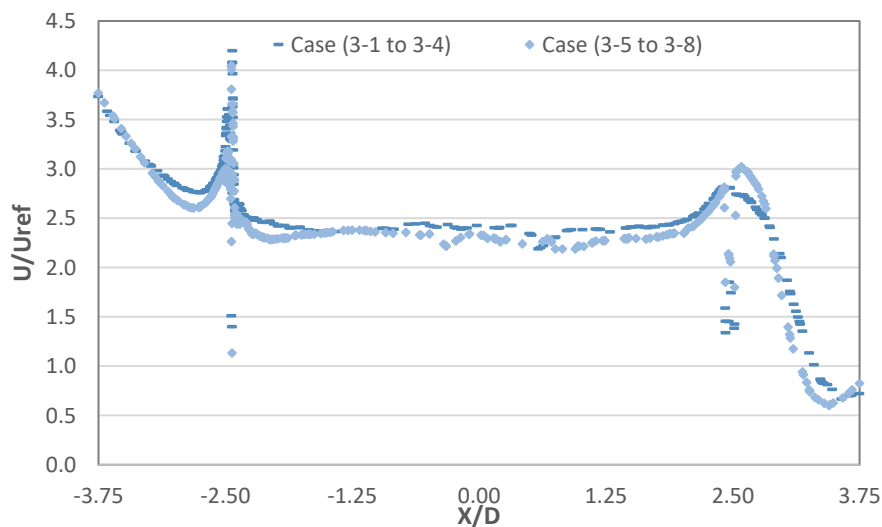
Figure 7-17 The airflow results of cases with horizontal slats compared to the other tilt "-20°" along a horizontal line going through the middle of the room openings

7.4.2.2 Temperature Distribution

Figure 7-18 shows the temperature distribution for the cases designed with horizontal slats, and Figure 7-19 when the slats were tilted -20°. It is clear that the room in these models was affected by the velocity profile, which allowed high heat transfer, thus limiting the effect of pipes on the room, as the drop did not exceed 1° in the best case (3-2). However, when the inlet temperature was set at 40°, using the pipes provided a better impact at room temperatures than the cases with an inlet temperature of 30°. Moreover, setting the pipes' temperature at 17° compared to 22° showed some improvement in decreasing the room temperature.

Despite the different conditions between the field experiment strategies and the simulation model, it is worth noting here their impact on the room thermal environment. In the field experiments, with an average outdoor temperature of 41.6 °C, the evaporative cooling technique "wet cloth" and thermal mass could provide temperature reduction for the room by up 6.8 °C, which was equivalent to a decrease of 19.3% compared to the single row pipes. And for a more efficient way of the piping system, it was needed to add another row of piping and test its performance to improve thermal comfort.
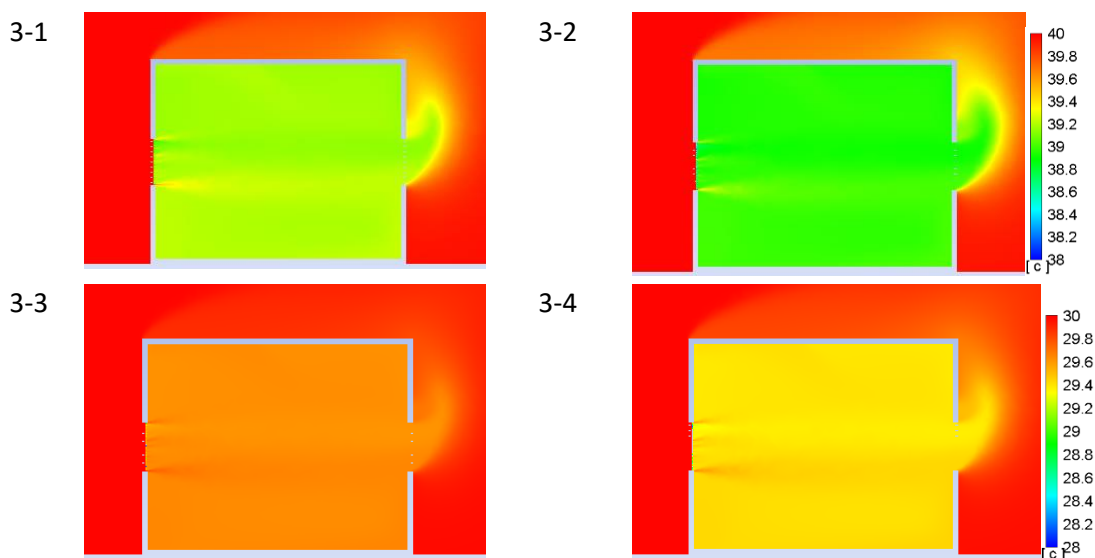
Figure 7-18 The cases with horizontal slats and the temperature distribution on the middle plane of the room
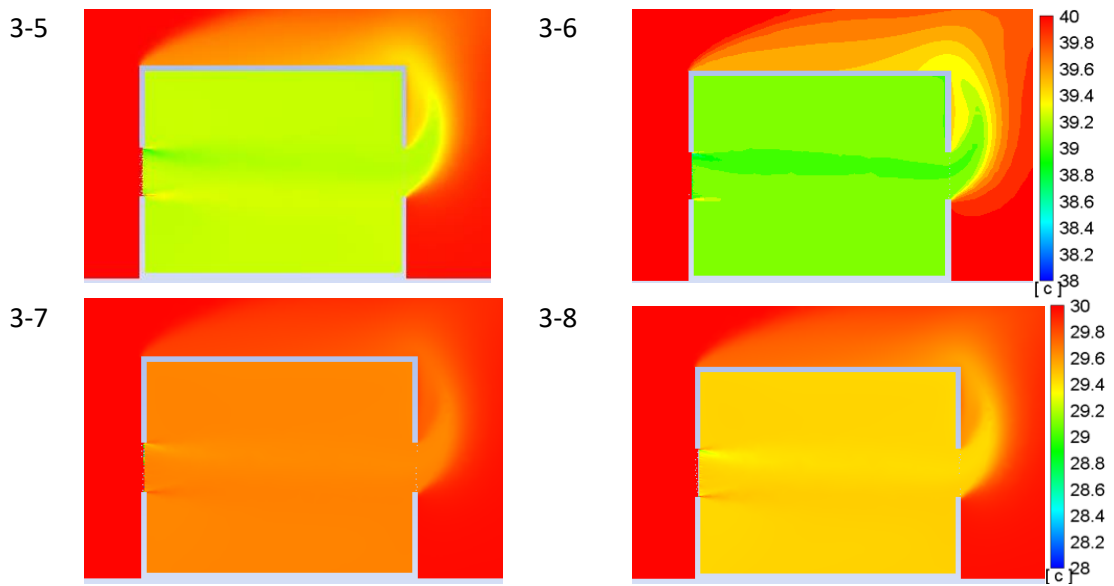
Figure 7-19 The cases with the inclination -20° and the temperature distribution on the middle plane of the room

7.4.3 Double Rows of Pipes Integrated with Mashrabiya

Another row of pipes has been added in this phase to increase the effect of the number of pipes on the room temperature. In this phase, five different air velocity profiles were tested on two models that differ in inclination angle of the slats (A) horizontal (B) -20°. In addition, the inlet temperature was set in worst case scenario at 40, while the pipes were set at 22°C. The velocity and temperature distribution results will be presented for 10 cases in this phase.

7.4.3.1 Velocity Distribution

Table 7-7 displays the contours of air velocity on the vertical middle plane based on selected different reference wind speed U_{ref}; 0.5, 1, 2, 4, and 5, and two configurations of slat angles; horizontal or -20°. Although the angle of inclination of the slats for cases 4-1 to 4-5 differed from the cases 4-5 to 4-10 and the air wind speed profile differed from 0.5 to 5 m/s, the flow patterns were similar in most cases. This is due to the additional row of pipes and thus had a more significant impact on the airflow distribution pattern. Therefore, the angle of inclination of the mashrabiya slats became less effective in forming the air pattern in this phase. Figure 7-20 shows the selected references wind speed and the averages of air velocity on different measurements levels, including the middle point. The figure shows how similar the rates of air measurements are despite the difference in the angle of inclination.

Table 7-7 Contours of air velocity on the vertical middle plane for the cases with double rows of pipes

Slat		Horizontal		-20°
Uref (m/s)	Case	Section and contour	Case	Section and contour
5	4-1		4-6	
4	4-2		4-7	
2	4-3		4-8	
1	4-4		4-9	
0.5	4-5		4-10	

Velocity Magnitude [m/s]

0	1.4	2.7	4.1	5.4	6.8	8.1	9
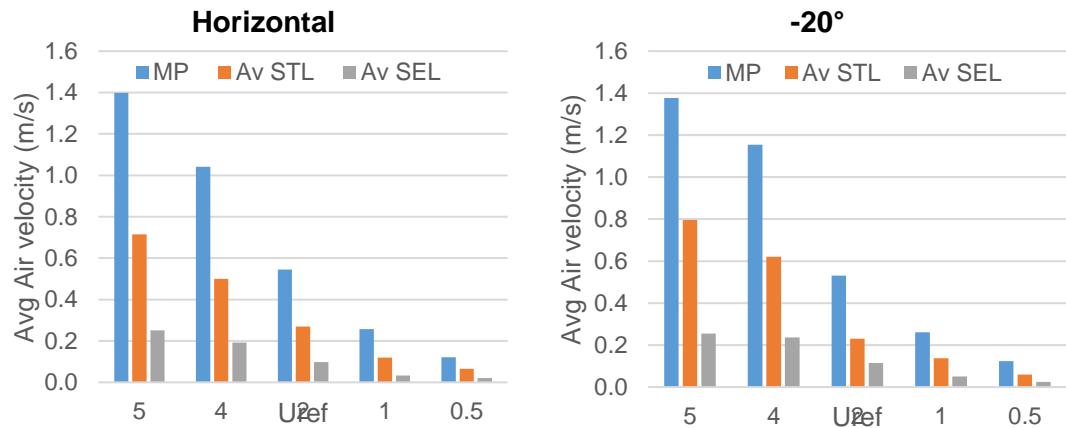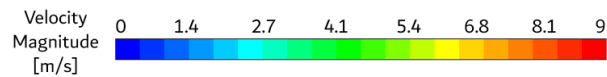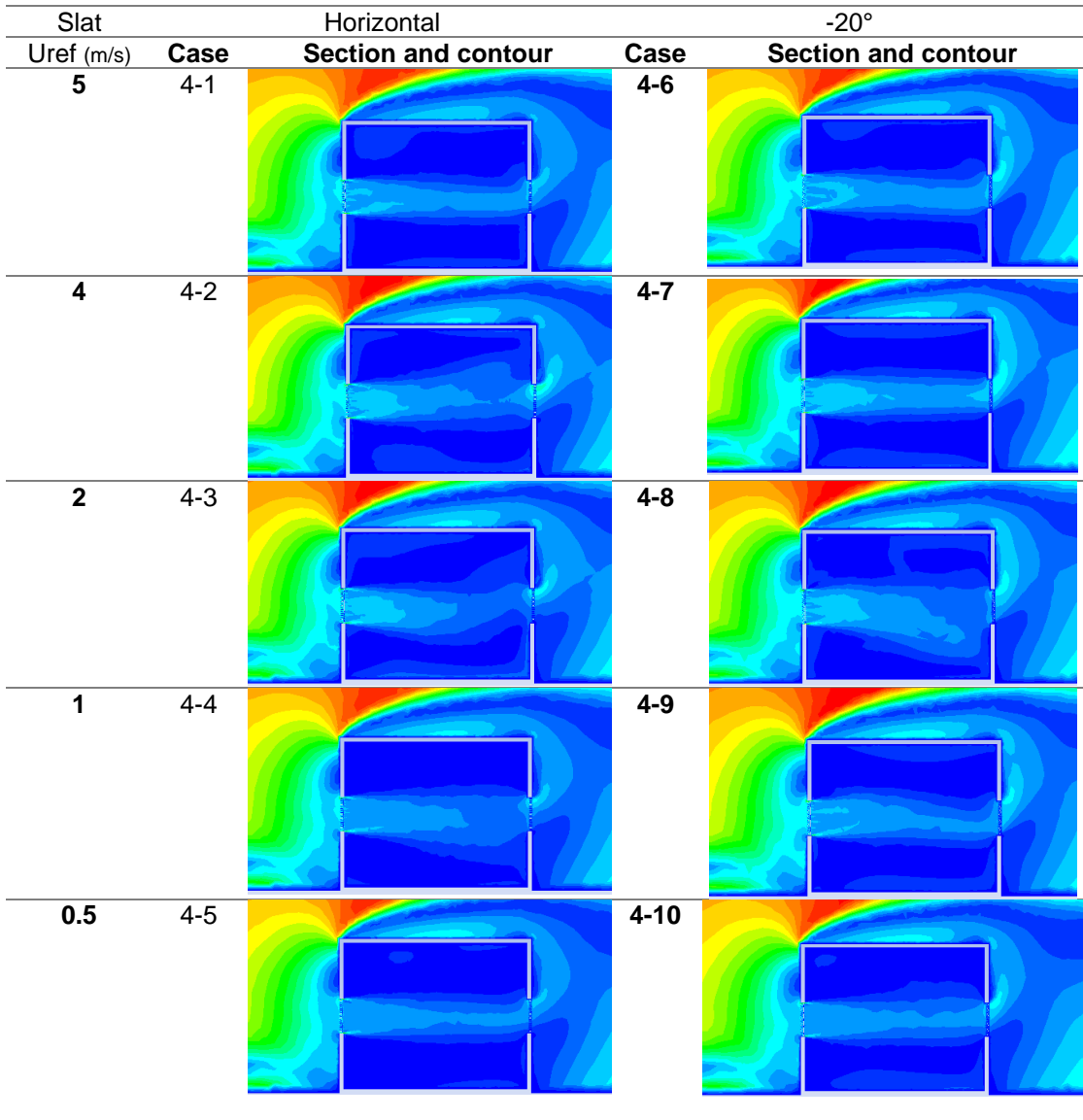
Figure 7-20 Different references wind speed and the averages of air velocity on different measurements levels and the middle point

7.4.3.2 Temperature Distribution

The temperature distribution for each case in this phase is presented in Table 7-8. As observed, both configurations follow the same temperature patterns. From the table charts, it can be said that cases 4-1 and 4-6 were the lowest practical cases, while cases 4-5 and 4-10 were the best cases in decreasing temperature. In other words, with the increase in the inlet airspeed, the effectiveness of the cooling strategy decreases. In contrast, with the decrease in the airspeed profile, the system becomes more efficient.

Table 7-8 The temperature distribution for two different configurations and five different air velocity profiles
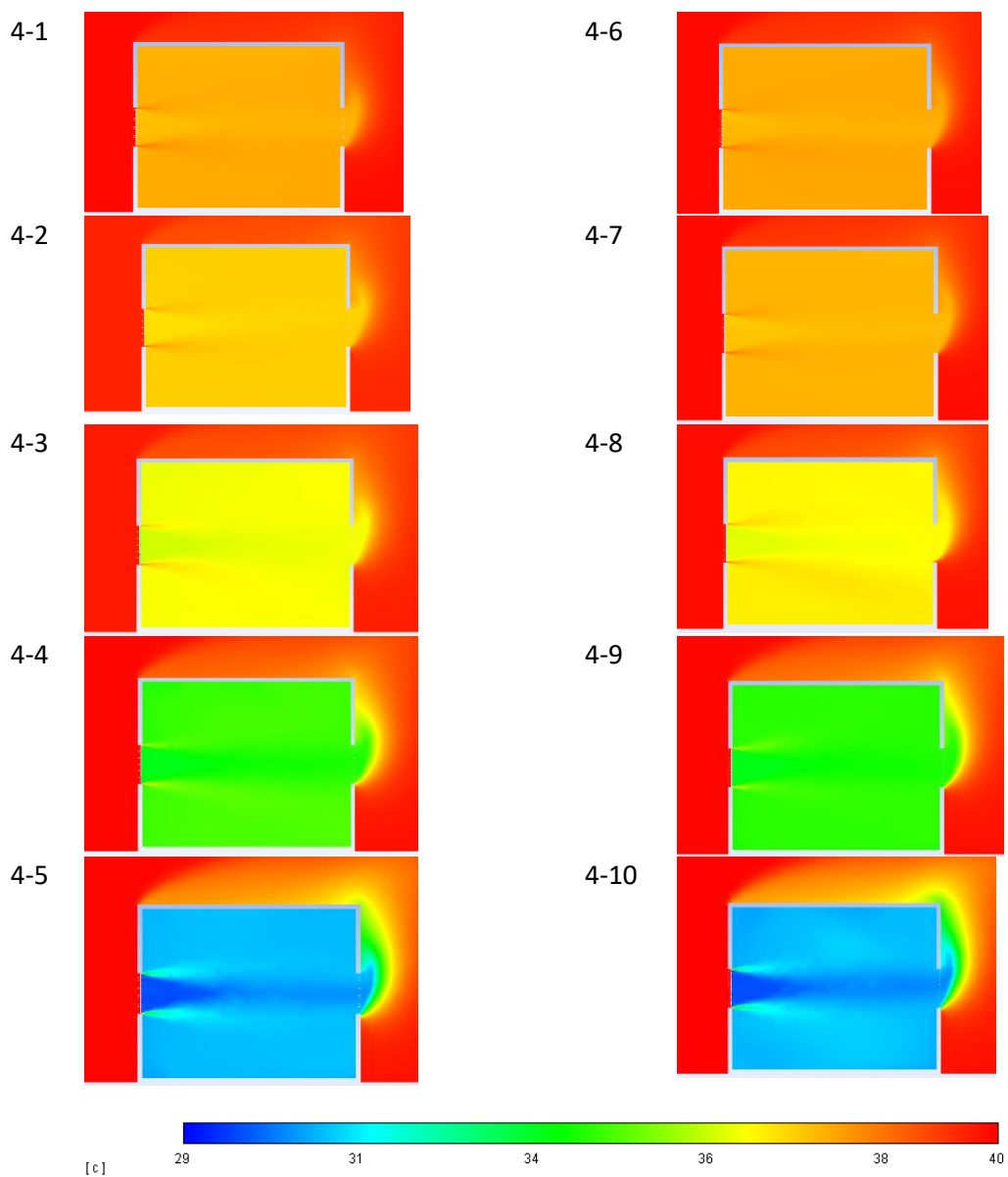
7.4.4 Comprehensive Comparison of the Simulation Phases

This part presents the main variation and improvement from the Base case to the last case and compares the simulation works' velocity and temperature, thus defining the optimal case among these simulations that provide the best indoor comfort.

7.4.4.1 The base case vs the benchmark model

Table 7-9 shows the results of air rates for the standard case compared to the results of adding mashrabiya and its effect on airflow rates when changing the angle of inclination of the slats. It is clear from this that case 2-1 afforded the best airflow at the standing level, shown in Figure 7-21. In addition, the graph shows that the mashrabiya contributed to the continuity of airflow on the standing level efficacy compared to the benchmark case. Case 2-3 indicates that with the slats inclinations of -30, the mashrabiya provided more flow in the seating area than the benchmark case. However, the second-best case based on the velocity averages was 2-5, considered the second design model in the pipes phase.

Table 7-9 The averages of airflow results for the benchmark case and the base case.

	Slats angel	(STL)	(SEL)
Benchmark case	NA	1.62	1.44
2-1	0°	1.86	0.43
2-2	+30°	0.70	0.80
2-3	-30°	1.21	1.62
2-4	+20°	1.63	0.43
2-5	-20°	1.51	1.41
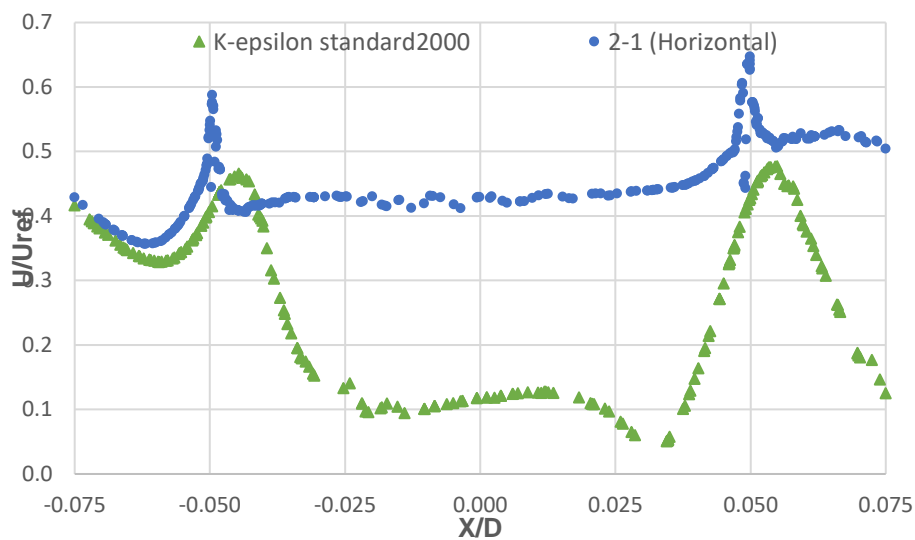
Figure 7-21 The impact of the best case (mashrabiya with horizontal slats) on the airflow results along the horizontal centerline compared to the benchmark case (no mashrabiya)

7.4.4.2 Single row of pipes vs Double rows of pipes

By comparing the results of the configurations of the pipes, it was found that the single pipes row had less reduction in the airflow. However, it has been observed that despite the change in the angle of inclination of the slats, the effect of adding pipes, either single row or double, contributed to the similarity of the airflow pattern, as shown in Figure 7-22.

The results of both phases were reflected in the velocity profile used for each case. The cases with the single-pipe row when using the profile of the mean wind speed U_{ref}=6.97 m/s as in the benchmark case, indicated a slight temperature drop of less than 1 degree C°. The mean wind speed profile allowed more heat transfer, thus limiting the impact of the pipes on the room. In the double pipes, the air wind speed profile was tested from 0.5 to 5 m/s, but the flow patterns were similar in most cases due to these additional rows of pipes. Therefore, the angle of inclination of the mashrabiya slats became less effective in forming the air pattern in this phase. Although the addition of another row of pipes reduced the airflow force, this contributed to an increase in the effectiveness of the pipes, which resulted in a clear reduction in room temperatures. Unfortunately, the application of these pipes may cause a lack of daylight and outside visibility.
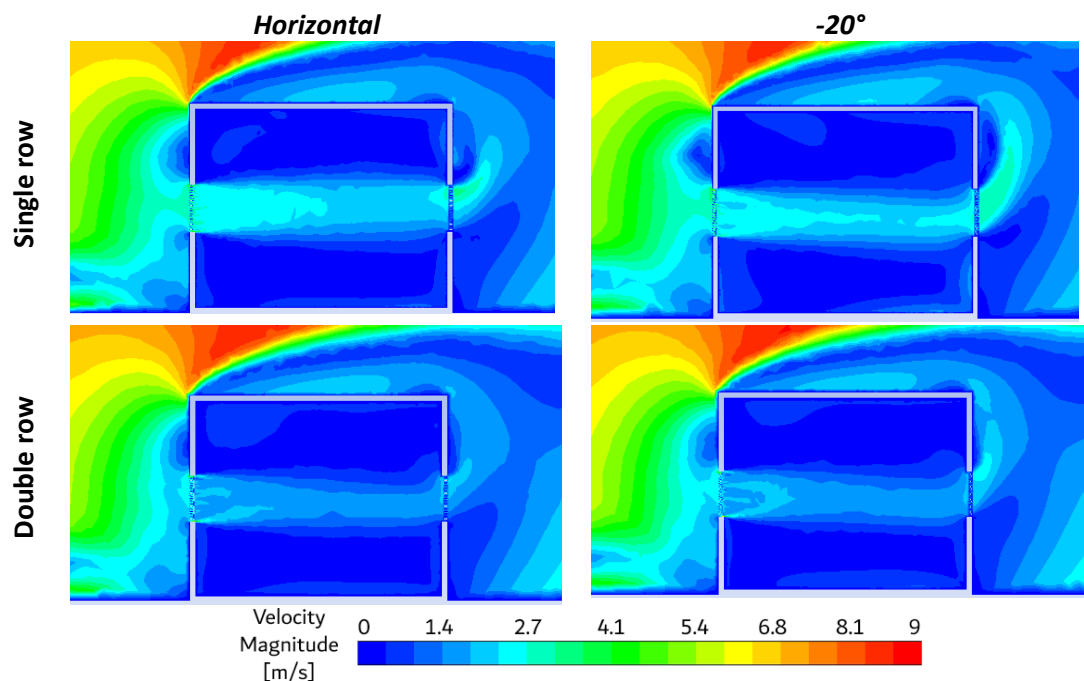
Figure 7-22 The overall airflow velocity contours at the measurement plane for both pipes phases and two configurations of inclination angle

The air velocity, temperature, and thermal comfort rates for the most effective phase are presented in Table 7-10. The thermal comfort was specified by using (de Dear and Berger, 2002) equation as follows;

$$T_c = 0.31\ T_o + 17.8 \qquad (7.1)$$

The equation was presented and discussed in detail in section 3.6.1 and section 5.4.4. However, based on the measured outdoor temperature during the experiment, T_o could be determined as 36.2 °C and hence calculated comfort temperature from the equation (7.1) was 30.2 °C. The other thermal comfort was specified based on the Nicol and Humphrey field study that indicated the participants felt comfortable at indoor temperatures around 33 °C.

Table 7-10 The averages of air velocity, temperature, and comfort for the double pipes cases

Case	U_{ref}	Velocity	Temperature	Thermal comfort	
		Avg.	Avg.	Ref. *30.2 C°*	Ref. 33 *C°*
4-1	5	0.48	38.97	-8.8	-5.97
4-2	4	0.35	38.81	-8.6	-5.81
4-3	2	0.18	38.02	-7.8	-5.02
4-4	1	0.08	36.06	-5.9	-3.06
4-5	0.5	0.04	32.50	-2.3	0.50
4-6	5	0.53	39.00	-8.8	-6.00
4-7	4	0.43	38.86	-8.7	-5.86
4-8	2	0.17	38.06	-7.9	-5.06
4-9	1	0.09	35.90	-5.7	-2.90
4-10	0.5	0.04	32.47	-2.3	0.53

In general, this method indicated lower temperatures while reducing the air velocity, which reduced heat flow from outside and increased system efficiency. Case 4-5 and 4-10, when the slats were set horizontally or tilt -20 with a mean wind speed profile U_{ref}=0.5 m/s indicated a temperature decrease of 7.5°C (18.8%), and hence resulted in enhanced thermal comfort.
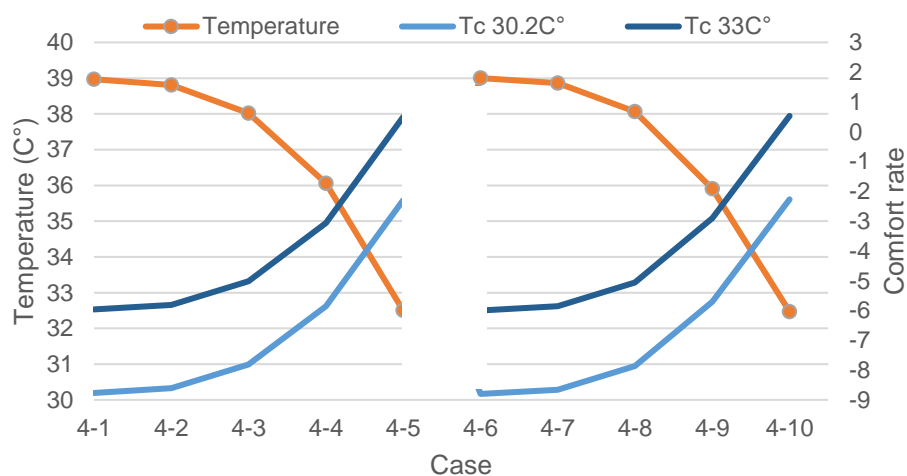
Figure 7-23 The effect of temperature on achieving indoor thermal comfort

From the pipes results, it can be said that higher air velocities with higher temperatures cause more heat transfer to the room and thus reduce the efficiency of the cooling strategy. Overall, the double pipes with the U_{ref} 0.5 m/s reference velocity profile indicated the highest reduction in room temperature, and thus thermal comfort was achieved.

7.5 Summary and Conclusions

Overall, this chapter presents modelling the mashrabiya in the simple design along with the change of the angle tilt slats, which has been analysed and discussed based on computational results of airflow. Moreover, to improve the mashrabiya performance in terms of indoor comfort, a relief thermal system "heat pipes" was used to decrease the indoor temperate by setting several configurations and parameters. The case of developing mashrabiya by combining with the pipes included two configurations: a row of pipes and another additional pipe row, both set behind the mashrabiya facing the windward. The computing results for air velocities and air temperature were analysed in both pipes cases. In the case of double pipes, several wind speed profiles U_{ref} were tested with two configurations of the angle of inclination, either horizontal or at an angle of -20, while the thermal comfort rates for each case were calculated.

The base case results indicated that the greater the angle of inclination towards the top or the bottom, the less the airflow rate in the middle of the room and the sharper the airflow pattern towards the ceiling or floor of the room. Moreover, the base case indicated that the mashrabiya contributed efficiently to better airflow inside the room than the benchmark case.

The result of pipes phases indicated that adding pipes, whether single or double row, greatly affected the similarity of the airflow patterns. By comparing the results of the configurations of the pipes, it was found that the double pipes rows cause more impact on reducing the airflow into the room. Also, it was found that the airflow for both phases was reflected based on the velocity profile used for each case.

The higher wind speed profiles U_{ref} contributed to the increased rates of heat transfer, which limited the effect of the pipes on the room and resulted in a slight temperature drop of less than 1 degree at best. Although the design of the pipes may cause a lack of daylight and

outside visibility, it reduced room temperature by up to 7.5 °C and achieved a level of thermal comfort. From the results, it can be said that high airspeeds with high temperatures reduce the efficiency of the applied strategy.

In general, mashrabiya slices play a key role in directing airflow according to the angle of inclination. In addition, the CFD was an excellent tool that allowed to test and analysis of different designs and variables of the mashrabiya, which contributed to a more accurate and better understanding of its performance and impact on the room. Although the mashrabiya could achieve better airflow than the benchmark case (without the Mashrabiya), reducing indoor temperatures required incorporating another strategy. The combined method with mashrabiya indicated a clear reduction in the room temperature, which resulted in thermal comfort and thus achieved this simulation work's objectives.

CHAPTER 8

Conclusions and Further Work

Introduction
Conclusions
Limitations
Recommendation for future work

8. CONCLUSIONS AND FURTHER WORK

8.1 Introduction

During the recent decades, the Kingdom of Saudi Arabia has witnessed many changes and developments in various sectors, including building development and construction. This was accompanied by the dependence of modern buildings on active "mechanical" systems and the neglect of the exploitation of natural resources such as passive ventilation. These factors, along with the hot climate of Saudi Arabia, contributed to the increase in energy use in residential buildings, while about half of this percentage is consumed to reach thermal comfort. Besides this consumption, most modern buildings have lost their local and authentic architectural style and identity.

Referring to the past, mashrabiya was one of the traditional architectural solutions used widely and characterized by its functionality suitable for the local environment. Although there are many research, experiments and studies were conducted to revive mashrabiya by several solutions and methods in the last years. Mashrabiya still needs more experimental and practical studies regarding evaluating its functional aspect and its effect on thermal comfort. This research investigated the effect of the mashrabiya on indoor air velocity and temperature and integrated different cooling techniques to enhance the indoor thermal comfort in the residential buildings a hot climate concerning Jeddah, Saudi Arabiya.

This research consisted of two approaches: theoretical and practical to achieve the research aim and objectives. The theoretical approach began with a literature review on the energy efficiency of residential buildings in Saudi Arabia. In addition, review some background about traditional and modern residential buildings in Saudi Arabia.

This research consisted of two approaches: theoretical and practical to achieve the research aim and objectives. The theoretical approach began with a literature review on the energy efficiency of residential buildings in Saudi Arabia. In addition, review some background about traditional and modern residential buildings in Saudi Arabia. The literature review included the impact of the building envelope represented by facades and windows on the thermal environment through different factors; daylight, heat loss, heat gain, ventilation, and focusing

on thermal comfort. Subsequently, the mashrabiya was reviewed and covered from different aspects; history, concept and structure, functions, advantages and disadvantages. Also, the literature review of mashrabiya covered the related previous studies and applications where the research gap has been determined.

The practical approach was carried out in two sequential stages: Field experiments and simulations. Accordingly, two field experiments were conducted during two separate summers in a historic building located in old Jeddah, Saudi Arabia. The first field experiment was considered a pilot study aimed mainly to assess the performance difference and the impact between open and closed mashrabiya in terms of thermal comfort. The second field experiment included the integration of the evaporative cooling technique with the mashrabiya. However, to evaluate the performance of the mashrabiya in detail and save cost, and have more flexibility of analysis and development, which required the use of a CFD simulation. The simulation work generated a benchmark case based on detailed wind tunnel experiments and a reference CFD model. After that, three sets were performed sequentially through a group of configurations and strategies: a) the base case, b) single row pipe, and c) double rows of pipe combined with mashrabiya.

The following sections draw the main conclusions based on the research findings, followed by recommendations for further work.

8.2 Conclusions

- The case study "Baeshen House" is one of the most prominent historical buildings in Old Jeddah, and where two similar rooms were selected in this building for the field experiments for investigating the effect of mashrabiya then test the integration of three different strategies for passive evaporative cooling with the Mashrabiya and their impact on the indoor thermal environmental comfort.

- The first field study was conducted during the summer of 2018 from 4th August to 1st September for 28 days. The results indicated that opening the mashrabiya allowed more airflow into the room during the day and reduced the indoor temperature by up to 2.4 °C as compared to the closed mashrabiya. Besides, the indoor thermal comfort evaluation

demonstrated that Room 1 typically were near to the temperature comfort of 33 °C and better than Room 2 by 0.3 degrees on average.

- The second fieldwork was carried out during the summer of July and August 2019. The results indicated that although the open mashrabiya provided some reduction in the heat in room 1, some cooling strategies (pots, water sprays, and wet cloth) were tested during those hot outdoor conditions. However, it was found that the most effective approach to improving the room air temperature was hanging a wet cloth facing the mashrabiya, where the R1 average temperature was reduced by up to 6.8°C. The results also showed that along with the mashrabiya and the evaporative cooling strategies, the thermal mass played a significant role in reducing indoor air temperatures' thermal swings.

- Although the fieldworks gave an overall and comprehensive perception of the performance of the mashrabiya and the impact of incorporating some passive evaporation cooling methods with the mashrabiya, the measurements were limited to a few points, especially concerning air velocity observations due to the limited time and the available equipment, which caused the lack of a clear perception of air movement and directions inside the room. In view of this, it was necessary to use a CFD simulation software as ANSYS to further understand and evaluate the performance of the mashrabiya and its impact on airflow and heat in the room.

- For the simulation works, the CFD model has been validated based on detailed wind tunnel data of the PIV velocity measurement with selected a CFD detailed reference in order to obtain an accurate and valid base model that reflect the actual impact on the model in the base case and optimisation phase. The total tested models for achieving the aim of the simulation work were 41 cases; 18 in the validation phase, 5 in the base case, and 18 in the pipes phase.

- In the validation phase, two types of mesh were tested: hexahedral mesh and tetrahedral mesh were solved with three turbulence models; (1) Shear Stress Transport (SST k-ω) model, standard k-epsilon (k-ε) model,(3) RNG k-epsilon (RNG k-ε) model;(4) K-omega (k-ω) model. The results indicated that the hexahedral mesh monitored strong agreement to PIV data; however, tetra has been proven effective in saving time and achieving good and compatible results to the PIV also and based on that, the model (k-ε

standard model with 2000 iterations) has been selected as a benchmark case for the subsequent phases.

- The base case was created as the benchmark case in addition to the mashrabiya, while five different angles of slats were tested: horizontal, +-30, and +-20°. It was observed that the greater the inclination of the slats towards the up or down, the lower the airflow rate in the middle of the room and the sharper the angle of the airflow towards the ceiling or floor. Overall, the results indicated that the mashrabiya contributed to the continuity of airflow into the room efficiently compared to the benchmark case.

- An inspired heat pipe strategy has been applied and combined with mashrabiya to extend indoor comfort more effectively and differently from the strategies used in the second field experiment. The applied technique used heat pipes as "thermal relief" devices to provide a continuous cooling cycle, thus lowering indoor temperatures. The case of developing mashrabiya by combining with the pipes included two configurations: a row of pipes and another additional pipe row, both set behind the mashrabiya facing the windward.

- In the single row of pipes phase, two different inclination angles of the slats were examined (a) horizontal (b) -20° with testing two different inlet temperatures; 40° and 30° and pipes temperatures 22° and 17°, aimed to reduce the indoor temperature. It was observed that the addition of the pipes played a primary role in the similarity of the airflow patterns. In contrast, the wind speed profile U_{ref}=6.97 m/s allowed high heat transfer into the room, thus limiting pipes' effect on the room where the temperature decreased by only 1 degree in the best case.

- In the phase of the double rows of pipes, five different air velocity profiles; (0.5, 1, 2, 4, and 5) were tested on two configurations of slat angles; horizontal or -20°. Concurrently, the inlet temperature was set in at 40 and pipes at 22°C. The results indicated that due to the additional row of pipes, the angle of inclination of the mashrabiya slats became less effective on the airflow direction, and the flow patterns became similar in this phase. Although the design of the pipes may cause a lack of daylight and outside visibility, the temperature decreased 7.5°C (18.8%) and resulted in achieving thermal comfort when Uref=0.5 m/s was used as profile mean wind speed. Overall, the applied technique played

an important role integrated with the mashrabiya in achieving thermal comfort and thus achieving the objectives of the simulation work.

- It can be said that the simulation method allowed the testing and analysis of different designs and variants of the mashrabiya in a more flexible manner than fieldwork, which contributed to a more accurate and better understanding of its performance and its effect on ventilation, temperature and thermal comfort inside the room.

8.3 Limitations

Overall, the work of this study was able to achieve the primary purpose and objectives of the research through the specified methods. However, like any research, it had some limitations. In the fieldwork, the measurements and observations covered the environmental factors for thermal comfort only, without covering the personal factors because the selected building is uninhabited, and the difficulty of involving people in this type of experiment in these climatic and spatial conditions. Furthermore, the field study was limited to studying one type of mashrabiya for one building during specific periods because of the time constraints, available tools, ability, and difficulty obtaining permission to enter such historical buildings. Also, due to the time and equipment available, monitoring was limited to specific measurement points, especially for air velocity.

In the simulation work, the investigation of the effect of mashrabiya was limited to one type and design. In addition, the computational room was not studied as part of a building but was studied as isolated. Although the hexahedral cases showed more correlated results with the PIV data, the tetra mesh was used due to the time and complexity of preparing the solution of the hexahedral mesh cases.

8.4 Recommendation for Future Works

- Further studies are needed to carry out field works in different conditions and climates where using this method in temperate climates may be more effective and result in more periods of thermal comfort.

- It is strongly recommended to conduct more field experiments on different types of mashrabiya and more buildings for comparison.

- Fieldwork was carried out on a western-oriented mashrabiya, while further investigation can be conducted on the influence of the mashrabiya with eastern and southern orientation, especially on indoor temperatures and heat gain.

- Further studies and tests of the effect of integrating different evaporative cooling techniques with mashrabiya should be conducted.

- It is recommended to study the effect of pipe configurations on the entry of daylight alongside the view, whereas testing different gaps between the slats and evaluating the effect of the heat transfer device on thermal conditions in parallel with its effect on daylight level will be useful.

- It is recommended to investigate more complex designs of mashrabiya and evaluate its impact on the airflow.

- It is very important to simulate a room as part of a building considering the influence of external elements, as this will give a better perception of the mashrabiya effect and more realistic results.

- Although the benchmark case has been successfully validated with actual experiments and selected CFD reference, the proposed design workflow that includes pipes has not been validated. Therefore, future work should consider creating an actual model and conducting fieldwork experiments to reconfirm the proposed design's reliability.

- Future work needs to investigate different alternatives to maintain pipes' water temperature as using water from the mainline or using fans solar-powered to cool the water tank.

- Future work should focus on investigating the incorporation of mashrabiya in a way that is in line with the requirements of modern buildings and their occupants.

REFERENCES

Proceedings of The 1st International Conference on Comfort at The Extremes: Energy, Economy and Climate. *In:* ROAF, S. & FINLAYSON, W., eds. CATE 2019, 2019 Heriot Watt University, Dubai. Ecohouse Initative Ltd.

ABDELGELIL, N. 2006. A New Mashrabiyya for contemporary Cairo: Integrating traditional latticework from Islamic and Japanese cultures. *Journal of Asian Architecture and Building Engineering,* 5**,** 37-44.

ABDULLAH, A., SAID, I. B. & OSSEN, D. R. 2019. A sustainable bio-inspired cooling unit for hot arid regions: Integrated evaporative cooling system in wind tower. *Applied Thermal Engineering,* 161**,** 114201.

ABOHORLU DOĞRAMACι, P. 2018. *Investigation of novel evaporative cooling material for Cyprus climate.* Doctor of Philosophy, University of Nottingham.

ADAS, A. A. Wooden Bay Window (Rowshan) Conservation in Saudi-Hejazi Heritage Buildings. ISPRS-International Archives of the Photogrammetry, Remote Sensing and Spatial Information Sciences, 2013 Strasbourg, France. 7-11.

ADDINGTON, D. M. & SCHODEK, D. L. 2005. *Smart Materials and New Technologies: For the Architecture and Design Professions,* Burlington, Massachusetts, USA, Architectural Press.

AFFAIRS, M. O. M. A. R. 2019. Jeddah City Profile. *Future Saudi Cities Programme.* UN-Habitat.

AIAA, C. F. D. C. 1998. Guide for the Verification and Validation of Computational Fluid Dynamics Simulations (AIAA G-077-1998 (2002)). United States of America: American Institute of Aeronautics and Astronautics, Inc.

AJAJ, A. & PUGNALONI, F. 2014. Re-Thinking Traditional Arab Architecture: A Traditional Approach to Contemporary Living. *International Journal of Engineering and Technology,* 6**,** 4.

AL-ANSARI, J., BAKHSH, H. & MADNI, I. 1986. Wind energy atlas for the kingdom of Saudi Arabia. *King Fahd University of Petroleum and Minerals Press, Dhahran*.

AL-BAN, A. Z. G. 2016. *Architecture and cultural identity in the traditional homes of Jeddah.* Doctor of Philosophy, University of Colorado at Denver.

AL-DOSSARY, A. M. & KIM, D. D. 2020. A Study of Design Variables in Daylight and Energy Performance in Residential Buildings under Hot Climates. *Energies,* 13**,** 5836.

AL-HAMID, N. & MOHAMMED, I. 2014. Centuries-old houses major attraction in Balad. *Arab News*, Oct 2018.

AL-HASHIMI, A. A. K. & SEMIDOR, C. 2013. Virtual Study of the Day-lighting Performance of Rawshan in Residential Buildings of Jeddah. *SB13 Dubai Paper***,** 8.

AL-HEMIDDI, N. A. & MEGREN AL-SAUD, K. A. 2001. The effect of a ventilated interior courtyard on the thermal performance of a house in a hot–arid region. *Renewable Energy,* 24**,** 581-595.

AL-LYALY, S. M. Z. 1990. *The Traditional House of Jeddah: a study of the interaction between climate, form and living patterns.* PhD, University of Edinburgh.

AL-MURAHHEM, F. 2010. The mechanism of the rawāshīn: the case study of Makkah. *WIT Transactions on Ecology and the Environment,* 128**,** 13.

AL-SANEA, S. A. & ZEDAN, M. F. 2008. Optimized monthly-fixed thermostat-setting scheme for maximum energy-savings and thermal comfort in air-conditioned spaces. *Applied Energy,* 85**,** 326-346.

AL-SANEA, S. A., ZEDAN, M. F. & AL-HUSSAIN, S. N. 2013. Effect of masonry material and surface absorptivity on critical thermal mass in insulated building walls. *Applied Energy,* 102**,** 1063-1070.

AL-SHAREEF, F. M. 1996. *Natural light control in Hadjazi architecture: an investigation of the Rowshan performance by computer simulation.* Doctor of Philosophy PhD thesis, University of Liverpool.

AL TAYASH, K. A. 2011. *Opinions in architecture and urban*.

ALAIDROOS, A. & KRARTI, M. 2015. Optimal design of residential building envelope systems in the Kingdom of Saudi Arabia. *Energy and Buildings,* 86**,** 104-117.

ALGBURI, O. & BEYHAN, F. 2019. Cooling Load Reduction in a Single–Family House, an Energy–Efficient Approach. *Gazi University Journal of Science,* 32**,** 385-400.

ALHARBI, A. 2014. *Investigation of sub-wet bulb temperature evaporative cooling system for cooling in buildings.* Doctor of Philosophy, University of Nottingham.

ALHARBI, A., ALMANEEA, A. & BOUKHANOUF, R. 2019. Integrated hollow porous ceramic cuboids-finned heat pipes evaporative cooling system: Numerical modelling and experimental validation. *Energy and Buildings,* 196**,** 61-70.

ALHARBI, T. H. 1989. *The development of housing in Jeddah: changes in built form from the traditional to the modern.* Doctor of Philosophy, University Newcastle.

ALITANY, A., BAIK, A., BOEHM, J. & ROBSON, S. 2013a. Jeddah historical building information modeling" JHBIM" Old Jeddah-Saudi Arabia. *International Archives of the Photogrammetry, Remote Sensing and Spatial Information Sciences-ISPRS Archives.* Strasbourg, FRANCE.

ALITANY, A., REDONDO, E. & ADAS, A. The 3D Documentation of Projected Wooden Windows (The Roshans) in the Old City of Jeddah (Saudi Arabia) Using Image-based Techniques. ISPRS Ann. Photogramm. Remote Sens. Spatial Inf. Sci., II-5/W1. XXIV International CIPA Symposium, 2013b Strasbourg, France. 7-12.

ALJOFI, E. 1995. *Effect of the Rawshan on the provision of daylight for shopping precincts.* PhD thesis, University of Wales, Cardiff.

ALJOFI, E. The potentiality of reflected sunlight through Rawshan screens. The International Conference "Passive and Low Energy Cooling for the Built Environment", Santorini, Greece, 2005 Santorini, Greece. 817-822.

ALKENAIDARI, A. 2019. *Moving toward energy efficient buildings : A growing economic challenge for Saudi Arabia.* Doctor of Philosophy University of Cincinnati.

ALLOCCA, C. 2001. *Single-sided natural ventilation: design analysis and general guidelines.* Master of Science in Mechanical Engineering, Massachusetts Institute of Technology.

ALMAANY. 2017. *Dictionary of Almaany* [Online]. Available: http://www.almaany.com/ [Accessed 2017].

ALMERBATI, N. 2016. *Hybrid Heritage: An Investigation into the Viability of 3D-Printed Mashrabiya Window Screens for Bahraini Dwellings.* Doctor of philosophy PhD Thesis, De Montfort University.

ALMERBATI, N., FORD, P., TAKI, A. & DEAN, L. 2014. From Vernacular to Personalised and Sustainable. *48th International Conference of the Architectural Science Association.* The Architectural Science Association & Genova University Press.

ALOTAIBI, F. 2015. The Role of Kinetic Envelopes to Improve Energy Performance in Buildings. *Journal of Architectural Engineering Technology,* 4**,** 2.

ALOTHMAN, H. 2017. *An Evaluative and Critical Study Of Mashrabiya: In Contemporary Architecture.* Master of Science, NEAR EAST UNIVERSITY.

ALRASHED, F., ASIF, M. & BUREK, S. 2017. The Role of Vernacular Construction Techniques and Materials for Developing Zero-Energy Homes in Various Desert Climates. *Buildings,* 7**,** 17.

ALSHAHRANI, J. & BOAIT, P. 2019. Reducing High Energy Demand Associated with Air-Conditioning Needs in Saudi Arabia. *Energies,* 12**,** 87.

ALSHARIF, A. 2016. *Towards Islamic Architecture: An Attempt to Understand Architecture from an Islamic Perspective.* Master of Architecture in Architecture Thesis (M.arch), Savannah College of Art and Design.

ALWETAISHI, M. 2019. Impact of glazing to wall ratio in various climatic regions: A case study. *Journal of King Saud University - Engineering Sciences,* 31**,** 6-18.

ALWETAISHI, M., BALABEL, A., ABDELHAFIZ, A., ISSA, U., SHARAKY, I., SHAMSELDIN, A., AL-SURF, M., AL-HARTHI, M. & GADI, M. 2020. User Thermal Comfort in Historic Buildings: Evaluation of the Potential of Thermal Mass, Orientation, Evaporative Cooling and Ventilation. *Sustainability,* 12**,** 9672.

AMER, O. 2017. *A heat pipe and porous ceramic based sub wet-bulb temperature evaporative cooler: a theoretical and experimental study.* Doctor of Philosophy, University of Nottingham.

AMER, O., BOUKHANOUF, R. & IBRAHIM, H. 2015. A Review of Evaporative Cooling Technologies. *International journal of environmental science and development,* 6**,** 111.

ANDERSEN, P. A., DUER, K., FOLDBJERG, P., ROY, N., CHRISTOFFERSEN, J., ASMUSSEN, T. F., ANDERSEN, K., PLESNER, C., RASMUSSEN, M. H. & HANSEN, F. 2014. *Daylight, Energy and Indoor Climate Basic Book,* Denmark, VELUX Knowledge Centre for Daylight, Energy and Indoor Climate (DEIC).

ANDERSON, J. D. 2009. *Computational fluid dynamics,* Berlin, Heidelberg, Springer.

ANSYS, I. 2017. *ANSYS Fluent Theory Guide,* U.S.A.

ANTIQUITIES, S. C. F. T. A. 2013. Historic Jeddah, The Gate to Makkah. *In:* ANTIQUITIES (ed.). Jeddah: Saudi Commission for Tourism and Antiquities

ASHOUR, A. F. 2018. Islamic Architectural Heritage: Mashrabiya. *WIT Transactions on The Built Environment,* 177**,** 245-253.

ASHRAE 2010a. ANSI/ASHRAE Standard 55. *Thermal environmental conditions for human occupancy*.

ASHRAE 2010b. ANSI/ASHRAE Standard 55. *Thermal Environmental Conditions for Human Occupancy.*

AULICIEMS, A. & SZOKOLAY, S. V. Thermal comfort. *In:* SZOKOLAY, S. V., ed. PLEA : Passive and Low Energy Architecture International in association with Department of Architecture, The University of Queensland, 2007. PLEA.

AUTODESK, S. W. 2014a. Human Thermal Comfort. *Climate & Site Analysis* [Online]. Available: https://sustainabilityworkshop.autodesk.com/buildings/human-thermal-comfort.

AUTODESK, S. W. 2014b. Psychrometric Charts. *Human Thermal Comfort* [Online]. Available: https://sustainabilityworkshop.autodesk.com/buildings/psychrometric-charts.

BABSAIL, M. O. & AL-QAWASMI, J. 2015. Vernacular architecture in Saudi Arabia: Revival of displaced traditions. *Vernacular Architecture: Towards a Sustainable Future.* London: Taylor & Francis Group.

BAGASI, A. A. & CALAUTIT, J. K. 2020. Experimental field study of the integration of passive and evaporative cooling techniques with Mashrabiya in hot climates. *Energy and Buildings,* 225**,** 110325.

BAGASI, A. A., CALAUTIT, J. K. & KARBAN, A. S. 2021. Evaluation of the Integration of the Traditional Architectural Element Mashrabiya into the Ventilation Strategy for Buildings in Hot Climates. *Energies,* 14**,** 530.

BAHADORI, M. N., MAZIDI, M. & DEHGHANI, A. R. 2008. Experimental investigation of new designs of wind towers. *Renewable Energy,* 33**,** 2273-2281.

BAIK, A. & BOEHM, J. 2017. Hijazi Architectural Object Library (HAOL). *Int. Arch. Photogramm. Remote Sens. Spatial Inf. Sci.,* XLII-2/W3**,** 55-62.

BAKER, N. & STEEMERS, K. 2005. *Energy and Environment in Architecture: A Technical Design Guide*, Taylor & Francis e-Library.

BARTZANAS, T., BOULARD, T. & KITTAS, C. 2002. Numerical simulation of the airflow and temperature distribution in a tunnel greenhouse equipped with insect-proof screen in the openings. *Computers and Electronics in Agriculture,* 34**,** 207-221.

BATOOL, A. 2014. *Quantifying environmental performance of Jali screen façadesfor contemporary buildings in Lahore, Pakistan.* Master of Architecture, University of Oregon.

BATTERJEE, S. A. 2010. *Performance of shading device inspired by traditional hejazi houses in Jeddah Saudi Arabia.* MSc MSc in Environmental Design of Buildings, The British University in Dubai.

BENEDETTI, C., BARATIERI, M., LEONE, G., MIMMO, T. & PAGLIALONGA, G. Wood technology for passive cooling. Proceedings of the 11th World Conference on Timber Engineering 2010, 2010. 20-24.

BOAKE, T. M. 2014. Hot climate Double Facades: Avoiding Solar Gain. *FACADE TECTONICS,* 14**,** 24.

BOGARI, F. 2011. Climate - its determinants - and its relationship to housing design in Jeddah. *The Egyptian Journal of Environmental Change,* 3.

BOUKHANOUF, R., ALHARBI, A., AMER, O. & IBRAHIM, H. 2015. Experimental and numerical study of a heat pipe based indirect porous ceramic evaporative cooler. *International Journal of Environmental Science and Development,* 6**,** 104.

CAIN, A., AFSHAR, F., NORTON, J. & DARAIE, M.-R. 1976. Traditional Cooling Systems in the Third World. *The Ecologist,* 6**,** 60-64.

CALAUTIT, J. K., CHAUDHRY, H. N., HUGHES, B. R. & GHANI, S. A. 2013. Comparison between evaporative cooling and a heat pipe assisted thermal loop for a commercial wind tower in hot and dry climatic conditions. *Applied Energy,* 101**,** 740-755.

CALAUTIT, J. K., CONNOR, D., SOFOTASIOU, P. & HUGHES, B. R. 2015. CFD Simulation and Optimisation of a Low Energy Ventilation and Cooling System. *Computation,* 3**,** 128-149.

CHAMBER, J. 2018. Jeddah Facts and Figures. *Jeddah Annual Report 2016–2017.* Jeddah.

CHEUNG, J. O. P. & LIU, C.-H. 2011. CFD simulations of natural ventilation behaviour in high-rise buildings in regular and staggered arrangements at various spacings. *Energy and Buildings,* 43**,** 1149-1158.

CHIANG, C.-M., CHEN, N., CHOU, P., LI, Y. & LIEN, I. A study on the influence of horizontal louvers on natural ventilation in a dwelling unit. The 10th International Conference on Indoor Air Quality and Climate, 2005.

D'AVIGNON, E. 2012. *Restoration manual for the rehabilitation in historical Jeddah : architectural and structural elements, characteristics, pathologies & restoration techniques and solutions,* Avignon, Ecole d'Avignon.

DAEMEI, A. B., EGHBALI, S. R. & KHOTBEHSARA, E. M. 2019. Bioclimatic design strategies: A guideline to enhance human thermal comfort in Cfa climate zones. *Journal of Building Engineering,* 25**,** 100758.

DE DEAR, R. J. & BRAGER, G. S. 2002. Thermal comfort in naturally ventilated buildings: revisions to ASHRAE Standard 55. *Energy and Buildings,* 34**,** 549-561.

DEHWAH, A. H. A., ASIF, M. & RAHMAN, M. T. 2018. Prospects of PV application in unregulated building rooftops in developing countries: A perspective from Saudi Arabia. *Energy and Buildings,* 171**,** 76-87.

DEL RIO, M. A., ASAWA, T., HIRAYAMA, Y., SATO, R. & OHTA, I. 2019. Evaluation of passive cooling methods to improve microclimate for natural ventilation of a house during summer. *Building and Environment,* 149**,** 275-287.

DI TURI, S. & RUGGIERO, F. 2017. Re-interpretation of an ancient passive cooling strategy: a new system of wooden lattice openings. *Energy Procedia,* 126**,** 289-296.

DICTIONARY. 2016. *Dictionary. com* [Online]. USA. [Accessed].

EISSA, K. W. 2005. *The design of shading louvres for solar energy collection.* Doctor of Philosophy PhD, University of Nottingham.

ELAIAB, F. M. 2014. *Thermal comfort investigation of multi-storey residential buildings in Mediterranean climate with reference to Darnah, Libya.* PhD of Architecture PhD, University of Nottingham.

ELKHATIEB, M. & SHARPLES, S. Climate Adaptive Building Shells for Office Buildings in Egypt: A Parametric and Algorithmic Daylight Tool. SBE16 Dubai, 2016 Dubai-UAE. British University in Dubai, 17-19.

ELSOUDANI, M. 2016. *Cooling techniques for building-greenhouse interconnections in hot-arid climates.* Doctor of Engineering Doctoral Thesis, University of Berlin.

ELWAN, M. M. 2020. The role of traditional Lattice window" Mashrabiya" in delivering single-sided ventilation-A CFD Study. *International Journal of Engineering Trends and Technology (IJETT),* 68.

ENERGY, U. S. D. O. 2020. *Energy Performance Ratings for Windows, Doors, and Skylights* [Online]. Available: https://www.energy.gov/energysaver/design/windows-doors-and-skylights/energy-performance-ratings-windows-doors-and [Accessed 6 Feb 2021].

ETHERIDGE, D. & SANDBERG, M. 1996. *Building Ventilation: Theory and Measurement*, John Wiley & Sons, Inc.

FACEY, W. 2015. *Back to earth: adobe building in Saudi Arabia,* Riyadh, Saudi Arabia, Al-Turath Foundation.

FALLAHTAFTI, R. & MAHDAVINEJAD, M. 2020. Window geometry impact on a room's wind comfort. *Engineering, Construction and Architectural Management*.

FANGER, P. O. 1970. *Thermal comfort: Analysis and applications in environmental engineering*, Copenhagen: Danish Technical Press.

FATHY, H. 1986. Natural Energy and Vernacular Architecture Principles and Examples with Reference to Hot Arid Climate. The United Nations University: The University of Chicago Press, USA.

FELIMBAN, A., PRIETO, A., KNAACK, U., KLEIN, T. & QAFFAS, Y. 2019. Assessment of Current Energy Consumption in Residential Buildings in Jeddah, Saudi Arabia. *Buildings,* 9**,** 163.

FRANKE, J., HELLSTEN, A., SCHLÜNZEN, H. & CARISSIMO, B. 2007. Best Practice Guideline for the CFD Simulation of Flows in the Urban Environment. *COST Office Brussels,* 732**,** 51.

GAN, G. 2010. Interaction between wind and buoyancy effects in natural ventilation of buildings. *The Open Construction and Building Technology Journal,* 4**,** 134-145.

GERMANÀ, M. L., ALATAWNEH, B. & REFFAT, R. M. Technological and behavioral aspects of perforated building envelopes in the Mediterranean region. 10th Conference on Advanced Building Skins, 2015 Bern, Switzerland. 846-854.

GIOVANNINI, L., VERSO, V. R. L., KARAMATA, B. & ANDERSEN, M. 2015. Lighting and Energy Performance of an Adaptive Shading and Daylighting System for Arid Climates. *Energy Procedia,* 78**,** 370-375.

GIVONI, B. 1992. Comfort, climate analysis and building design guidelines. *Energy and buildings,* 18**,** 11-23.

GREENLAW, J.-P. 1976. *The coral buildings of Suakin,* Stocksfield, Oriel press.

HAREDY, A. 2016. *Simulation of photovoltaic airflow windows for indoor thermal and visual comfort and electricity generation.* Doctor of Philosophy PhD, University of Nottingham.

HARIRI, M. 1992. Design of Rowshan and its importance to the dwelling. *Journal of the Umm-Al-Qura University,* 3**,** 175-237.

HARRY, S. 2016. Dynamic Adaptive Building Envelopes–an Innovative and State-of-The-Art Technology. *Creative Space,* 3.

HAUSLADEN, G., DE SALDANHA, M. & LIEDL, P. 2008. *Climateskin: building-skin concepts that can do more with less energy*, Birkhäuser.

HAWKES, D. 1982. The theoretical basis of comfort in the 'selective' control of environments. *Energy and Buildings,* 5**,** 127-134.

HE, J. & HOYANO, A. 2011. Experimental study of practical applications of a passive evaporative cooling wall with high water soaking-up ability. *Building and Environment,* 46**,** 98-108.

HELLINGA, H. 2013. Daylight and view: The influence of windows on the visual quality of indoor spaces.

HUMPHREYS, M. A. & NICOL, J. F. 2000. Outdoor temperature and indoor thermal comfort: raising the precision of the relationship for the 1998 ASHRAE database of field studies. *ASHRAE Transactions,* 106**,** 485-492.

IBRAHEEM, O. 2018. *The feasibility of Passive Downdraught Evaporative Cooling (PDEC) of multi-storey office buildings in Cairo: a modelling study.* Doctor of Philosophy, University of Nottingham.

IBRAHIM, A. 1995. The development of architecture in the Kingdom of Saudi Arabia through different ages. *For architects and planners* [Online]. Available: http://www.cpas-egypt.com/Articles/Baki/Study/23.html.

IRVING, S. & CLEMENTS-CROOME, D. 2005. *Natural ventilation in non-domestic buildings,* Norwich, Great Britain, Chartered Institution of Building Services Engineers CIBSE.

JEONG, W. & SEONG, J. 2014. Comparison of effects on technical variances of computational fluid dynamics (CFD) software based on finite element and finite volume methods. *International Journal of Mechanical Sciences,* 78**,** 19-26.

KAMAL, M. A. 2014. The morphology of traditional architecture of Jeddah: Climatic design and environmental sustainability. *Global Built Environment Review,* 9**,** 4-26.

KANAAN, M. & CHAHINE, K. 2018. CFD study of ventilation for indoor multi-zone transformer substation. *International Journal of Heat and Technology,* 36**,** 88-94.

KANG, D. & STRAND, R. K. 2018. Performance control of a spray passive down-draft evaporative cooling system. *Applied energy,* 222**,** 915-931.

KARAMATA, B., GIOVANNINI, L., VERSO, V. R. L. & ANDERSEN, M. 2014. Concept, Design and Performance of a Shape Variable Mashrabiya as a Shading and Daylighting System for Arid Climates. *30th International Passive and Low Energy Architecture conference (PLEA 2014).* Ahmedabad, India: CEPT University Ahmedabad.

KARAVA, P., STATHOPOULOS, T. & ATHIENITIS, A. K. 2011. Airflow assessment in cross-ventilated buildings with operable façade elements. *Building and Environment,* 46**,** 266-279.

KHADRA, A. A. & CHALFOUN, N. 2014. Development of an integrated passive cooling façade technology for office buildings in hot arid regions. *WIT Transactions on Ecology and the Environment,* 190**,** 13.

KHAN, S. M. 1986. Jeddah Old Houses. *Department of Scientific Research, King Abdulaziz City for Science and Technology, Saudi Arabia.*

KIAMBA, L. N. 2016. *Optimising environmental design strategies to improve thermal performance in office buildings in Kenya.* PhD, University of Nottingham.

KIENZL, N. 1999. *Advanced building skins: translucent thermal storage elements.* Master of Science in Building Technology, Massachusetts Institute of Technology.

KLEIVEN, T. 2003. *Natural Ventilation in Buildings Architectural concepts, consequences and possibilities.* PhD, Norwegian University of Science and Technology.

KOSUTOVA, K., VAN HOOFF, T., VANDERWEL, C., BLOCKEN, B. & HENSEN, J. 2019. Cross-ventilation in a generic isolated building equipped with louvers: Wind-tunnel experiments and CFD simulations. *Building and Environment,* 154**,** 263-280.

KOTBI, M. 2013. *Investigating thermal comfort models.* Doctor of philosophy, University of New South Wales.

KOTTEK, M., GRIESER, J., BECK, C., RUDOLF, B. & RUBEL, F. 2006. World map of the Köppen-Geiger climate classification updated. *Meteorologische Zeitschrift,* 15.

KROELINGER, M. 2002. Daylight in Buildings. *Informe Design.* University of Minnesota.

LECHNER, N. 2014. *Heating, Cooling, Lighting,* United States of America, John wiley & sons.

LEE, K. S., HAN, K. J. & LEE, J. W. 2016. Feasibility Study on Parametric Optimization of Daylighting in Building Shading Design. *Sustainability,* 8**,** 1220.

LI, N. 2015. *Comparison between three different CFD software and numerical simulation of an ambulance hall.* Master of Science, KTH ROYAL INSTITUTE OF TECHNOLOGY.

LOTFABADI, P. & HANÇER, P. 2019. A Comparative Study of Traditional and Contemporary Building Envelope Construction Techniques in terms of Thermal Comfort and Energy Efficiency in Hot and Humid Climates. *Sustainability,* 11**,** 3582.

LUDLOW, A. 1976. The functions of windows in buildings. *Lighting Research and Technology,* 8**,** 57-68.

LUKIANTCHUKI, M. A., PRATA SHIMOMURA, A., MARQUES DA SILVA, F. & CARAM, R. M. 2020. Wind tunnel and CFD analysis of wind-induced natural ventilation in sheds roof building: impact of alignment and distance between sheds. *International Journal of Ventilation,* 19**,** 141-162.

MAAJIM 2013. ARABIC DICTIONARY.

MAGHRABI, A. A. 2000. *Airflow characteristics of modulated louvered windows with reference to the Rowshan of Jeddah, Saudi Arabia.* Doctor of Philosophy, University of Sheffield.

MAGHRABI, A. A. & SHEHATA, A. M. 2005. Room Airflow Characteristics with Reference to The Rowshan (Window Bay) Configurations: CFD Study. *The 17th International Conference on Systems Research, Informatics and Cybernetics.* Baden-Baden, Germany.

MALDONADO, J. M., DE GRACIA, A. & CABEZA, L. F. 2020. Systematic review on the use of heat pipes in latent heat thermal energy storage tanks. *Journal of Energy Storage,* 32**,** 101733.

MARKUS, T., MORRIS, E. N., REED, P., MCGEORGE, W. D. & YANESKE, P. P. 1980. *Buildings, climate, and energy*.

MARKUS, T. A. 1967. The function of windows— A Reappraisal. *Building Science,* 2**,** 97-121.

MARTIN, L. W. 1996. A Guide to Energy Efficient Ventilation. *Air Infiltration and Ventilation.* Coventry, Great Britain: Air Infiltration and Ventilation Centre (AIVC).

MAXWELL, E., CORNWALL, C., WILCOX, S., ALAWAJI, S. & BIN MAHFOODH, M. Assessment of solar radiation resources in Saudi Arabia. Renewable Energy, Proceedings of World Renewable Energy Conference, 1996. 21.

MCDONOUGH, J. M. 2009. *Lectures In Elementary Fluid Dynamics: Physics, Mathematics and Applications,* University of Kentucky, Lexington, KY, Mechanical Engineering Textbook Gallery.

MEIR, I. & ROAF, S. Thermal comfort–thermal mass: housing in hot dry climates. *In:* LEVIN, H., ed. The 9th International Conference on Indoor Air Quality and Climate, 2002 Monterey, California. Indoor Air 2002, 1050-1055.

MERONEY, R. N. CFD prediction of airflow in buildings for natural ventilation. Proceedings of the Eleventh Americas Conference on Wind Engineering, 2009 San Juan, Puerto Rico.

METEOBLUE. 2020. *Jeddah Climate* [Online]. Available: https://www.meteoblue.com/en/weather/historyclimate/climatemodelled/jeddah-king-abdul-aziz-international-airport_saudi-arabia_6300018 [Accessed 2020].

METEOROLOGY, N. C. F. 2019. *Monthly Climate Reports* [Online]. Available: https://ncm.gov.sa/Ar/MediaCenter/Reports/Pages/medialibrary.aspx?folderID=a8807580-fef8-425c-8981-c757ec9f33ea [Accessed 2020].

MISRA, D. & GHOSH, S. 2018. Evaporative cooling technologies for greenhouses: a comprehensive review. *Agricultural Engineering International: CIGR Journal,* 20**,** 1-15.

MOHAMED, J. 2015. *The traditional arts and crafts of turnery or mashrabiya.* Master of Art, Rutgers, The State University of New Jersey.

MOHD NASIR, S. D. N. 2017. *The Influence of Building Configuration on the Urban heat Island Effect.* PhD, University of Sheffield.

MORALES, X., SIERRA-ESPINOSA, F. Z., MOYA, S. L. & CARRILLO, F. 2021. Thermal effectiveness of wind-tower with heated exit-wall and inlet-air humidification: Effects of winter and summertime. *Building and Environment,* 204**,** 108110.

MURALI, S. 2013. *Design of a Climate Adaptive Façade System using Bamboo for Urban India.* Master, Delft University of Technology

NACIRI, N. 2007. Sustainable features of the Vernacular Architecture: A Case Study of Climatic Controls in the Hot-Arid regions of the Middle Eastern and North African Regions.

NAKANISHI, T., NAKAMURA, T., WATANABE, Y., HANDOU, K. & KIWATA, T. 2007. Investigation of Air Flow passing through Louvers. *Komatsu Technical Report 2,* 53.

NAKANO, J. 2003. *Evaluation of Thermal Comfort in Semi-outdoor Environment.* Waseda University.

NICOL, J. F. & HUMPHREYS, M. A. 2002. Adaptive thermal comfort and sustainable thermal standards for buildings. *Energy and Buildings,* 34**,** 563-572.

NIKAS, K. S., NIKOLOPOULOS, N. & NIKOLOPOULOS, A. 2010. Numerical study of a naturally cross-ventilated building. *Energy and Buildings,* 42**,** 422-434.

NOROOZI, A. & VENERIS, Y. S. 2018. Thermal Assessment of a Novel Combine Evaporative Cooling Wind Catcher. *Energies,* 11**,** 442.

O'CONNOR, D. 2016. *A Novel Heat Recovery Device for Passive Ventilation Systems.* Doctor of Philosophy, The University of Sheffield.

OLIVER, P. 2006. *Built to meet needs: cultural issues in vernacular architecture,* Italy, Elsevier.

OTUSANYA, O. P., AJWANG, P. & ONDIMU, S. N. 2020. Reducing Cooling Demands in Sub-Saharan Africa: A Study on The Thermal Performance of Passive Cooling Methods in Enclosed Spaces. *Journal of Sustainable Development of Energy, Water and Environment Systems*.

PARSONS, K. 2014. *Human Thermal Environments,* New York, CRC press.

PASSE, U. & BATTAGLIA, F. 2015. *Designing Spaces for Natural Ventilation: An Architect's Guide,* New York, Routledge.

PEETERS, L., DEAR, R. D., HENSEN, J. & D'HAESELEER, W. 2009. Thermal comfort in residential buildings: Comfort values and scales for building energy simulation. *Applied Energy,* 86**,** 772-780.

PERÉN, J. I., VAN HOOFF, T., LEITE, B. C. C. & BLOCKEN, B. 2015. CFD analysis of cross-ventilation of a generic isolated building with asymmetric opening positions: Impact of roof angle and opening location. *Building and Environment,* 85**,** 263-276.

PHILLIPS, D. 2004. *Daylighting,* Italy, Architectural Press.

PRAKASH, D. & RAVIKUMAR, P. 2015. Analysis of thermal comfort and indoor air flow characteristics for a residential building room under generalized window opening position at the adjacent walls. *International Journal of Sustainable Built Environment,* 4**,** 42-57.

RAEL, R. & FRATELLO, V. S. 2015. *Cool Brick* [Online]. Available: http://www.emergingobjects.com/projects/cool-brick/ [Accessed 10 Dec 2019 2019].

RAFIQUE, M. M., REHMAN, S., LASHIN, A. & AL ARIFI, N. 2016. Analysis of a Solar Cooling System for Climatic Conditions of Five Different Cities of Saudi Arabia. *Energies,* 9**,** 75.

RAMPONI, R. & BLOCKEN, B. 2012. CFD simulation of cross-ventilation for a generic isolated building: Impact of computational parameters. *Building and Environment,* 53**,** 34-48.

RAMZY, N. & FAYED, H. 2011. Kinetic systems in architecture: New approach for environmental control systems and context-sensitive buildings. *Sustainable Cities and Society,* 1**,** 170-177.

RIFFAT, S. & ZHU, J. 2004. Experimental Investigation of an Indirect Evaporative Cooler Consisting of a Heat Pipe Embedded in Porous Ceramic. *The Journal of Engineering Research [TJER],* 1**,** 46-52.

ROBERTSON, K. 2003. *Daylighting guide for Buildings*, Canada Mortgage and Housing Corporation.

RODRIGUES, L. T. 2010. *An investigation into the use of thermal mass to improve comfort in British housing.* Doctor of Philosophy, University of Nottingham.

ROSENLUND, H. 2000. Climatic design of buildings using passive techniques. *Building Issues.* LUND UNIVERSITY: Lund University, Housing Development and Management.

RUCK, N., ASCHEHOUG, O., AYDINLI, S., CHRISTOFFERSEN, J., EDMONDS, I., JAKOBIAK, R., KISCHKOWEIT-LOPIN, M., KLINGER, M., LEE, E. & COURRET, G. 2000. Daylight in Buildings-A source book on daylighting systems and components. Lawrence Berkeley National Laboratory, Berkeley (USA).

SABRY, E. & DWIDAR, S. 2015. Contemporary Islamic Architecture towards preserving Islamic heritage. *ResearchGate*.

SABRY, H., SHERIF, A., GADELHAK, M. & ALY, M. 2014. Balancing the daylighting and energy performance of solar screens in residential desert buildings: Examination of screen axial rotation and opening aspect ratio. *Solar Energy,* 103**,** 364-377.

SAID, S., HABIB, M. & IQBAL, M. 2003. Database for building energy prediction in Saudi Arabia. *Energy conversion and management,* 44**,** 191-201.

SAID, S. A. M. & AL-ZAHARNAH, E. T. 1994. Development of comfort zone charts using the isopleth chart technique. *Building and Environment,* 29**,** 13-20.

SAINI, B. S. 1991. *Building In Hot Dry Climates,* Chichester, John Wiley & Sons.

SAJJAD, U., ABBAS, N., HAMID, K., ABBAS, S., HUSSAIN, I., AMMAR, S. M., SULTAN, M., ALI, H. M., HUSSAIN, M., TAUSEEF UR, R. & WANG, C. C. 2021. A review of recent advances

in indirect evaporative cooling technology. *International Communications in Heat and Mass Transfer,* 122**,** 105140.

SALEM, R. 2019. *Evaluating Environmental Performance of Mashrabiya.* Master, University of Westminster.

SALLOUM, A. El-Rawashin of Jeddah, Saudi Arabia. Passive and Low Energy Architecture: Proceedings of the Second International PLEA Conference, 28 June-1 July 1983 1983 Crete, Greece. Elsevier, 245-252.

SAMUELS, W. 2011. *Performance and Permeability: An investigation of the Mashrabiya for Use within the Gibson Desert.* Master of Architecture (Professional), Victoria University of Wellington.

SANTAMOURIS, M. 2006. Adaptive thermal comfort and ventilation. *Air Infiltration and Ventilation Center***,** 8.

SAUDI COMMISSION FOR TOURISM AND NATIONAL HERITAGE. 2016. Historical Old Jeddah. *Internationally Registered Sites* [Online]. Available: https://www.scta.gov.sa/en/Antiquities-Museums/InternationallyRegisteredSites/Pages/OldJeddah.aspx [Accessed 15/07/2017].

SAUDI, M. 2020. Rijal Almaa and the Flower Men of Asir. Saudi Tourism Authority.

SAULLES, T. D. 2015. Thermal Mass Explained. *The Concrete Centre.* Camberley, Surrey: MPA The Concrete Centre.

SCHIANO-PHAN, R. The development of passive downdraught evaporative cooling systems using porous ceramic evaporators and their application in residential buildings. 28th International Conference on Passive and Low Energy Architecture, PLEA2004, 2004 Eindhoven, The Netherlands. Architectural Association, 9-12.

SCHIANO-PHAN, R. 2010. Environmental retrofit: building integrated passive cooling in housing. *Architectural Research Quarterly,* 14**,** 139-151.

SEEC. 2019. *Buildings sector* [Online]. Saudi Arabia: Saudi Energy Efficiency Center. Available: https://www.seec.gov.sa/en/energy-sectors/buildings-sector/ [Accessed 19 Feb 2021].

SHAERI, J., YAGHOUBI, M., AFLAKI, A. & HABIBI, A. 2018. Evaluation of Thermal Comfort in Traditional Houses in a Tropical Climate. *Buildings,* 8**,** 126.

SHAHZAD, S., CALAUTIT, K., WEI, S., TIEN, P. W., CALAUTIT, J. & HUGHES, B. 2020. Analysis of the thermal comfort and energy performance of a thermal chair for open plan office. *Journal of Sustainable Development of Energy, Water and Environment Systems,* 8**,** 373-395.

SHEN, C. & LI, X. 2016. Solar heat gain reduction of double glazing window with cooling pipes embedded in venetian blinds by utilizing natural cooling. *Energy and Buildings,* 112**,** 173-183.

SHUKLA, K. 2015. Heat pipe for aerospace applications—an overview. *Journal of Electronics Cooling and Thermal Control,* 5**,** 1.

SOFOTASIOU, P. 2017. *Aerodynamic optimisation of sports stadiums towards wind comfort.* Doctor of Philosophy, The University of Sheffield.

SOLARGIS. 2018. *Solar resource maps for Saudi Arabia* [Online]. Slovakia. Available: http://solargis.com/products/maps-and-gis-data/free/download/saudi-arabia [Accessed 06/2017].

SPARK, W. 2022. *Climate and Average Weather Year Round in Jeddah* [Online]. Available: https://weatherspark.com/y/101171/Average-Weather-in-Jeddah-Saudi-Arabia-Year-Round [Accessed 2022].

STATISTICS, G. A. F. 2019. Household Environment Survey 2019. *Environment Indicators.* Riyadh.

STAVRAKAKIS, G., KOUKOU, M., VRACHOPOULOS, M. G. & MARKATOS, N. 2008. Natural cross-ventilation in buildings: Building-scale experiments, numerical simulation and thermal comfort evaluation. *Energy and Buildings,* 40**,** 1666-1681.

STAVRAKAKIS, G. M., STAMOU, A. & MARKATOS, N. C. 2009. Evaluation of thermal comfort in indoor environments using Computational Fluid Dynamics(CFD).

STEIN, B. & S. REYNOLDS, J. 1992. *Mechanical and electrical equipment for buildings,* the University of Michigan, John Wiley & Sons. Inc.

SUBYANI, A. M. & HAJJAR, A. F. 2016. Rainfall analysis in the contest of climate change for Jeddah area, Western Saudi Arabia. *Arabian Journal of Geosciences,* 9.

SUDY, S. 2011. *The architectural language of park51 understanding cultural and historical connections.* Washington State University.

SUNEARTHTOOLS. 2017. *Sun Position, Jeddah* [Online]. [Accessed 2018].

SZOKOLAY, S. 2004. *Introduction to Architectural Science: The Basis of Sustainable Design,* Architectural Press, Routledge.

TALEB, H. M. 2012. *Towards sustainable residential buildings in the Kingdom of Saudi Arabia.* Doctor of Philosophy, University of Sheffield, School of Architecture.

TALEB, H. M. & ANTONY, A. G. 2020. Assessing different glazing to achieve better lighting performance of office buildings in the United Arab Emirates (UAE). *Journal of Building Engineering,* 28**,** 101034.

TALIB, K. 1984. *Shelter in Saudi Arabia,* New York, USA, Academy Editions/ St. Martin's Press.

TAP, M. M., KAMAR, H. M., MARSONO, A. K., KAMSAH, N. & SALIMIN, K. A. M. 2011. Simulation of Thermal Comfort of a Residential House. *International Journal of Computer Science Issues (IJCSI),* 8**,** 200.

TOMINAGA, Y., MOCHIDA, A., YOSHIE, R., KATAOKA, H., NOZU, T., YOSHIKAWA, M. & SHIRASAWA, T. 2008. AIJ guidelines for practical applications of CFD to pedestrian wind environment around buildings. *Journal of Wind Engineering and Industrial Aerodynamics,* 96**,** 1749-1761.

VALLEJO, J. 2018. *Design integration of novel porous ceramic evaporative cooling systems.* Doctor of Philosophy, University of Nottingham.

VAN DER LINDEN, A. C., BOERSTRA, A. C., RAUE, A. K., KURVERS, S. R. & DE DEAR, R. J. 2006. Adaptive temperature limits: A new guideline in The Netherlands: A new approach for the assessment of building performance with respect to thermal indoor climate. *Energy and Buildings,* 38**,** 8-17.

VAN HOOFF, T., BLOCKEN, B. & TOMINAGA, Y. 2017. On the accuracy of CFD simulations of cross-ventilation flows for a generic isolated building: Comparison of RANS, LES and experiments. *Building and Environment,* 114**,** 148-165.

VEFIK ALP, A. 1991. Vernacular climate control in desert architecture. *Energy and Buildings,* 16**,** 809-815.

VERSTEEG, H. & MALALASEKERA, W. 1995a. *An Introduction to computational fluid dynamics*, Longman Group.

VERSTEEG, H. K. & MALALASEKERA, W. 1995b. *An Introduction to computational fluid dynamics*, Longman Group.

VINCENT, P. 2008. *Saudi Arabia: an environmental overview*, CRC Press.

WAHEEB, S. A. 2006. *Impact of shading devices on indoor sunlight distribution and building energy performance, with reference to Saudi Arabia.* Doctor of Philosophy, University of Nottingham.

WIGGINTON, M. & HARRIS, J. 2002. *Intelligent skins,* Itlay, Gray.

WILSON, S. & HEDGE, A. The office environment survey : a study of building sickness. Building Use Studies, 1987 London.

WINDFINDER. 2017. *Monthly wind speed statistics and directions for Jeddah King Abdulaziz Airport* [Online]. Available: https://www.windfinder.com/windstatistics/jeddah [Accessed 2017].

WORLDDATA.INFO. 2020. *The climate in Saudi Arabia* [Online]. German Weather Service. Available: https://www.worlddata.info/asia/saudi-arabia/climate.php [Accessed 1 June 2020 2021].